DISSERTATION

ISOLATION AND CHARACTERIZATION OF DENGUE VIRUS MEMBRANE-ASSOCIATED REPLICATION COMPLEXES FROM *AEDES AEGYPTI*

Submitted by

B. Katherine Poole-Smith

Department of Microbiology, Immunology, and Pathology

In partial fulfillment of the requirements

For the Degree of Doctor of Philosophy

Colorado State University

Fort Collins, Colorado

Summer 2010

COLORADO STATE UNIVERSITY

May 28, 2010

WE HEREBY RECOMMEND THAT THE DISSERTATION PREPARED UNDER OUR SUPERVISION BY B. KATHERINE POOLE-SMITH ENTITLED ISOLATION AND CHARACTERIZATION OF DENGUE VIRUS MEMBRANE-ASSOCIATED REPLICATION COMPLEXES FROM *AEDES AEGYPTI* BE ACCEPTED AS FULFILLING IN PART REQUIREMENTS FOR THE DEGREE OF DOCTOR OF PHILOSOPHY.

Committee on Graduate Work

_____
Kenneth E. Olson

_____
Brian D. Foy

_____
Eric D. Ross

_____
Advisor: Carol D. Blair

_____
Department Head: Edward A. Hoover

ABSTRACT OF DISSERTATION

ISOLATION AND CHARACTERIZATION OF DENGUE VIRUS MEMBRANE-ASSOCIATED REPLICATION COMPLEXES FROM *AEDES AEGYPTI*

Ultrastructural studies of flavivirus replication have long observed proliferation of host membranes. Membrane-bound replication compartments have recently been isolated and characterized from flavivirus-infected mammalian cells, providing insight into the morphology, organelle of origin, and protein components of the flavivirus membrane-associated replication complex. Our laboratory has proposed that a balance exists between dengue virus (DENV) replication in *Aedes aegypti* and the mosquito's RNA interference (RNAi) based antiviral response. Here, we have isolated and characterized membrane-bound replication compartments from mosquito cell culture and *Ae. aegypti* to evaluate the role that these membranes may play in shielding DENV double-stranded RNA (dsRNA) from RNAi.

Membrane isolation techniques and immunofluorescent staining techniques for dsRNA identification were developed to isolate and characterize membrane-associated replication complexes in DENV-infected mosquito cell culture and *Ae. aegypti*. Here we show that double-membrane vesicles arise from the endoplasmic reticulum (ER) and are associated with DENV dsRNA in mosquitoes. These data suggest that DENV dsRNA replicative intermediates may be shielded from the RNAi response in the mosquito.

DENV membrane-associated replication complexes were characterized in mosquito cell culture and *Ae. aegypti* using immunofluorescent staining for dsRNA, confocal microscopy, sucrose gradient cellular fractionation, and electron microscopy. In addition, we compared immunofluorescent staining for dsRNA between DENV and Sindbis virus (SINV). We also evaluated replication of DENV mutants in the DENV-resistant transgenic mosquito strain known as Carb77 and whether mutations in DENV genome sequence lead to evasion of the enhanced RNAi response of Carb77 mosquitoes.

This is the first isolation of membrane-associated replication complexes and first characterization of dsRNA staining from DENV-infected mosquito cell culture and *Ae. aegypti*, providing knowledge which can be used to develop improved RNAi-based control strategies for DENV in mosquitoes.

Betty Katherine Poole-Smith
Department of Microbiology, Immunology, and Pathology
Colorado State University
Fort Collins, CO 80523
Summer 2010

Table of Contents

List of Figures

List of Tables

Chapter 1

Literature Review

Introduction

In modern times, dengue is a major re-emerging disease that afflicts 50-100 million individuals with 22,000 deaths annually (NIAID, 2008). In spite of the importance of dengue disease, we still have many gaps in our knowledge of dengue viruses. We, as researchers, still have much work to do to develop safe and efficacious vaccines, animal models, promote and enforce control measures, and promote sharing of clinical and epidemiological observations to prevent disease transmission (CDC, 2008; Halstead, 2008; NIAID, 2008). In spite of the many researchers working on these goals, there are still many basic research questions to be answered regarding all aspects of dengue disease. Our laboratory is focused on understanding the interaction between dengue virus (DENV) and the mosquito host at the molecular level. In this pursuit, we study the mosquito's most important antiviral response to DENV infection, RNA interference (RNAi).

In the past, research in our laboratory has shown that mosquitoes have a robust RNAi response and that suppression of the RNAi response leads to increased replication of arboviruses in the mosquito host (Keene et al., 2004; Sanchez-Vargas et al., 2004). More recent research suggests that there is a fine balance between replication of DENV and the antiviral RNAi response in *Aedes aegypti* mosquitoes (Sanchez-Vargas et al., 2009). In an effort to further understand how this balance between DENV replication and mosquito immunity is maintained, the goal of this project is to evaluate mechanisms by which DENV is able to evade the RNAi response.

DENV Taxonomy

DENV is a member of the taxonomic family Flaviviridae, genus *Flavivirus*. Flaviviridae includes other pathogenic mosquito borne viruses: yellow fever virus (YFV), West Nile virus (WNV), St. Louis encephalitis virus (SLEV), and Japanese encephalitis virus (JEV). There are four serotypes of DENV, each of which likely emerged separately from the sylvatic cycle (Vasilakis and Weaver, 2008). Although the four serotypes of DENV could be considered different viruses based on 62-67% amino acid homology, the differences between the viruses were originally based on serologic analysis and the viruses were assigned to the same antigenic complex and deemed different serotypes instead of different viruses (Calisher et al., 1989; Kyle and Harris, 2008).

DENV replication

DENV has a positive sense genome with a 5' 7-methylguanosine cap and no polyadenylic acid. DENV replicates in a variety of cells in the human host including monocytes, hepatocytes, and dendritic cells (DCs), which the virus enters via receptor-mediated endocytosis through interaction with possible receptors including CD4, DC-SIGN, mannose receptor, and possibly integrins (Bartenschlager and Miller, 2008) Once inside the endosome, the envelope (E) protein trimerizes due to conformational changes mediated by the acidic environment, causing fusion between the virion envelope and cellular membranes (Modis et al., 2004). The viral genome is uncoated and released into the cytoplasm. As the genome is translated, the viral polyprotein is co- and post-translationally cleaved by cellular proteases and NS2B/NS3 (Figures 1.1 & 1.2). The

replication complex consisting of the RNA-dependent RNA polymerase (RdRp) NS5, other NS proteins, positive strand RNA, and probably host cellular factors associates with the host cell rough endoplasmic reticulum (rER). All flaviviruses including DENV have inverted complementary regions at the 3' and 5' ends and the genome circularizes during replication (You and Padmanabhan, 1999). Replication occurs in association with membranes, and genomic length negative or antisense strand RNA is synthesized, then serves as a template for positive strand RNA synthesis. The positive or sense strand RNA when base-paired with the negative strand is called the replicative form (RF) (Uchil and Satchidanandam, 2003). The RF serves as the template for positive RNA synthesis and this is called the replicative intermediate (RI). As positive strand RNA is released from the RI it is either translated by ribosomes or packaged into virions in the rER. The viral glycoproteins undergo maturation in the Golgi, becoming glycosylated, prM is cleaved by furin, and the E protein homodimerizes. Finally, the mature virion exits the infected cell.

During DENV replication there are three points at which double-stranded viral RNA (dsRNA) has the potential to be exposed to the host immune response (Figure 1.2). The first point at which DENV dsRNA is exposed occurs after the virion enters the cell and secondary structure of DENV genome produces regions of dsRNA. Next dsRNA is produced as the anti-genome strand RNA is transcribed from the DENV genome and again as the anti-genome strand is used as a template to transcribe DENV genomes. If the viral RNA is recognized by the host at any of these points, the virus may need to combat the RNAi response to establish a productive infection.

Protein	Roles	References
Structural		
C	forms nucleocapsid with + RNA	(Sangiambut et al., 2008)
PrM	prevents fusion by E during maturation	(Li et al., 2008b)
E	virus-cell binding and fusion with pH change	(Nayak et al., 2009)
Non-structural		
NS1	unknown, possible role in pathogenesis	(Chen et al., 2009)
NS2a	anchors replication complex	(Mackenzie et al., 1998)
	blocks IFN α/β	(Munoz-Jordan et al., 2003)
NS2b	proteolytic processing	(Falgout et al., 1991) (Amberg et al., 1994)
NS3	proteolytic processing	(Falgout et al., 1991) (Amberg et al., 1994)
	enhances NS4b helicase	(Umareddy et al., 2006)
	serine protease activity (NS2b cofactor)	
	nucleotide triphosphatase	
NS4a	membrane rearrangement	(Miller et al., 2007)
	anchors replication complex	
	block interferon α/β	(Munoz-Jordan et al., 2003)
	interacts with NS1	(Lindenbach and Rice, 1999)
NS4b	anchors replication complex	(Mackenzie et al., 1998)
	blocks interferon α/β	(Munoz-Jordan et al., 2003)
	colocalizes with NS3 and dsRNA	(Puig-Basagoiti et al., 2007)
NS5	viral RdRp	(Yap et al., 2007)
	N-terminal methyltransferase	(Egloff et al., 2007)

Figure 1.1 Dengue virus polyprotein

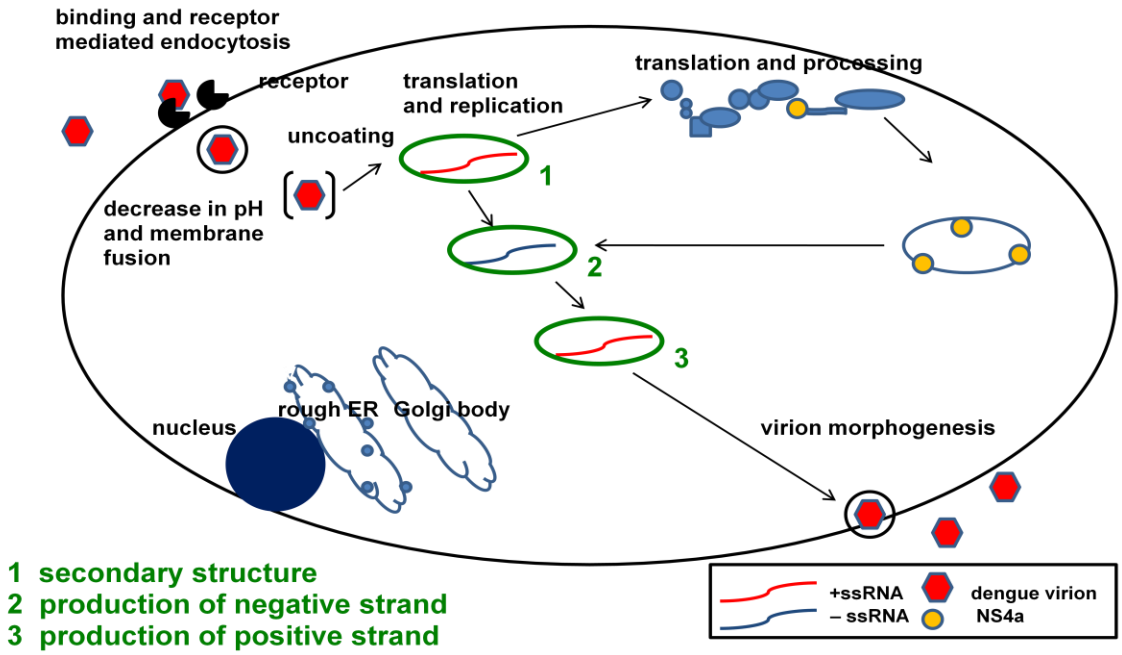

Figure 1.2 DENV replication: three points of vulnerability. During DENV replication, there are three points at which double-stranded viral RNA could be at risk for degradation by Dicer, **1** at initial uncoating the secondary structure of the genomic RNA forms dsRNA, **2** during replication production of the negative strand template of RNA from the positive or genomic strand of RNA, and **3** during production of the positive strand of RNA from the negative template.

DENV natural cycle

DENV is an arbovirus (arbo: arthropod borne) which has two transmission cycles. The urban cycle of DENV consists of virus transmission between humans by anthropophilic mosquitoes. In the sylvatic cycle, DENV is transmitted between non-human primates by *Aedes* species mosquitoes (Diallo et al., 2003). Although humans are periodically infected by sylvatic strains of DENV, unlike many other arboviruses DENV does not require a sylvatic cycle for maintenance because of the high titer viremia, 10^5–10^6 infectious units per ml) that occurs in the human host (Cardosa et al., 2009; Whitehead et al., 2007). This work will focus on the urban cycle of DENV.

DENV exists in an urban cycle throughout the neotropics and a sylvatic cycle in Africa (de Thoisy et al., 2004). The major vector of urban dengue is *Aedes aegypti*, an anthropophilic mosquito that has readily adapted to thrive in major urban areas throughout the tropics. *Ae. aegypti* breed in or near houses and feed frequently and almost exclusively on humans, behavior which makes them quite effective disease vectors in densely populated urban areas (Getis et al., 2003; Harrington et al., 2001). Once infected with DENV, humans have a 5-7 day incubation period, then a high titer viremia develops and lasts up to 12 days (McBride and Bielefeldt-Ohmann, 2000). During this viremic period, mosquitoes feeding on an infected individual will most likely become infected unless the mosquito is resistant to virus infection and dissemination (Bennett et al., 2005; Bennett et al., 2002). After an 8-12 day extrinsic incubation period (EIP), the mosquito is capable of infecting another human host and the cycle continues (Black et al., 2002). In addition to DENV transmission by *Ae. aegypti*, *Aedes albopictus*

is a secondary vector for dengue and was spread from Southeast Asia around the world with tire shipments (Moore et al., 1988; Rudnick and Chan, 1965).

History of dengue disease

Dengue is a mosquito-borne, virally induced illness that was first described as early as 992 A.D. in China (Kyle and Harris, 2008). Dengue disease existed as basic dengue fever until after World War II (WWII) (Snowden, 2008). Not until the 1950s, with the possible exception of cases in Japan, were the more severe forms of dengue that we know as dengue hemorrhagic fever (DHF) and dengue shock syndrome (DSS) observed (Kuno, 2007; Kuno, 2009). DHF and DSS will be discussed in more detail later.

DENV resurgence

The Pan American Health Organization (PAHO) project to eradicate *Aedes aegypti* (1946-1970s) from the Americas using larval control and dichlorodiphenyltrichloroethane (DDT) had profoundly reduced dengue disease (Gubler, 2005). The success of the eradication campaign resulted in a disbandment of the program and government funding for vector control in the early 1970s (Gubler, 2005; Snowden, 2008). Unfortunately, the abandonment of vector control programs led to the rebound of *Ae. aegypti* populations, and from 1970 to the early 1980s *Ae. aegypti* had re-infested all of the countries from which it had been eradicated (Gubler, 1989). This rebound of *Ae. aegypti* populations coincided with increased global population growth, travel, and trade, all which combined to cultivate the emergence and spread of severe

forms of dengue. Movement of commercial goods and transport of viremic humans continues to spread both vectors and serotypes of DENV today (Kitchener et al., 2002 ; Moore et al., 1988; Shu et al., 2005).

Post WWII, there has been a five hundred-fold increase in DHF and DSS cases, so now one-third of the worldwide population is at risk for dengue and the only available prevention method for dengue is mosquito control (Kyle and Harris, 2008; Rothman, 2004). There are no licensed vaccines or antiviral drugs for dengue. Based on global warming predictions and the effects of temperature change and rainfall on vector populations, it is unlikely that dengue cases will diminish without our intervention (Vezzani and Carbajo, 2008).

Dengue fever, dengue hemorrhagic fever, and dengue shock syndrome

There is a range of illness caused by infection by DENV from unapparent infection to severe shock and death. Classic dengue fever (DF) consists of symptoms including retro-orbital pain, myalgia, arthralgia, and usually rash (CDC, 2003). According to the WHO, DHF cases are defined by fever, thrombocytopenia (reduced platelet count), hemorrhagic tendencies, and plasma leakage. DSS cases have all of the symptoms of DHF plus weak pulse, low blood pressure, clammy skin, and confusion (WHO, 2008).

Severe disease: antibody-mediated or determined by virus genotype?

There are two major theories as to the cause of the more severe forms of dengue, DHF and DSS: antibody-dependent enhancement and strain specific virulence. The

antibody-dependent enhancement (ADE) theory is based on observations that secondary dengue infections are associated with increased severity of disease. An epidemiologic study of occurance of DHF in children admitted to hospitals in Thailand in the early 1960s noted a bimodal distribution of DHF cases by age with the first peak before 1 year of age and again at 4 years of age (Halstead, 1970). Based on serologic testing of the children in this study, Halstead et al. (1970) noted that presence of maternal antibody or secondary infections increased the risk of DHF. From this data, Halstead et al. (1970) presented the hypothesis that antibodies from the initial infection are cross-reactive with a second DENV serotype but instead of neutralizing the infection, they aid infection of Fc receptor-bearing cells leading to higher titer viremia. This prediction was also supported by testing in cultured human monocytes and non-human primates (Halstead, 1979). Secondary dengue infection was also found to be a major risk-factor, especially if the infecting serotype in the second infection was DENV-2, for the development in DSS during a prospective study of DSS in Myanmar (Thein, 1997). More recent research on T cells associated with dengue infection modifies the ADE hypothesis slightly. A synergistic effect caused by the interaction interferon gamma (IFN γ), interferon alpha (IFN α), and activation of complement causes a "cytokine storm" which creates the capillary leakage which leads to DHF (Rothman and Ennis, 1999). Another group of researchers found that cross-reactive memory T cells from primary dengue infection dominate the response to a secondary infection and they determined that magnitude of the T cell response correlated with dengue disease severity and DHF (Mongkolsapaya et al., 2003).

The virulence theory points out that not all of the predictions of ADE are supported by epidemiological evidence and that severe infections could also be explained by the introduction of more virulent strains of DENV (Rosen, 1977). Research evaluating the displacement of DF-causing viruses by DHF-causing viruses, have found that Southeast Asian (SEA) virus strains grow to higher titers in mosquito midguts and SEA virus strains have a shorter extrinsic incubation period (EIP) both which explain how these virus strains are replacing less virulent strains (Anderson and Rico-Hesse, 2006; Armstrong and Rico-Hesse, 2001; Armstrong and Rico-Hesse, 2003; Cologna et al., 2005). There continue to be new cases to support the virulence theory as evidenced by the sudden occurance of DHF and DSS cases associated with new genotypes of DENV being introduced into Sri Lanka, or Central America, Peru, Mexico, Cuba, etc. (Messer et al., 2003).

Although there is much data to support both the ADE and virulence theories, there are also data that cannot be explained by the predictions of either theory alone. In the case of ADE, the prediction of higher titer viremia in secondary infections is not always correct (Rothman and Ennis, 1999). Researchers who modeled dengue outbreaks based on the assumptions of ADE or virulence found that neither theory alone predicts actual case data, and that seasonal variation in vector distribution and short-lived cross-reactive immunity better predict dengue cases (Wearing and Rohani, 2006). It seems the real mechanism of severe disease is complex and might involve both the ADE and virulence theories, as neither theory can explain every outbreak of severe disease.

Cost of dengue disease

In addition to being the primary cause of pediatric morbidity and mortality in many countries, dengue is a costly disease in terms of missed schooling and work days (Gubler, 1998). A prospective study of eight countries in South and Central America and Asia estimated the costs in 2005 US dollars to be $514 per ambulatory case and $1,394 per hospitalized case of dengue (Suaya et al., 2009). Based on this calculation, the total cost of dengue for these countries was $1.8 billion. On a global scale, the cost of dengue is several billion dollars per year. A study to determine the cost of a dengue vaccine in 1999 US dollars found that vaccination costs would be $150/1000 members of the total population but the net cost would be US $17/1000 if the savings in healthcare costs were taken into account (Shepard et al., 2004). Research leading to the reduction in the number of worldwide dengue cases will have a huge impact on the economic well-being of dengue endemic countries.

Vaccine

Currently there are no licensed dengue vaccines available. There are unique difficulties in the production of a dengue vaccine because of the concerns about antibody-dependent enhancement and increased severity of secondary infections. Immune response to heterologous dengue antigens has the potential to tilt the balance of immunity from protection to immunopathology (Huisman et al., 2009; Rothman, 2004). A successful dengue vaccine will need to meet many requirements: to produce balanced immunity to all four serotypes, to cause minimal vaccine-induced illness, to provide lifelong protection, and be economically feasible (Whitehead et al., 2007). In spite of the

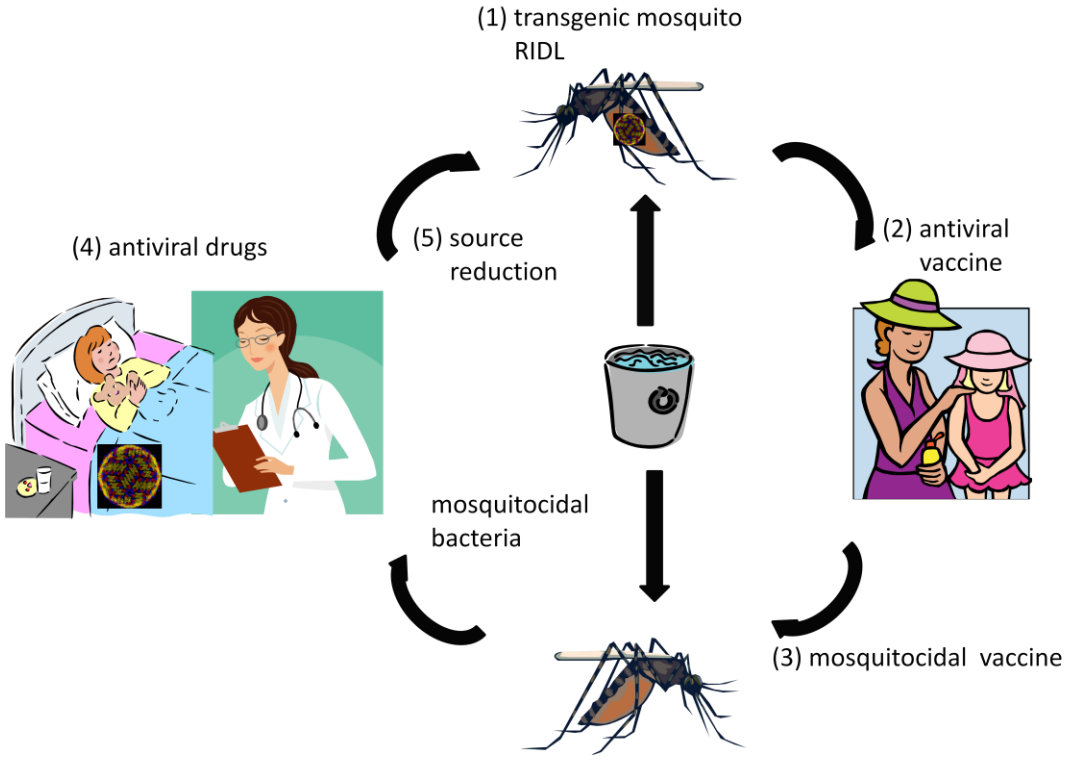

Figure 1.3 Opportunities to disrupt the dengue host-pathogen cycle. Researchers are looking to disrupt the dengue cycle at all points: **1** by preventing mosquito infection with transgenic mosquitoes or release of insects carrying a dominant lethal (RIDL), **2** preventing human infection with dengue vaccine, **3** preventing survival of bloodfed mosquitoes with mosquitocidal vaccines, **4** limiting chance of mosquito infection with antiviral drugs to decrease titer and duration of viremia and, **5** source reduction and mosquitocidal bacteria to minimize vectors.

barriers to control discussed, researchers are pursuing opportunities to disrupt the pathogen at every stage of the cycle (Figure 1.3).

Insect immunity

Insects have several layers of protection from pathogens. The first line of defense is passive, consisting of structural defenses such as the exoskeleton, chitin lining of the trachea, and peritrophic matrix to protect the midgut (Dimopoulos, 2003). The next layer of immunity is a rapid response to pathogen threats that is the insect correllary to the vertebrate innate immune system. Much of our knowledge of insect immunity is based on research on *Drosophila* innate immune response, which identified the Toll receptor and immunodeficiency (Imd) intracellular signaling pathways (Barillas-Mury et al., 2000). The Toll pathway responds to gram positive bacteria and fungi while the Imd pathway responds to gram negative bacteria.

The first step in an insect's response to a pathogen involves recognition of pathogen associated molecular patterns (PAMPs) by an insect's pathogen recognition receptor (PRR). Different pathogens have different PAMPs as in the following examples: gram negative bacteria have lipopolysaccharides, gram positive bacteria have teichoic acids, viruses have dsRNA, and yeasts have mannans. Upon recognition of a bacterial PAMP, immune organs including the fatbody, midgut, and salivary glands synthesize antimicrobial peptides. In mosquitoes, these antimicrobial peptides are defensins for gram positive bacteria and cecropins for both gram negative and positive bacteria (Levashina, 2004). In addition to the Toll and Imd pathways, insects have a melanization reponse which is mediated by phenyloxidases and occurs within the first

twenty-four hours to filarial worms and *Plasmodium* (Ho et al., 1982; Paskewitz et al., 1988; Sidjanski et al., 1997). There are variations between different insects in antimicrobial peptide concentrations, how specific proteins are used, and exactly how immune response is extended (Dong et al., 2006; Kurtz, 2004). The success of insects in exploiting a wide variety of ecological niches has been attributed to this rapid innate response (Lowenberger, 2001).

Insects have long been said to lack an acquired immune or "memory" response; however, this concept is being revisited based on evidence that the invertebrate innate response may have a type of memory (Kurtz, 2004). Research over the last decade on autophagy and RNA interference (RNAi) may now be considered to be part of the insect response to viral infection. Autophagy has recently been suggested as an antiviral mechanism in insects (Shelly et al., 2009). However, the validity of the insect-virus pairing of *Drosophila* and vescicular stomatitis virus (VSV) used to test his theory is questionable, as it is unlikely that *Drosophila* would encounter and support VSV infection in nature. The support for RNAi as an antiviral immune response is much more robust. Researchers have repeatedly demonstrated that RNAi in mosquitoes aids in virus control (Adelman et al., 2002; Campbell et al., 2008; Keene et al., 2004; Sanchez-Vargas et al., 2009)

The seeming thoroughness of insect immune response begs the question, how do pathogens survive to transmissible levels in vector insects? Malaria and, more recently, DENV researchers have suggested that there is a fine balance between host vector and pathogen, which maintains the lowest possible parasite or virus load that permits

pathogen transmission (Cirimotich et al., 2009; Dimopoulos, 2003; Myles et al., 2008; Sanchez-Vargas et al., 2009).

Host reactions to dsRNA

DsRNA can occur naturally from heterogeneous nuclear riboprotein particles (hnRNPs) which arise from aberrant bidirectional transcription and complementary transcripts in prokaryotic and eukaryotic cells (Kumar and Carmichael, 1998). However, dsRNA is typically recognized as a threat by host cells because it is associated with viral infection. Viruses that have DNA or RNA genomes both produce dsRNA during replication or expression of their genomes. There are a variety of host defense responses to dsRNA including: the interferon pathway (IFN), 2'5' oligoadenylate synthestase pathway (2'5' OAS), RNA dependent protein kinase pathway (PKR) and RNA silencing. Since we are interested in the interaction between the virus and the mosquito host, and only the RNA silencing pathway exists in mosquitoes, we will focus on RNA silencing.

History of RNA silencing

RNA silencing was first observed by researchers who overexpressed chalcone synthase (CHS), an enzyme that produces flavonoids, in an attempt to intensify the color of a petunia flower. Unexpectedly, the petunia flowers were white and the reversible phenomenon was associated with a 50-fold decrease in CHS mRNA expression by an unknown mechanism (Napoli et al., 1990). *Caenorhabditis elegans* researchers also observed anomalous results during an attempt to express RNA homologous to a *C. elegans* gene. The resulting phenotype resembled that of a null mutation (Fire et al.,

1991). More detailed experimentation revealed that this phenomenon was dsRNA-mediated, gene specific, and likely catalytic in origin because the signal seemed to amplify and the signal appeared to travel (Fire et al., 1998). Now these two phenomena, post-transcriptional gene silencing (PTGS) in plants and RNA interference in *C. elegans*, are considered to be related mechanisms that are known as RNA silencing (Ding et al., 2004).

General mechanism of RNA silencing

There is a wealth of research on RNA silencing but for the purpose of understanding the mosquito, we will focus on the si- and miRNA producing pathways. RNA silencing is triggered by double-stranded RNA (dsRNA) from sources including hairpin transcripts, virus replicative intermediates, and transposable element transcripts. DsRNA is recognized by a RNase III family protein called Dicer that contains a dsRNA binding domain (dsRBD). Dicer cleaves long dsRNA into smaller duplex RNAs known as small interfering RNAs (siRNAs). Next, Argonaute cleaves one strand of the duplex si/miRNA. The remaining strand, known as the guide strand, is incorporated into an RNA induced silencing complex (RISC) that contains both Dicer and Argonaute. The guide strand binds to messenger RNAs (mRNAs) with complementary sequence and Argonaute cleaves the transcript, leading to specific silencing (Figure 1.4).

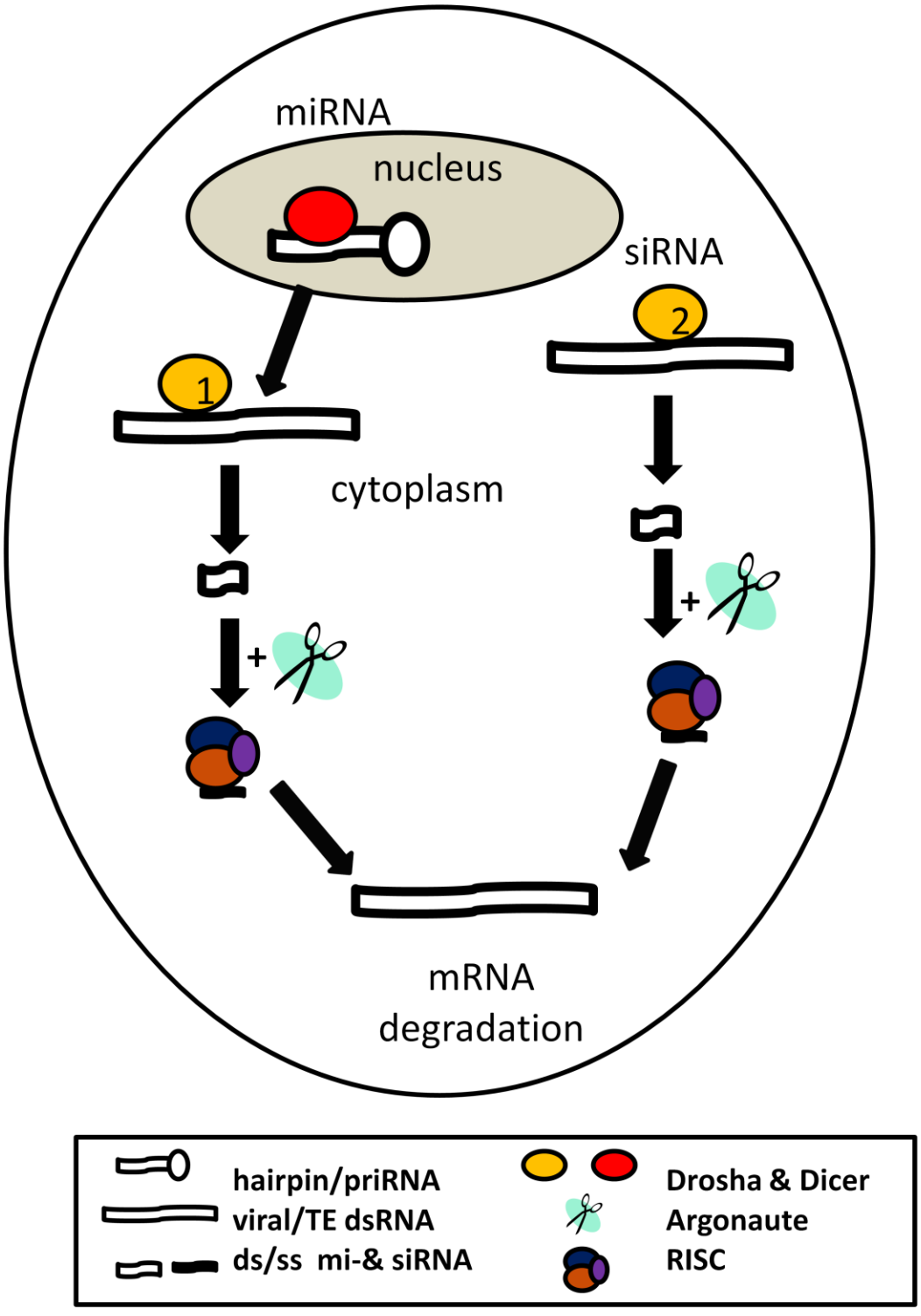

Figure 1.4 RNA silencing: **1** miRNA and **2** siRNA pathways

Details of RNA interference

RNA silencing is effective in plant, mammalian, insect, and tick cells (Garcia et al., 2006; Li and Ding, 2006). Several possible outcomes of RNA silencing in insects have been discovered in *Drosophila*: chromatin modification, mRNA cleavage and translational repression (Meister and Tuschl, 2004). However, since we are focusing on si- and miRNA pathways, we will only be discussing the mRNA cleavage outcome of RNA silencing. Dicer-1 generates miRNAs from hairpin precursor RNAs known as pri-mRNAs, and Dicer-2 generates siRNAs from long dsRNAs (Lee et al., 2004). These si- and miRNAs have characteristic ends consisting of a 5' phosphate and a 2 nucleotide 3' overhang (Elbashir et al., 2001; Nykanen et al., 2001). A protein called R2D2 guides the passage of small RNAs in combination with Dicer to RISC (Liu et al., 2003). Analysis of siRNAs in plants found siRNAs that could not be derived directly from input RNA. These secondary siRNAs also had a 5' to 3' orientation on the antisense strand suggesting that they had been primed by existing siRNAs and amplified by RdRp activity (Sijen et al., 2001). Plants possess RdRp genes but no homologous RdRp genes are found in insects. There are some data that suggest that siRNAs may be able to travel between cells in mosquito cell culture but whether this occurs in mosquito tissues is still unknown (Attarzadeh-Yazdi et al., 2009).

RNAi is an antiviral response

Dicer-2 mutant *Drosophila* have increased susceptibility to viral infection but not to bacteria or fungi, indicating that the RNAi pathway is a virus-specific mechanism

(Galiana-Arnoux et al., 2006). There is some debate as to whether RNAi also could be an antiviral response in mammalian cells (Bennasser et al., 2005; Schutz and Sarnow, 2006). It seems unlikely that the mammalian RNAi response is active against viruses naturally, as this would make the IFN response redundant, unless this is another example of redundancy in biological pathways.

There is evidence for a strand-specific bias in the RNAi response to virus infection in plants, suggesting that the major trigger for RNAi is secondary structure in ssRNA (Molnar et al., 2005; Szittya et al., 2002). However, it does not appear that this pattern of bias holds true for flaviviruses, and so far, in the case of DENV it appears that both strands are represented among siRNAs while reports on alphaviruses indicate a positive strand bias (Brackney et al., 2009; Campbell et al., 2008; Myles et al., 2008; Sanchez-Vargas et al., 2009; Scott, 2009). Recent evidence indicates that certain regions of the West Nile virus (WNV) genome that are highly targeted by the mosquito RNAi response are more likely to mutate (Brackney et al., 2009). Since the RNAi response is highly sequence specific, point mutations like those observed in the WNV study could be sufficient to evade the RNAi response.

Virus versus host: viral suppressors of RNAi

Suppressors of RNA interference or RNA silencing have been discovered for many plant and insect pathogenic viruses (Table 1.1). Many suppressors were originally identified as determinants of pathogenicity or host range (Qu and Morris, 2005). Many of the originally discovered suppressors were found in plants using *Agrobacterium tumefaciens*. Since the Agrobacterium method is rather complicated, requiring the

Table 1.1: Well-known virus-encoded suppressors of RNA silencing

Host organisms	Protein	Virus	Mechanism of suppression	References
Plant	HC-Pro	potyvirus	inhibits Dicer processing	(Yelina et al., 2002)
	2b	cucumoviruses	inhibits Ago1 cleavage	(Zhang et al., 2006)
	p19	tombusvirus	direct binding of siRNAs	(Koukiekolo et al., 2007)
	p25	potato virus X	inhibits accumulation of 24 nt RNAs	(Bayne et al., 2005)
Animal	B2	Flock House virus	prevents dsRNA processing by binding dsRNA	(Lingel et al., 2005)

creation of transgenic plants, several other methods have been developed by researchers interested in viral suppressor activity in insects (Takeda et al., 2002). *Drosophila* S2 cells can be used to evaluate suppressors by transfecting the cells with green fluorescent protein (gfp) or gfp-suppressor fusion construct. One day post transfection with gfp, dsRNA to gfp is introduced. If gfp is still expressed, the construct contains an active suppressor; if gfp is knocked down then no suppressor is present (Li et al., 2004). More recently, a tick cell assay has been developed in which tick cells are infected with a Semliki Forest virus (SFV) replicon that expresses firefly luciferase. Normally, the SFV replicon will induce RNAi because dsRNA is produced during replication (Garcia, 2005). To test potential RNAi silencers, plasmids containing potential RNAi silencers are expressed in cells infected with the SFV replicon containing luciferase, and luciferase expression level is monitored. Suppressors will cause an increase in luciferase levels by inhibiting RNAi which is triggered by the replicon (Garcia et al., 2006). In addition to the cell culture assays, a strain of *Ae. aegypti* mosquitoes has been developed that can be used to evaluate potential arbovirus suppressors of RNAi (Adelman et al., 2008).

Some suppressors of RNA interference, or silencing, have been shown to have broad activity in both plants and vertebrate animals and insects (Cirimotich et al., 2009; Li and Ding, 2006; Myles et al., 2008; Scott, 2009). Research on dsRNA binding proteins (dsRBPs) suggests that this broad spectrum suppressor activity may be a characteristic of any protein with RBP domains simply because they inhibit access to the RNA (Lichner et al., 2003). Suppressors play a crucial role in the interaction of the host immune response with viruses, shifting the balance to allow establishment of a systemic

infection (Vance and Vaucheret, 2001). When viruses lose their suppressor proteins, viral infectivity is poor (Galiana-Arnoux et al., 2006).

LaCrosse virus NSs protein has been shown to be a suppressor of RNAi in mammalian cells, but no evidence of suppressor activity was observed in mosquito cells (Blakqori et al., 2007; Soldan et al., 2005). It could be argued that arboviruses may have no need for suppressors of RNAi if their replicative intermediates are shielded from the RNAi machinery.

Other methods of evading RNAi

In addition to encoding suppressors that block steps of the RNAi pathway, RNA viruses have other methods of evading RNAi, specifically sequestering their RNA so that it is inaccessible to host anti-dsRNA responses. RNA of rabies virus and vesicular stomatitis virus (indeed, all negative strand RNA viruses) associate very tightly with their nucleoproteins during replication. Structural analysis of these nucleoprotein-RNA complexes has shown that two lobes or domains of the N protein clamp so tightly around the RNA that a conformational change in the protein would be required to gain access to the RNA (Figure 1.5) (Albertini et al., 2006; Green et al., 2006). Albertini et al. (2006) suggest that this nucleoprotein-RNA complex exists to protect viral RNA from the innate immune response in human cells. Additionally, an arbovirus with a negative-sense genome, La Crosse virus (LACV), is known to replicate in tight association with its nucleocapsid (Knipe, 2005). Researchers surveying dsRNA in virus-infected cells via immunofluorescent assay with a dsRNA antibody could not detect dsRNA in mammalian

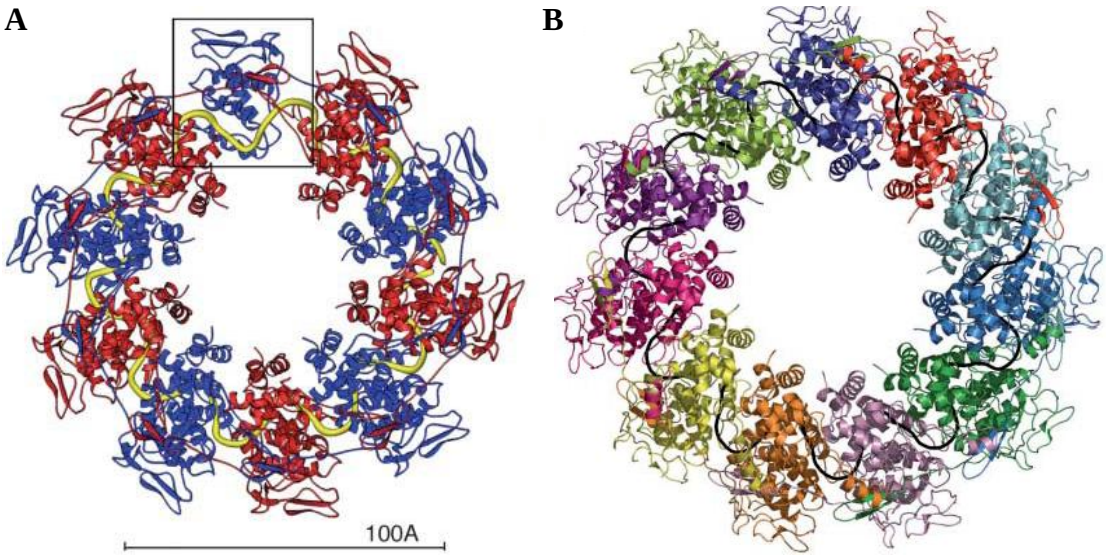

Figure 1.5 Structure of the nucleoprotein-RNA complex in **A**. vesicular stomatitus virus, RNA in yellow (Green et al., 2006) and **B**. rabies virus, RNA in black (Albertini et al., 2006)

cells actively replicating LACV; dsRNA is not produced during LACV replication (Weber et al., 2006).

During positive-sense RNA arboviral replication, dsRNA intermediates are formed that should trigger RNAi. However, in spite of the existence of a robust RNAi system in mosquitoes, arboviruses are still able to replicate to transmissible titers in mosquitoes (Sanchez-Vargas et al., 2004). Flavivirus replication complexes have been shown to be sequestered in membrane-bound compartments in mammalian cells (Uchil and Satchidanandam, 2003). Similar sequestration of dsRNA in replication compartments could potentially allow dengue virus to evade RNAi in mosquito cells.

Viral replication-associated membranes: co-opting existing cellular pathways

Viruses are completely dependent on their host cells for replication. Cells have two major directional transport pathways that involve membrane rearrangement: endocytosis to bring in required nutrients and exocytosis to remove waste materials. In addition to these methods of cellular transport, there are additional cellular processes leading to membrane rearrangement, autophagy, and the unfolded protein response (UPR) that could be the source of virus-induced membrane rearrangement (Figure 1.6). Both RNA and DNA viruses benefit from or even co-opt these existing cellular pathways to increase replication. Autophagy is a cellular process of degradation that allows cells to reallocate nutrient resources by engulfing and degrading surplus proteins or organelles during starvation or growth. Autophagy was first observed as a phenomenon occurring in rapidly growing cells (De Duve and Wattiaux, 1966). Autophagy can also be triggered by cellular stressors such as nutrient deprivation, which results in the formation of a

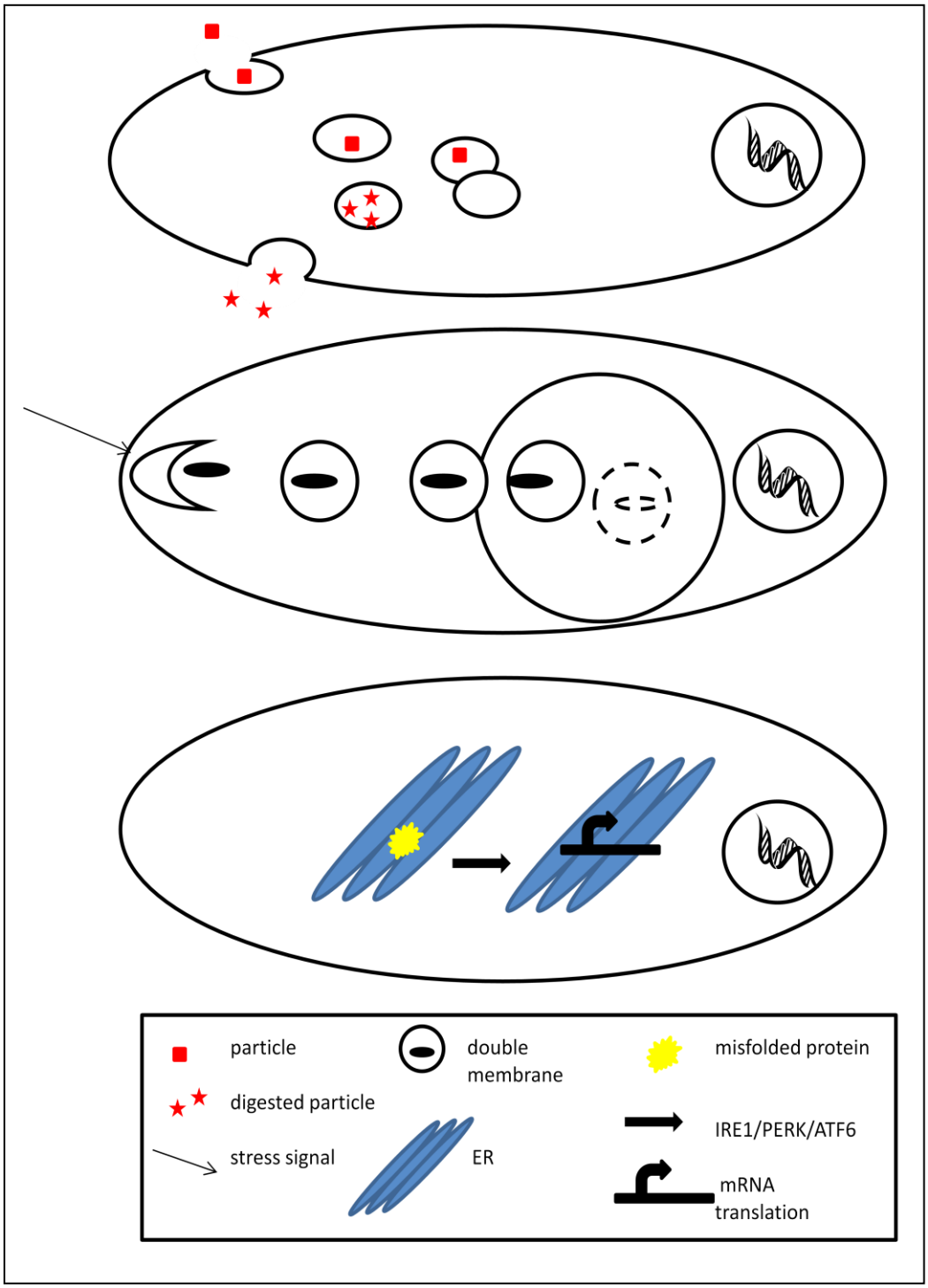

Figure 1.6 Generalized membrane-associated cellular pathways A endosome brings in particles, fuses with the lysosome, particles are digested then exocytosed **B** autophagy is induced by a stress signal inducing double membrane formation around proteins or organelles, then the double membrane vesicle fuses with lysosome **C** UPR is triggered by misfolded protein in the ER, IRE1/PERK/ATF6 inhibits mRNA translation

double-membraned vesicle of ER origin around organelles or proteins (Dunn, 1990a). This membrane fuses with the prelysosome, acidifies, and fuses with the lysosome, serving to aid cellular survival in times of stress by minimizing the number of proteins and organelles that are not in active use (Dunn, 1990b; Klionsky and Emr, 2000; Reggiori and Klionsky, 2002). The similarities between the double membrane structures observed during autophagy and the double membrane vesicles (DMVs) observed during positive RNA virus replication has led some researchers to suggest that these viral membranes arose from the autophagy pathway. Membrane-bound vesicles that arise from autophagy are typically 500-1000 nm in diameter and contain microtubule-associated protein 1 light chain 3 (LC3).

Positive sense RNA viruses, like coronaviruses and polioviruses, have been shown to induce and benefit from the cellular autophagy pathway (Jackson et al., 2005; Prentice et al., 2004). Additionally, DENV infection of mammalian cell culture has been shown to trigger the production of the double-membrane structures and rearrangement of LC3 protein that are characteristic of autophagy (Lee et al., 2008b). Recent research has shown co-localization of the LC3 marker of autophagy and dengue virus NS1 protein and dsRNA (Panyasrivanit et al., 2009). While these data are interesting, there is a discrepancy between the size of typical autophagic membrane-enclosed vesicles 500-1000 nm, and the observed diameter of dengue virus-induced vesicles of approximately 75 nm (Welsch et al., 2009). Also, the co-localization of LC3 and markers of dengue virus replication could be a correlation, not causation. Autophagy is a response to cellular stress leading to resource reallocation, so it is plausible that LC3

would localize to regions of virus replication where dengue virus is co-opting cellular resources for RNA replication (Jackson et al. 2005).

The unfolded protein response (UPR) is triggered by the defective folding of proteins, nutrient stress or pathogen infection. Once the UPR is triggered, three transmembrane signal transducers are activated: inositol-requiring enzyme 1 (IRE1) phosphorylated extracellular signaling-regulated kinase (PERK), and activating transcription factor 6 (ATF6). A signaling cascade is induced that halts translation of mRNA by inhibiting translation initiation (Malhotra and Kaufman, 2007). The UPR also controls enzyme genes that are involved in phospholipid synthesis (Federovitch et al., 2005). Phospholipid synthesis may be induced to increase the capacity of the ER, and ER proliferation has been observed in dengue virus infected cells (Niwa, 2006). DENV has been shown to induce and regulate the UPR in mammalian cells, leading to increased viral titers (Umareddy et al., 2007). Perhaps DENV uses the UPR to increase the capacity of the ER for RNA replication.

Membranes associated with viral replication

Scientists studying viral pathogenesis have long observed proliferation and rearrangement of host cellular membranes associated with viral replication. These early observations noted similarities in morphology between virus-induced membrane structures and membranes associated with natural cellular processes. Electron microscopy of SLEV-infected *Culex pipiens pipiens* showed "intravesicular cylindrical membranous structures" and proliferation of the endoplasmic reticulum but no virus associated with the Golgi (Whitfield et al., 1973). A study of virus maturation in C6/36

Aedes albopcitus cells that were infected with DENV-2 at an extremely high multiplicity of infection (MOI) of 50-60 noted membrane proliferation later followed by membrane loss (Hase et al., 1987).

These early studies noted infected cell-specific membranes that were named convoluted membranes (CMs), double membrane vesicles (DMVs), and smooth membrane structures (SMSs). Convoluted membranes are electron dense groupings of membranes, DMVs are vesicles of a variety of sizes that are enclosed by two closely associated membranes, and SMSs are proliferated membranes that do not contain ribosomes. Although membrane proliferation in association with virus replication has long been observed, the details and mechanisms of these membrane modifications are still not well understood.

Modern methods of studying viral membranes

Most of the research on intracellular processes that cause membrane rearrangement has been carried out in mammalian cells. In trying to determine what cellular pathway a virus is utilizing, it is important to note certain details, including the trigger for membrane rearrangement, the morphology, and especially the intracellular membrane from which the structure arose.

Researchers studying the mechanisms by which viruses co-opt cellular pathways have made great strides in the last ten years (Table 1.2). Recent studies of viral replication consider protein markers of cellular organelles, timing of cellular processes, and cellular membranes with similar morphologic characteristics to understand the origin of membranes associated with viral replication. To tease out these details, in addition to

Table 1.2: +RNA viral membranes in mammalian cells & their characteristics

Family	Virus	Vesicle Dia. (nm)	Membrane of origin	Mechanism of formation	References
Togaviridae	SFV	150	lysosome	interaction of nsP1 and RNA replication complex	(Kujala et al., 2001)
Coronaviridae	SARS CoV	200-300 (8 nm neck)	ER and and unidentified membrane	unknown	(Knoops et al., 2008)
Flaviviridae	KUNV YFV HCV	50-100 80-100 varies	Golgi unknown web from ER vesicles not ER	unknown unknown NS4b forms membrane web	(Mackenzie et al., 1999) (Deubel and Digoutte, 1981) (Quinkert et al., 2005) (Gouttenoire et al., 2009)
Nodaviridae	FHV	50 (10 neck)	mitochodria	viral protein A forms shell	(Kopek et al., 2007)
Arteriviridae	EAV	80 (10 neck)	ER	formed by ORF1a encoded replicase components	(Pedersen et al., 1999)
Picornaviridae	PV	70-400	lysome or rER	COPII proteins interact with 2BC	(Suhy et al., 2000) (Egger et al., 2000) (Cho et al., 1994)

Key: Dia. = Diameter, SARS CoV = severe acute respiratory syndrome coronavirus, KUNV = Kunjin virus, HCV = hepatitis C virus, EAV = equine arteritis virus, PV = poliovirus
Note: A comparison of viral vesicle sizes suggests that genome RNA must circularize during replication (Salonen et al., 2005).

electron microscopy, modern researchers studying viral replication use fluorescent microscopy with antibodies to organelle markers, confocal microscopy, and electron tomography (ET). Fluorescent microscopy can be used to locate proteins within cells by using a fluorescently labeled antibody specific for the protein of interest. In combination with other types of microscopy, proteins can be located to specific subcellular compartments (Giepmans, 2008). Fluorescent microscopy can be used to determine whether structures that arise in association with virus replication can be labeled with markers for cellular organelles. Confocal microscopy produces images consisting of light from only one plane of the sample through the use of a pinhole lens that excludes out-of-focus light. This exclusion of light from all other planes of focus results in crisply focused images with better resolution than standard fluorescent microscopy. When these high resolution images are coupled with computer software-controlled focusing, a series of optical sections can be taken by focusing through a specimen. These images can be re-built by computer software to yield three-dimensional visual data of cellular structures (Dailey et al., 1999). Confocal microscopy is useful in the study of viral replication compartments because it allows colocalization of cellular organelle markers and viral antigen or genome in three-dimensional space. Electron tomography takes a series of two-dimensional images of a specimen tilted by a one or two degree angle between images via electron microscopy. These images are weighted using computer software used to generate three-dimensional images that are 40-100 times higher resolution than confocal microscopy because electron microscopy allows for thinner slices, resulting in an average resolution of 4nm (McIntosh et al., 2005).

Arbovirus-associated membranes

Several studies on flavivirus pathology in mosquitoes and flavivirus replication in mammalian cells using fluorescent microscopy in combination with electron microscopy have provided some important insights into arbovirus replication. Ultrastructural studies of WNV replication in *Culex pipiens quinquefasciatus* using transmission electron microscopy (TEM) noted membrane proliferation in midgut tissues, midgut associated muscles, and salivary glands after infection via artificial bloodmeal (Girard et al., 2004; Girard et al., 2005; Girard et al., 2007). *Aedes albopictus* injected in the thorax with Sindbis virus (SINV) showed antigen localization in the salivary glands and midgut associated muscles as well as gross pathology in the lateral lobes of the salivary glands via fluorescent microscopy and TEM (Bowers et al., 2003). Electron microscopic *in situ* hybrization showed labeling of genomic RNA in association with SMS in the ER of mosquito cells (Grief et al., 1997).

All of these studies noted membrane rearrangement in the major tissues where arboviruses are known to replicate: the midgut and salivary gland. Membrane rearrangement occurred within known timeframes for virus replication for each virus-host pair and RNA association with novel membranes was established. All of these insights are consistent with the theory that viral RNAs are sequestered within compartments formed by novel membranes during replication of arboviral genomes.

Electron tomography: three-dimensional insights into formation of replication compartments

Electron tomography (ET) studies of SARS CoV, FHV, and DENV have confirmed stalk-like structures associated with double membrane vesicles (DMVs) that had only been noted once previously, in PV-infected cells (Knoops et al., 2008; Rust et al., 2001; Welsch et al., 2009). These stalk-like structures were designated "necks" or "collars." The necks are 8-10 nm in diameter and suggest that the replication compartments are not completely isolated from the rest of the cell. In the case of DENV and PV, the necks provide a connection between the viral replication compartments and the cytoplasm, allowing import of materials needed for viral replication and possibly export of RNA. In the case of SARS CoV, it appears that these structures do not allow access to the cytoplasm, but this could be an artifact of the fixation. In fact, Welsch et al. (2009) noted that the necks were visible in some of their dengue virus samples but not in others, depending on fixation method. Also, Welsch and colleagues' ET study of DENV replication in mammalian cells demonstrated the CM, ER, and the outer membrane of the DMVs.

Models of virus–induced membrane rearrangement

There are many theories as to how viral replication membranes may be formed, and these theories seem to be influenced by observations based on the model system the researcher studies. Flavivirus researchers hypothesize that viral proteins cause rearrangement of host membranes based on structural and functional properties of the viral proteins. A conical shaped viral protein can cause membrane bending around the

protein, while viral proteins that contain amphipathic helixes or are able oligmerize may pull membranes together, forming a curved structure (Miller and Krijnse-Locker, 2008). Arterivirus researchers suggest that double membrane structures are formed by budding through two tightly associated membranes; into the ER and again to exit the ER (Pedersen et al., 1999). Poliovirus researchers suggest that viruses co-opt either anterograde or retrograde vesicle pathways (Rust et al., 2001).

Which viral proteins induce membrane rearrangement?

In an effort to discover the mechanism of viral-induced membrane rearrangement, many researchers studying replication compartments have attempted to reproduce the membrane structures by expression of individual viral proteins. Hepatitis C virus researchers have shown that expression of nonstructural protein 4b (NS4b) is sufficient to reproduce the membranous web that is characteristic of HCV replication (Gouttenoire et al., 2009). Expression of DENV NS3 was shown to cause membrane rearrangement, but the pattern was not consistent with the membrane rearrangement observed in a typical infection via fluorescent microscopy (Chua et al., 2004). Expression of DENV NS4b in mammalian cells was more successful, recreating membrane rearrangement characteristic of DENV infection as observed via electron microscopy (Miller et al., 2007). The flaviviral NS4a and NS4b nonstructural proteins are transmembrane proteins that cross the membranes they interact with multiple times, which is consistent with the theory that membrane rearrangement is caused by membrane-bending amphipathic helices.

What is the purpose of viral-induced membranes?

A variety of purposes for membrane proliferation have been suggested: to concentrate materials and coordinate replication to increase replication efficiency, to provide structural support for replication, to provide lipids necessary for replication, and to prevent host reaction to viral replication (Knoops et al., 2008; Lyle et al., 2002; Miller and Krijnse-Locker, 2008; Salonen et al., 2005). In mosquitoes, viral replication within membrane-bounded structures could protect dsRNA from RNAi.

Transgenic mosquitoes: a history

Development of genetically modified or transgenic insects that are resistant to disease has been a scientific goal for many years. The first transgenic insect was developed in 1982 (Rubin & Spradling, 1982). This original transgenic insect was a strain of *Drosophila* that was transformed with P transposable element and had a transformation success rate of 20-50%. There were many early problems with production of transgenic insects: remobilization of transposable elements, lack of control over insertion location, and lack of specific promoters. The remobilization problem was solved by careful selection of transposable element for minimal remobilization and molecular manipulation of the element to separate the transposase from the insert (O'Brochta et al., 2003; Sethuraman et al., 2007; Wilson et al., 2003). Additionally, the transposon-based development of transgenic mosquitoes may be a cause for concern since RNAi has been shown to naturally silence transposons in the germline (Sijen and Plasterk, 2003). Precise insertion of transgenes is still difficult but the phi C31 and

CRE/lox systems show promise (Nimmo et al., 2006). In addition, many specific promoters have been identified for use in mosquito systems (Olson et al., 2002).

How to engineer a transgenic mosquito

In the last ten years, technology for developing transgenic insects has matured greatly, and several transgenic mosquito lines have been created. After careful selection of transposable element, promoter, and effector gene, the basic method for creation of transgenic mosquitoes begins with microinjection of preblastoderm embryos, collection of individuals expressing a reporter gene, creation of single female families that are backcrossed with a genetic background strain, and screening for the desired phenotype or genotype (Jasinskiene et al., 1998).

Engineering resistance: transgenic mosquitoes with enhanced immunity

As a proof of principle, the first transgenic *Aedes* mosquito was developed in 1998, a white-eyed *Aedes aegypti* line transformed with *Hermes* to express the cinnabar eye gene, thus restoring a wildtype eye phenotype (Jasinskiene et al., 1998). Two years later another transgenic *Ae. aegypti* strain was developed, this mosquito expressed the immune gene Defensin under the control of a vitellogenin promoter, rendering it resistant to bacterial infection (Kokoza et al., 2000). During the next few years, RNAi was used both to study immunity via knockdown in a mosquito and enhance virus resistance in mosquito cells (Adelman et al., 2002; Levashina et al., 2001). In 2002, another transgenic mosquito strain was reported, an *Anopheles stephensi* strain expressing SM1, an antiparasitic gene under a carboxypeptidase promoter that rendered it resistant to

Plasmodium parasite infection (Ito et al., 2002). In addition to these insects engineered to increase pathogen resistance, there have been several reports of insects that have natural integration of viral sequences into their genome, which may lead to virus resistance (Crochu et al., 2004; Maori et al., 2007).

Transgenic mosquitoes with enhanced RNAi

Since RNAi has been successfully used to create viral resistance in transformed mosquito cells and RNAi affects viral titers in mosquitoes, the next step was to create transgenic mosquitoes that are pathogen resistant due to RNAi (Adelman et al., 2002; Keene et al., 2004). Transgenic mosquitoes, known as the Carb77 strain, were transformed to express hairpin RNA containing DENV sequences that enhance the natural antiviral RNAi response (Franz et al., 2006). Carb77 mosquitoes express a virus-specific dsRNA when the mosquito under control of a carboxypeptidase promoter after an infectious bloodmeal and the virus is at the beginning of replication and therefore most vulnerable (Franz et al., 2006). With few individual exceptions, these Carb77 mosquitoes are resistant to infection with DENV-2 via an RNAi-mediated mechanism.

Prospects for use of transgenic mosquitoes

Although transgenic mosquitoes are promising in the laboratory, there are many hurdles to overcome before transgenic mosquito strains could be released in the wild. Two major concerns for viability of transgenic mosquitoes in the wild are fitness and gene drive. Fitness is defined as the success of a genotype in promoting its genes into the next generation (Marrelli et al., 2006). Testing of transgenic mosquito strains

transformed with *hermes* or *Mos* TEs to express eGFP showed reduced fitness relative to laboratory stains. Specifically, fitness evaluation of the transgenic strains revealed fecundity, increased sterility, and sex ratio distortion in the *Mos* strain (Irvin et al., 2004).

Modeling predicts that transgenic mosquitoes require either a very minimal fitness load or strong genetic drive to be competitive in natural populations (Lambrechts et al., 2008). Cage experiments involving crosses of transgenic mosquitoes with wildtype mosquitoes confirm the requirement for a driver and emphasize the importance of outbreeding of transgenic lines to increase fitness (Catteruccia et al., 2003; Li et al., 2008a). With the possible exception of *Plasmodium* resistant mosquitoes, which have a distinct loss of fitness when infected with *Plasmodium* so the transgene is highly beneficial, a strong genetic drive mechanism will be required for the success of transgenic mosquitoes in the wild (Marrelli et al., 2007).

The most promising or strong genetic drive mechanisms are maternal effect selfish genetic elements, transposable elements, and *Wolbachia*. All of these genetic drive mechanisms have been shown to move though insect populations extremely rapidly by giving their carriers a distinct advantage during breeding. Maternal effect genetic elements, like Medea, are strong enough to cause population replacement in *Drosophila* (Chen et al., 2007). Medea is a selfish genetic element that kills offspring that do not inherit the element. Some transposable elements, like P elements, are promising genetic drive mechanisms because of their ability to overcome large geographic barriers and reach isolated populations (Silva and Kidwell, 2004). P elements spread by causing mating incompatibilities, so viable offspring only result from matings that produce offspring carrying the P element. P elements have been shown to spread rapidly through

populations of *Drosophila*. *Wolbachia* bacterial infection shows promise as a genetic drive mechanism because it reaches fixation at very high levels fairly quickly in populations of mosquitoes (Rasgon and Scott, 2003). However, there are technical difficulties coupling *Wolbachia* drive to a transgene. These strong genetic drive elements, if they can be successfully adapted to mosquito systems, seem to be the key to successful population replacement by transgenic mosquitoes in the future.

Can pathogens develop resistance to transgenic mosquitoes?

The development of resistance by the pathogen is a concern for all methods of controlling vector-borne diseases. Naturally occurring resistance develops when selective pressure acts on pre-existing phenotypic variants, selecting the variant that has greater fitness under the new conditions. There is a risk that pathogen resistance will develop more rapidly when under selection pressure in transgenic insects with enhanced immune systems. In the case of malaria parasite- and virus-resistant mosquitoes, antigenic variance is inherent in the pathogen's development. *Plasmodium*, the pathogen that causes malaria, naturally undergoes antigenic variation; moreover, this can lead to rapid development of drug resistance (Dzikowski and Deitsch, 2009; Khatoon et al., 2009). In the case of RNA viruses, the error rate of the RdRp is naturally 10^{-3} per nucleotide per round of replication, which for DENV means at least one mutation per replication cycle (Domingo and Holland, 1997).

RNA viruses exist in a quasispecies state or a distribution of non-identical but closely related genomes (Domingo, 2002). Theoretically, an RNAi-based transgenic mosquito could lead to selection for a resistant arbovirus. La Crosse virus researchers

have reported development of viruses resistant to siRNA treatment after 72 hours in cell culture (Soldan et al., 2005). There is also evidence for increased mutation rates in viral sequences that are RNAi "hotspots" (Brackney et al., 2009).

Summary and hypotheses

Previous research has shown that DENV replication occurs in membrane-bound compartments in mammalian cells. Isolation and characterization of these membrane-bound vesicles has shown that these replication compartments have a double-membrane morphology and are tightly sealed enough that they should exclude effector proteins produced by the host immune response (Uchil and Satchidanandam, 2003; Welsch et al., 2009). RNAi is known to be active in mosquito cell culture and mosquito tissues and likely plays a role in modulating the balance between viral replication and mosquito health (Sanchez-Vargas et al., 2009). If membrane-bound compartments of similar morphology are created during DENV replication in mosquitoes, these membranes may prevent Dicer from accessing the replicative intermediate (Figure 1.2). The existence of membrane-bound replication in mosquito cells could explain how DENV evades the mosquito RNAi response to replicate successfully.

We hypothesized that DENV replication in mosquito cells occurs within membrane-bound vesicles with many of the same characteristics of DENV-associated vesicles observed in mammalian cells: originate from the ER, are double-membrane bound, contain DENV dsRNA, and are induced by the expression of DENV NS4a-2k. We also hypothesized that the morphology of these membranes should prevent Dicer from accessing replicative intermediates, allowing DENV-2 to escape RNAi in the

mosquito. Finally, we hypothesized that DENV-2 would mutate to evade the complementary base-pairing required for RNAi in transgenic mosquitoes designed to target DENV-2 immediately after entry to the cell prior to formation of replication vesicles.

The work discussed in the following chapters set out to localize and characterize the association between viral double-stranded RNA and membranes in mosquito cells and tissues. In addition to this goal, we attempted to determine whether the dengue NS4a and NS4b proteins played any role in the formation of the replication-associated membranes. Also, viruses that successfully replicated to high titers in transgenic mosquitoes with an enhanced RNAi response were characterized to determine whether mutation of the targeted viral sequence could be another mechanism that allows DENV to evade the RNAi response.

We found DENV dsRNA to be initially localized in punctuate perinuclear patterns then spread throughout each mosquito cell. DsRNA was observed in close association with viral envelope and capsid proteins in both mosquito cells and midgut tissues. Isolation and microscopic examination of membrane fractions from DENV-infected cells and midguts revealed double-membrane structures with similar size and other characteristics to those isolated from mammalian cells. The attempt to induce membrane rearrangement via expression of DENV NS4a and NS4b proteins was largely unsuccessful. Characterization of DENV isolates that escaped the enhanced RNAi response of transgenic mosquitoes revealed no mutations within the targeted viral sequence that could account for RNAi escape or mutations in other regions of the genome associated with enhanced replication phenotypes. Overall, this work suggests that there

may be a point in the dengue viral life cycle where the replication complex of viral RNA is protected from the mosquitoes' RNA interference pathway.

Chapter 2

Evaluation of dengue virus replication-associated membranes in mosquito cell culture

Introduction

Rearrangement and proliferation of intracellular membranes has long been observed in association with flavivirus replication, as discussed in Chapter 1. Replicative forms of viral RNA have been isolated from these membranes (Mackenzie et al., 1999; Uchil and Satchidanandam, 2003). Most of our knowledge of flavivirus replication-associated membranes has been gathered from experiments in mammalian cells. In addition to the primary purpose of concentrating replication components to increase replication efficiency, many researchers have speculated that replication of viruses within membrane-enclosed compartments may serve to protect the viral genome from detection by the host immune response. Endoplasmic reticulum-derived double-membrane bound vesicles that could serve this purpose have been described in association with flavivirus replication in mammalian cells (Uchil and Satchidanandam, 2003). The hypothesis examined in this chapter is that, as in mammalian cells, DENV replicates in association with membranes in mosquito cells and these membranes are derived from endoplasmic reticulum (ER).

If this hypothesis is correct, double-stranded RNA (dsRNA) should be detected in sites of DENV replication, specifically in association with the ER. An additional hypothesis tested in this chapter is that the morphology of these vesicles should be similar to the double-membrane vesicles isolated from mammalian cells. If the vesicles are indeed of ER origin, then viral dsRNA should co-localize with ER markers.

DsRNA has been detected via immunofluorescent assay (IFA) with a highly specific dsRNA antibody in mammalian cells infected with a wide variety of positive

sense RNA and DNA genome viruses but not from cells infected with negative strand RNA viruses such as La Crosse and influenza viruses (Schonborn et al., 1991; Weber et al., 2006). Electron microscopic studies of DENV replication in mammalian cells have shown that genomic RNA localizes to proliferated membranes of ER origin and that replicating RNA can be isolated from vesicles 75-100 nm in diameter that are resistant to a non-ionic detergent (Grief et al., 1997; Uchil and Satchidanandam, 2003). An electron tomographic (ET) study reconstructed three-dimensional images of DENV replication in mammalian cells, which revealed that the several types of proliferated membranes, smooth membrane structures (SMSs), double membrane vesicles (DMVs) and convoluted membranes (CMs), are interconnected and serve as sites of RNA replication and viral assembly (Welsch et al., 2009). Additionally, this study provided precise measurements of the DMVs as 87.5 nm in diameter with an 11.2 nm pore and noted that the vesicles showed correlation with ER markers and no observed colocalization with markers of autophagy.

Previous research in this laboratory has shown that RNA interference (RNAi) is an active antiviral response in mosquito cells and tissues (Adelman et al., 2002; Keene et al., 2004; Sanchez-Vargas et al., 2004). In addition to this evidence that RNAi is active in mosquitoes, these data suggest that there is a fine balance between DENV replication and the mosquito's RNAi-based immune response (Sanchez-Vargas et al., 2009). These results are consistent with the hypothesis that replication within membranes may play a role in protecting viral genomes from detection by the host immune response. In the case of DENV in mosquitoes, replication within membranes should protect the dsRNA replicative intermediates from RNAi.

To test the hypotheses outlined here, the localization of dsRNA associated with DENV replication was characterized via immunofluorescent assay. DENV-specific RNA and virions were isolated from fractionated mosquito cells and characterized via reverse-transcription polymerase chain reaction (RT-PCR), strand-specific northern blots, and infectivity assays. Co-localization of dsRNA with antigenic markers of mature DENV and ER markers was examined via immunofluorescent microscopy and confocal microscopy. Additionally, DENV-associated dsRNA localization in mosquito cells was compared to alphavirus and bunyavirus replication associated dsRNA. Also, isolated fractions of detergent-treated mosquito cells infected with DENV were examined via transmission electron microscopy to verify the presence of vesicles associated with DENV replication.

The experiments discussed here were designed to establish a link between DENV replication within vesicles and the exclusion of the mosquito RNAi response. The data presented here established a link between DENV replication and production of DMVs. Exclusion of DENV-specific dsRNA from the mosquito RNAi response was not clearly established but based on similarities in size and morphology between vesicles isolated from mosquito and mammalian cells, we can speculate that if the vesicle pore size is consistent between mammalian and mosquito cells, the pore size might exclude Dicer from accessing the DENV dsRNA replicative intermediates.

Materials and Methods

Cell culture lines

C6/36 (*Aedes albopictus*) cells were obtained from the American Type Culture Collection (ATCC, Manassas, VA). C6/36 cells were grown in Leibowitz 15 (L-15) medium supplemented with 10% heat-inactivated fetal bovine serum (FBS), 100 U/mL penicillin, 100 U/mL streptomycin, and 0.2 mM L-glutamine (growth medium) at 28°C.

Aag2 (*Aedes aegypti*) cells were a gift from Dr. Alexander Raihkel at University of California, Riverside. Aag2 cells were grown in Schneider's medium supplemented with 10% heat-inactivated FBS, 100 U/mL penicillin, 100 U/mL streptomycin, and 0.2 mM L-glutamine at 28°C.

FB9.1 (*Aedes albopictus*) cells are a clonally selected cell line made by Dr. Zach Adelman from C6/36 cells by transformation with a plasmid to express an inverted repeat RNA derived from the DENV-2 genome under the control of the baculovirus *Immediate early 1* (Ie1) promoter and selected by expression of a hygromycin B resistance gene (Adelman et al., 2002; Gaines et al., 1996). The inverted repeat sequence in FB9.1 cells is derived from Mnp, a non-translatable prM gene from DENV-2 (New Guinea C) RNA (Gaines et al., 1996). When this inverted repeat sequence is transcribed, it produces a 290 bp hairpin RNA that can trigger RNAi. H9.1 cells were transformed with the same plasmid lacking the DENV-2 RNA sequence. To maintain the expression of the plasmid, these cell lines were grown at 28°C with L-15 medium with 10% FBS supplemented as above with the addition of 300 U/mL hygromycin B (Calbiochem, EMD Biosciences, Inc., San Diego, CA) and changed every 3 days. The particular FB9.1 and H9.1 cell lines

used in these experiments were obtained from frozen cell culture stocks made by Dr. Emily Travanty.

Viruses

All virus stocks were obtained from the AIDL core support program with the exception of the La Crosse virus (LACV) prototype strain. All titrations were performed via the AIDL core support program using the protocol described in Chapter 5 except that plaques were counted instead of picked at the end.

DENV-2 For preparation of working virus stocks, 4 mL of DENV-2 strain Jamaica 1409 (JAM1409) (Genbank #M20558) were inoculated onto subconfluent C6/36 cells in a 75 cm^2 tissue culture flask at a multiplicity of infection (MOI) of 0.01 and rocked at room temperature for 1 hr before adding 20 mL of medium. Infected C6/36 cells were maintained in L-15 medium supplemented with 2% FBS, 100 U/mL penicillin, 100 U/mL streptomycin, 1x MEM non-essential amino acids, and 0.2 mM L-glutamine (maintenance medium) at 28°C for a total of 14 days with a medium change at 7 days post-infection (dpi). At the end of the 14 day incubation, virus was harvested by using a cell scraper to detach cells, then cells and virus were resuspended and divided into 0.5 mL aliquots and stored at -80°C.

For immunofluorescent assay (IFA) experiments, DENV-2 was inoculated onto subconfluent C6/36 cells grown on 18 mm, No.1, sterile glass coverslips in 12-well tissue culture plates, at an MOI of 0.1. Infected C6/36 cells were maintained in L-15 maintenance medium at 28°C for a total of 14 days with a medium change at 7 dpi. For

cellular fractionation experiments, DENV-2 was inoculated into C6/36 cells grown in a 75 cm^2 tissue culture at an MOI of 0.1 and used for experiments at 5 dpi.

Sindbis viruses MRE16 (Klimstra et al., 1998; McKnight et al., 1996) and TE3'2J (Hahn et al., 1992; Lustig et al., 1988) stocks were prepared as follows. Two milliliters of Sindbis virus (SINV) were inoculated onto C6/36 cells in 75 cm^2 tissue culture flasks at an MOI of 0.01 and rocked at room temperature for 1 hr before adding 10 mL of medium. Infected C6/36 cells were maintained in L-15 maintenance medium and virus was harvested at 4 days. Cells were detached from tissue culture flasks using a cell scraper, then cells and virus were resuspended and divided into 0.5 mL aliquots and stored at -80°C.

For IFA, SINV was inoculated onto C6/36 cells at an MOI of 0.01. Infected C6/36 cells were maintained in L-15 maintenance medium for a total of 4 days.

LACV Prototype strain was obtained from Dr. Mark Hughes (AIDL, Colorado State University). For IFA, LACV was inoculated onto C6/36 cells at an MOI of 1.0. Infected C6/36 cells were maintained in L-15 maintenance medium for a total of 4 days.

Cellular fractionation

Sucrose solutions Sucrose solutions were made as described by Uchil et al. (2003, 2006) with sucrose dissolved in a buffer consisting of 10 mM Tris (pH 8.8), 10 mM sodium acetate, and 1.5 mM magnesium chloride in distilled water called TNMg. Solutions contained 75%, 55%, and 5% sucrose by weight, which are equivalent to 8.7 M, 3.6 M, and 153 mM concentrations respectively. A 75% sucrose solution was substituted for the

80% sucrose solution used by Uchil et al. (2003), which repeatedly precipitated out of solution in Colorado.

Isolation of vesicles Viral replication-associated vesicles were isolated based on the technique used by Uchil et al. (2003) with mammalian cells. C6/36 cells were infected with DENV-2 (JAM1409) at an MOI of 0.1. Infection was verified via IFA with 3H5-21 monoclonal antibody at 4 dpi by a method described in more detail later in the chapter (page 54). Infected cells were harvested by centrifugation (2500 rpm, 5 min) at 5 dpi. The pellet was incubated in 1% Triton X100 (TX100) on ice for 1 hr to disrupt cellular plasma membranes, then the heavy membrane fraction (S16) was sedimented at 16,000 x g, 15 min. A discontinuous sucrose gradient was prepared in 14 x 89 mm polyallomer ultracentrifuge tubes (Beckman Coulter, Fullerton, CA) as follows: 0.5 mL 75% sucrose, followed by a layer consisting of the S16 pellet resuspended in 0.5 mL TNMg and mixed with 4 mL 75% sucrose, followed by 4 mL 55% sucrose, and topped with 0.5 mL 5% sucrose. The S16 fraction was separated by sucrose density gradient centrifugation in a Beckman L8-80 model ultracentrifuge (18 hr, 35,000 rpm, 4°C). Ten 1 mL fractions were collected from the top of the gradient with the top fraction designated 1, etc.

This cellular fractionation method uses sucrose gradient centrifugation to separate subcellular components based on buoyant density. More buoyant subcellular components rise to the top of the gradient while dense components sink lower within the gradient.

Localization of virions To determine location of non-ionic detergent-resistant (TX100) membranes and virions within the sucrose gradient fractions, the medium from pelleted infected cells was loaded onto separate tubes of the discontinuous sucrose gradient and

treated as described for cell fractionation. Fractions were collected, washed and analyzed as described for vesicles.

Washing and concentrating fractions Sucrose was washed out of all fractions by resuspending each 1 mL fraction in 50 mL ice cold RNase-free PBS (Ambion, Austin, TX) and centrifuging for 30 min, 30,000 rpm, 4˚C to concentrate samples before further analysis via RT-PCR, strand specific northern blot, and infectivity assay.

Characterizing RNA in gradient fractions

RNA extraction All solutions were obtained from Amresco (ISC Bioexpress, Kaysville, UT) except the RNase-free phosphate buffered saline (PBS), which was obtained from Ambion as a 25x solution and diluted in nuclease-free water.

Concentrated fractions obtained from cell fractionation gradients were analyzed for presence of DENV-2 RNA. Fractions were resuspended in 0.5 mL RNase-free PBS and extracted once using saturated 5:1 phenol-chloroform, once with 24:1 chloroform-isoamyl alcohol followed by precipitation in one-tenth volume of 5 M ammonium acetate and two volumes 100% ethanol. RNA pellets were washed once in 70% ethanol and air dried. Pellets were resuspended in nuclease-free water.

RT-PCR Viral RNA was detected via RT-PCR using the SuperScript III One-Step RT-PCR System with Platinum Taq kit (Invitrogen, Carlsbad, CA) using the following primers to amplify DENV-2 NS1 cDNA: 5'GATAGTGGTTGCGTTGTGAG3' and 5'TCCAAGCTCTGTTTGTGTTG3'. The RT-PCR conditions were: 60°C 30 min, 94°C 2 min, 40 cycles of 94°C 15 sec, 60°C 30 sec, and 68°C 30 sec, followed by a final incubation of 68°C 5 min. Each sample had a PCR control, in which the RT enzyme was

omitted from the reaction to verify that amplification was occurring from RNA template during the RT step instead of from possibly contaminating cDNA in the PCR step. Amplification product size of 500 base pairs was verified via gel electrophoresis.

Strand-specific northern blot Gradient fractions from four cellular fractionation experiments were pooled and stored at -80°C were combined and washed. RNA was extracted as described above.

RNA probe preparation

Briefly, probe preparation involved three amplification steps: RT-PCR to generate a 500 bp cDNA template from the DENV-2 NS3, followed by a separate PCR reaction which amplified a 200 bp product and added a T7 promoter, and T7-specific transcription to generate a labeled RNA probe. The second PCR reaction added strand-specfic T7 promoters to the transcription templates. One PCR reaction added a 5' T7 promoter to the genome sense strand and a separate reaction added a 5' T7 promoter to the anti-genome sense strand.

RNA was extracted from 2 (0.5 mL) aliquots of DENV-2 JAM1409 stock (approximately 10^6 pfu/mL) with phenol-chloroform as described above. A 50 µL RT-PCR to amplify the region of the DENV-2 NS3 gene was performed with the SuperScript III One Tube RT-PCR with Platinum Taq kit (Invitrogen). The RT-PCR program to prepare the cDNA template consisted of one RT reaction at 50°C 30 min, followed by denaturation at 94°C 2 min, and 40 PCR cycles of 94°C 15 sec, 55°C 30 sec, 68°C 30 sec, and a final incubation at 72°C 10 min. Product size was verified to be 500 bp via gel electrophoresis and cDNA concentration determined via absorbance at 260 nm. The cDNA product was further amplified and T7 promoter sequences added at the 5' end of

each to create transcription templates using the following primer pairs: KP13 5’ TAATACGACTCACTATAGGGCACAAGAAAGCCACCTACGAGAC3’ and KP 14 5'CTGTGTCACCATAGGGACGACGTC3' for anti-genome sense probe to detect genome sense strand RNA, KP 15 5'TAATACGACTCACTATAGGGCTGTGTCA CCATAGGGACGACGTC3' and KP 16 5'CACAAGAAAGCCACCTACGAGAC3' for a genome sense probe to detect anti-genome sense strand. PCR conditions were: 1.5 mM $MgSO_4$, 0.8 mM dNTPs, 10x PCR buffer at a final concentration of 1x, 2 µL of the cDNA from the RT-PCR reaction, 0.2 µM forward primer, 0.2 µM reverse primer, 1 unit Platinum Taq, nuclease-free water (Invitrogen) to 100 µL. PCR amplification was carried out under the following parameters: 94°C 2 min; 35 cycles, 94°C 30 sec, 50°C 30 sec, 68°C 1 min, followed by a final incubation of 68°C 10 min. Product size was verified to be 200 bp via gel electrophoresis and DNA concentration determined via absorbance at 260 nm.

Transcription of the strand specific northern blot probes used Megascript T7 High Yield Transcription Kit. Following the directions in the kit, a 20 µL reaction, using biotin-labeled UTP to give 9% of total UTP and 1 µg template cDNA, was incubated overnight at 37°C. The transcription product was treated with the provided DNase as instructed in the kit to remove template DNA and purified by phenol-chloroform extraction followed by isopropanol precipitation at -20°C for 15 min. Transcription product was collected by centrifugation for 15 min at 14,000 rpm at 4°C, and resuspended in nuclease-free water, aliquoted and stored at -80°C. Biotin labeling of probe was verified by pipetting 1 and 2 µL drops of the transcription product onto blot paper, cross-linking by UV irradiation twice, then detecting as directed with the

BrightStar Biodetect Nonisotopic Detection kit (Ambion). Blot was exposed to Blue Lite Autoradiography film (ISC Bioexpress) until labeling could be detected.

Gel electrophoresis, blotting, and detection of RNA

Gel electrophoresis materials including sample buffer, gels, and loading buffer were obtained from Invitrogen. Each fraction was run in duplicate on identical gels. RNA extracted from gradient fractions were resuspended in 10 µL nuclease free water, split in half, and then mixed with 2x Novex TBE-UREA sample buffer to 1x. Each fraction was loaded onto one well of a 12-well Novex 6% TBE-UREA polyacrylamide gel in 1x Novex TBE running buffer, which had been pre-run for 3 min at 180 V and urea flushed from wells with running buffer. Gel electrophoresis was run at a constant 180 V for 90 min.

RNA was transferred from gel to Brightstar Plus positively charged membrane (Ambion) via electroblotting at a constant 30 V for 1 hr. RNA was cross-linked to the membrane by 2x treatment with a UV Stratalinker (Stratagene, La Jolla, CA). Blot was pre-hybridized for 30 min in 0.7 mL/cm^2 UltraHYB (Ambion) at 68°C in a rotating hybridization oven. Probe was added at a concentration of 10 ng/mL directly to the pre-hybridized blot. Blots were hybridized overnight. Biotinylated probe hybridized to blots was detected as directed using the BrightStar Biodetect Nonisotopic Detection kit (Ambion). The blot was then exposed to X-ray film as described above.

Infectivity assay

Fractions obtained from sucrose gradient centrifugation were resuspended in 0.2 mL RNase free PBS (Ambion) and transferred to microcentrifuge tubes.

Concentrated fractions plus 1 mL of L-15 maintenance medium were filtered using 0.2 μm Acrodisc syringe filters (Pall, Port Washington, NY) and placed into sterile microcentrifuge tubes. Filtrate from each fraction diluted in 1 mL medium was inoculated onto one well of a 12-well plate of subconfluent C6/36 cells grown on circular glass coverslips. Cells were maintained to support possible virus growth for 14 days with a change of medium at 7 days. Cells were fixed at 14 days in cold acetone and processed for IFA.

Immunofluorescent assay IFAs for DENV envelope (E) antigen were performed with monoclonal antibody 3H5-21 (1:400) as the primary antibody (1 hr), biotinylated sheep anti-mouse IgG (1:400) as secondary (1 hr), and finally with strepavidin-fluorescein and Evan's blue (1:400) counterstain (30 min). Coverslips were washed three times following each incubation in PBS. After the final incubation with strepavidin-fluorescein and Evan's blue, coverslips were washed with distilled water and mounted on glass slides in Vectashield with 4',6-diamidino-2-phenylindole (DAPI) (VWR) and scored as positive or negative by observation with a Leica DM4500B fluorescent microscope.

Dicer exclusion trial

To determine whether dsRNA in cell fractions was susceptible to Dicer cleavage, sucrose gradient samples were prepared and washed as described above. Samples were tested for access of Dicer to RNA using the Recombinant Human Dicer Enzyme Kit (Genlantis, San Diego, CA). Ten microliter enzymatic reactions containing 1 unit of recombinant Dicer enzyme were set up for each fraction and incubated for 18 hr at 37°C. Controls included extracted genomic DENV-2 RNA in buffer without enzyme and

genomic RNA with enzyme. RNA was extracted from samples at the end of 18 hr using the phenol-chloroform method described previously. RNA was detected via RT-PCR with the Superscript III kit as previously described. RT-PCR products were analyzed by gel electrophoresis.

Optimization of antibodies

All antibodies used for single and double-staining experiments were optimized to minimize non-specific background staining prior to usage in experiments. Typical samples used for optimization consisted of DENV-2, SINV, or LACV-infected C6/36 cells, as described previously. Antibodies were initially tested at the dilution recommended by the manufacturer and two additional 10-fold dilutions, one more concentrated and one less concentrated than recommended. Optimal staining dilution was defined as the dilution that showed the expected staining pattern described by the manufacturer with little to no background in experimental samples or non-specific staining in negative controls.

If needed, antibody optimization was repeated an additional two times, with new dilutions being tested each time based on the most promising staining from the previous test as a starting dilution. If the results of a third test were non-optimal but promising, additional optimization was initiated. ER tracker red (Molecular Probes, Carlsbad, CA), anti- *Drosophila* calnexin antibody (Abcam, Cambridge, MA), and J2 anti-dsRNA and 3H5-21 anti-flavivirus E protein labeled with a rhodamine labeling kit (Pierce, Rockford, IL), were not used experimentally because staining could not be optimized.

ER marker testing was also done using Aag2 cells and C6/36 cells treated with (4-2-hydroxyethyl)-1-piperazineethanesulfonic acid (HEPES) to promote cell attachment and spreading to evaluate concerns that non-optimal ER staining was an artifact due to spherical shape of C6/36 cells.

Antibodies for single label immunofluorescence assays

J2 antibody A commercial antibody used for detection of dsRNA was obtained from Scions (Scions/English and Scientific Consulting, Hungary, http://www.engscicons.de). J2 antibody is a mouse monoclonal antibody (IgG2a) that is highly specific for dsRNA. Research to characterize the antibody showed that dsRNA of length ≥40 bp is recognized in a non-sequence specific manner (Schonborn et al., 1991). Lyophilized preparations of J2 were reconstituted in 0.5 mL sterile distilled water as recommended by the manufacturer, then divided into 10 µL aliquots and frozen at -20˚C for longer term storage.

Biotinylated sheep anti-mouse IgG A commercial secondary anti-mouse IgG antibody and strepavidin-fluorescein were obtained from Pierce (Pierce/Thermo Fisher, Rockford, IL).

3H5-21 Mouse ascites fluid containing monoclonal antibody 3H5-21 to DENV E protein was prepared by and obtained from Dr. Irma Sanchez-Vargas (AIDL, Colorado State University).

30.11a Mouse ascites fluid containing monoclonal antibody to SINV E1 protein was prepared by and obtained from Dr. Irma Sanchez-Vargas (AIDL).

807-13αN A directly FITC-conjugated mouse polyclonal antibody reactive to all LACV structural proteins was obtained from Cynthia Meredith (AIDL).

Immunofluorescence assay for dsRNA

IFA to detect dsRNA in DENV-2 infected cells Samples were prepared by seeding C6/36 cells onto sterilized 18 mm diameter No.1 coverslips in 12-well tissue culture plates and infecting with DENV-2 (JAM1409) at an MOI of 0.1. Predetermined fixation timepoints were every 24 hr post infection, as needed for the experimental design, in 4% electron microscopy grade paraformaldehyde (Electron Microscopy Sciences, Hatfield, PA) in RNase free PBS (Ambion). Plates containing coverslips in PBS were stored at 4°C wrapped in parafilm. Samples were checked periodically so they were not allowed to dry, which leads to increased background fluorescence.

Experimental IFAs consisted of incubation with 1:1000 antibody J2 (2 hr), followed by 1:400 biotinylated sheep anti-mouse IgG (1hr) then 1:400 strepavidin-fluorescein (1hr) at 28˚C with gentle rocking (Weber et al., 2007). All antibodies were diluted in PBS with 0.2% bovine serum albium (BSA) (Sigma, St. Louis, MO) and 0.5% TX100 (Sigma). Each incubation was followed by three washes in PBS (Ambion). Coverslips were mounted on glass slides using Vectashield with DAPI (VWR) and observed with a Leica DM4500B fluorescent microscope. Control IFAs were as described for J2 antibody except the primary antibody was 3H5-21 at a dilution of 1:400.

SINV-infected cells Samples were prepared by seeding C6/36 cells onto sterilized coverslips in 12-well tissue culture plates and infecting with MRE16 or TE3’2J at an MOI of 0.01. Cells were fixed every 24 hr post infection in 4% paraformaldehyde in

PBS at 4˚C for 15 min, then rehydrated in PBS for 5 min. Protocol was as described above except the primary antibody was 30.11a at a dilution of 1:150.

LACV-infected cells Samples were prepared by seeding C6/36 cells onto sterilized coverslips in 12-well tissue culture plates and infecting with LACV prototype strain at an MOI of 1.0. Cells were fixed 4 dpi in 4% paraformaldehyde in PBS at 4˚C for 15 min, then rehydrated in PBS for 5 min. Experimental and control IFAs were as described above for SINV except for use of primary antibody 807-13αN (1:150) dilution, a directly labeled antibody, so no secondary antibody was required.

Detection of dsRNA in transformed cell lines

DENV challenge and dsRNA IFA of FB9.1 cells FB9.1 cells and C6/36 cell controls were challenged with DENV-2 as previously described (Adelman, 2000; Adelman et al., 2002). Briefly, cells were seeded onto glass coverslips in 12-well tissue culture plates as described for IFA experiments. When cells were approximately 90% confluent, they were challenged with DENV-2 (JAM1409), MOI 0.01 in 300 µL L-15 medium. Cells were incubated at room temperature with rocking for 30 min, medium was removed and replaced with 10% FBS-containing growth medium containing 300 U/mL hygromycin and incubated overnight. Then growth medium was removed and replaced with L-15 maintenance medium plus 300 U/mL hygromycin. At 7 days post challenge, cells were fixed in paraformaldehyde as described for dsRNA IFAs. FB9.1 and C6/36 cells were stained with fluorescent antibodies specific for dsRNA or DENV E protein as described previously.

RT-PCR to test transformed cell lines FB9.1 and H9.1 for LACV contamination

RNA was extracted from 1 mL medium from FB9.1 and H9.1 cell culture flasks using the RNeasy Mini kit (Qiagen, Valencia, CA). Controls consisted of extraction of 1 mL medium from uninfected cultured C6/36 cells and from 50 µL of LACV prototype stock using the same kit. Extracts were tested for the presence of LACV RNA via RT-PCR with reaction and program conditions as described above for RT-PCR analysis of cellular fractionation samples using the Invitrogen SuperScript III One-Step RT-PCR System with Platinum Taq kit (Invitrogen). The following primers specific to LACV S segment (AF528167) were designed and used to detect LACV RNA: LACVFWD (KP 105) 5'TGCAGGGTATATGGACTTCTGTG3' and LACVREV (KP 106) 5'AGCAGTATCGCTCAGGCCTCC3'. RT-PCR products were analyzed via gel electrophoresis.

Biotinylation of J2 antibody

IFAs for localization of dsRNA and DENV E and capsid (C) antigens used biotinylated monoclonal antibody J2 prepared with ProtON Biotin Labeling Kit (Vector Laboratories Inc., Burlingame, CA), which creates a stable linkage between biotin and terminal amino groups on lysine residues of the antibody. Antibody labeling was carried out using kit instructions with a few exceptions as noted below.

Solutions were prepared as described in the kit. Labeling reagent plus 15 µL dimethylsulfoxide (DMSO) was vortexed to mix. This mixture was divided into 2 µL aliquots in 0.2 mL PCR tubes and stored at -20˚C for no longer than 1 yr.

Approximately 0.1 mg monoclonal antibody J2 was dissolved in 100 µL manufacturer's protein solution. The labeling reaction was initiated by the addition of

2 µL of biotin labeling reagent and mixed by pipeting up and down gently. The reaction was incubated at room temperature. Departing from the protocol provided with the kit, reactions were incubated in the dark for 1 hr to increase labeling efficiency. The labeling reaction was halted by adding 2 µL of manufacturer's stop solution and incubated for 5 min at room temperature.

Labeled antibody was purified by a gel filtration step provided with the kit. Labeled J2 antibody was divided into 10 µL aliquots and stored at -20˚C for no longer than 1 month prior to use. (Note that J2 antibody batch J2-0702 was used for preparation of biotin-labeled antibody. Scicons advised that this batch of antibody was determined to be half as concentrated as previous batches used for single IFAs as determined by their internal quality testing.)

IFAs for colocalization of dsRNA and DENV proteins

Primary antibodies

J2. For all assays, biotinylated mouse monoclonal J2 antibody prepared as described above was reacted with Streptavidin Alexa Fluor 546 conjugate as described below.

PDI. Mouse monoclonal antibody reactive to *Drosophila* protein disulfide isomerase (PDI), a microsomal enzyme that localizes to the endoplasmic reticulum (ER) was used to define location of ER in mosquito cells (Abcam).

3H5-21. Mouse ascites fluid containing monoclonal antibody to DENV E protein was prepared by and obtained from Dr. Irma Sanchez-Vargas (AIDL).

1A2A-1. Mouse monoclonal antibody specific for DENV capsid protein was obtained from Dr. John Roehrig at DVBID-CDC (Fort Collins, CO).

Secondary antibodies and labels

Streptavidin Alexa Fluor 546 conjugate. To label biotinylated J2 antibody, Streptavidin Alexa Fluor 546 was incubated with biotinylated J2 antibody to allow the strepavidin to react with biotin, forming a stable bond (Molecular Probes).

FITC antimouse IgG antibody. A goat polyclonal antibody to mouse heavy and light chain IgG conjugated with fluorescein isothiocyanate (FITC) (Abcam) was used as the secondary antibody to viral antigen specific antibodies (3H5, 30.11a, 1A2A-1) and PDI antibodies.

Localization of DENV E antigen, C antigen, or cellular PDI with dsRNA

To determine relative locations of E antigen and dsRNA, samples were prepared as described for dsRNA IFAs using DENV-2 infected C6/36 cells at 1-14dpi. Experimental IFAs consisted of incubation of infected cells with 1:400 mAb 3H5-21 (2 hr) followed by 1:400 FITC conjugated sheep anti-mouse IgG (1hr), then 1:250 biotinylated J2 mAb (2hr) followed by 1:250 streptavidin Alexa Fluor 546 conjugate (1hr). All incubations were at 28˚C with rocking. Control IFAs were with single monoclonal antibody J2 or 3H5-21. All antibodies were diluted in PBS containing 0.2% BSA (Sigma) and 0.5% TX100 (Sigma) except the Strepavidin Alexa Fluor 546 conjugate, which was diluted in PBS alone. Prior to antibody incubations, all samples were washed in PBS with 0.01% Tween20 (PBST). Between antibody incubations, all samples were washed three times with PBST, and after the final incubation, an additional wash with distilled water was included. Coverslips were mounted on glass slides in Vectashield with DAPI (VWR) and observed initially with a Leica DM4500B fluorescent microscope to verify labeling.

Localization of dsRNA and E protein staining was analyzed using confocal microscopy as described below.

To determine relative locations of dsRNA and DENV C protein, samples were prepared as described for dsRNA IFAs using C6/36 cells infected with DENV-2 (JAM1409) at 1-14 dpi. Experimental IFAs consisted of incubations of infected cells with 1:250 mAb 1A2A (2 hr) followed by 1:250 FITC conjugated sheep anti-mouse IgG (1hr), then 1:250 mAb biotinylated J2 (2hr), followed by 1:250 streptavidin Alexa Fluor 546 conjugate (1hr) at 28˚C with rocking. All washes between and after incubations, mounting, control IFAs, and microscopy were as described above.

To localize dsRNA and PDI as a marker of ER, samples were prepared as described previously at 1-12 dpi. Experimental IFAs consisted of incubation of infected cells with 1:30 anti-PDI (2 hr), followed by 1:30 FITC-conjugated sheep anti-mouse IgG (1hr) then 1:250 biotinylated J2 mAb (2hr), followed by 1:250 streptavidin Alexa Fluor 546 conjugate (1hr) at 28˚C with rocking. All washes between and after incubations, final washes, mounting, control IFAs, and microscopy as described above.

Confocal microscopy

All three-dimensional imaging and analysis were carried out using the Zeiss Laser Scanning Axiovert Confocal Microscope in the Infectious Diseases Annex (IDA) on the Foothills campus (Colorado State University). The LSM510 Meta software was used for all imaging. Original confocal microscope training was provided by a Zeiss representative and training on updated confocal microscope software was provided by the confocal technician, Eric Lee, M.S.

Confocal microscope settings Confocal settings were optimized for each set of samples using unstained and singly stained positive and negative control slides prior to imaging experimental samples.

Three-dimensional localization Three-dimensional localization of dsRNA in mosquito cells was determined by examining optical Z sections of samples prepared for IFA as described above. Sections were selected manually between the apical and basal planes of each sample and by choosing an optical section thickness from the recommended optimal thickness as calculated by the LSM510 Meta software. Sections were reconstructed and animated as three-dimensional images using the LSM Image Examiner software.

Differential contrast microscopy Differential contrast microscopy (DIC) is a high resolution method of visualizing transparent materials when brightfield microscopy produces no observable contrast. DIC uses two prisms and a polarized light beam to create contrast. One prism splits the illuminating light beam before it enters the sample and an additional prism recombines after passing through the sample (Frohlich, 2008). If the light beam passes through the sample without refraction, that region of the sample will appear gray. However, if the beams encounter regions with different refractive indices as they pass through the sample, when the beams are recombined they can interfere either destructively, producing a dark area, or constructively, producing a bright area. DIC was used in combination with confocal microscopy to help delineate the edges of the mosquito cells being imaged. Where DIC increased the clarity of the image, it was included in the data figures. If DIC added no information to the image, the DIC images were not shown in results.

Electron microscopy

All electron microscopic imaging was carried out with the assistance of Dr. Suzanne Royer, operating the JEOL JEM 2000 EXII transmission electron microscope (TEM) in the Anatomy and Zoology building (Colorado State University). All grid preparation was performed by the author, and embedding after the initial fixation steps was carried out by Dr. Royer.

Sample preparation: controls For positive controls, DENV-2 was inoculated at a 0.1 MOI onto subconfluent C6/36 cells grown in a 75 cm^2 cell culture flask, and infected C6/36 cells were maintained in L-15 maintenance medium at 28°C for 5 dpi. Negative controls were prepared as described excluding the addition of virus.

To verify that any structures observed in TEM observations of sucrose gradient fractions were not artifacts introduced by fixation, mosquito cell culture samples were divided for fractionation on sucrose density gradients or fixed as follows for whole tissue controls. Cells in a 75 cm^2 tissue culture flask were harvested with a cell scraper and resuspended in 1 mL medium and centrifuged at 1,500 rpm, 1 min at 4°C. Cells were washed by pipetting off supernatant, resuspending in ice-cold PBS, and centrifuging at 14,000 rpm, 5 min. Fixative consisting of 2.5% glutaraldehyde in 0.1 M sodium cacodylate buffer (pH 7.2), was added dropwise down the side of the microcentrifuge tube and samples were allowed to incubate for 10 min at room temperature. Pellet was loosened from the bottom of the tube with a sterile pipette tip and allowed to incubate in fixative for an additional 20 min at room temperature before transferring to 4°C for storage until embedding and sectioning.

Pre-fixed samples were post-fixed, embedded, and sectioned by Dr. Royer as follows. Fixed cell pellets were secondarily fixed in 1% osmium tetroxide in 0.1 M sodium cacodylate for 1 hr at room temperature then dehydrated with graded ethanol solutions: 50%, 60%, 70%, 80%, 90%, and 100%. Dehydrated samples were transferred from 100% ethanol to 50:50 ethanol:acetone, and finally to 100% acetone before being infiltrated with Eponate 12 resin (Ted Pella Inc., Redding, CA), and polymerized overnight at 60^{o}C. Ultra-thin sections (70-90 nm in thickness) were cut on a Reichert Ultracut E ultramicrotome using a Diatome diamond knife, mounted on Formvar-coated slot grids, and post-stained with 5% uranyl acetate, and stored in a 0.08 M solution of lead citrate in distilled water.

Sample preparation: isolated vesicles Vesicle samples were prepared as described previously in the cellular fractionation protocol and mounted on EM grids as described below.

Grid preparation Samples were concentrated as described for cellular fractionation in 0.2 mL TNMg buffer. Samples were transported on ice to the EM center for preparation.

Samples for TEM were prepared and stained based on the methods of Uchil and Satchidanadam (2003), exposing Formar coated copper grids to 20 µL drops on parafilm starting with a drop of sample (1 min) then a drop of negative stain (3 min)(Harris, 1999). Grids were blotted with a point of filter paper between drops and after staining, then allowed to dry resting on parafilm for 15 min. The negative stain was 2% uranyl acetate in distilled water. Samples were examined and images recorded after grids were dry.

Characterization of isolated vesicles: detergent sensitivity To determine the detergent sensitivity of vesicles, samples were prepared by the cellular fractionation protocol,

except samples were incubated in 1.5% sodium deoxycholate (DOC) on ice instead of TX100. Grids were prepared as described above. TX100-treated samples from upper fractions likely to contain buoyant vesicles were compared with DOC-treated equivalent fractions.

Imaging Samples were examined by Dr. Royer and the author by TEM as described above. Images were taken at a magnification of 100,000x and 100 kV unless otherwise noted. Vesicles were imaged as a through-focal series consisting of three images of each vesicle. Negative control and DOC-treated sample grids were scanned for five times the average time required to identify the vesicles on TX100-treated sample grids to ensure that adequate time was allowed to be reasonably certain that such grids contained no vesicles. All images were taken with Kodak electron microscopy 4489 film (Electron Microscopy Sciences).

Prediction of DENV RNA secondary structure

The mFold webserver for RNA folding available through the Rensselaer bioinformatics web server (http://mfold.bioinfo.rpi.edu/cgi-bin/rna-form1.cgi) was used to analyze the 5'-terminal 6000 nt and 3' 4723nt of the DENV-2 (JAM1409) genome (Genbank #M20558) under the statistical nucleic acid predictions described by Zuker (2003).

Results

Characterization of sucrose-gradient fractions: analysis of viral RNA via RT-PCR

RT-PCR amplification of viral RNA from fractions of sucrose gradients showed two major regions containing DENV-2 RNA: buoyant upper fractions (1 and 2) and dense lower fractions (8, 9, and 10) of the gradient. When RT-PCR was used to compare cellular fractions to equivalent fractions from cell culture, medium cDNA amplicons were observed from many fractions, but the major cDNA amplicon differed between DENV-infected cell culture and medium from these cells. The major DENV cDNA amplicon was found in buoyant upper fraction 2 from cellular fractionation (top panel, Figure 2.1), and the major cDNA amplicon was found in dense lower fraction 7 in medium gradients (bottom panel, Figure 2.1).

Characterization of sucrose gradient fractions: analysis of viral RNA via strand-specific northern blot

The northern blot analysis of samples, from gradient fractions of detergent-treated cellular material hybridized with an anti-genome sense probe showed genome sense RNA at ~10.7 Kb in several buoyant upper fractions (2-3) and a similar-sized band in dense lower fractions (5-8) (Figure 2.2a, left panel). The equivalent northern blot hybridized with a genome sense probe showed a 10.7 Kb band of anti-genome sense RNA only in buoyant upper fraction 2 of the sucrose gradient (Figure 2.2a, right panel). There was little or no detectable RNA in the middle fractions with either probe.

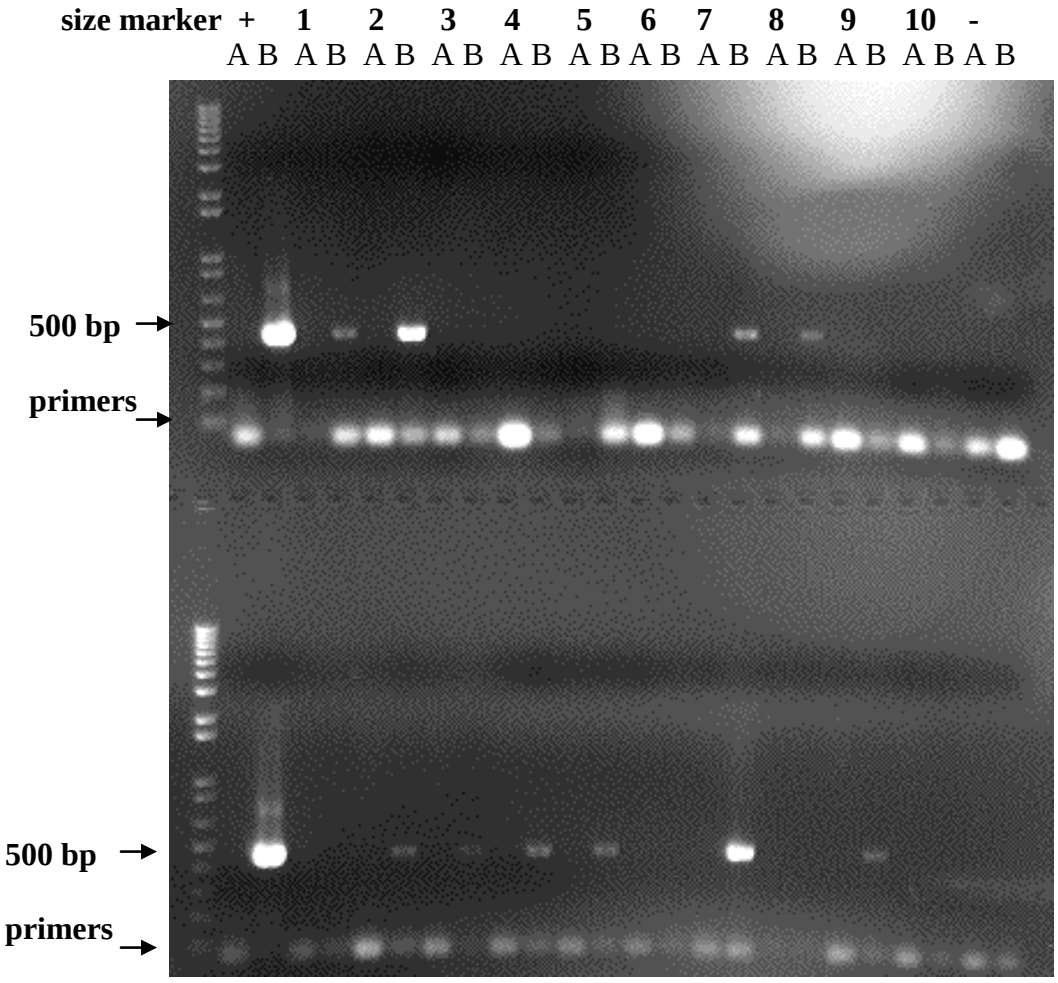

Figure 2.1 RT-PCR of sucrose gradient fractions The top panel shows agarose gel electrophoresis of RT-PCR products amplified from cell fractionation gradient fractions of DENV-2 infected C6/36 cells, and the bottom panel shows analysis of equivalent fractions from a gradient separation of medium from infected cells. Each sample had a PCR control (A) and RT-PCR (B). The left-most lane contains the DNA size markers, and the next two lanes contain the PCR and positive control RT-PCR from extracted DENV-2 RNA. Remaining lanes contain products from top to bottom fractions, and the final two lanes contain controls without template RNA. In the top panel, fractions 1, 2, 7, and 8 had amplified cDNA from DENV-2 infected C6/36 cells. In the bottom panel, fractions 2, 3, 4, 5, 7, and 9 contain amplified cDNA products from infected cell culture medium.

Figure 2.2 Strand-specific northern blots and infectivity assay DENV-infected mosquito cells were treated with detergent and separated into subcellular components via density-dependent sucrose gradient fractionation. Samples were taken as one mL fractions from the top of this gradient and the top-most fraction was labeled 1, etc. To determine which fractions of the sucrose gradient contained DENV RNA resembling the genome sense and anti-genome sense RNA found in DENV replication compartments, fractions were analyzed via strand-specific northern blot. To determine which fractions contained infectious virions, each fraction was inoculated onto C6/36 cells, which were analyzed via IFA for DENV E protein.

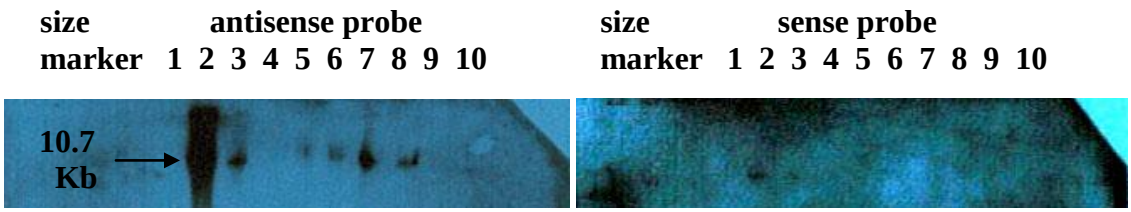

Figure 2.2a. Strand-specific northern blots. The left-most lane contains DNA size marker. Numbers correspond with gradient fractions: 1 at the top and 10 at the bottom.

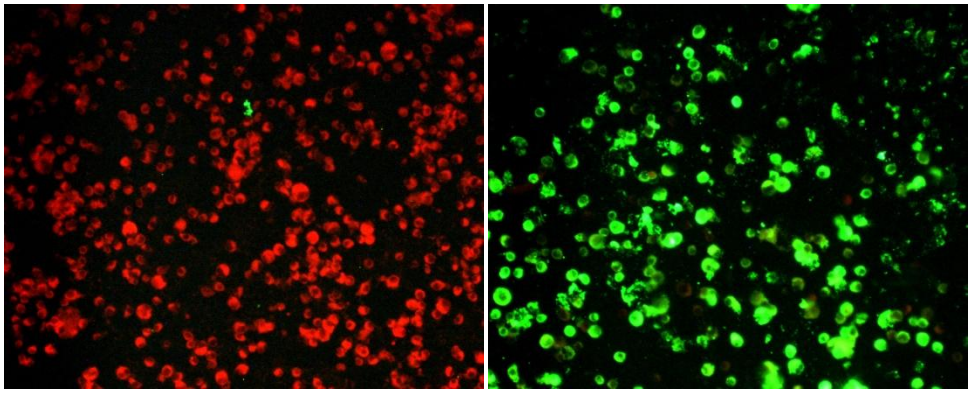

Figure 2.2b. Infectivity assay. IFA of C6/36 cells 14 days after inoculation with top fractions (2-3) of sucrose gradient on left and exposed to lower fractions (7-8) on the right (40x, fluorescent microscope).

Characterization of sucrose gradient fractions: analysis of infectious DENV

To determine which fractions from sucrose gradient centrifugation contain infectious DENV, fractions were concentrated, mixed with medium, and applied to mosquito cell cultures. Immunofluorescent detection of DENV envelope (E) antigen as a marker of viral replication showed few to no positive cells via IFA after exposure to samples from the upper (1-3) and middle (4-6) fractions of the sucrose gradient and a large proportion of positive cells via IFA after exposure to lower (7-10) sucrose gradient fractions (Figure 2.2b).

Characterization of sucrose gradient fractions: Dicer exclusion trial

To determine whether viral RNA in sucrose gradient fractions that were suspected to contain DENV replication complexes enclosed in vesicles was protected from Dicer, concentrated gradient fractions were incubated with Dicer, then RNA was extracted and subjected to RT-PCR and gel electrophoresis to detect protected genomic RNA. The positive controls indicated that the Dicer enzyme kit was functional in digesting long dsRNA. Viral RNAs were not detected by RT-PCR in any of the samples. We had expected to find viral RNA in the upper (1-3) fractions and in the lower (7-10) fractions where viral RNA would be protected from Dicer by vesicles or C protein respectively. We suspect that lysis of the occurred as vesicles were transferred from concentrated sucrose gradient fractions in pH 8.8 TNMg buffer used in cellular fractionation to the more neutral buffer used in the Dicer reactions. Researchers working on SARS-coronavirus replication-associated vesicles have also noted the fragility of the vesicles and how easily they can be accidentally lysed during experiments (Knoops et al., 2009).

Localization of dsRNA in mosquito cells: DENV

To visualize where virus-associated dsRNA localized in mosquito cells, DENV-infected cells were stained with antibodies for dsRNA or DENV E protein and examined via fluorescent microscopy. DsRNA associated with DENV replication was observed in a diffuse pattern throughout the cytoplasm in C6/36 cells that were infected with DENV-2 (JAM1409) at an MOI of 0.1 and fixed at 5 dpi. DENV E protein was observed primarily along the plasma membrane or in larger foci than dsRNA in the cytoplasm in C6/36 cells that were infected with DENV-2 and fixed at 5 dpi (Figure 2.3B). Mock-infected C6/36 cells had no staining for dsRNA or DENV E protein (Figure 2.3A).

Localization of dsRNA in mosquito cells: SINV

To determine where virus-associated dsRNA localizes in mosquito cells infected with SINV (strains MRE16 and TE3'2J), infected cells were fixed at 3 dpi and stained with fluorescent antibodies for dsRNA or SINV E1 protein and examined via fluorescent microscopy. DsRNA staining was observed in large foci throughout the cytoplasm in both MRE16 and TE3'2J infected cells, and the intensity of staining for dsRNA appeared to be slightly greater in MRE16 than TE3'2J infected cells (Figure 2.4, B and C). Mock-infected cells showed no staining for SINV envelope 1 (E1) protein or dsRNA (Figure 2.4). Cells infected with each strain of SINV showed localization of E1 protein in large foci throughout the cytoplasm. There were only minor differences in staining intensity of dsRNA or E1 antigen in agreement with observations of similar growth curves of the two strains in C6/36 cells (Myles et al., 2008) (Figure 2.4).

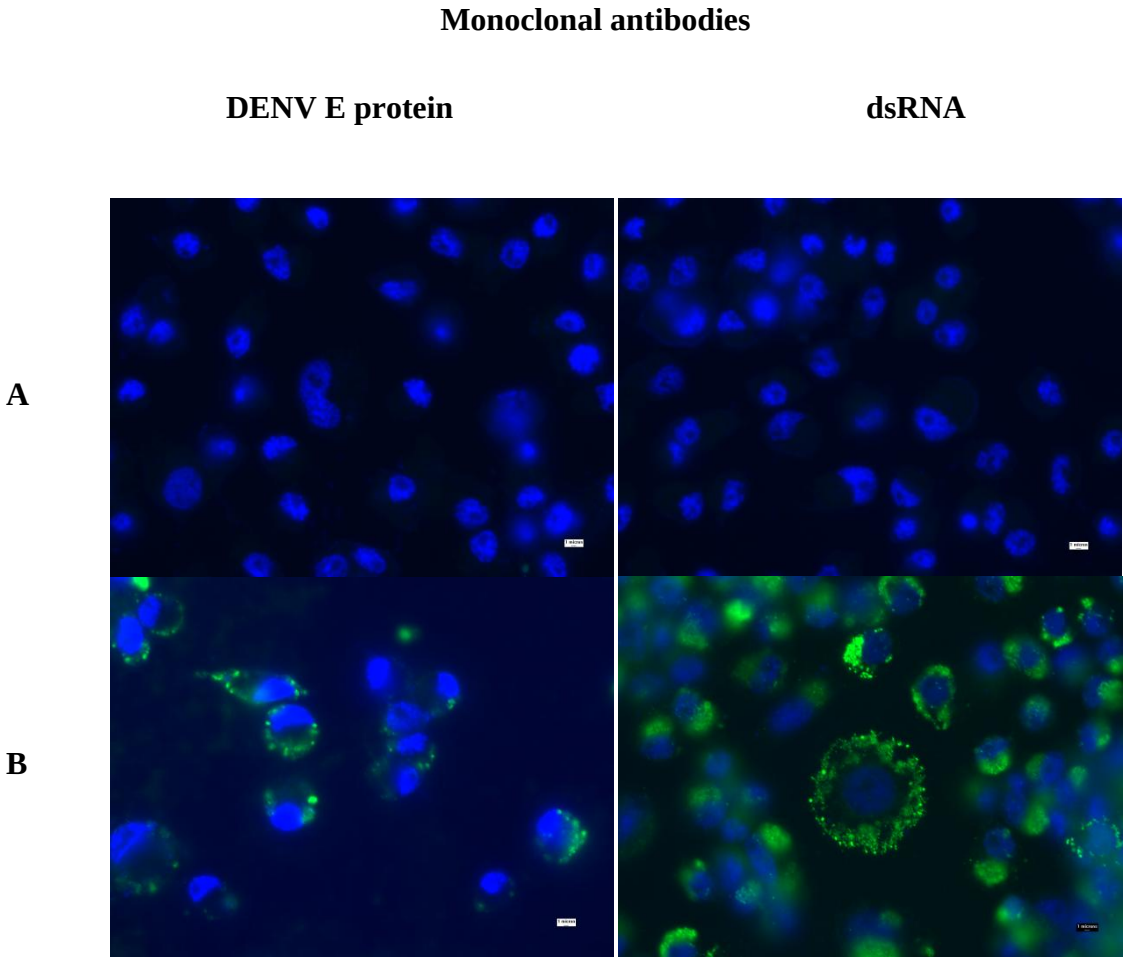

Figure 2.3 Localization of viral antigen and dsRNA in DENV-infected mosquito cells 5 dpi C6/36 cells **A** mock-infected, and **B** DENV-infected in left panels were stained for DENV or E antigen (green) and counterstained with DAPI nuclear stain (blue). The right panels were stained for dsRNA (green) and counterstained with DAPI nuclear stain (blue) (4 micron bar) (100x oil, fluorescent microscope).

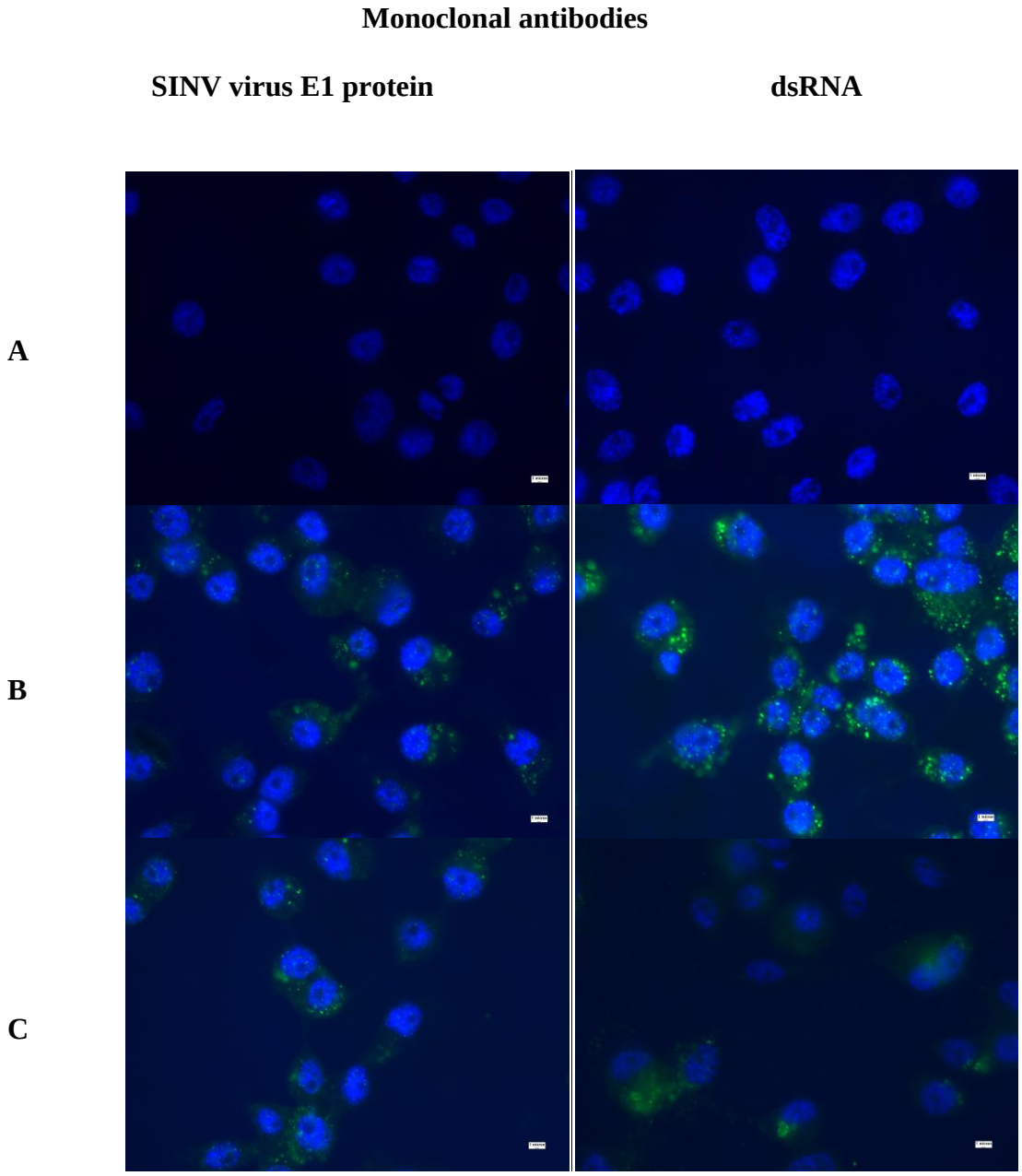

Figure 2.4 Localization of viral antigen and dsRNA in SINV-infected mosquito cells at 3 dpi C6/36 cells: **A** mock-infected, **B** MRE16-infected, and **C** TE3’2J-infected, in the left panels were stained for SINV E1 protein (green) and counterstained with DAPI nuclear stain (blue). The right panels were stained for dsRNA (green) and counterstained with DAPI nuclear stain (blue) (4 micron bar) (100x oil, fluorescent microscope).

Localization of dsRNA in mosquito cells: LACV

No dsRNA associated with LACV replication was observed via IFA at 4 dpi in C6/36 cells infected with LACV at an MOI of 1 (Figure 2.5). Mock-infected C6/36 cells also had no staining for dsRNA. Cells infected with LACV and mock-infected cells were stained for LACV structural proteins to verify infection. Mock-infected cells showed no staining for LACV structural proteins and cells infected with LACV prototype strain showed structural proteins in large foci throughout the cytoplasm.

Localization of dsRNA in transformed mosquito cell lines: FB9.1 cells

To determine whether dsRNA outside the context of viral infection could be detected in mosquito cells, FB9.1 cells, a C6/36 cell line transformed to express a 290 bp hairpin RNA, were challenged with DENV-2, fixed, stained with fluorescent antibodies for dsRNA or DENV E protein, and examined via fluorescent microscopy. DsRNA in mock-infected FB9.1 cells appeared to localize primarily to the nucleus and in both the nucleus and the cytoplasm after DENV-challenge. Unprotected dsRNA is rapidly degraded in the cytoplasm, so transgene derived dsRNA would be destroyed (Houseley and Tollervey, 2009). DsRNA in C6/36 cells localized as previously observed for both mock-infected and DENV-infected cells (Figures 2.3 and 2.6). Unexpectedly, DENV E antigen staining was observed in approximately 10-30% of the DENV-challenged FB9.1 cells, 25% shown. Mock-infected C6/36 and FB9.1 cells showed no staining for DENV E protein. C6/36 cells infected with DENV-2 (JAM1409) and some DENV-challenged FB9.1 cells had E protein in large foci at the plasma membrane of some cells and in other cases, near the nucleus (Figure 2.3). There were a great percentage of cells,

Antibodies

LACV structural proteins **dsRNA**

A

B

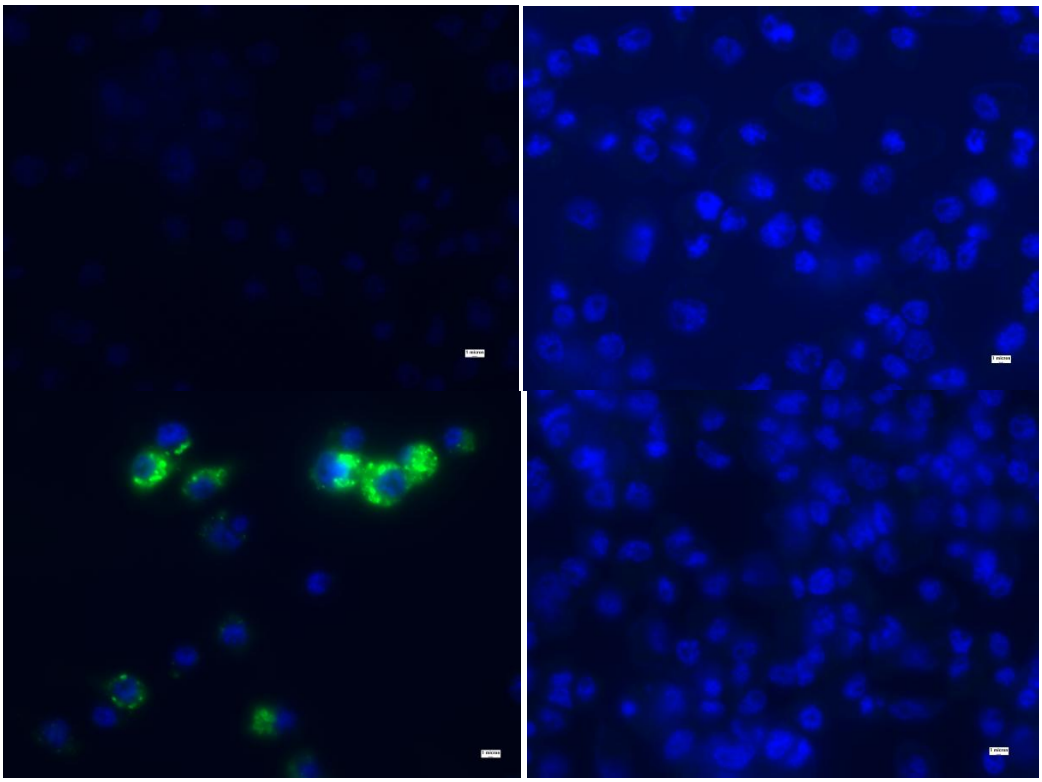

Figure 2.5 Staining for viral antigens and dsRNA in LACV-infected mosquito cells at 4 dpi C6/36 cells **A** mock-infected and **B** LACV-infected in left panels were stained for LACV structural proteins (green) and counterstained with DAPI nuclear stain (blue). The right panels were stained for dsRNA (green) and counterstained with DAPI nuclear stain (blue) (bar 4 microns) (100x oil, light microscope).

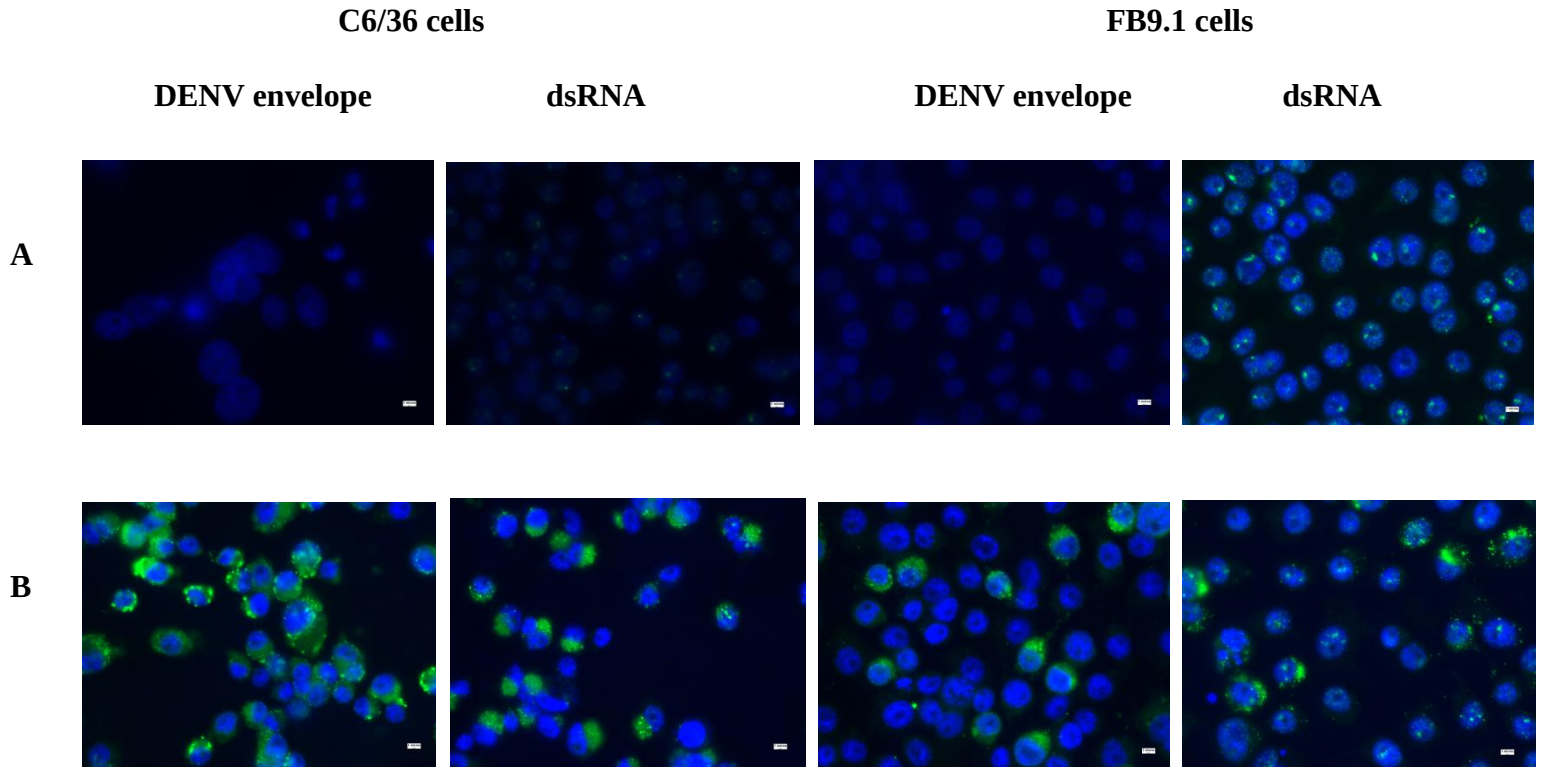

Figure 2.6 Localization of dsRNA in mock-infected and DENV-2 challenged FB9.1 transformed mosquito cells and C6/36 mosquito cells at 7 dpi In **A** mock-infected and **B** DENV-infected cells, first and third panels in each row were stained for DENV E protein (green); the second and fourth panels were stained for dsRNA (green). All panels were counterstained with DAPI nuclear stain (blue) (bar 4 microns) (100x oil, fluorescent microscope).

approximately 90% C6/36 versus 25% FB9.1 stained for dsRNA and DENV E protein in infected C6/36 cultures than in DENV-challenged FB9.1 cultures, suggesting that some of the FB9.1 cells were still resistant to DENV infection (Figure 2.6). The number of FB9.1 cells staining with DENV antigen after challenge with DENV had increased from the originally reported 1% to an estimated 10-30% based on counts of imaged cells (Figure 2.6). The FB9.1 cells that showed dsRNA staining in the cytoplasm had probably lost resistance and were infected with DENV. We planned to further evaluate the hypothesis that some FB9.1 cells had lost resistance by staining for co-localization of dsRNA and DENV E protein. At the time the IFA experiments were performed, the FB9.1 cell line was believed to be free of viral contamination. In preparation for co-localization studies for dsRNA and DENV E protein, both the FB9.1 and H9.1 cell lines were found to be positive for LACV RNA via RT-PCR (Figure 2.7).

Time course of localization of DENV E antigen and dsRNA in infected cells

To determine whether DENV E protein and dsRNA localize throughout replication, DENV- infected C6/36 cells were fixed at 1-14 dpi, stained for DENV E protein and dsRNA, and examined via fluorescent microscopy. At all timepoints, dsRNA and DENV E appeared to co-localize in the cytoplasm of C6/36 cells infected with DENV-2 (JAM1409) via fluorescent microscopy (Figures 2.8a and 2.8b). There was no visible staining of either dsRNA or E protein at 1 dpi and there was little variation in the observed levels of dsRNA and E protein staining at 2-14 dpi except a slight decline in both by 14 dpi. Both dsRNA and E protein staining were found throughout the

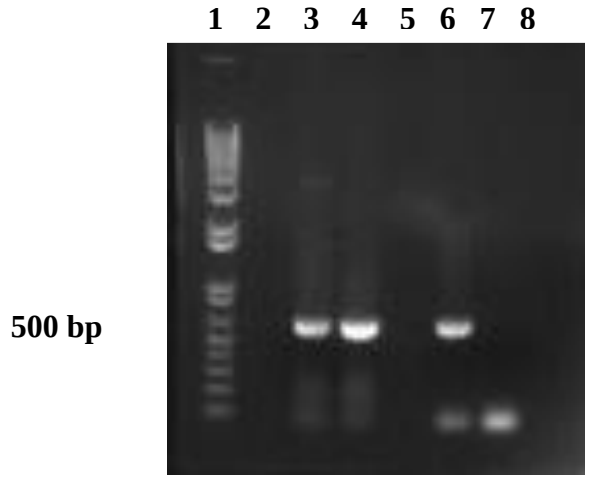

Figure 2.7 Gel electrophoresis of RT-PCR products from LACV RNA RT-PCR products from FB9.1 and H9.1 transformed mosquito cell lines indicate both are contaminated with LACV. Lane 1 contains markers, lane 2 is empty, lane 3 is the amplicon from H9.1 cells, lane 4 is the amplicon from FB9.1 cells, lane 5 empty, lane 6 positive control, and lane 7 negative control, and lane 8 empty.

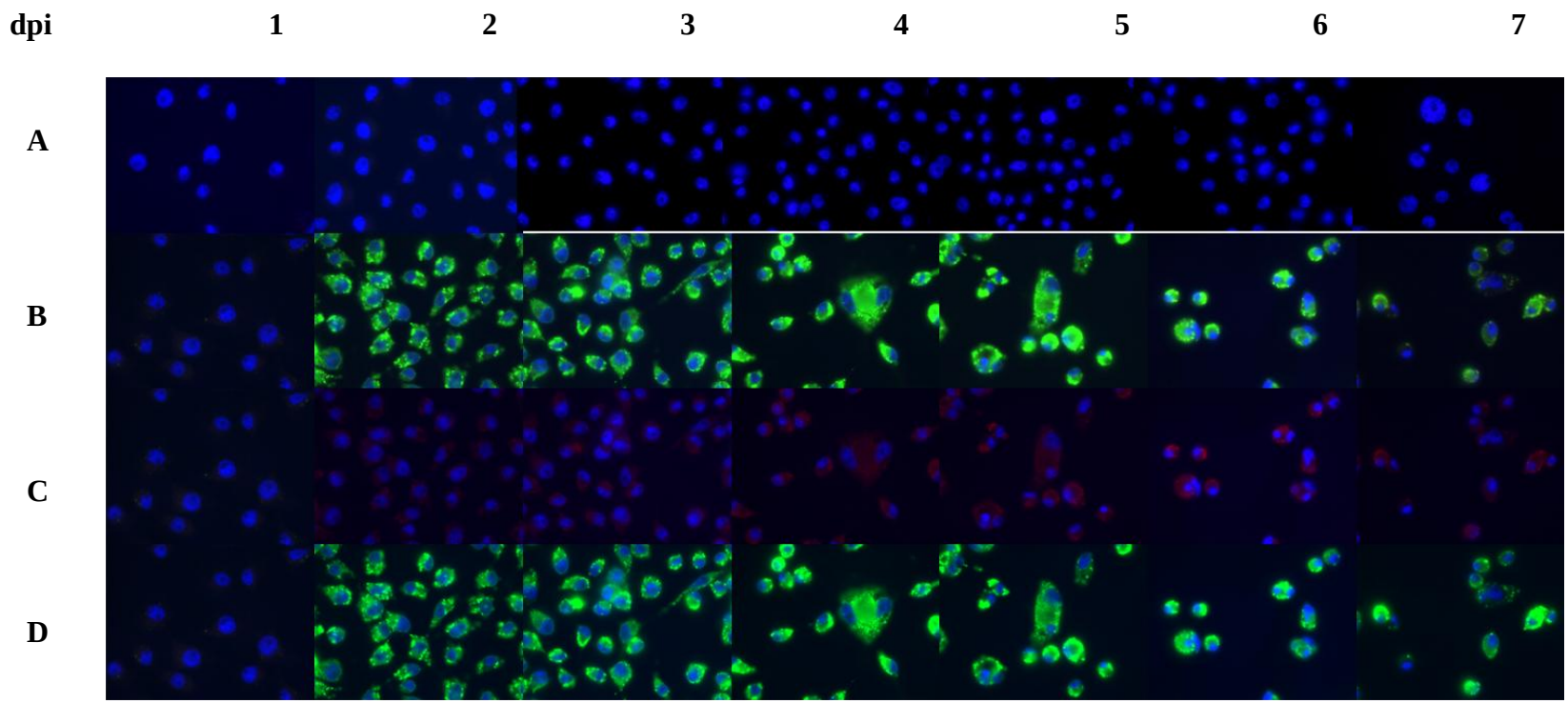

Figure 2.8a Time course of localization of dsRNA and DENV E protein **A** Mock-infected C6/36 cells stained for dsRNA and DENV E protein. **B** DENV-infected cells stained for dsRNA and DENV virus E protein (merged C & D). DENV-infected cells stained for **C** dsRNA, and **D** DENV E protein. The nuclei are stained with DAPI (blue), (100x oil, fluorescent microscope). dpi = days post infection

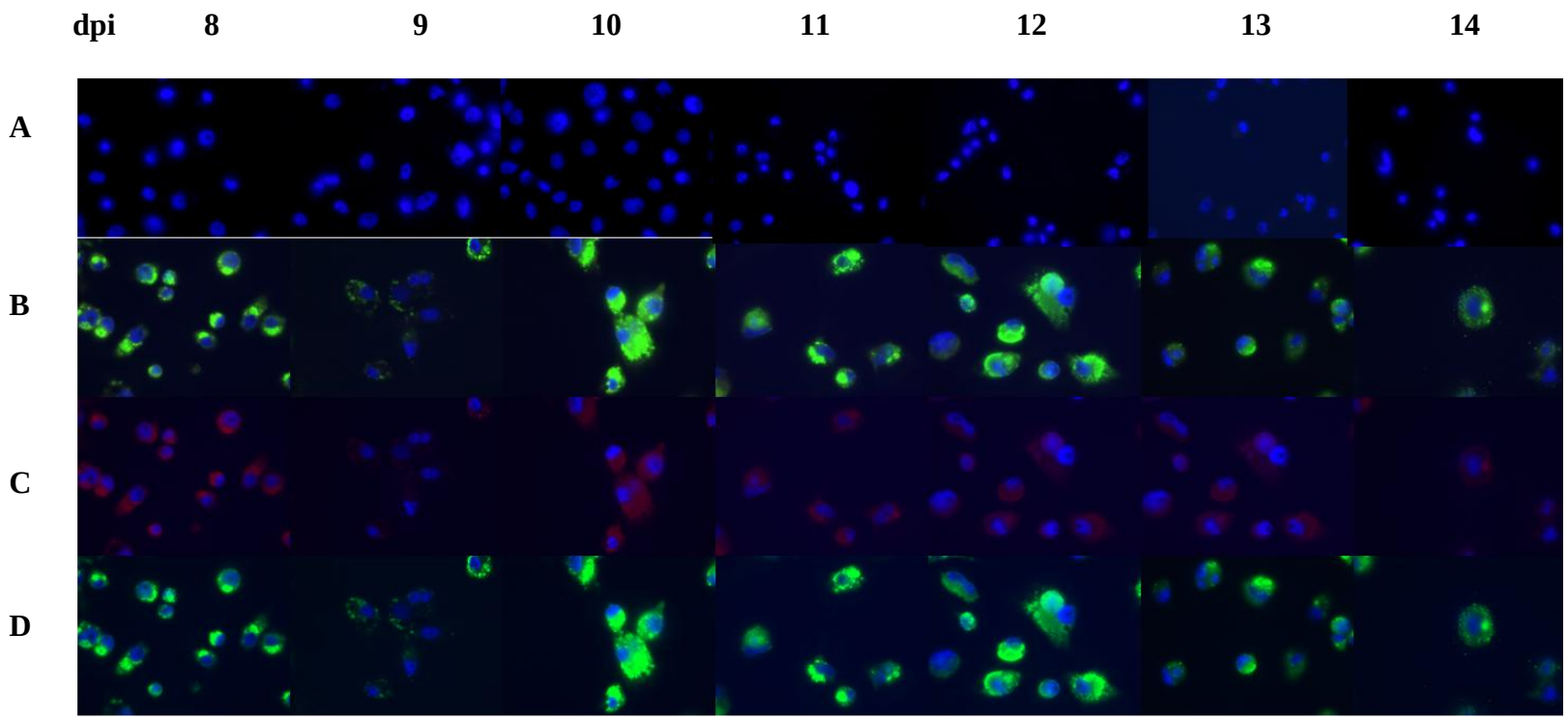

Figure 2.8b Time course of localization of dsRNA and DENV E protein **A** Mock-infected C6/36 cells stained for dsRNA and DENV E protein. **B** DENV-infected C6/36 cells stained for dsRNA and DENV E protein (merged C & D). DENV-infected cells stained for **C** dsRNA, and **D** DENV E protein. The nuclei are stained with DAPI (blue), (100x oil, fluorescent microscope). dpi = days post infection

cytoplasm with more intense staining foci scattered throughout the cytoplasm. On examination at higher magnification of a fluorescent microscopic image of infected C6/36 cells at 7 dpi, it appeared that co-localization of dsRNA and DENV E protein may not be complete as there appeared to be some red (dsRNA) staining not overlaid with green (E protein) (Figure 2.9).

Examining infected cells via confocal microscopy confirmed that there may be dsRNA not co-localized with E antigen and that dsRNA may be closer to the nucleus than the E protein (Figures 2.10, 2.11, 2.12).

Localization of DENV C antigen and dsRNA over time

To determine whether DENV C antigen and dsRNA co-localized during DENV replication, DENV- infected mosquito cells were prepared for IFA to both antigens at 1-12 dpi. DENV C protein and dsRNA did not consistently localize in C6/36 mosquito cells infected with DENV-2 (JAM1409). From 1-6 dpi, both dsRNA and C protein staining was faint and diffuse and was difficult to observe at 1, 2, and 4 dpi, but slightly more intense and more easily observed at 3, 5, and 6 dpi (Figure 2.12). C protein and dsRNA staining did not show the same localization patterns 7-12 dpi, dsRNA staining was diffuse and C protein staining was intense and localized to one side of the nucleus. Recently translated C protein was near RNA replication sites as in 1-6 dpi, but viral C protein accumulated at virion assembly sites at 7-12 dpi. Confocal microscopic analysis of cells stained with monoclonal antibodies for dsRNA and C protein at 10 dpi showed diffuse dsRNA staining with single intense C protein foci typically on one side of the nucleus (Figures 2.13 and 2.14).

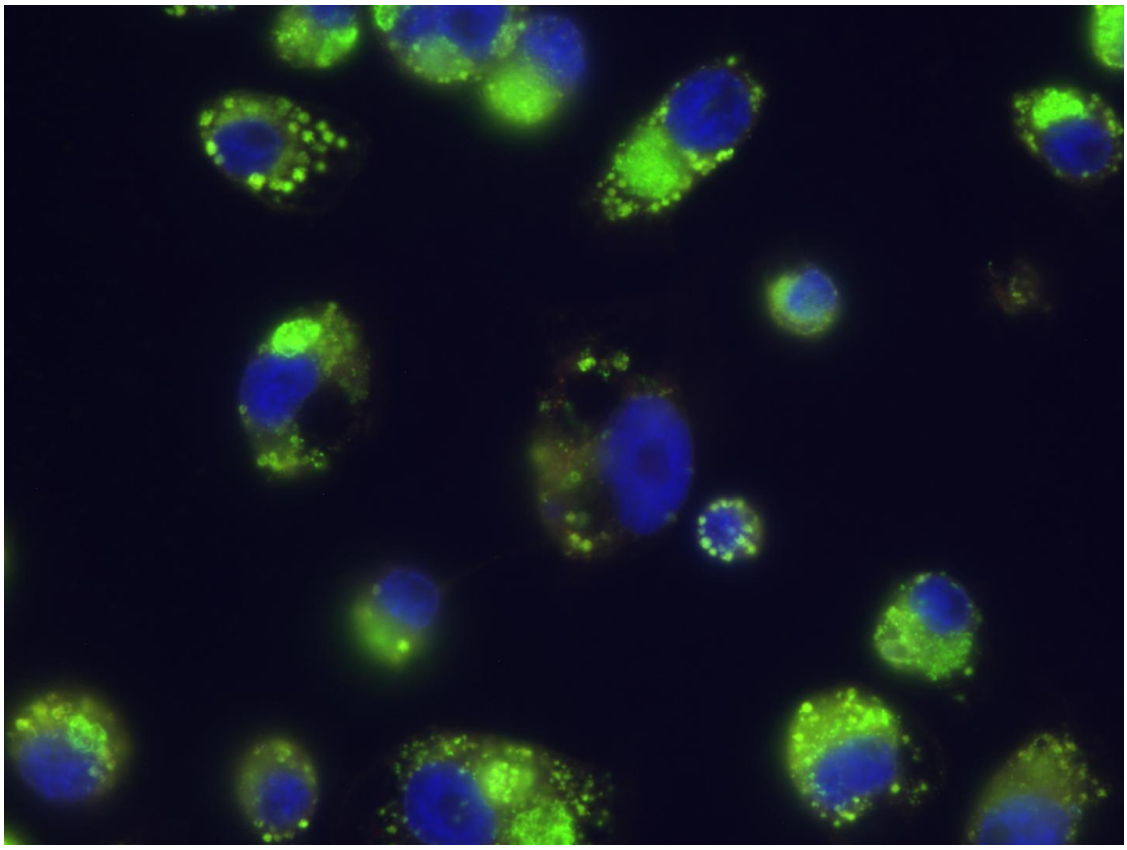

Figure 2.9 Is dsRNA completely co-localized with DENV E protein? Fluorescent microscopic image of C6/36 cells infected with DENV-2 (JAM1409) 7 dpi, nucleus stained with DAPI (blue), E antigen stained with FITC-conjugated 3H5-21 (green), dsRNA stained with biotinylated J2 and Streptavidin-Alexa 546 conjugate (red) (100x oil, fluorescent microscope).

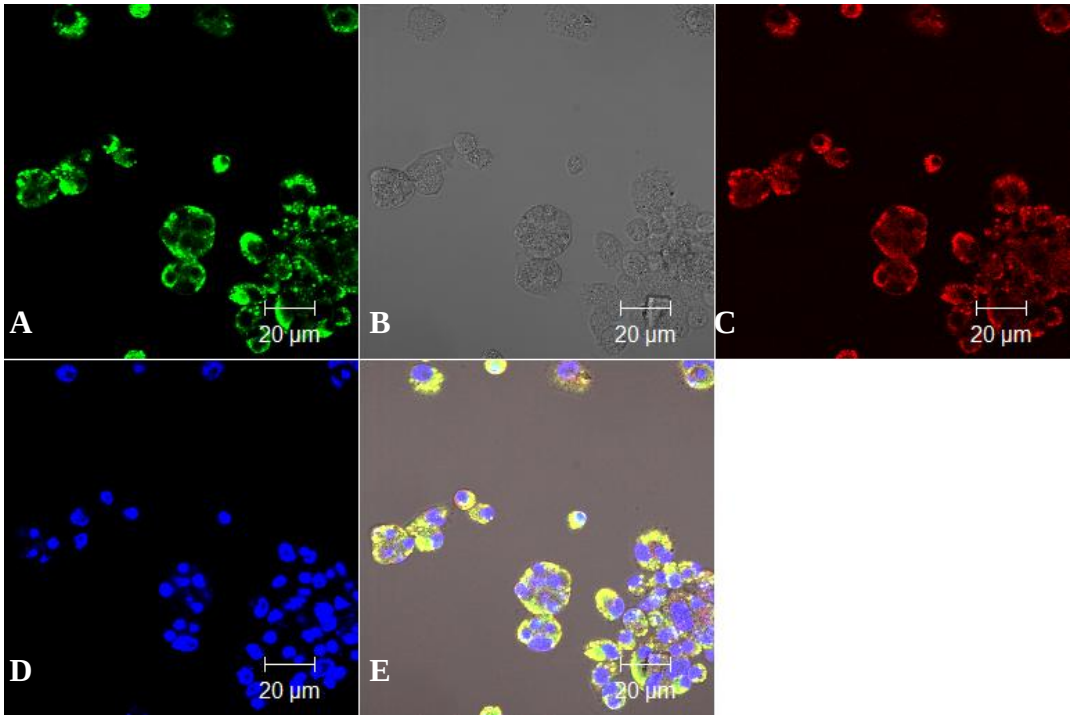

Figure 2.10 Localization of DENV-2 E protein and dsRNA in C6/36 mosquito cells
Imaging of the same field of C6/36 cells infected with DENV-2 at 7 dpi stained for **A**, E protein antigen (green), **B**, differential interference contrast DIC (gray) to delineate plasma membrane of cells, **C** dsRNA (red), **D** DNA (blue), and **E** merged (63x oil, confocal microscope). Merged red and green staining appears yellow.

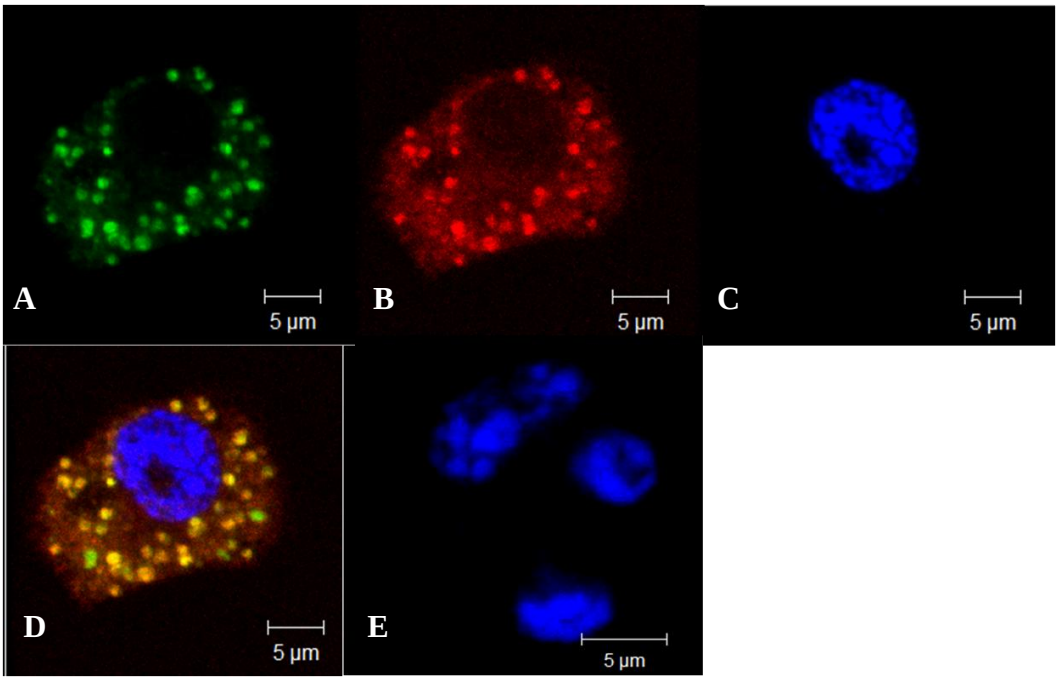

Figure 2.11 Localization of DENV E protein and dsRNA in mosquito cells Images of C6/36 cells **A-D** DENV-infected, and **E** mock-infected at 7 dpi. **A**, stained for E protein (green), **B,** dsRNA (red), **C**, DNA (blue), and **D** merged A, B, and C. Please note that **E** is also a merged image but because the cells are mock-infected there is no observable staining for E protein (green) or dsRNA (red) (cropped 63x oil, confocal microscope). Merged red and green staining appears yellow.

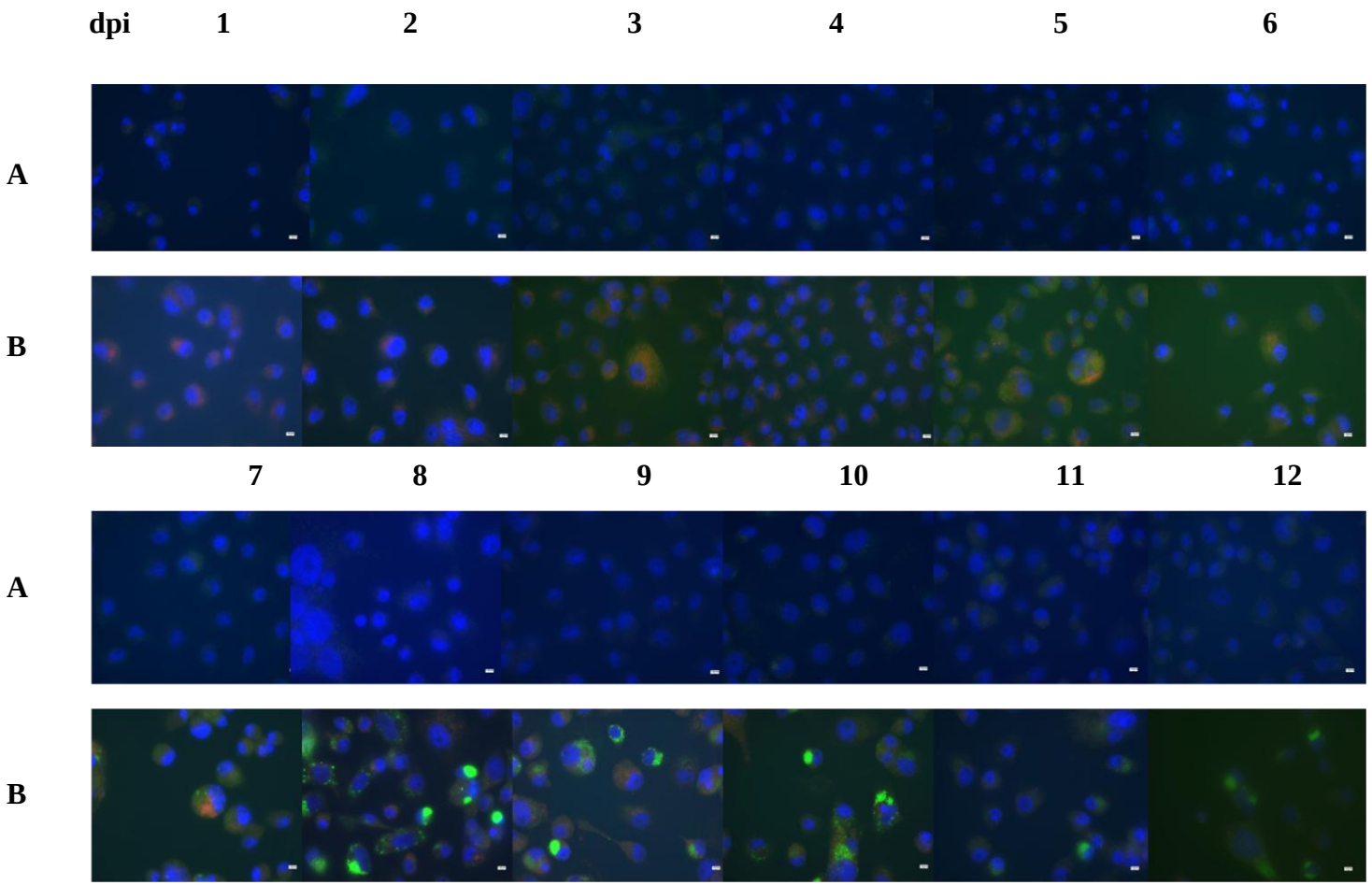

Figure 2.12a DsRNA and DENV C protein do not co-localize in infected C6/36 cells Fluorescent microscopy images of **A** mock-infected C6/36 cells and **B** DENV-infected C6/36 cells stained for both dsRNA and DENV C protein. The nuclei are stained with DAPI (blue), dsRNA with biotinylated J2 antibody (red), and DENV C protein antibody (green) (100x oil, fluorescent microscope). dpi = days post infection.

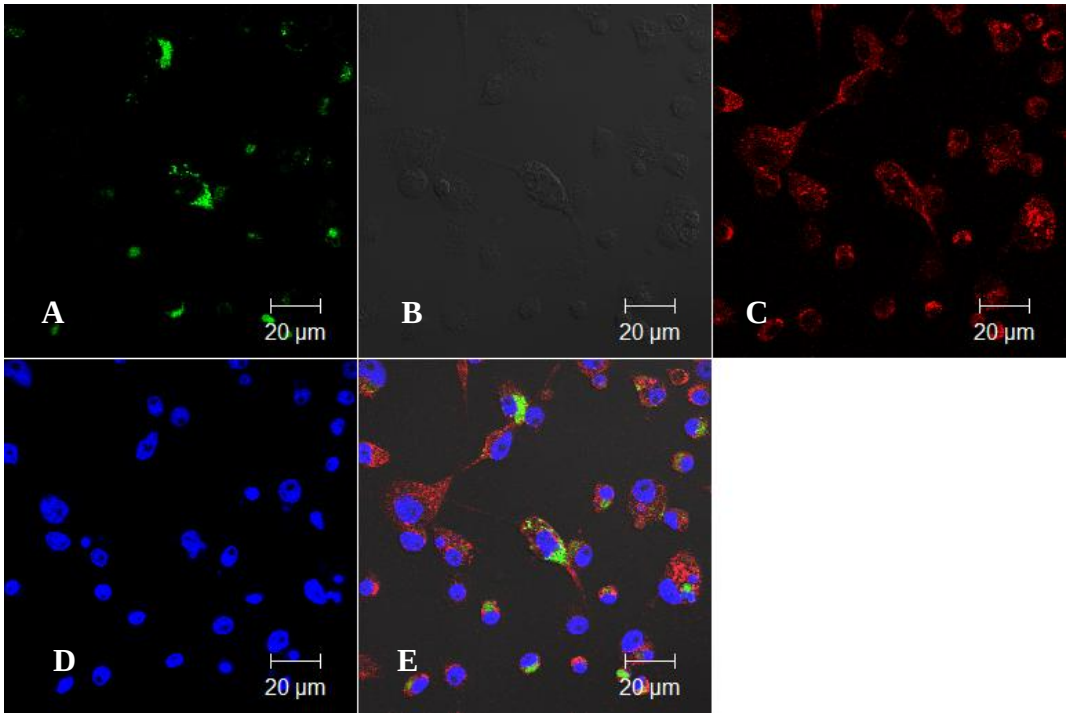

Figure 2.13 Localization of dsRNA and DENV C protein 10 dpi Images of **A-D**, DENV-infected, and **E**, mock-infected C6/36 cells stained for both dsRNA and DENV C protein. The stains are **A**, DENV C protein (green), **B**, dsRNA with biotinylated J2 (red), **C**, nuclei stained with DAPI (blue), and **D**, merged A, B, and C. **E** is also a merged image but because the cells are mock-infected there was no observable staining for C protein (green) or dsRNA (red) (63x oil, confocal microscope).

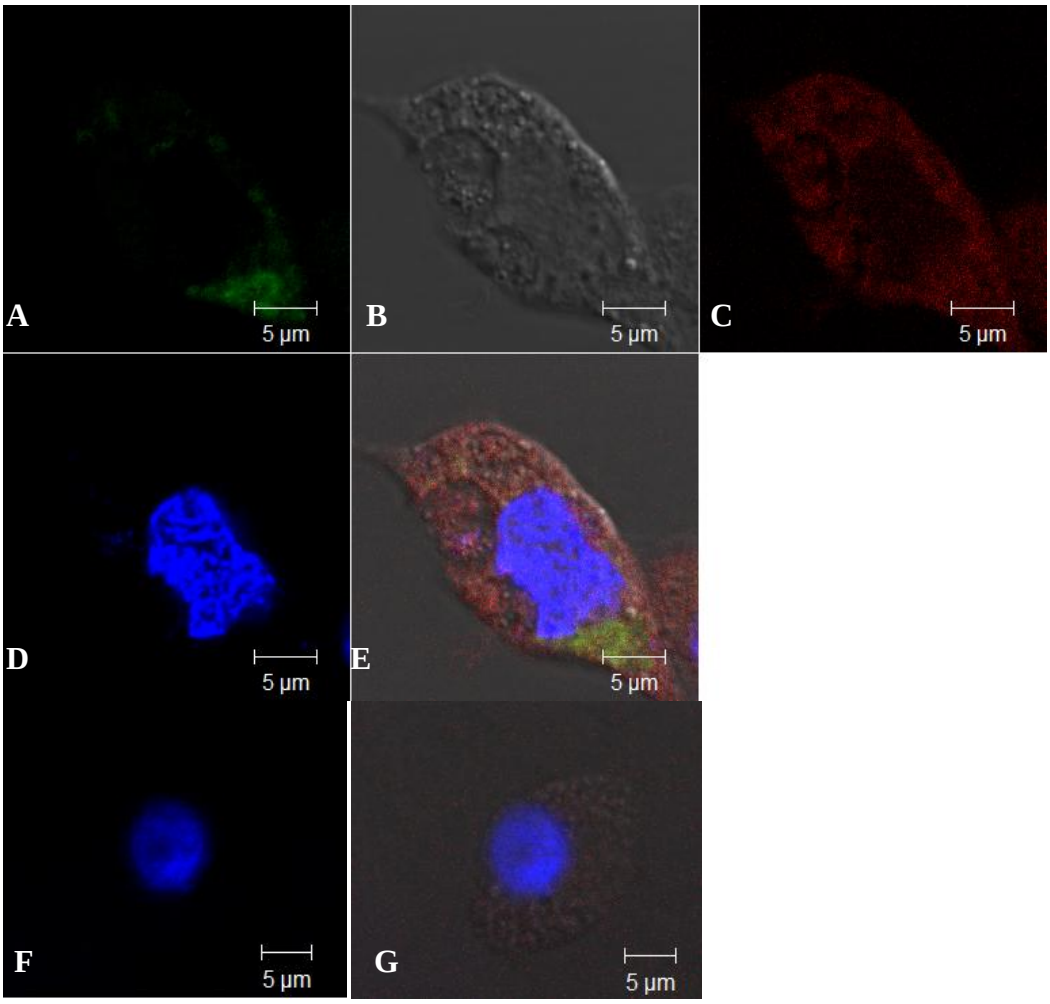

Figure 2.14 Localization of dsRNA and DENV C protein 10 dpi in single cell
Images of **A-E**, DENV-infected and **F-G**, mock infected C6/36 cell stained for both dsRNA and DENV C protein. The stains are **A**, DENV C protein (green), **B**, DIC (gray), **C**, dsRNA with biotinylated J2 (red), **D & F**, nuclei stained with DAPI (blue), and **E**, merged A, B, C, and D. **G** is also a merged image but because the cells are mock-infected there is no observable staining for C protein (green) or dsRNA (red) (cropped 63x oil, confocal microscope).

Localization of ER marker protein and dsRNA

To determine whether DENV replication causes proliferation of the ER, mosquito cells infected with DENV were stained for a protein marker of the ER, PDI, and examined via fluorescent and confocal microscopy. Fluorescence microscopy images of cells stained with antibodies specific for dsRNA and PDI showed minimal staining for PDI in C6/36 cells. Confocal microscopic analysis was sensitive enough to detect faint staining of the ER in mock-infected C6/36 cells at 7 dpi (data not shown). Confocal microscopic analysis revealed co-localization of dsRNA and PDI as well as an increase in intensity of staining for ER in the DENV-infected C6/36 cells at 7 dpi (Figure 2.15).

Electron microscopy

To visualize membranes associated with DENV replication, mosquito cells were infected, treated with detergent, cell fractions were separated via sucrose gradient density centrifugation, and concentrated material from fractions was examined via TEM. Electron microscopy imaging showed membrane bound vesicles that were 50-75 nm in diameter in samples from buoyant upper (1-3) fractions of sucrose gradients and through-focal imaging series confirmed that the structures were approximately spherical (Figure 2.16). Membrane-bound vesicles were sparse but consistently found in fraction 2 of the gradient. Detergent sensitivity testing further confirmed the likelihood that the structures were derived from membranes because they were not visible after treatment with DOC. The fact that the structures were resistant to treatment with TX100 but not DOC provides biochemical evidence that the structures were derived from ER (Figure 2.17).

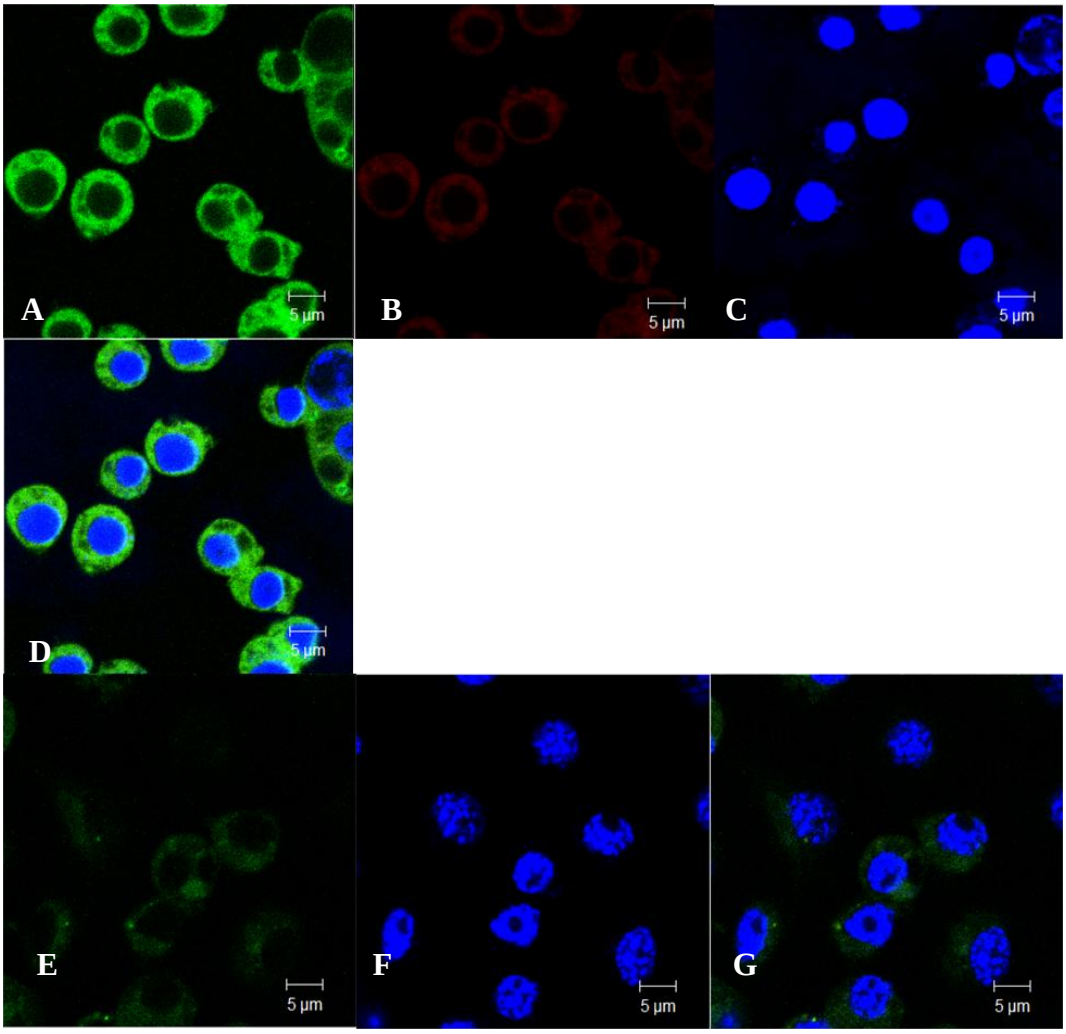

Figure 2.15 Co-localization of dsRNA and ER marker protein PDI in DENV-2 infected mosquito cells at 7dpi Images of **A-D,** DENV-infected, and **E-G,** mock-infected C6/36 cells stained for both dsRNA and PDI. The stains are **A & E,** ER marker protein PDI (green), **B,** dsRNA with biotinylated J2 (red), **C & F,** nuclei stained with DAPI (blue), and **D & G,** merged (cropped 63x oil, confocal microscope).

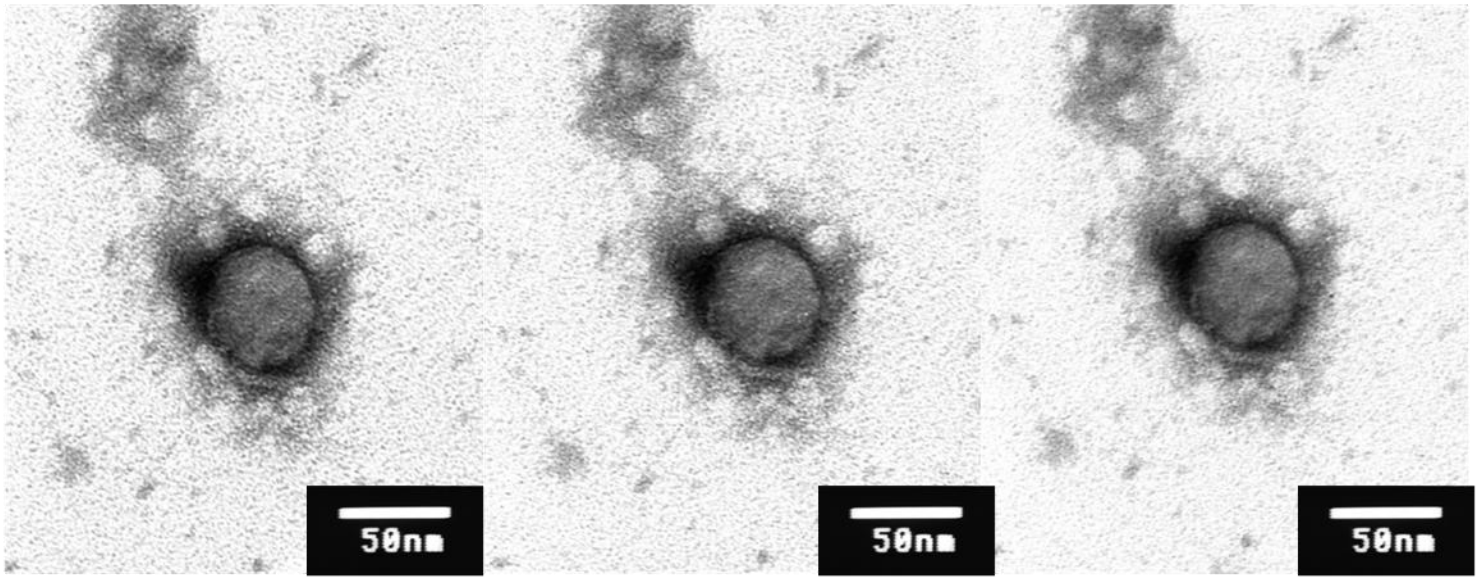

Figure 2.16 Transmission electron micrograph through-focal series of Trition-X100 resistant vesicle isolated from DENV-infected mosquito cells Images ranging through vesicle from fraction 2 of cell fractionation sucrose gradient of detergent-treated C6/36 cells. All images use the same size bar (100,000x, 100 kV, TEM).

A **B** **C**

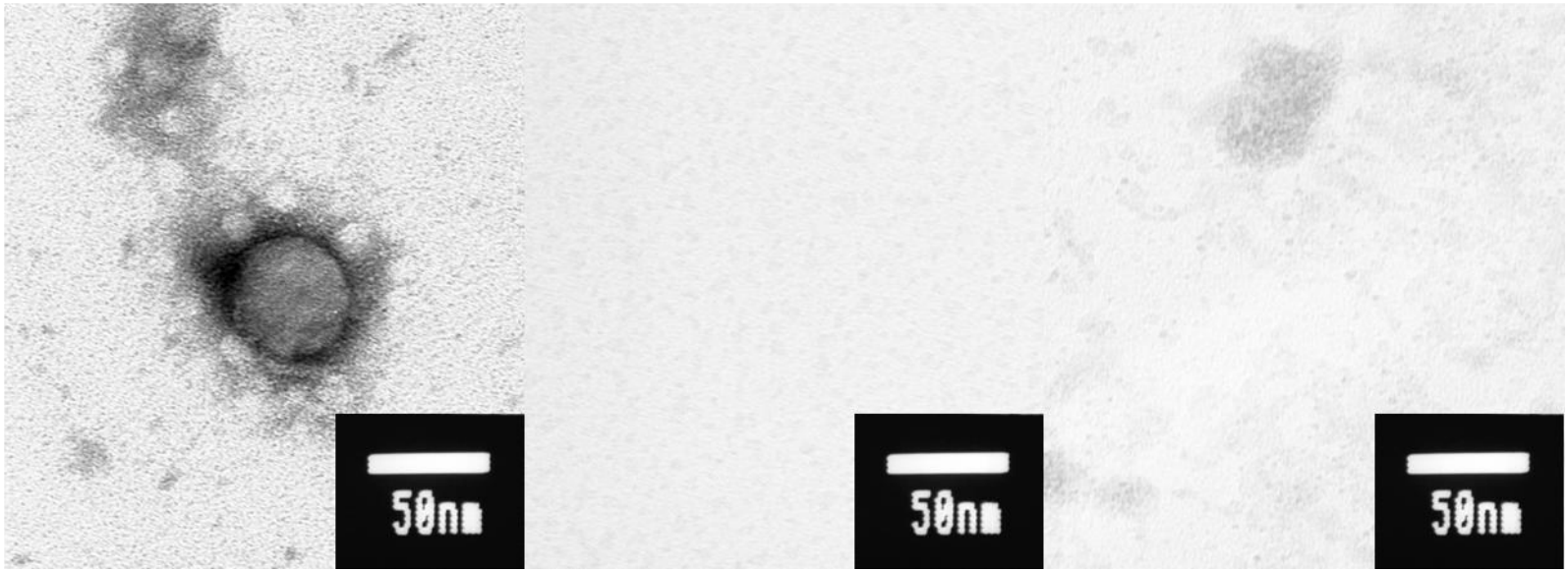

Figure 2.17 Transmission electron micrographs of detergent-treatment of isolated vesicles **A** vesicle from Triton-X100 treated DENV-infected mosquito cells, **B** no vesicles from Triton-X100 treated mock-infected mosquito cells, **C** no vesicles from sodium deoxycholoate treated DENV-infected cells (100,000x, 100 kV, TEM).

Membranes, like ER, which are enriched in sphingomyelin and cholesterol are TX100 resistant and DOC sensitive.

To ensure that vesicle-like structures observed in the cellular fractionation samples were not artifacts of sample preparation for TEM, infected and mock-infected cells from the same cell cultures used to prepare cellular fractionation samples were fixed, embedded, sectioned, and examined via TEM. Sections of DENV-infected C6/36 cells were thoroughly scanned via TEM and both vesicles and viral particles were observed. A representative image of a DENV-infected cell is shown in Figure 2.18 (A). Sections of mock-infected C6/36 cells were thoroughly scanned via TEM and no vesicle-like structures were observed. A representative image of a mock-infected cell is shown in Figure 2.18 (B). Vesicles ranged in size from 50 to 75 nm in diameter and virions within vacuoles were slightly smaller than 50 nm in diameter. Vesicles were observed within the cytoplasm of cells while virions were observed both within cells and just outside the plasma membrane.

In silico prediction of secondary structure of DENV genome

Forty-eight possible secondary structure configurations were produced and these results were enlarged and examined for dsRNA regions ≥40 bp in length. Several predicted structures had dsRNA regions ≥40 bp in length (Figure 4.19), but base-pairing of these structures was imperfect (Figure 2.20), and this imperfect base-pairing likely affects the binding of the J2 antibody. Schonborn et al. (1991) characterized the J2 antibody and found that it did not bind to naturally occurring dsRNA with imperfect base-pairing and short such as transfer RNAs (tRNAs).

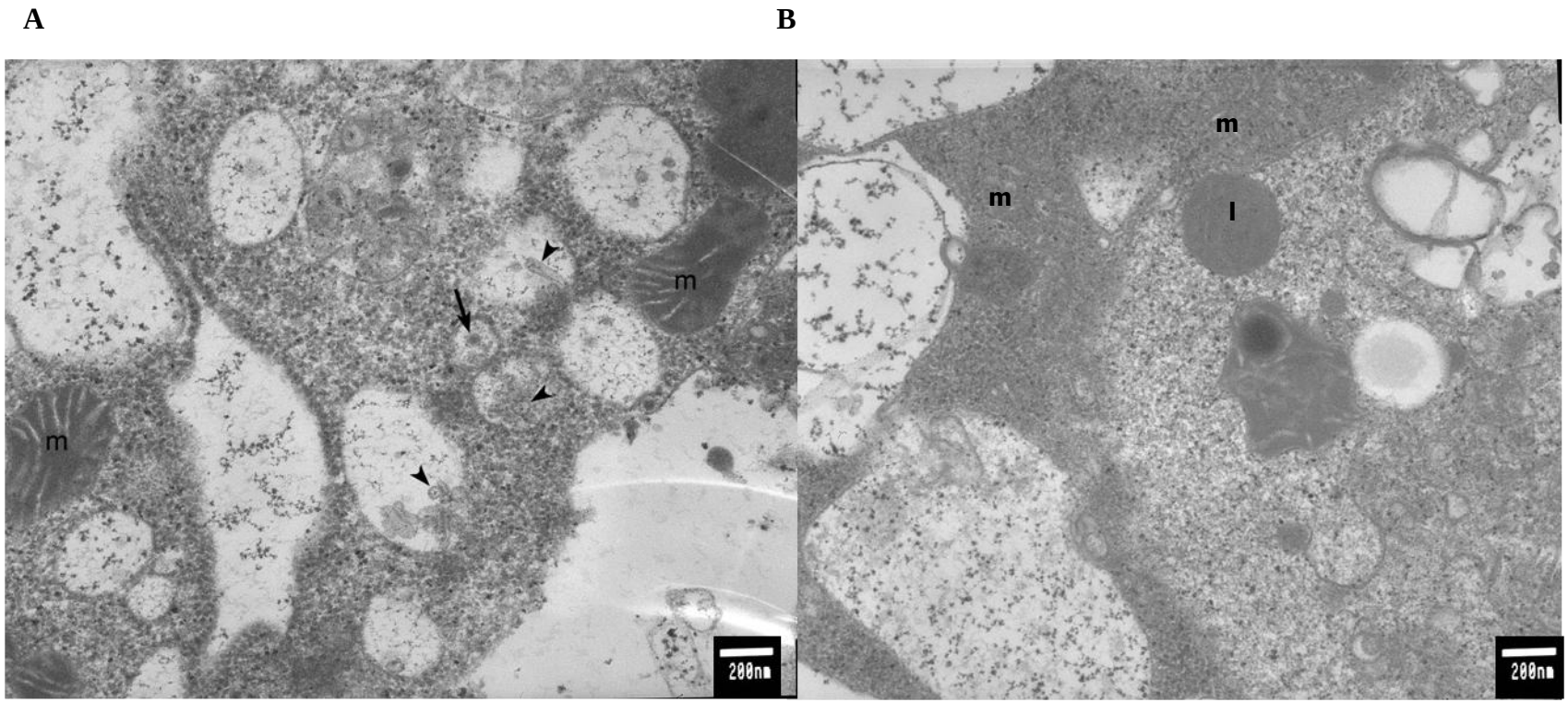

Figure 2.18 Transmission electron micrographs of mosquito cell thin sections at 5dpi C6/36 cells **A** DENV-infected **B** mock-infected C6/36 cells from which the sucrose gradient cellular fractionation samples shown in figures 2.16 and 2.17 were derived. Arrow = viral particle, arrowheads = vesicles, m = mitochondria, l = lysosome (30,000x, 100 kV, TEM).

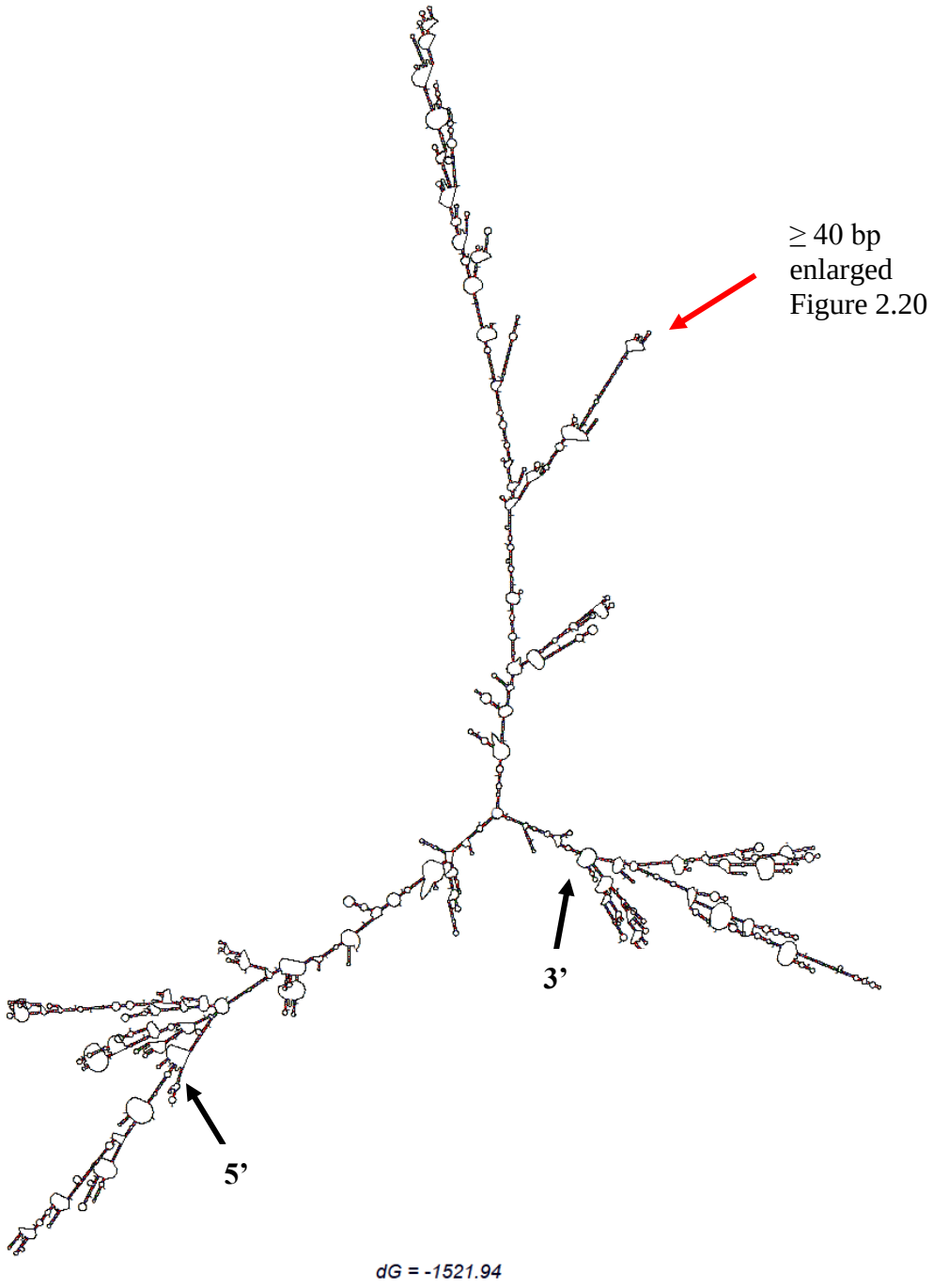

Figure 2.19 One prediction of secondary structure of DENV-2 (JAM1409) genome
One of the forty-eight possible secondary structures produced from first 6000 nt (input limit of the software) of DENV-2 RNA from mFold a software program used to predict nucleic acid folding. Mfold structures were used to determine whether genomic DENV could produce ≥40 bp dsRNA capable of detection by the J2 dsRNA antibody, which specifically detects dsRNAs ≥40 bp in length. Arrow indicates region ≥40 bp.

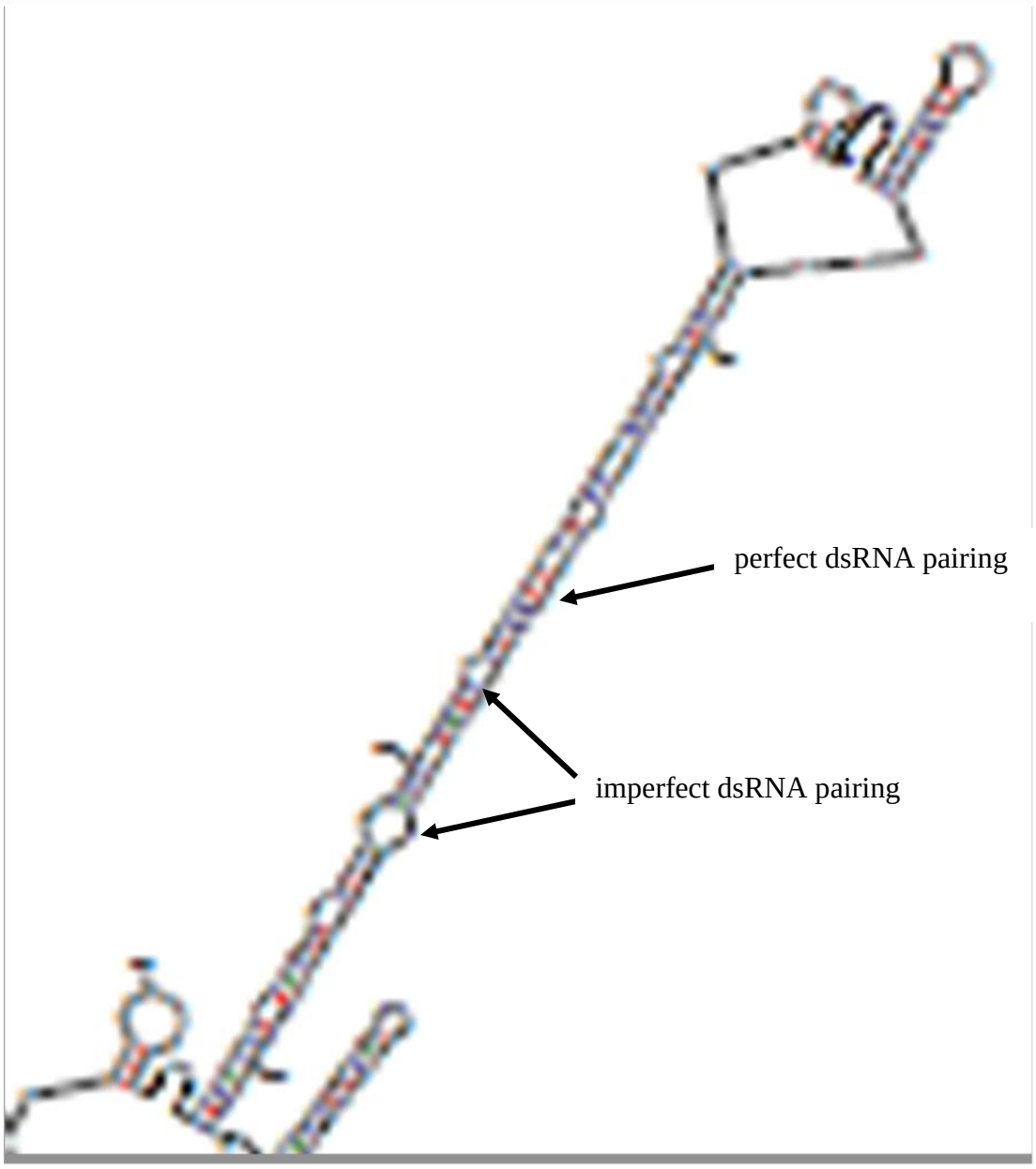

Figure 2.20 Enlarged area of predicted secondary structure of DENV-2 (JAM1409) genome Enlargement of Mfold structure predicted for genomic DENV showing imperfectly paired ≥40 bp dsRNA which would probably not be detected by the the J2 dsRNA antibody, which specifically detects dsRNAs ≥40 bp in length.

Discussion

We hypothesized that DENV replicates in association with ER-derived membranes in mosquito cells, and these membranes might protect replicative dsRNA from RNAi. We isolated DENV RNA-associated vesicles and examined their morphology, detergent sensitivity, and association with PDI. To determine whether vesicles we isolated could protect DENV dsRNA from RNAi, we compared vesicle size and Dicer dimensions and determined the vesicles might be sufficient to prevent Dicer from accessing the DENV dsRNA.

Detection of viral RNA species via RT-PCR

In a discontinuous sucrose gradient, sample materials that are placed in the middle of the gradient will be separated according to their buoyant density during centrifugation. RT-PCR detection of viral RNA in cellular fractions was consistent with the existence of the two expected intracellular forms of viral RNA associated with DENV replication, membrane bound replication complexes and virions. Membrane bound replication complexes would be predicted to be buoyant due to their higher lipid content, and virions would be denser because of their compact, protein-dense composition (Kuhn et al., 2002). RT-PCR results were consistent with the prediction that both the upper more buoyant fractions likely to contain the buoyant membrane-associated replication complexes and lower denser fractions likely to contain virions contained DENV-RNA (Figure 2.1). However, further characterization of viral RNA polarity and infectivity characteristics were needed to confirm this prediction.

Characterization of viral RNA species via strand-specific northern blot hybridization

Further characterization of viral RNA collected from cellular fractionation of detergent-treated DENV-infected mosquito cells via strand-specific northern blot hybridization revealed a broad distribution of genomic sense RNA in the upper fractions and a less intense band of anti-genome sense RNA in the same fraction. This is consistent with the composition of the replicative intermediate as discussed in Chapter 1, which is composed of paired genome sense and anti-genome sense strands during positive RNA synthesis. The compact band of full-length genome sense RNA with no corresponding anti-genome sense RNA found in the lower fractions is consistent with the genomic RNA expected in mature DENV virions (Figure 2.2). The intensity of the genome sense strand RNA detected was greater than the intensity of anti-genome sense RNA, which is consistent with the estimated 1 to 10 ratio of anti-genome sense to genomic sense strand in DENV replication intermediates observed by Richardson et al. (2006) at 5 dpi in *Aedes aegypti* mosquitoes. These results further support the hypothesis that the DENV-specific RNA detected in the buoyant upper fractions might be associated with membrane bound replication complexes and that the RNA from the denser lower fractions might be from virions.

The ratio of background to signal in these strand-specific northern blots for detection of anti-genome sense RNA, even after pooling samples from multiple experiments, suggests that this method might not be optimal for analyzing viral RNA species isolated via cellular fractionation. For this reason, in Chapter 4, strand-specific RT-PCR replaced strand-specific northern blot hybridization for RNA analysis.

Other researchers studying flavivirus membrane-associated replication complexes used radioisotopes to label viral RNA in mammalian cells instead of RT-PCR or strand-specific northern blot to track the location of flaviviral RNA (Uchil et al., 2003; Mackenzie et al., 1999). In our hands, attempts to directly label replicating viral RNA were unsuccessful, so we used RT-PCR and strand-specific northern blot analysis instead; there are no published data using RT-PCR or strand-specific northern blots to compare with our data. However, Westaway et al. (1999) localized newly synthesized Kunjin viral RNA to cytoplasmic foci that were imaged via TEM and resemble the vesicles observed in our micrographs of infected mosquito cells (Figure 2.18).

Characterization of gradient fraction contents via infectivity assay

To further characterize gradient fractions from sucrose gradient fractionation of detergent-treated DENV-infected mosquito cells, fractions were inoculated onto C6/36 cells and subsequently stained for DENV antigen to assay for the presence of infectious virus. This infectivity assay showed infectious material in lower fractions and minimal infectious material in the upper fractions, consistent with the hypothesis of buoyant replication compartments and dense virions (Figure 2.3). Combined with results from the RT-PCR and strand-specific northern blot hybridization, these data provide convincing evidence that we have isolated buoyant membrane-associated DENV replication complexes and dense virions in the cellular fractionation sucrose gradient.

Localization of dsRNA in infected mosquito cells: DENV

The perinuclear localization of dsRNA associated with DENV replication at 5 dpi in mosquito cells is consistent with the viral dsRNA localization patterns observed in mammalian cells (Figure 2.4) (Weber et al., 2006; Welsch et al., 2009). This suggests that, like DENV replication in mammalian cells, dsRNA as a marker of DENV replication in mosquito cells is associated with endoplasmic reticular membranes. DsRNA spatial localization in DENV-infected mosquito cells changes over time and will be discussed in more detail later in the discussion. The observation that DENV E protein is found throughout the cytoplasm is consistent with expectations for an antibody, 3H5-21, that recognizes a linear epitope and thus binds the DENV E protein, as it is post-translationally modified and matures in association with cytoplasmic membranes (Roehrig et al., 1998).

Localization of dsRNA in infected mosquito cells: SINV

The cytoplasmic localization of dsRNA associated with SINV replication, both MRE16 and TE3’2J strains, is consistent with published accounts of alphavirus replication compartments in cytoplasmic vacuoles (Kujala et al., 2001). The minimal intensity differences observed between dsRNA or antigen patterns for the two strains of SINV is consistent with published reports comparing replication of MRE16 and AR339-based strains like TE3’2J showing similar growth curves in mosquito cell culture (Figure 2.4) (Myles et al., 2004). Based on Myles et al.’s (2004) observations of titer differences in the mosquito midgut, we predict that differences between the two virus strains,

MRE16 and TE3’2J, will be readily observable in the mosquito midgut. Chapter 4 will address this possibility in more detail.

Localization of dsRNA in infected mosquito cells: LACV

As expected from literature on detection of dsRNA by IFA of LACV-infected mammalian cells, no dsRNA was observed in association with LACV replication mosquito cells; since LACV does not have a dsRNA replicative intermediate (Weber et al., 2006) (Figure 2.5). This lack of staining for dsRNA could not be attributed to lack of replication as infection was verified by staining for LACV structural proteins. LACV resembles other negative strand RNA viruses, which are known to replicate and transcribe RNA in tight association with their nucleocapsid protein (Albertini et al., 2006; Green et al., 2006). This tight association of nucleocapsid and template RNA could render replicating RNA completely inaccessible to antibody detection; alternatively, the extent of the dsRNA regions might have been too short to be detected by J2 monoclonal antibody which detects ≥40 bp regions (Schonborn et al., 1991).

Short regions of LACV dsRNA are not detectable by IFA staining in mammalian cells (Weber et al. 2006) or in mosquito cells (Figure 2.5). These data have implications for the role of LACV NSs protein as a viral suppressor of RNAi or interferon (IFN) suppressor (Blakqori et al., 2007; Soldan et al., 2005). Virus-specific Small RNAs are produced during LACV infection of mosquito cells, but no LACV specific dsRNA is detectable by IFA staining (Blakqori et al., 2007; Weber et al., 2006). These two facts raise the question of whether the LACV small RNAs were derived from secondary

structure of LACV genomic or messenger RNA because no dsRNA replicative forms are present.

Comparison of localization of dsRNA in mosquito cells: DENV, SINV, and LACV

In spite of significant differences in replication strategies, there are minimal differences in localization of dsRNA associated with DENV and SINV replication in mosquito cells. In both cases, dsRNA is located where replication complex components are known to be assembled, perinuclear foci for DENV and cytoplasmic vacuoles for SINV. LACV-associated dsRNA could not be detected by IFA using the dsRNA monoclonal antibody discussed here. Perhaps comparison of dsRNA localization using confocal microscopy in three-dimensions or dsRNA localization within the mosquito midgut, as discussed in Chapter 4, will be more enlightening about localization differences of dsRNA, as a marker of arbovirus replication. The experiments described in this chapter provided the methodological basis for the imaging of dsRNA in mosquitoes.

Localization of dsRNA in transformed mosquito cell lines: FB9.1 cells

FB9.1 cells are C6/36 mosquito cells that have been transformed with a plasmid that constitutively expresses an inverted repeat RNA derived from the DENV-2 genome. The observation that dsRNA in FB9.1 cells appears to localize primarily to the nucleus prior to DENV challenge confirms that the prM RNA hairpin is not transported out of the nucleus. DsRNA in the nucleus has been described previously in LT C-7 *Aedes albopictus* cells and was attributed to heterogeneous nuclear RNA (Stollar et al., 1978).

There is no evidence to suggest that the dsRNA observed in the FB9.1 cells is heterogeneous nuclear RNA as it has not been observed in IFAs for dsRNA in non-transformed C6/36 cells or H9.1 cells that did not express inverted repeat RNA.

Staining of DENV E antigen by IFA in approximately 25% of the DENV-challenged FB9.1 cells, which should be resistant to DENV infection, suggests that FB9.1 cells had partially lost their resistance at the time of challenge (Figure 2.6). Adelman et al. (2002) reported that their cell lines transformed to produce prM foldback RNA typically retained resistance, defined as less than 1% of cells expressing DENV E antigen via IFA, for 40-50 passages. The FB9.1 cell lines used for dsRNA staining were at passage 29 according to Dr. Travanty's records. According to Adelman et al. (2002), FB9.1 cells at this passage should still be resistant. However, if the passage number was re-initiated at zero when the cells were transferred from Dr. Adelman to Dr. Travanty, the actual passage number may have been higher than 29 and the inverted repeat plasmid may have had more time to develop mutations leading to a loss of resistance. We could have tested this by extracting the RNA from FB9.1 cells, amplifying the prM region via RT-PCR, sequencing the prM region, and analyzing the FB9.1 prM region for mutations.

This loss of DENV resistance may have foreshadowed the loss of resistance that occurred in the Carb77 transgenic mosquito line. However, the Carb 77 transgenic mosquito line lacked a gene drive mechanism while the FB9.1 cells were under hygromycin selection pressure. So the mechanism of resistance loss in the FB9.1 cells was probably different from the Carb77 mosquitoes in which the transgene was found to be present but inactivated by an unknown mechanism (Franz et al., 2009). However, 10-30% FB9.1 cells that had lost resistance to DENV were surviving in the presence of

hygromycin, so perhaps the prM sequence was lost, suppressed, or dissociated from the hygromycin resistance marker. Loss of the prM sequence in FB9.1 cells could occur from a random deletion or mutation that disrupted the expression or function of the prM region or otherwise separated the prM region from the hygromycin selection sequence by an unknown mechanism. Additionally, the FB9.1 cells were found to have a high copy number of the prM expression transcript from plasmid in Dr. Travanty's Southern blot testing, so perhaps the fitness cost of expressing the plasmid was too high for C6/36 cells to maintain for many passages (Travanty, 2005). These questions could have been resolved by Southern blot detection of the prM transcript in FB9.1 cells which have lost resistance to DENV-2.

We had planned to further evaluate the FB9.1 cells that had lost resistance to DENV by comparing DENV-challenged FB9.1 and H9.1 cells via virus titration and IFA. Since both the FB9.1 and H9.1 cell lines were shown to be positive for LACV RNA via RT-PCR, we did not do further experiments involving DENV challenge (Figure 2.7). The LACV infection could also explain why FB9.1 cells lost resistance to DENV.

Temporal and spatial co-localization of DENV E antigen and dsRNA

The observation that DENV E protein and dsRNA are in temporal and spatial close proximity in mosquito cells (Figures 2.8 - 2.11) is not surprising in light of the three-dimensional structure of the DENV replication compartment in mammalian cells as seen by EM tomography (Welsch et al., 2009). This EM tomography model of DENV replication reveals that virus particles are found in a region of the ER that is contiguous with replication vesicles. In immuno-EM staining, this same group found that antibody to

the E protein did not label the vesicles or convoluted membranes (CM); however, it did label the ER, confirming the EM tomography data. Although the greater resolution of electron microscopy used by Welsch et al. (2009) allows for more precise observations about the localization of dsRNA and E protein than confocal microscopy, our confocal microscopic images showing large foci of E protein near dsRNA could also support a model of DENV replication and assembly in a network of membranes. The co-localization of dsRNA and DENV E protein was confirmed by three-dimensional sectioning by confocal microscopy of the samples used in the timecourse experiments.

It is unclear whether the J2 dsRNA antibody recognizes secondary structure of single-stranded viral genomic RNA or dsRNA associated with viral replication. This could have been determined by an antibody-RNA association or "pull-down" experiment. It is possible that the fairly constant level of dsRNA detection and localization throughout the entire cytoplasm may indicate that both forms of viral dsRNA are being recognized by the J2 antibody.

Localization of DENV C antigen and dsRNA

DENV C protein and dsRNA did not consistently co-localize in DENV-infected C6/36 mosquito cells. DsRNA staining was diffuse from 1-12 dpi while C protein was diffuse 1-6 dpi and from 7-12 dpi dsRNA C protein staining was intense and localized to one side of the nucleus. Our C protein localization pattern of an intensely stained focus on one side of the nucleus is consistent with previous observations of DENV C protein staining in DENV-infected C6/36 cells (Sangiambut et al., 2008).

The nuclear magnetic resonance (NMR) structure of the DENV C protein homodimer suggests that there is a fold in the structure where the C protein interacts with the genomic viral RNA (Ma et al., 2004). The small area of overlap between locations of DENV C protein and dsRNA could correspond with where C protein and newly-synthesized viral genomes associate in the cytoplasm, and if the dsRNA being recognized at this point is the secondary structure of the genomic RNA. The J2 antibody can detect completely complementary dsRNA duplexes ≥40 bp but doesn't detect naturally occurring dsRNAs with basepair mismatches like transfer RNAs (tRNAs). Predictions of secondary structure of DENV-2 (JAM1409) using mFold software did not predict perfectly matched dsRNA regions of ≥40 bp (Figure 2.19). Instead the predicted secondary structures of genomic DENV RNA more closely resemble a more complicated tRNA-like structure. Transfer RNAs have shorter regions of perfect dsRNA pairing rather than a simple perfectly paired dsRNA such as would be produced by pairing of genome sense and anti-genome sense RNAs during replication. The affinity of J2 for short dsRNAs ≤11 bp is very low, but it seems plausible that secondary genomic RNA structures like those in Figures 2.19 and 2.20 might be detected but at lower affinity than perfectly matched dsRNA regions of ≥40 bp (Schonborn et al., 1991).

Co-localization of ER marker protein and dsRNA

The co-localization of an ER marker protein and dsRNA was expected based on many reports of ER proliferation associated with flavivirus infection (Chu and Westaway, 1992; Girard et al., 2005; Grief et al., 1997; Ng, 1987). The faint PDI staining in uninfected cells and increase in staining intensity in DENV-infected C6/36 cells (Figure

2.15) was consistent with previously published attempts to stain for ER markers during flavivirus replication in mammalian cells, which noted the pattern of PDI staining undergoes rearrangement and an increase in intensity in flavivirus-infected cells (Mackenzie et al., 1999; Welsch et al., 2009). In agreement with our results, Welsch et al. found that replication vesicles were immunolabeled with PDI, but in contrast to our results, they observed ER staining at lower levels in DENV-infected cells than non-infected ER in mammalian cells, which they suggested indicates that PDI is partially excluded from the structures. A similar observation in poliovirus research found no co-fractionation of poliovirus vesicles with ER, Golgi, lysosomal, or mitochondrial protein markers. Suhy et al. (2000) proposed this loss of intracellular markers might be due to a vesicle budding mechanism in which the clustering of viral proteins on the ER led to an ER-derived vesicle that excluded the typical cellular protein markers of ER. Overall, these confocal images of increased intensity of PDI staining in DENV-infected mosquito cells suggest that ER membranes proliferate in DENV-2 infected mosquito cells.

Electron microscopy

Electron microscopic imaging of subcellular fractions suggested that the viral specific RNA observed in more buoyant samples of cellular fractionation experiments was associated with membrane-enclosed structures that resemble the membrane-bound replication compartments observed in mammalian cells (Uchil and Satchidanandam, 2003) (Figure 2.16). Additionally, the through-focal EM series of material concentrated from gradient fractions and detergent sensitivity testing support a model of ER-derived, spherical membrane vesicles of 50-75 nm diameter that are sensitive to strong non-ionic

detergent, which are formed in association with DENV replication in mosquito cells (Figure 2.17).

The TEM images of thin sections of DENV-infected mosquito cells showed that the vesicle structures are not an artifact of the cellular fractionation method and that they were specific to DENV-infected cells, as vesicles were not found in mock infected cells (Figure 2.18). We did not observe the paracrystalline arrays noted by Grief et al.(1997) or the large quantities of virions observed by Hase et al. (1987). This discrepancy could be explained by differences in infecting MOIs. The infecting MOI used by Hase et al. was 50-60 compared to our MOI of 0.1. *In situ* hybridization electron microscopy by Grief et al. (1997) on DENV-infected mosquito cells localized single-stranded RNA (ssRNA) to smooth membrane structures (SMS). Mackenzie et al. (1999) localized dsRNA to vesicle packets on Kunjin virus-infected mammalian cells via immunoEM. The Grief and Mackenzie groups looked at different parts of the replication complex described by Welsch et al. (2009). The ssRNA in Grief et al. (1997) probably localized to the virion assembly region as suggested early in infection when overlap of our DENV C protein and dsRNA staining was observed. Mackenzie et al. (1999) observed buoyant vesicle packets that localized with NS proteins and dsRNA that was consistent with our isolation of buoyant vesicles from fractions that typically contain dsRNA, and Welsch et al. (2009) recently reported immuno-EM localization of viral NS proteins to vesicle packets.

Based on the work of Uchil and Satchidanadam (2003), the detergent sensitivity of our vesicles suggested that the vesicles are ER derived. Membranes that are enriched in sphingomyelin and cholesterol, such as the ER membrane, cannot be disrupted in cold

non-ionic detergent, like the ice cold TX100 we used to isolate vesicles from DENV-infected mosquito cells before sucrose gradient fractionation (Jacobson and Dietrich, 1999; Uchil and Satchidanandam, 2003). Since DENV DENV replication-associated vesicles are resistant to cold TX100, they may be enriched in cholesterol and sphingolipids. Cholesterol and sphingolipids have been shown to be required for both fusion and budding of alphaviruses, but less data is available as to whether flaviviruses require these lipids for replication (Lu and Kielian, 2000; Smit et al., 1999). However, a recent study suggested that disruption of detergent-resistant membranes in Japanese encephalitis or DENV-infected mammalian cells inhibits replication (Lee et al., 2008a). Lee et al. (2008) used a method similar to our cellular fractionation on sucrose gradients and showed that NS3 localizes to bouyant fractions in sucrose gradients of DENV-infected mammalian cells. These data fit with our hypothesis that our detergent resistant membranes are replication compartments as they would be likely to contain NS proteins.

Vesicle structures and virions were observed in thin sections of DENV-infected cells via TEM but not in mock-infected cells (Figure 2.18). This further confirms that vesicles are specific to DENV infection. The observed diameters of vesicles (50-75 nm) and virions (approximately 50 nm) were consistent with the observations of Welsch et al. (2009). This size range is also similar to the vesicle size range reported for other flaviviviruses such as Kunjin (50-100 nm) and yellow fever (80-100 nm) (Deubel and Digoutte, 1981; Mackenzie et al., 1999). This raises the question of whether conserved vesicle size may indicate a conserved mechanism of vesicle-production in flaviviruses.

Overall, the observed vesicle structure was in agreement with data from Uchil and Satchidanadam (2003) but not Welsch et al. (2009), due to the lack of observation of a

pore; however, Welsch et al. noted that the observation of a pore was dependent on the method of fixation used in their experiments. The presence of the vesicles raises the question of how DENV RNA exits through the pore of the replication vesicles? Uchil and Satchidanadam (2003) speculated that "viroporins" could extrude the RNA from the vesicles, but they did not observe pores. Welsch et al. (2009) suggest that the pore would allow nucleotides in and RNA out but did not suggest a possible mechanism. Perhaps a viral or host RNA binding protein could be used as a chaperone. Future research into the mechanism of vesicle formation and pore composition should include experiments to determine how RNA movement in and out of the replication vesicles is regulated.

Can Dicer access the dsRNA of replicating DENV in mosquito cells?

After finding that replicating hepatitis C virus (HCV) RNA is mostly resistant to experimental nuclease treatment, Quinkert et al. (2005) proposed a model of HCV replicative complex vesicles with a pore size that excludes proteinase K (29 kD) and S7 nuclease (17 kD). Unfortunately, our experiments to address the corresponding hypothesis in DENV replication, that Dicer cannot access the dsRNA of DENV replicative intermediates, were inconclusive. Uchil and Satchidanadam (2003) had similarly inconclusive results when they found that after ionic detergent was used to disrupt membranes associated with flavivirus RNA, the exposed RNA was not vulnerable to RNase treatment. They suggested that this indicated that flaviviral RNA was surrounded by a protein coat. However, when they sequentially treated RNA-associated membranes with detergent, then trypsin, RNA was still resistant to RNAse treatment, and this discrepancy was attributed to incomplete trypsin digestion. Our data showing DENV

dsRNA staining with J2 does not support their hypothesis that DENV RNA is protected by proteins. If DENV RNA was protected by protein, we might expect the dsRNA of DENV-infected cells staining to resemble LACV-infected cells in which replicating RNA is likely to be protected by nucleoprotein like other negative-strand RNA viruses (Albertini et al., 2006; Green et al., 2006). We compared dsRNA staining between LACV-infected cells and DENV-infected cells and detected no dsRNA staining in LACV-infected cells and dsRNA staining in DENV-infected cells, suggesting that DENV dsRNA should be vulnerable to RNases.

Based on the comparison of our electron microscopy results with the Welsch et al. (2009) EM tomography model, it is reasonable that ER-derived vesicles created during DENV replication in mosquito cells should have a pore size of approximately 10 nm. So what size is Dicer? The crystal structure of mosquito Dicer 2 is not available, but the structure has been solved for Dicer from *Giardia intestinalis* (http://www.rcsb.org/pdb /results/results.do?tabtoshow=Current) and is approximately 65 angstroms by 100 angstroms (6.5 nm x 10 nm) (MacRae et al., 2006). If the mosquito Dicer 2 protein is similar in size, it would be difficult but not impossible for Dicer to access the dsRNA through a 10 nm pore.

Overall, the RT-PCR, northern blot data, infectivity assay, fluorescent microscopy data, co-localization of DENV E protein with dsRNA throughout replication and lack of co-localization of C protein with dsRNA at 7-12 dpi, is consistent with the electron tomography model proposed by Welsch et al. (2009). The electron microscopy data reported in this chapter suggest that DENV replication occurs in association with vesicles in mosquito cells. These vesicles are 50-75 nm in diameter, of ER origin, and

specifically associated with DENV replication as they cannot be isolated from mock-infected cells.

This is the first isolation of DENV replication-associated membranes from mosquito cells. These vesicles have similar characteristics to vesicles isolated from DENV-infected mammalian cells. Replication of DENV RNA within a vesicle, which may make it difficult for Dicer 2 to reach dsRNA replicative intermediates, has implications for the antiviral activity of RNAi in the mosquito cell and implications for the development of an RNAi-based DENV-resistant transgenic mosquito. Since small RNAs from the anti-genome strand of DENV are produced and anti-genome strand is likely protected by membranes during replication, the question of where Dicer accesses anti-genome strand remains. Is the anti-genome sense strand vulnerable to Dicer before replication-associated membranes are formed or after it has served as a template for transcription of DENV genomes. The next chapter will discuss possible mechanisms for the formation of these DENV replication associated membranes.

Chapter 3

Does expression of dengue virus nonstructural proteins 4A and 4B cause membrane rearrangements in transformed mosquito cell lines?

Introduction

One of the major questions for researchers studying viral replication compartments is how viruses orchestrate the rearrangement of host intracellular membranes. Many non-structural (NS) proteins from positive-strand RNA genome viruses have hydrophobic regions, which suggests that they may interact with or become embedded in cellular membranes (Salonen et al., 2005). Miller and Krijnse-Locker (2008) have suggested three different ways that viral NS proteins may cause membrane rearrangement: proteins with amphipathic helices cause membranes to bend and curve as the helices pull across the lipid bilayer, proteins with a conical structure cause membranes to curve around them, and oligomerization of proteins can distort or curve membranes.

Studies of membrane-bound viral replication complexes (RC) look at the interactions of viral NS proteins with host membranes, host proteins, and viral RNA. To begin to examine viral RCs, typically researchers investigate the roles of NS proteins or localization of replicating viral RNA. To study NS proteins outside of natural virus infections, researchers often use protein expression plasmids and then track the localization of the proteins by fluorescent or confocal microscopy. Further experiments typically seek to co-localize NS proteins with replicating RNA or membranous organelles like the Golgi or ER via immunofluorescent microscopy and immunoEM. Once the NS proteins that comprise the viral RC are known, yeast two-hybrid (Y2H) or co-immunoprecipitation techniques are used to identify interactions beween host proteins and NS proteins. These experiments have led to the suggestion of various cellular

membrane-associated processes that viruses could co-opt to form RC-associated membranes. Various cellular membrane-associated processes have been suggested as the mechanism that flaviviruses or other +RNA viruses could co-opt to use for RC compartment membranes. Mechanisms of RC compartment membrane formation include co-opting autophagy, unfolded protein response (UPR), or lipid raft formation. We will briefly explain the mechanisms of RC compartment membrane formation, review the literature on RCs of +RNA genome viruses here, then discuss how we investigated the role of DENV NS proteins in RC compartment membrane formation.

Autophagy is typically triggered by starvation and leads to the breakdown and recycling of cellular organelles (Dunn, 1990a). How the starvation or other autophagy initating signal is relayed to the autophagic membrane forming mechanism is not understood but autophagy related gene 6 (Atg6), also known as Beclin-1, initiates the formation of the autophagosome. The vesicle elongates, engulfing foreign material, and Atg proteins 4, 5, 6 and 12 recruit Atg8 or microtubule-associated protein 1 light chain 3 (LC3) as the double membrane bound autophagosome formation is completed. LC3 becomes lipidated and associates with the membrane (Orvedahl and Levine, 2008). The autophagosome fuses with the lysosome, which contains lysosome associated marker proteins (LAMP), and forms a single membrane bound autolysosome that degrades its contents.

The membrane-bound form of LC3-II is the only universally accepted and experimentally demonstrated accepted marker of autophagy in mammalian cells (Kabeya et al., 2000). Lysosomal-associated membrane protein (LAMP) is also used as a marker of autophagy since the protein is essential for early autophagic vacuoles to become

degradative vacuoles (Tanaka et al., 2000). However, since lysosomes may also contain LAMP as a marker, LAMP alone is not considered an infallible marker of autophagy.

The unfolded protein response (UPR) is triggered by ER stress due to unfolded or misfolded proteins. The UPR can both halt translation and increase production of chaperone proteins to increase the capacity to fold translated proteins. There are three UPR pathways: (1) the protein ER resident kinase (PERK), which stops translation by phosphorylating initation factor 2 alpha (eIF2α); (2) the inositol-requiring kinase (IRK), which activates transcription factor XBP1 mRNA by promoting an alternate splice site and XBP1 migrates to the nucleus and upregulates stress genes and can increase the capacity of the ER; and (3) ATF6, which also upregulates stress genes (Harding et al., 1999; Molinari et al., 2002; Sriburi et al., 2004). Immunoblot detection of phosphorylated eIF2α, RT-PCR showing XBP1 splicing, and immunoblots showing increased levels of ATF6 protein are all used as experimental markers of the UPR.

Lipid rafts are characterized by sphingomyelin and saturated phospholipids that are resistant to extraction by cold TritonX-100 (Jacobson and Dietrich, 1999). The mechanism of lipid raft formation is unclear but lipid rafts are generally unstable unless the lipids interact with proteins. The presence of lipid rafts can be experimentally determined by fluorescent resonance energy transfer (FRET) which shows clustering (Anderson and Jacobson, 2002). There are two types of lipid rafts, planar and caveolae, which appear as concave areas on the plasma membrane and contain caveolin protein markers (Pietiainen et al., 2005).

The mechanism of +RNA virus RC-associated membrane rearrangement is probably best understood for poliovirus (PV). Doedens et al. (1997) expressed PV

protein 3A and showed via immuno EM that 3A localized to the ER and caused the organelle to dilate, which they suggested was the result of 3A-mediated inhibition of ER to Golgi trafficking. A study using strand-specific FISH and IFA to proteins 2C and 2B found that PVRNA co-localizes with 2C and 2B to the periphery of the nucleus (Bolten et al., 1998). Using cellular fractionation and immuno EM, Schlegel et al. (1996) suggested a mechanism similar to autophagy for the origin of PV replication compartment membranes. Continued investigation of the mechanism of PV RC compartment formation has produced data supporting both the autophagy and secretory pathways of vesicle origin.

Suhy et al. (2000) found that transfection of plasmids expressing PV 3BC and 3A produced vesicles that resembled vesicles in PV-infected cells via buoyancy gradients and immunoEM. Since no ER proteins or other organelle proteins colocalized with these membranes, Suhy et al. (2000) argued that they must arise from the autophagy pathway. In an effort to evaluate the role of autophagy in PV infection, Jackson et al. (2005) found that chemical stimulation of autophagy increased PV titers. Taylor et al. (2007) looked at artificial expression of the LC3 marker of autophagy and found that it became lipidated and membrane-associated during PV infection just as in natural autophagy. Taylor et al. (2009) found artificially expressed LC3 localizes in vesicles during PV infection that resemble autophagosomes except that unlike autophagosomes, which move along microtubules, they are immobilized. Additionally, using a microtubule disrupting agent, nocodazole, and mutant PV with reduced interactions with the host cytoskeleton, Taylor et al. (2009) found that extracellular virus increased with increased vesicle mobility, so

they suggested that an autophagy-like mechanism may provide an additional exit pathway for PV.

Meanwhile, Dodd et al. (2001) showed through characterization of PV 3A mutants that PV 3A causes disruption of normal cellular secretion, thus reducing cytokine secretion and the host immune response to the virus. Rust et al. (2001) used confocal imaging to show co-localization of plasmid-expressed PV 2BC with Sec 13 and 31, cellular coat protein complex (COP II) components which are involved in vesicle transport between the ER and Golgi. Based on this evidence, Rust et al. (2001) argued for a COP II-mediated anterograde transport pathway origin for PV vesicles. Belov et al. (2007) have taken a closer look at host proteins involved in PV membrane formation and found that 3A and ACD directly interact with ADP-ribosylation factors (Arf) proteins that control membrane rearrangement for COPII-mediated ER to Golgi trafficking. Belov et al. (2008) evaluated a Brefeldin A (BFA) sensitive step of RC formation, which they hypothesized meant PV replication was dependent on the cell secretory pathway and found mutations in host Arf proteins that allowed production of RC-associated vesicles in the presence of BFA. However, these RC compartments formed in the presence of BFA, which inhibited the cell secretory pathway, so that infected cells were unable to produce PV (Belov et al. 2008).

Current consensus is that PV definitely uses a cellular membrane rearrangement pathway, and the mechanism is analogous to autophagy and uses COP II pathway components. Experiments to test both hypotheses have limitations. LC3 experiments to test the autophagy hypothesis use artificial expression of LC3, which may not be representative of natural LC3 localization. Experiments to test the COPII hypothesis use

artificially expressed PV proteins or mutant viruses, which may not be representative of mechanisms occuring during natural infections.

The most well understood RC of the family Flaviviridae is the Kunjin virus RC. KUNV is now considered to be a subtype of West Nile virus, but will be referred to here as KUNV for ease of discussion (Hall et al., 2001). In studying the DENV RC, it is helpful to review the KUNV RC literature to learn useful techniques for the study of viral RCs and gain a broader understanding of flavivirus membrane-associated RCs by comparing the two viruses. Using IFA to NS proteins, confocal microscopy, and immunoEM, the KUNV NS1, NS2a, NS2b, NS3, NS4a, NS4b, and NS5 proteins were shown to localize mainly within the vesicle packets in the cytoplasm as well as colocalize with each other and dsRNA (Mackenzie et al., 1996; Mackenzie et al., 2007; Mackenzie et al., 1998; Westaway et al., 1997a; Westaway et al., 1997b). Newly synthesized RNA was shown to be located near genomic dsRNA via bromouridine labeling and BFA experiments (Westaway et al., 1999). IFA and immunoEM staining for trans-Golgi, where secretory vesicles exit the Golgi, and the intermediate compartment, a possible intermediate between the ER and Golgi in cellular trafficking, showed changes in staining patterns with KUNV replication, implicating these compartments as the membrane source for the RC compartments (Mackenzie et al., 1999; Marie et al., 2009). Experiments using KUNV packaging mutants and Brefeldin A, which blocks the secretory pathway indicated that RNA replication and virion packaging were coupled (Khromykh et al., 2001; Mackenzie and Westaway, 2001). Immunoblot analysis of components of buoyant sucrose gradient used to separate membranes showed that there are two sets of KUNV replication induced membranes: vesicle packets containing NS3,

RNA dependent RNA polymerase (RdRp), and dsRNA as well as the convoluted membranes and paracrystalline arrays containing NS3 helicase (Kim et al., 2004). EM imaging of cells transfected with plasmids expressing KUNV NS4a-4b and NS2b-NS3-NS4a showed that full-length NS4a caused membrane rearrangement and NS4a-2K region did not (Roosendaal et al., 2006). EM studies of KUNV replication mutants implicated NS2a as a viroporin, a viral protein that spans the lipid bilayer of host cells and can create hydrophobic pores in oligomeric form promoting release of virions from cells, based on its characteristic hydrophobic residues and interaction with dsRNA (Gonzalez, 2003; Leung et al., 2008). Based on their observations and some of the KUNV observations described above, Leung et al. (2008) also proposed a model in which KUNV RNA replication occurs in close association with virus assembly, with NS2a acting either as a chaperone to move viral RNA between replication and assembly sites or a viroporin allowing RNA to exit the vesicle packets where nascent strand replication occurs. Much less is known about membrane-associated RCs for other flaviviruses than for KUNV replication.

For DENV, co-immunoprecipitation and immunoblot experiments have shown that NS3 interacts with the viral replicase NS5 (Kapoor et al., 1995). Experiments using digoxigenin strand-specific probes have localized ssRNA near DENV-replication associated vesicles (Grief et al., 1997). Chua et al. (2004) used a plasmid-based expression system to express DENV NS3 and found NS3 caused cellular membrane rearrangement, as observed by confocal microscopy, and interacted with nuclear receptor binding protein (NRBP) via yeast two-hybrid (Y2H). The Y2H technique uses the dual properties of transcription factors to discover protein-protein interactions. Transcription

factors have two domains: the binding domain (BD) which binds to an upstream activating factor (UAF), and the activation domain (AD) that activates transcription of a downstream gene. To determine whether proteins interact using Y2H, proteins of interest are expressed as fusion proteins with the BD and AD in yeast. The protein-BD will bind an UAF and if the protein-AD interacts with the protein-BD, the AD will be brought into contact with the reporter gene and activates transcription of a reporter gene. However, one flaw in the experiments of Chua et al. is that membrane rearrangement was not confirmed via EM. Umareddy et al. (2006) found that DENV NS4b also interacts with NS3 via yeast two-hybrid experiments and suggested that DENV NS4b may play a role in DENV replication. Miller et al. (2006) found by artificially expressing DENV NS4b and confocal microscopy that NS4b is membrane-associated and localizes to ER-derived cytoplasmic foci. Contradicting Chua et al. (2004), Miller et al. (2007) found that expression of NS4a caused ER-derived membrane rearrangement via confocal microscopy and EM. After the experiments described in this chapter had been designed and begun, Welsch et al. (2009) described extensive co-localization of DENV NS proteins, confocal microscopic fluorescent staining for organelles, and EM tomography of DENV-infected mammalian cells, revealing a physical connection between the DENV replication and assembly sites. DENV RC-associated membranes originate from the ER, and pores from the RC vesicles are in close proximity to where virions are budding from the ER according to Welsch et al (2009). From these observations, Welsch et al. (2009) proposed a model for DENV replication, which in brief, begins with association of genomic viral RNA with ribosomes of the RER, translation, and co- and post-translational cleavage of the polyprotein. After cleavage, NS4a and unknown host

proteins cause formation of vesicles, RNA is synthesized within the lumen of these vesicles, and nucleocapsids form around the RNA and bud from the ER near the RNA exit site.

In general, very little is known about the role of NS proteins in the formation of viral RCs for other members of the family Flaviviridae. From the genus Hepacivirus, hepatitis C virus (HCV) researchers expressed individual NS proteins as well as the whole polyprotein in cells. NS4b expression created a membranous web and other NS proteins were found to localize to this NS4b generated web via immuno EM (Egger et al., 2002). Gosert et al. (2003) confirmed that the HCV membranous web contained the RC by localizing viral RNA to this membrane via bromouridine labeling of RNA in the presence of actinomycin D. Additional work suggests that HCV replication may require association with lipid droplets during replication for virion infectivity, which we speculate may be required for the formation of RC-associated membranes (Boulant et al., 2007). Expression of HCV NS4b activates the unfolded protein response (UPR) by XBP1 splicing and ATF6 cleavage as shown by RT-PCR and confirmed by immunoblot (Li et al., 2009)

For the Pestivirus genus of the family Flaviviridae, one study examined the role of viral NS protein, and chemical cross-linking experiments showed that NS3, NS4b, and NS5a interact during bovine diarrheal virus (BVDV) replication (Qu et al., 2001). Additionally, Qu et al. (2001) found that the NS4b amino acid residues that mediate association with the ER are highly conserved in otherwise divergent cytopathic and non-cytopathic forms of BVDV, which they suggested indicates these residues may be crucial for replication. We speculate that these amino acid residues, like the NS4 residues of

DENV, may integrate BVDV NS4b into membranes, helping to form the vesicles that protect the BVDV RC from the host innate immune response.

To test the hypothesis that DENV NS4 expression creates DENV RC-associated vesicles, four different DENV NS4 constructs: NS4a, NS4a-2k, NS4b, and NS4b+2k coding regions (Figure 3.1) were tagged with six histidine residues, inserted into plasmids, and expressed under control of the baculovirus derived immediate early 1 promotor (ie1) (Adelman et al., 2002; Huynh and Zieler, 1999). This method was unsuccessful in protein expression, so a commercial plasmid designed for expression of fluorescently tagged proteins was modified by excision of the original cytomegalovirus (CMV) promoter. The CMV promoter has poor activity in insect cells, so we replaced it with an ie1 promoter, and the four NS4 constructs were inserted. This method was also unsuccessful in protein expression, so a Sindbis virus (SINV) (family Togaviridae) replicon system was used to express NS4a-2K (Geiss et al., 2007). Unfortunately, mosquito cells infected with this SINV replicon could not be used to evaluate whether expression of DENV NS4a-2K causes membrane rearrangement because alphavirus replication is also known to cause membrane rearrangements (Kujala et al., 2001).

Overall, the experiments discussed in this chapter did not establish whether expression of DENV NS4 causes membrane rearrangement in mosquito cells. Expression of NS4 via commercial protein expression systems was unsuccessful, leading to the hypothesis that expression of DENV NS4 was either unstable or toxic to mosquito cell culture outside of a natural infection. Attempts to co-express NS4 constructs in mosquito cell culture or express NS4 in DENV-infected cell culture did not increase NS4

NS4a

pTMS is also known as the 2K region

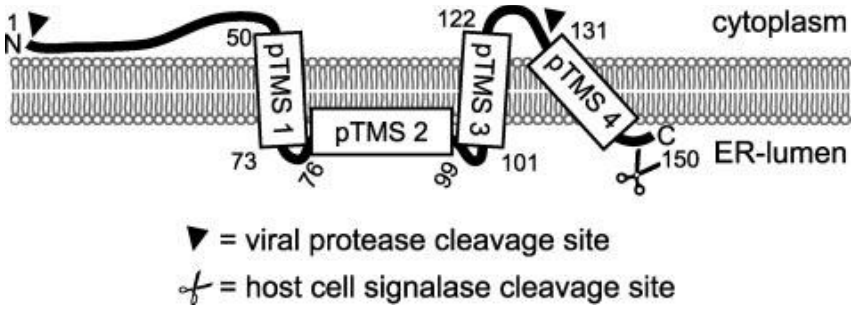

NS4b

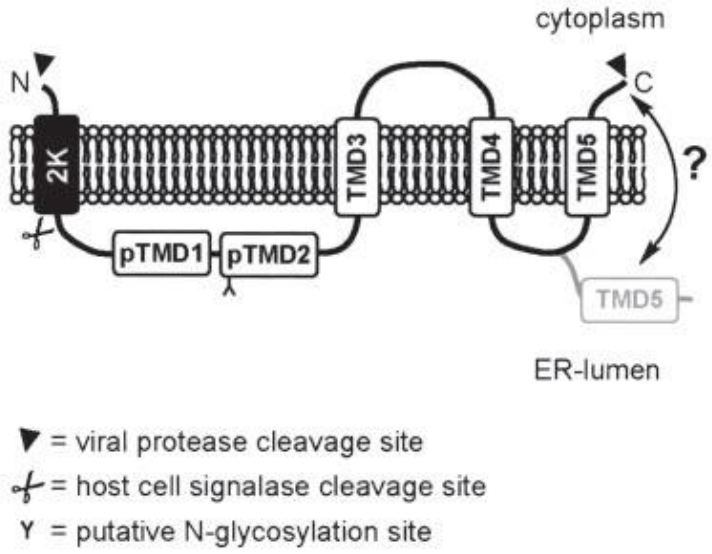

Figure 3.1 DENV NS4a and NS4b constructs NS4a has a C-terminal region known as the "2K" or 2 kDa region. Note that the 2K region in NS4a diagram is labeled as "pTMS4." During DENV gene expression, this region is cleaved, resulting in NS4a minus 2K (NS4a-2K). The 2K region associates with the N terminus of NS4b as a signal peptide, resulting in NS4b plus 2K (NS4b+2K). The four constructs used for cloning were full length NS4a, NS4a-2K, NS4b, and NS4b+2K. (Miller et al., 2007; Miller et al., 2006).

expression from the experimental plasmids, leading to the hypothesis that expression of NS4 constructs under a constitutive promoter was overwhelming or toxic to mosquito cells. Possible reasons for the failure of the these experiments will be discussed in more detail at the end of this chapter in the context of recently published information on DENV NS proteins triggering the cellular unfolded protein (UPR) pathway.

Materials and Methods

Cell lines

C6/36 (*Aedes albopictus*) cells were grown in Leibowitz's 15 (L-15) medium supplemented with 10% fetal bovine serum (FBS), 100 U/mL penicillin, 100 U/mL streptomycin, and 0.2 mM L-glutamine (L-15 growth medium) at 28°C.

Aag2 (*Aedes aegypti*) cells were a gift from Dr. Alexander Raihkel at University of California, Riverside. Aag2 cells were grown in Schneider's medium supplemented with 10% heat-inactivated FBS, penicillin, streptomycin, and L-glutamine (Schneider's growth medium) at 28°C.

BHK-21 (*Mesocricetus auratus*) baby hamster kidney cells were obtained from the American Type Culture Collection (ATCC) (Manassas, VA). BHK-21 cells were grown in Dulbecco's modified minimum essential medium (DMEM) (Mediatech, Arlington Heights, IL) supplemented with 10% heat-inactivated FBS, penicillin, streptomycin, and L-glutamine (DMEM growth medium) at 37°C with 5% CO_2.

Viruses

DENV stocks were originally obtained from the AIDL CORE support system and all titrations were performed via the AIDL CORE support system using the protocol described in Chapter 5, except that plaques were counted instead of picked at the end of the assay.

DENV-2 For preparation of working virus stocks, 4 mL medium containing DENV (JAM1409) (Genbank #M20558) was inoculated onto subconfluent C6/36 cells in a 150

cm^2 cell culture flask at an MOI of 0.01 and rocked at room temperature for 1 hr before adding 20 mL of medium. Infected C6/36 cells were maintained in L-15 medium maintenance medium, at 28°C for a total of 14 days, with a medium change at 7 dpi. At the end of the 14 day incubation, virus was harvested by using a cell scraper to detach cells, then cells and medium were suspended and divided into 0.5 mL aliquots and stored at -80°C. These aliquots were used for extracting RNA used in cloning steps described below.

Cloning 6His tagged DENV NS4a and NS4b inserts using pIE plasmid with hygromycin selection marker

pIE HYG plasmid The pIE HYG plasmid was constructed by Dr. Zachary Adelman while at AIDL (Adelman et al., 2002). Full sequence data are not available for this plasmid but it is known to contain a baculovirus ie1 promoter, XbaI non-directional insertion site, and a selectable hygromycin resistance marker.

RNA extraction RNA to be used for RT-PCR was extracted from 0.5 mL working virus stocks described above using the RNeasy Mini kit (Qiagen, Valencia, CA).

RT-PCR The NS4a, NS4a-2k, NS4b, and NS4b+2k coding regions of DENV RNA were amplified via high-fidelity RT-PCR using Superscript III One Step RT-PCR High Fidelity kit (Invitrogen, Carlsbad, CA). The NS4a and NS4b inserts were amplified using the following primer pairs: KP59 and KP63, KP59 and KP62, KP60 and KP64, KP61 and KP64 (Table 3.1). Primers were used to add XbaI restriction enzyme sites at both 5' and 3' ends for insertion into pIE HYG plasmid and 3' tags consisting of 6 histidine codons (6His) to aid later detection of protein expression. Amplification product size was

verified via gel electrophoresis and RT-PCR products were purified to remove template RNA using QIAquick PCR Kit (Qiagen).

Sequencing Purified cDNAs of all 4 NS4a and NS4b constructs with added restriction sites and 6His tags were sequenced in both forward and reverse directions by the Proteomics and Metabolics Facility (Colorado State University).

Intermediate cloning Sequenced cDNAs were first inserted into a TOPO plasmid using the TOPO TA cloning kit (Invitrogen) for reliable amplification of inserts. Colonies expressing TOPO clones were selected with ampicillin, PCR was used to identify positive colonies based on manufacturer's instructions, then several colonies containing clones of each insert were cultured overnight and plasmid DNA was purified using the QIAprep Spin Miniprep kit (Qiagen). Purified plasmid was sequenced to verify inserts by the Proteomics and Metabolics Facility.

Colony PCR Colonies were screened by touching a sterile pipette tip to each colony and swirling tip in a PCR reaction as follows: 2 mM $MgSO_4$, 0.2 mM each dNTP, PCR buffer at a final concentration of 1x, 0.2 µM forward primer, 0.2 µM reverse primer, 1 U Platinum Taq, nuclease-free water to 10 µL (Invitrogen). PCR amplification was carried out under the following conditions: 94°C 10 min; 30 cycles 94°C 1 min, 55°C 1 min, 72°C 1 min, followed by a final extension at 72°C 10 min. Product size was verified via gel electrophoresis.

Table 3.1 Primers for amplification of 6His tagged DENV NS4a and NS4b for insertion into pIE HYG expression plasmid

Primer	Purpose (sequence added)	Sequence
KP59	NS4a fwd	GATCTCTAGATATGTCTTTGACCCTGAACCTAATC
KP60	NS4b+2k fwd	GAT CTC TAG ATA TGC CAG AAC CAG AAA AAC AGA GAA C
KP61	NS4b fwd	GATCTCTAGATATGGAGATGGGTTTCCTGGAAAAAACC
KP62	NS4a full rev (NS4a 6His Stop XbaI)	GATCTCTAGACTAGTGATGATGGTGATGATGGTTTGCCATGGTTGCGGCCAC
KP63	NS4a-2k rev (NS4a w/o 2k 6His Stop XbaI)	GATCTCTAGACTAGTGATGATGGTGATGATGAATGAGCAGAACTATGAG
KP64	NS4b rev (NS4b 6His Stop XbaI)	GATCTCTAGACTAGTGATGATGGTGATGATGGTTCCTCTTCTTGTGTTTGTTGTG

pIE = plasmid with baculovirus derived immediate early 1 (ie1) promoter, fwd = forward primer, rev = reverse primer, 6His = tag coding for 6 histidine residues, Stop = stop translation site, XbaI = restriction site for XbaI

Insertion of histidine-tagged NS4a and NS4b cDNA into pIE-HYG NS4a and NS4b inserts with added 3' and 5' XbaI restriction enzyme sites were excised from the intermediate TOPO plasmid with XbaI (New England Biolabs, Ipswich, MA) after amplification. Digested plasmids and inserts were separated by agarose gel electrophoresis and inserts were extracted using the QIAquick gel extraction kit (Qiagen). Plasmid pIE-HYG was digested with XbaI. Inserts were ligated into pIE-HYG using T4 DNA ligase (New England Biolabs), electroporated into XL1 *E. coli* cells and plated onto Luria broth plates containing 50 µg/mL ampicillin. Plates were checked for growth and colonies screened via colony PCR.

Preparation of plasmids from colonies containing correct insert size as shown via colony PCR Colonies with PCR amplification products of the appropriate size were grown for no more than 16 hr in Luria broth with 50 µg/mL ampicillin. Plasmids from overnight cultures were purified using QIAprep spin miniprep kit (Qiagen). Presence of appropriate size insert was again verified via PCR as for colony PCR except 1 µL liquid culture was used for the template. Samples were sequenced by the Proteomics and Metabolics Facility and sequences analyzed using Contig Express from Invitrogen's VectorNTI Advance 10 (Invitrogen).

Determination of insert orientation in pIE-HYG Since the pIE HYG expression plasmid has a non-directional insertion site, orientation of the NS4 insertions had to be determined prior to expression in mosquito cells.

Directional PCR To determine the orientation of the NS4a and NS4b inserts in pIE-HYG, PCR as described above was used with the KP20 primer specific to the ie1 promoter sequence, KP20 5'TGGATATTGTTTCAGTTGCAAG3', with one of the

reverse primers KP63, KP62, and KP64 (Table 3.1) or KP 65-68 (Table 3.2) as needed for the specific insert being tested (Figure 3.2). Product size was verified via gel electrophoresis.

Directional sequencing To determine the orientation of NS4a and NS4b inserts in plasmids extracted from colonies positive via PCR, the primers designed for orientation PCR were used for sequencing. Samples were sequenced by the Proteomics and Metabolics Facility and sequences analyzed using Contig Express from Invitrogen's VectorNTI Advance 10.

Transfection to evaluate expression To determine whether NS4a and NS4b inserts determined to have correct orientation could be expressed, plasmid DNA was purified from overnight cultures as described previously and was transfected into C6/36 cells using Mirus 293T (Mirus, Madison, WI). To transfect cells, 0.5 mL serum free L-15 medium was incubated with 10 µL transfection reagent for 5 min at room temperature, then 1 µg of plasmid DNA was added and incubated for an additional 20 min at room temperature. Medium was removed from one well of a 6-well tissue culture plate containing 60% confluent C6/36 cells and transfection mixture was added in dropwise manner. After 30 min, L-15 growth medium was added. Cells were allowed to grow for 3 days to express the plasmid. At the end of 3 days medium was removed from the tissue culture plate and RNA was extracted from medium and cells using Trizol LS (Invitrogen).

All chemicals used for RNA extraction were obtained from Ameresco (ISC Bioexpress, Evans, UT) except the Trizol LS. RNA extraction using Trizol was carried

Table 3.2 Orientation primers for checking directionality of NS4a and NS4b inserts

Primer	Purpose	Sequence
KP 65	NS4a fwd dir ck	CTTCTTATTCTTAATGAGCGGAAAAGGTATAGAA
KP 66	NS4a rev dir ck	TTCTCTGTGACTGTGGCCAGGAGTGTCAGTAAAAGG
KP 67	NS4b fwd dir ck	GCACATTATGCCATTATAGGGCCAGGACTTCAAGC
KP 68	NS4b rev dir ck	TGCTACCAATAAAGAAGAGCTGTGAGAGTTATAGG

fwd = forward primer, rev = reverse primer, dir ck = insertion orientation check

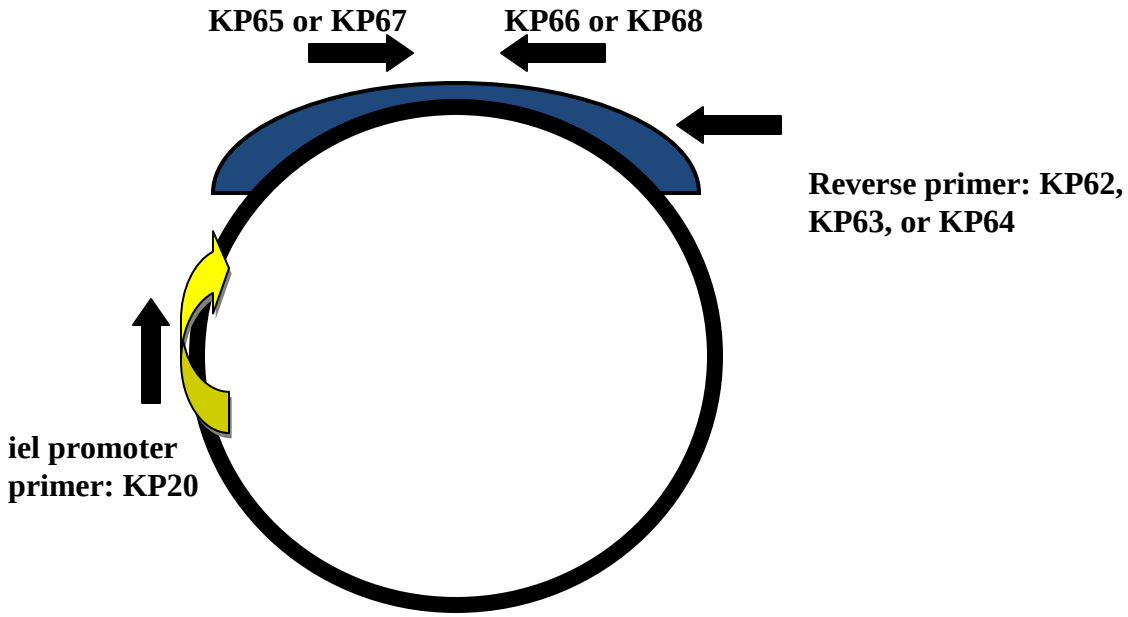

Directional PCR **forward KP20 & reverse KP62, KP63, or KP 64 = PCR product = correct orientation**
forward KP20 & reverse KP62, KP63, or KP 64 = no PCR product = incorrect orientation

forward KP 20 & reverse KP 65 or KP 67 = PCR product = reverse orientation
forward KP 20 & reverse KP 66 or KP 68 = PCR product = desired orientation

Figure 3.2 Directional PCR To determine the orientation of DENV NS4a and NS4b constructs inserted into the pIE HYG plasmid, combinations of primers were used to amplify the inserts.

out according to the manufacturer's instructions. Two milliliters of Trizol LS were added to each well and incubated at room temperature for 5 min, and then Trizol treated samples were transferred to microcentrifuge tubes. Next 0.4 mL of chloroform was added to each tube and samples were shaken for 15 sec followed by incubation at room temperature for 2 min. Phases were separated by centrifugation at 12,000 x g for 15 min at 4°C. The aqueous phase was transferred to a new microcentrifuge tube, 1 mL isopropanol was added and samples incubated at room temperature for 10 min to allow RNA to precipitate. RNA was concentrated by centrifugation at 12,000 x g for 10 min at 4°C. Supernatant was removed and samples were washed by the addition of 2 mL 75% ethanol and centrifuged 7,500 rpm for 5 min at 4°C. Pellets were air-dried briefly.

Expression of NS4a and NS4b constructs was detected via RT-PCR with the SuperScript III One-Step RT-PCR System with Platinum Taq kit (Invitrogen) using the appropriate forward primer and an 18 mer oligdT reverse primer (Integrated DNA Technologies, Coralville, IA) (Table 3.1) in 20 µL reactions exactly as described in the kit. The RT-PCR conditions were: 45°C 30 min; 94°C 2 min, 40 cycles of 94°C 15 sec, 60°C 30 sec, and 68°C 30 sec, followed by a final incubation of 68°C 5 min. Product size was verified via gel electrophoresis.

Cloning and expression of DENV NS4a and NS4b inserts using commercial fluorescent tagged protein expression plasmid

Construction of pIE-dsRed plasmid The pDsRed-monomer-HYG-N1 plasmid (Clontech, Mountain View, CA) was modified to contain a baculovirus ie1 promoter by removing the CMV promoter via excision at the 5' PciI and 3' XhoI restriction enzyme sites. The

baculovirus immediate early promoter region was amplified out of the pIE-3 plasmid obtained from Dr. Alexander Franz (Colorado State University) with the following primers: ie1 FWD with RE 5'ATGCACATGTACGCGTAAAACACAATCAAGTA TG3' and ie1 REV with RE 5'GCATGCTAGCTGGTACTTGGTTCACGATC3', which added 5' PciI and 3' XhoI restriction enzyme sites. Size of amplification product was verified via gel electrophoresis, and product was digested with PciI and XhoI (New England Biolabs, Ipswich, MA) to create ligation sites. Digested plasmids and inserts were separated by agarose gel electrophoresis and inserts were extracted using the QIAquick gel extraction kit (Qiagen). Inserts were ligated into pDsRed-monomer-HYG-N1 plasmid using T4 DNA ligase (New England Biolabs). Ligation products were electroporated into XL1 *E. coli* cells and plated onto Luria broth plates containing 50 µg/mL ampicillin. Plates were incubated, checked for growth and colonies screened via PCR. Colonies with PCR amplification products of the appropriate size to contain the dsRed plasmid with the new ie1 promoter were grown for no more than 16 hr in Luria broth with 50 µg/mL ampicillin. Plasmids from overnight cultures were purified using QIAprep spin miniprep kit (Qiagen).

The NS4a and NS4b inserts were amplified from DENV-2 (JAM1409) RNA via RT-PCR with the primer sets that added 5' PciI and 3' XbaI restriction enzyme sites (Table 3.3). Additional cloning and sequencing steps were as for the promoter region. Presence of appropriate size NS4a or NS4b insert was again verified via colony PCR and gel electrophoresis, as previously described. Samples were sequenced by the Proteomics and Metabolics Facility and sequences analyzed using Contig Express from Invitrogen's VectorNTI Advance 10.

Table 3.3 Primers for modifying commercial plasmid promoter and inserting NS4a/b

Primer	Purpose	Sequence
KP69	ie1 fwd w/ RE	ATCCACATGACGCGTAAAACACAATCAATCAAGTATG
KP70	ie1 fwd w/o RE	CGCGTAAAACACAATCAAGTATG
KP71	ie1 rev w/ RE	GCATGCTAGCTGGTACTTGGTTGTTCACGATC
KP72	ie1 rev w/o RE	GGTACTTGGTTGTTCACGATC
KP85	A fwd w/ RE	ATGCCTCGAGATGTCTTTGACCCTGAACCTAATC
KP86	B fwd w/ RE	ATGCCTCGAGATGGAGATGGGTTTCCTGGAAAAAACC
KP87	A - rev w/ RE	GCATGGTACCTAATGAGCAGAACTATGAG
KP88	A rev w/ RE	GCATGGTACCCTGTTTGCCATGGTTGCGGCCACC
KP89	B rev w/ RE	GCATGGTACCCTCCTCTTTTGATGCCTTCTTTTGC
KP90	B+ fwd w/ RE	ATGCCTCGAGATGATTCCAGAACCAGAAAACAGAG
KP91	B+ rev w/ RE	GCATGGTACCCCCTCCTCTTTTGATGCCTTCTTTTGC
KP92	A fwd	ATGTCTTTGACCCTGAACCTAATC
KP93	B rev	ATGGAGATGGGTTTCCTGGAAAAAACC
KP94	A- rev	CTAATGAGCAGAACTATGAG
KP95	A rev	TGTTTGCCATGGTTGCGGCCACC
KP96	B rev	CTCCTCTTTTGATGCCTTCTTTTGC
KP97	B fwd	ATGATTCCAGAACCAGAAAAACAGAG
KP98	B+ rev	CCCTCCTCTTTTGATGCCTTCTTTTGC

ie1 = immediate early 1 promoter, fwd = forward, rev = reverse, w/ = with, w/o = without, RE = restriction enzyme

Establishment of transformed cell lines Plasmids pIEdsRed (no insert control), pIEdsRedNS4a, pIEdsRedNS4a-2k, pIEdsRedNS4b, and pIEdsRedNS4b+2k were transfected into C6/36 cells using Mirus 293T (Mirus, Madison, WI). To transfect cells, 0.5 mL serum free L-15 medium was incubated with 10 μL transfection reagent for 5 min at room temperature, then 1 μg of plasmid DNA was added and incubated for an additional 20 min. Medium was removed from T-25 cell culture flasks containing 60% confluent C6/36 cells, and transfection mixture was added in dropwise manner. After 30 min, growth medium was added. After 24 hr recovery period, this medium was replaced with maintenance medium containing 300 U hygromycin B/mL (Calbiochem, EMB Biosciences, Inc., San Diego, CA) (Adelman, 2000). Medium was changed every 3 days to maintain hygromycin selection. Cells were screened with an inverted fluorescent microscope for red fluorescence as a marker of NS4a or NS4b expression (Olympus inverted microscope, AIDL).

Co-transfection of NS4a and NS4b constructs To determine whether co-expression of NS4a and NS4b would increase stability of protein expression, all possible pairwise combinations of plasmids expressing NS4a, NS4a-2K, NS4b, and NS4b+2K were co-transfected into C6/36 cells as described for establishing transformed cell lines. The quantity of transfected DNA consisted of 0.5 μg of each plasmid for a total of 1 μg of DNA.

Infection and transfection of cells To determine whether expression of NS4a or NS4b would be more stable in the context of a natural infection, C6/36 cells were infected with DENV and transfected with NS4a or NS4b constructs. Briefly, batches of cells were

infected and then transfected at 24, 48, and 72 hr post infection. Other batches of cells were transfected then infected at 24, 48, and 72 hr post transfection.

For infection, C6/36 cells in 12-well tissue culture plates were infected with DENV (JAM1409) at an MOI of 0.1, 0.01, or 0.001 and rocked at room temperature for 1 hr in 0.5 mL/well before adding 1.5 mL more medium. Infected C6/36 cells were maintained in L-15 maintenance medium at 28°C. For transfection, C6/36 cells grown in 12-well tissue culture plates were transfected as described above. After transfection, medium containing 300 U/mL hygromycin was used to maintain the cells and medium was changed every 3 days.

Transfection of Aag2 cells To determine whether expression of NS4a and NS4b was more stable in Aag2 cells, Aag2 cells were grown in 12-well tissue culture plates and transfected using Effectene (Qiagen). Transfection methods followed the manufacturer's guidelines. One microgram of plasmid DNA was mixed with Buffer EC in a microcentrifuge tube for a volume of 150 µL, then 8 µL of enhancer solution was added and the mixture was vortexed for 1 sec. The mixture was incubated at room temperature for 5 min and briefly centrifuged to collect mixture at the bottom of the tube. Twenty-five microliters of Effectene was added to the tube and pipetted up and down five times to mix, and then the mixture was incubated at room temperature for 5 min. Meanwhile, medium was removed from the Aag2 cells, cells were rinsed with PBS, and fresh maintenance medium was added to the cells. One milliliter of medium was added to the transfection mixture and the mixture was pipetted up and down twice to mix. Mixture was added dropwise to cells and dish was swirled to mix transfection reagents and fresh medium. Cells were incubated for 18 hr before medium was changed.

Infection and transfection of Aag2 cells Infection and transfection of Aag2 cells was identical to methods used for C6/36 cells except transfection used Effectene as described above. Infected cells were maintained in Schneider's maintenance medium at 28°C. After transfection, medium containing 300 U/mL hygromycin was used to maintain the cells and medium was changed every 3 days.

Cloning using recombination-ready SINV replicon expression vectors

To determine whether NS4a and NS4b constructs could be expressed in mosquito cells, the constructs were inserted into a SINV replicon expression vector using a system designed by Dr. Brian Geiss (Geiss et al., 2007). In brief, inserts were amplified via PCR, purified and cloned into an intermediate vector, sequenced to verify insert, recombined into a replicon plasmid, and transfected into BHK-21 cells with a packaging plasmid, then the replicon-containing supernatant from transfected cells was used to infect C6/36 cells.

RT-PCR amplification of NS4 inserts To test the replicon method, only two insert constructs were designed initially, NS4a-2k tagged with V5 at either the 3' or 5' ends (Figure 3.3). V5 tag is a protein encoding sequence derived from simian virus five RNA (Southern et al., 1991). RNA to be used for RT-PCR was extracted from 0.5 mL DENV (JAM1409) stocks prepared as described above using the RNeasy Mini kit (Qiagen). The inserts were amplified via high-fidelity RT-PCR using the Superscript III One Step RT-PCR High Fidelity kit (Invitrogen). The NS4a and NS4b inserts were amplified using the following primer pairs: KP103 and KP104, KP105 and KP106 (Table 3.4). Primers were used to add CACC sequence needed for recombination and translation 5' start sites and

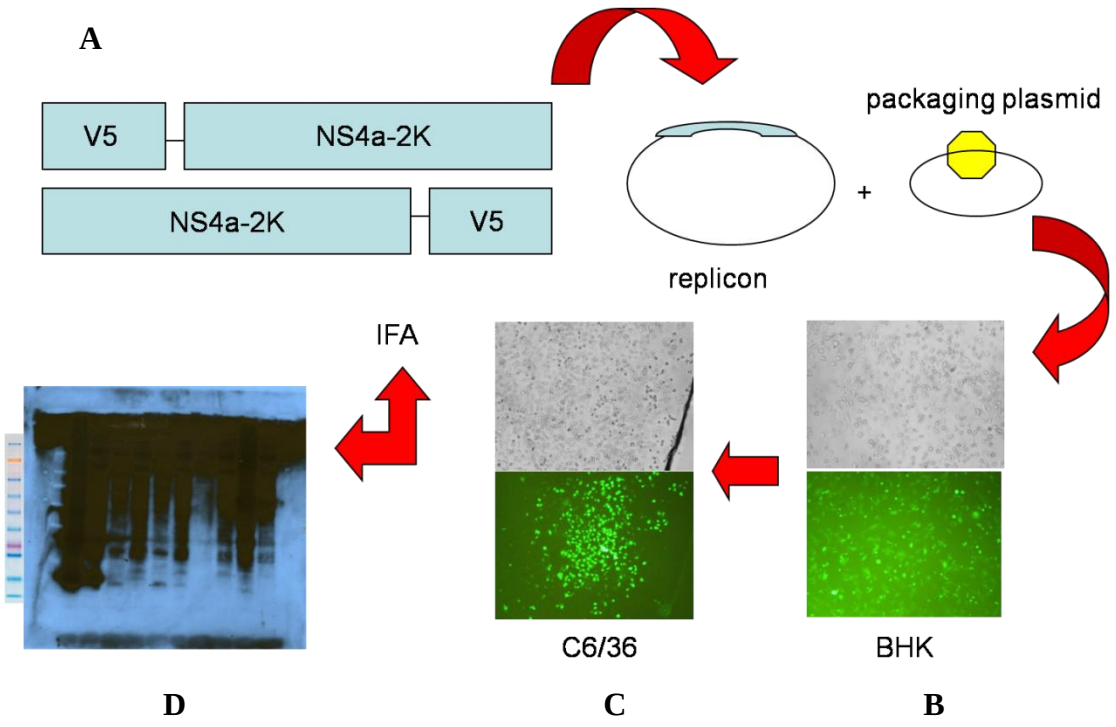

Figure 3.3 Cloning of NS4-2K using recombination-ready SINV replicon expression vectors **A.** A V5 tag was added to DENV NS4a-2k in either the 5' or 3' ends, then NS4a was cloned into an intermediate plasmid and recombined *in vitro* into a SINV replicon plasmid, the replicon plasmid and packaging plasmid were co-transfected into **B.** BHK-21 cells, showing expression of GFP from control GFP containing plasmid, then medium was transferred to **C.** C6/36 cells, showing expression of GFP from control GFP containing plasmid, then cells were harvested and proteins were separated by polyacrylamide gel electrophoresis and **D.** immuno-blotted to detect V5-tagged proteins or fixed and stained to detect V5-tagged proteins.

Table 3.4 Primers for amplification of inserts for recombination-ready SINV replicon expression vectors

Primer	Purpose (site added)	Sequence
KP103	fwd NS4a-2K SINV w/ 3' V5 (translation start)	CACCATGTCTTTGACCCTGAACCTAATC
KP 104	rev NS4a-2K SINV w/ 3' V5 (V5, translation stop)	TCAGGTGCTATCCAGGCCCAGCAGCGGGTTCGGAATCGGTTTGCC GGAATGAGCAGAAC ATGAG
KP105	fwd NS4a-2K SINV w/ 5' V5 (translation start, V5)	CACCATGGGCAAACCGATTCCGAACCCGCTGCTGGGCCTGGATAG CACCTCTTTGACCCTGACCTAAT C
KP106	rev NS4a-2K SINV w/ 5' V5 (translation stop)	TCAGGAATGAGCAGAACTATGAG

V5 = a protein encoding sequence derived from simian virus five RNA

3’ stop sites. The RT-PCR was done in 20 µL reactions as described in the kit. The reaction parameters were: 45°C 30 min, 94°C 2 min; 40 cycles of 94°C 15 sec, 60°C 30 sec, and 68°C 1 min, followed by an extension of 68°C 5 min. Amplification product size was verified via gel electrophoresis and RT-PCR products were purified to remove template RNA using the QIAquick PCR Kit (Qiagen).

TOPO cloning The constructs were inserted into the Gateway Directional TOPO vector (Invitrogen, Carlsbad, CA) using a 2:1 molar ratio of the PCR product to the TOPO vector as recommended in the kit. The ligation reaction and transformation of chemically competent cells was as recommended by the manufacturer. The transformed cells were grown overnight on Luria Broth (LB) plates with 50 mg/mL Kanamycin.

Colony PCR Transformed colonies were evaluated via colony PCR as described above using M13 primers, forward primer 5’GTAAAACGACGGCCAG3’ and reverse primer 5’CAGGAAACAGCTATGAC3’. Amplification product size was verified via gel electrophoresis. Colonies with the appropriate size NS4 insert were cultured overnight and plasmids were purified using the QIAprep Spin Miniprep kit (Qiagen) and sequenced using the M13 primers by the Proteomics and Metabolics Facility.

Recombination The NS4a-2K insert tagged with V5 was recombined *in vitro* using the Gateway LR Clonase II Enzyme kit, into the replicon plasmid described by Dr. Geiss (Geiss et al., 2007). The Gateway LR Clonase II enzyme kit uses bacteriophage lambda recombination proteins and an *Escheria coli* integration factor for *in vitro* recombination designed recombine inserts from the TOPO vector described above into another vector, like the replicon plasmid based on *att*-recombination sites. After recombination, plasmids were electroporated into *E. coli*, and transformed colonies were evaluated via

PCR with M13 primers. Overnight cultures of colonies with the proper size product were grown and plasmids purified as described above. In addition to these replicon plasmids containing NS4a-4k tagged with V5, the BG25 packaging plasmid (previously known as pBG256), as described by Dr. Geiss, was grown and purified. The packaging plasmid expressed the SINV structural proteins from TE 3'2J under a CMV protein.

Transfection The replicon plasmids and packaging plasmids were transfected into BHK-21 cells grown to 70% confluency in 6-well tissue culture plates using Lipofectamine LTX (Invitrogen). The packaging and replicon plasmids were transfected in a 1:1 ratio. A total of 2.5 µL of DNA was diluted in 2.5 mL DMEM without serum, mixed gently, then 2.5 µL of Plus reagent was added, and after mixing gently, incubated for 5 min at room temperature. After the incubation, Lipofectamine LTX was mixed and 6.25 µL was added to the DNA mixture then incubated for 30 min at room temperature, added to the BHK-21 cells, and gently rocked and incubated at 37°C. At 24 hr post transfection, medium was removed from cells, added to 2 wells of C6/36 cells grown in 12-well tissue culture plates on coverslips and incubated for 30 min at 37°C before removing DMEM and returning C6/36 cells to the L-15 medium and 28°C.

A green fluorescent protein (GFP) expressing replicon, BG78, and a V5-tagged protein-expressing replicon, BG156, were obtained from Dr. Brian Geiss and transfected alongside the experimental NS4a-2K inserts as transfection and V5 detection controls, respectively. Untransfected BHK-21 cells were maintained as negative controls.

Detection of NS4a-2K expression To determine whether NS4a-2k was being expressed from the SINV replicon, samples of BHK-21 and C6/36 cells were used for IFA and immunoblot.

IFA C6/36 cells were fixed at 72 hr post infection in 4% electron microscopy grade paraformaldehyde (Electron Microscopy Sciences, Hatfield, PA) diluted in RNase-free PBS (Ambion). All antibodies were diluted in phosphate buffered saline with 0.2% bovine serum albumin (Sigma) and 0.5% Triton X-100 (Sigma). IFA to detect V5-tagged NS4a-2K used anti-V5 monoclonal antibody (1:400) (Invitrogen) as the primary (1 hr), FITC-labeled antimouse IgG (1:400) as secondary antibody (1 hr). All incubations were at 28°C with gentle rocking. Coverslips were washed three times following each incubation in PBS. After the final incubation, coverslips were washed with distilled water and mounted on glass slides in Vectashield with 4',6-diamidino-2-phenylindole (DAPI) (VWR) and scored as positive or negative by observation with Leica DM4500B fluorescent microscope.

Immunoblot All reagents and antibodies used for immunoblot procedure were acquired from Invitrogen. Medium was removed from BHK-21 and C6/36 cells and they were washed three times in PBS and scraped off tissue culture plates into 20 µL of PBS and stored at -20°C. Ten microliters of each thawed infected cell sample was mixed with 5 µL of 6x NuPage LDS sample buffer. Five microliters of See Blue Plus 2 protein marker were loaded into the first well of a NuPAGE Bis Tris gel. Then paired samples for each plasmid from BHK-21 and C6/36 cells were loaded. Positive control consisted of V5 tagged R2D2-expressing plasmid, and negative control was GFP-expressing plasmid without V5 tag as described above in transfections.

Proteins were separated via polyacrylamide gel electrophoresis at a constant 200 V for 35 min. Proteins were transferred to a nitrocellulose membrane at a constant 30 V for 1 hr. Membrane was blocked for 1 hr at room temperature in a blocking buffer

consisting of PBS plus 0.1% Tween-20 (PBS-T) and 5% nonfat dry milk. Expression of V5 tagged NS4a-2K inserts was detected with mouse anti-V5 antibody (1:5000) in blocking buffer at 4°C overnight. The blot was washed three times with PBS-T between incubations. The blot was rocked in horseradish peroxidase-conjugated goat anti-mouse IgG secondary antibody (1:1000) in blocking buffer at room temperature for 30 min. The Novex ECL Plus Chemiluminescent Reagent Kit was used for detection according to the manufacturer's instructions. Chemiluminescence was detected by briefly exposing blot to Blue Lite Autoradiography film (ISC Bioexpress) until labeling could be detected.

Results

Cloning 6His tagged DENV NS4a and NS4b inserts using pIE plasmid with hygromycin selection marker

The 6His tagged NS4a and NS4b constructs were successfully inserted in pIE HYG plasmid, but orientation and expression could not be verified. Attempts to determine orientation via directional PCR using primers at the ends of the NS4 inserts produced faint product bands that appeared to be slightly smaller than predicted for the correct inserts (data not shown). The directional PCR with primers within the NS4 inserts revealed that some inserts were in the reverse orientation and produced some unexpectedly large PCR products (data not shown). Attempts to verify expression of mRNA from the NS4a and NS4b containing plasmids in transfected cells via RT-PCR amplification yielded no PCR bands.

Cloning DENV NS4a and NS4b inserts using commercial fluorescent tagged protein expression plasmid

The second method used to express DENV NS4a and NS4b proteins by modifying a commercial plasmid to contain an ie1 promotor and selection of transformed mosquito cells using hygromycin resistance was also unsuccessful. The NS4a and NS4b constructs were successfully inserted. The ie1 promotor driven expression of dsRed from the altered commercial plasmid without an insert was observed, but no expression of NS4a or NS4b from inserts could be detected (data not shown). This led to the question

of whether expression of the NS4 genes was unstable without the expression of other DENV proteins or if the experimental NS4 constructs could be toxic.

In an attempt to determine whether NS4 expression could be stabilized, NS4a and NS4b constructs were co-transfected or expressed singly in the background of infected cells. Neither of these methods led to expression of dsRed-tagged NS4 protein. Sequencing of experimental NS4 constructs revealed no mutation of inserts or the dsRed tag, no stop codons, or any other mutations that could explain the observed lack of protein expression. This led us to consider that constitutive expression of NS4a or NS4b could be toxic in mosquito cells, perhaps by overwhelming the protein folding capacity of the ER, triggering the UPR, and if the UPR could not upregulate protein folding, eventually leading to cell death. This hypothesis is plausible, because the transformed C6/36 cells rounded and detached from the flask more readily than normal, and in fact there were extremely few viable cells in the NS4 transfected flasks. This cell death was initially attributed to low transfection efficiency combined with the typical cell death observed with hygromycin selection; however, NS4-dsRed experimental cell lines never showed signs of recovery and growth as did cells transfected with the control plasmid expressing only dsRed.

Cloning of NS4a-2K using recombination-ready SINV replicon expression vectors

To force expression of NS4a-2K, both 5' and 3' V5-tagged NS4-2k constructs were cloned into SINV replicon vectors. GFP expression from expression control plasmid was observed by fluorescent microscopy but expression of NS4a-2K was

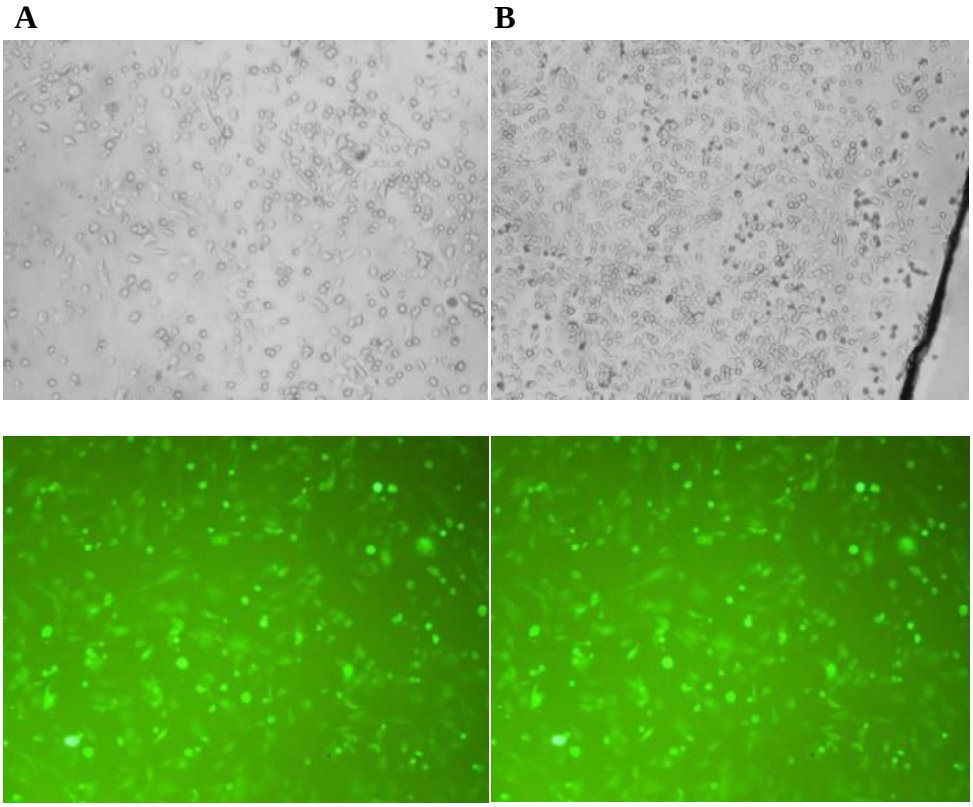

Figure 3.4 GFP expression from SINV replicon control plasmid To verify that V5-tagged NS4-2K expression from recombination-ready SINV replicon expression vectors should be detectable, a GFP expression replicon was transfected into **A.** BHK-21 cells, top panel phase contrast image, bottom panel fluorescent image, **B.** C6/36 cells, top panel phase contrast image, bottom panel fluorescent image (40x, fluorescent microscope).

not detected via IFA with V5-specific monoclonal antibody (Figure 3.4) nor was expression of V5 could be detected via V5-specific immunoblot when overexposed (Figure 3.5).

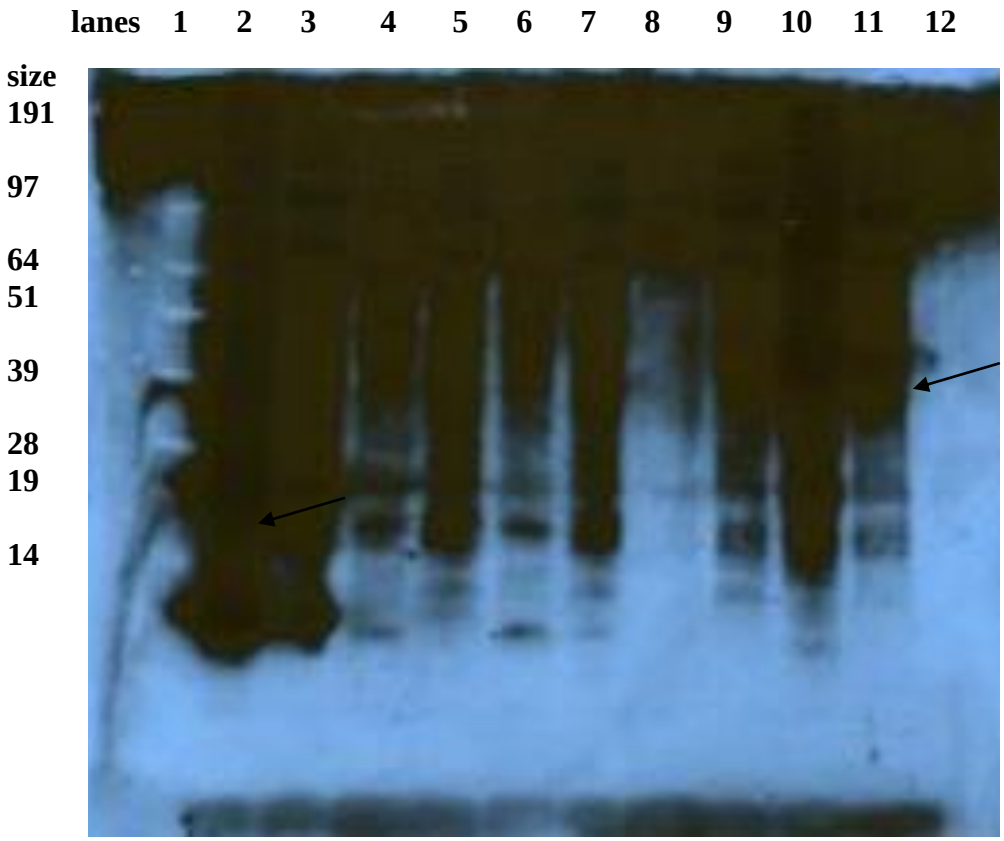

Figure 3.5 Immunoblot of attempted expression of V5 tagged NS4-2K expression from recombination-ready SINV replicon expression vectors Paired protein samples from BHK-21 cells transfected with SINV replicon expression vectors and C6/36 cells infected with packaged replicons were separated by gel electrophoresis and immuno-blotted to detect V5-tagged proteins. Lane 1 contains size markers, lanes 2 and 3 the 5' V5 NS4-2k (arrow indicates 16.5 kDa NS4a-2k + 1.5kDa V5) BHK-21 and C6/36 samples, Lanes 4 and 5 another clone of 5' V5 NS4-2k the BHK-21 and C6/36 samples, lanes 6 and 7 contain the 3' V5 NS4-2k BHK-21 and C6/36 samples, lanes 8 and 9 the transfection and infection control GFP-expression plasmid BHK-21 and C6/36 samples, lanes 10 and 11 the immunoblot control V5-tagged R2D2 BHK-21(arrow indicates 40kDa R2D2 + 1.5kDa V5) and C6/36 samples, and lane 12 is empty.

Discussion

Cloning and expression of DENV NS4a and NS4b inserts in C6/37 cells

Although cloning NS4a and NS4b inserts into the pIE HYG plasmid appeared to be successful when evaluated via PCR, evaluation of directionality of the insert revealed some possible problems with the pIE HYG plasmid. The cells transfected with the NS4a and NS4b containing plasmids did not contain mRNA corresponding to transcripts from the inserts detectable by RT-PCR, which could have been attributable to poor transfection efficiency. Unfortunately, we did not have a pIE HYG plasmid with confirmed protein expression to use as a transfection control.

The directional sequencing data revealed repetitive sequences around the XbaI insertion site of the pIE HYG plasmid which differed from the information known about the plasmid from Dr. Adelman's dissertation (Adelman, 2000). This sequence discrepancy suggests that the pIE HYG plasmid had mutated from original construct. Additionally, discussion of use of the pIE HYG plasmid with Dr. Alexander Franz revealed that he also had great difficulty working with this plasmid. His attempts to sequence the plasmid revealed that it appeared to have multiple insertions of the ie1 promoter (Franz, 2008). Overall, the difficulty working with this pIE HYG plasmid and unsuccessful attempts to evaluate the problems encountered, led to abandoning this method of expressing DENV proteins NS4a and NS4b.

Cloning and expression of DENV NS4a and NS4b inserts using commercial fluorescent-tagged protein expression plasmids was also unsuccessful but led to hypothesis that constitutive expression of NS4a or NS4b could be toxic after we

evaluated stability issues by trying to stabilize NS4 expression by co-transfection of constructs and transfecting DENV infected cells. The stability hypothesis was further pursued by cloning NS4a-2K in a replicon system to force expression of NS4a-2k, which resulted no detectable expression of tagged protein via immunoblot (Figure 3.5). We found that DENV-2 NS4a-2k might be expressed from the SINV replicon but because alphavirus infection also causes membrane rearrangement we felt this method of expressing DENV NS4 was not optimal. It now appears that to successfully express DENV proteins NS4a or NS4b, the proteins should be cloned and expressed under an inducible promoter, cells selected for expression of proteins, and membrane rearrangement visualized via electron microscopy.

Mechanisms of membrane rearrangement

Once the viral proteins that induce replication complex-associated membrane rearrangement are discovered, the next major experimental question is the mechanism by which viral proteins cause membrane rearrangement. Miller and Krisjie-Locker (2008) have suggested that viral NS proteins may cause membrane rearrangements by insertion of amphipathic helices or oligomerization of conical membrane proteins. At an ultrastructural level these mechanisms are hypothesized to resemble double-membrane budding or protrusion and detachment as observed when equine arteritis virus (EAV) nsp2-7 are expressed (Miller and Krijnse-Locker, 2008; Pedersen et al., 1999)

Membrane rearrangements associated with viral replication could be attributed to *de novo* viral processes, like the replication of the RNA genome by a virally encoded RNA-dependent RNA polymerase (RdRp). However, since +RNA viruses are

completely dependent on their host cells for other processes such as translation of viral proteins it seems plausible that viruses are also dependent on the membrane generating processes of host cells. Researchers studying viral replication complexes have noted ultrastructural similarities between infection-induced membranes and membranes arising from typical host cell processes. We had planned to evaluate ultrastructure of membrane rearrangements caused by DENV-2 NS4 proteins via confocal and EM microscopy after expressing NS4 in mosquito cells to provide some insight into what cellular processes might be co-opted by DENV-2 to provide membranes for the replication complex. Cellular processes including autophagy, the unfolded protein response (UPR), and the formation of lipid rafts have been proposed as possible sources for viral RC-associated membranes.

Autophagy

Autophagy can be triggered by cellular stress and results in the formation of double membrane bound vesicles of ER origin (Dunn, 1990a). The double membrane vesicles produced by autophagy and those induced by replication of +RNA genome viruses have led many researchers to hypothesize that viral RC-associated membranes arose from autophagy. Hypotheses suggesting autophagy as a source of viral RC-associated membranes are typically based on morphological observations of RC-associated membranes, without biochemical markers of autophagy, so these membranes may or may not be autophagosomes (Lee and Iwasaki, 2008). To examine the role of NS proteins in RC-associated membrane formation, Pedersen et al. (1999) expressed nsp2-nsp7 of equine arteritis virus (EAV) (family Arteriviridae) and observed RC-associated membrane formation by a protrusion and detachment mechanism that

resembled autophagy. Poliovirus (PV) researchers initially suggested an autophagic origin of PV RC-associated membranes because they found no markers of any other cellular organelles that co-fractionated with RC-associated membranes and the membrane morphology resembled the DMVs formed during autophagy (Suhy et al., 2000). Jackson et al. (2005) presented more convincing data for an autophagic origin of PV-induced vesicles, showing co-localization of the RC with LC3 via IFA. In addition, Jackson et al. (2005) stimulated and inhibited autophagy with taxomoxfin and 3-methyladenine respectively, and used RNAi to knockdown autophagy components and showed the predicted increase and decrease of PV yields.

Research on other +RNA genome viruses has generated conflicting data on the role of autophagy in the formation of RC-associated membranes. Prentice and colleagues (2004) co-localized LC3 with the mouse hepatitis virus (MHV) (family Coronaviridae) RC via IFA, so they suggested an autophagic origin for the RC-associated membranes. Zhao et al. (2007) further examined the role of autophagy in MHV replication and found that MHV was able to replicate in two cell lines impaired for autophagy, an ATG5 deletion cell line and a primary murine cell line that lacked ATG5. However, this discrepancy as to whether autophagy is required for MHV replication could be explained by redundancy in the autophagy pathway like the Dicer redundancy observed in plants (Deleris et al., 2006).

Some researchers have suggested a role for autophagy in the antiviral response. Liang et al. (1998) found that SINV encephalitis in mice could be reduced by upregulating autophagy through enhanced expression of Beclin 1. Lee et al. (2007) found an impaired interferon alpha (IFNα) antiviral response to vesicular stomatitis virus

(VSV) (family Rhabdoviridae) in the absence of ATG proteins and suggested that autophagy may mediate detection of negative-strand ssRNA viral genomes and secretion of IFNα.

The literature discussing the possibility of autophagic membranes for DENV RC-associated membranes is relatively new. Lee et al. (2008) expressed a GFP-linked form of LC3 in mammalian cells, infected the cells with DENV, and observed LC3 aggregation, which they argued could be used as a marker of autophagy. When DENV infected cells were treated with chemical inhibitors of autophagy, Lee et al. (2008) found that LC3 aggregation and DENV titers both decreased, so they suggested that DENV induces autophagy. Panyasrivanit et al (2009) took Lee and colleagues' hypothesis a step further and argued for presence of DENV RC in autophagic vacuoles based on fluorescent co-localization of DENV-2 NS1 or LC3 with dsRNA. Based on their fluorescent microscopic observations that NS1 and LC3 co-localize, Panyasirvant et al. (2009) suggested DENV uses amphisomes or autophagosomes, autophagic membranes prior to fusion with lysosomes as sites for viral replication. Interestingly, Panyasirvant's colleagues published very similar experiments using LC3-GFP and DENV-3 in mammalian cells and observed that DENV-3 localized with autophagolysomes, autophagic vesicles after fusion with lysosomes (Khakpoor et al., 2009). Khakpoor et al. (2009) suggested the difference in data between the DENV-3 experiments and the DENV-2 could be explained by the difference in DENV serotype used. It seems unlikely that two different virus serotypes would evolve different mechanisms for induction of membranes when KUNV and DENV have very similar RC-associated membranes.

After reviewing the literature on DENV RC-associated membranes and autophagy, we would like to propose an alternative explanation for colocalization of the DENV RC and autophagic vesicles. Autophagy is one of several antiviral responses, with autophagic vesicles serving as a viral clearance mechanism. Since viral RCs are engulfed by autophagosomes during an antiviral response, this could also explain co-localization of LC3 and components of viral RCs and dsRNA. In the future researchers studying the role of autophagy in the DENV RC should consider evaluating the effects of enhancement of autophagy on DENV titers as well as evaluating other markers of autophagy such as XBP-1 splicing to make a more convincing argument for the role of autophagy in the formation of DENV RC-associated membranes.

Unfolded Protein Response

The unfolded protein response (UPR) is a response to ER stress caused by improperly folded proteins, nutrient stress, or pathogen infection. As discussed in Chapter 1, one of the UPR-mediated responses to ER stress is to increase the capacity of the ER by enlarging the ER, since ER proliferation is observed in +RNA virus infected cells, researchers have speculated that viruses may be co-opting the UPR. Bechill et al. (2008) used RT-PCR and immunoblot of MHV-infected cells to show that MHV replication triggers UPR transducers like IRE1 and ATF6 but downstream UPR-targeted genes are not induced, suggesting that MHV can modify the UPR. Instead of viral protein translation overwhelming the ER, thus triggering the UPR, MHV may modify the UPR to evade the host immune response (Bechill et al., 2008).

Research on the interaction between viruses from the family Flaviviridae and the UPR is not as advanced as the MHV and UPR studies. Plasmid based expression of

HCV envelope glycoproteins causes ER stress and HCV NS4b has been shown to induce the UPR by RT-PCR and immunoblot-monitoring of XBP1 mRNA splicing and ATF6 cleavage (Chan and Egan, 2009; Li et al., 2009). For the genus Flavivirus, WNV has been shown to activate the UPR using RT-PCR showing XBP1 mRNA splicing and immunoblot-monitoring of ATF6 cleavage and phosphorylation of EIF-2α (Medigeshi et al., 2007). Medigeshi et al. (2007) also showed that WNV triggered UPR can eventually lead to apoptotic cell death. Yu et al. (2006) used an XBP1 slicing reporter system to show that JEV and DENV-2 interact with the UPR differently; DENV-2 NS2B-3 induces XBP-1 splicing but JEV does not. The reason for the discrepancy in XBP1 splicing between these two flaviviruses is not understood. Umareddy et al. (2007) used immunoblot to show phosphorylation of eIF2α, nuclear localization of ATF-6 via IFA, and splicing of XBP-1 via RT-PCR in DENV-infected mammalian cells, showing that DENV globally activates the UPR. The mechanism by which DENV activates the UPR is unclear and Umareddy et al. (2007) suggest that the mechanism may involve up- and down-regulation of the UPR since unsuccessful UPR leads to apoptosis.

Since most of the UPR and virus work has been done in mammalian cells, this raises many questions as to whether the UPR plays a role in DENV replication in mosquito cells. Plongthongkum (2007) showed that the UPR is active in *Drosophila melanogaster* S2 cells and mediates XBP1 mRNA splicing. A more recent RNAi screen of insect host factors associated with DENV infection in *D. melanogaster* cells identified two components of the UPR as essential host factors (Sessions et al., 2009). It is currently unclear whether the UPR plays a role in membrane formation for enclosure of DENV RCs in mosquitoes. We think that interaction of DENV NS proteins with the

UPR to enhance ER capacity is a plausible hypothesis for the origin of DENV RC-associated membranes, perhaps by a mechanism similar to what Bechill (2008) observed for MHV. One of the next experimental steps to evaluate this possibility might be a crosslinking or co-immunoprecipiation experiment in DENV-infected mosquito cells and tissues to identify interactions between DENV NS proteins and UPR proteins.

Lipid Rafts

Since lipid rafts contain cholesterol and sphingomyelins, making them resistant to extraction with cold non-ionic detergent, and flavivirus RC-associated membranes are resistant to extraction with cold TritonX-100, researchers suggested that lipid rafts could be involved in formation of flavivirus RC-associated membranes (Jacobson and Dietrich, 1999; Uchil and Satchidanandam, 2003). Van der Goot et al. (2001) proposed that lipid rafts could serve as concentration sites for viruses and other pathogens, and one of the major purposes of viral RC-associated membranes is believed to be concentration of RC (Salonen et al., 2005). Shi et al. (2003) used membrane flotation and IFA co-localization of newly synthesized viral RNA with incorporated bromouridine and caveolin markers of lipid rafts to show that HCV replication occurs on detergent-resistant membranes, which might be lipid rafts. Cherry et al. (2006) conducted a genome-wide RNAi screen for host factors required for Drosophila C virus replication (family Picornaviridae) in *D. melanogaster* cells, revealing that fatty acid biosynthesis is required for viral replication. Ng et al. (2008) showed that SINV requires cholesterol and sphingelomyelins for proper replication, using cholesterol depleted fibroblasts. Noiskarama (2008) found that DENV and JEV NS1 co-localize with lipid raft markers in TX100 resistant cellular lysates. Depletion of cholesterol, resulting in the disruption of lipid raft formation, also resulted

in decreased JEV and DENV titers, so lipid raft components appear to be required for flavivirus replication (Noisakran et al., 2008). The hypothesis of a lipid raft origin of RC-associated membranes needs further evaluation. The available data to support this hypothesis are minimal. Also these data, suggesting that the DENV RC localizes to lipid rafts, conflict with Welsch and colleagues' (2009) EM tomography images of an ER origin of the DENV RC. The hypothesized lipid raft origin of the RC-associated membranes seems more plausible for HCV. Shi et al. (2003) showed co-localization of newly synthesized viral RNA and caveolin markers of lipid rafts. A useful follow-up experiment to confirm the HCV RC lipid raft hypothesis would be to determine whether caveolin localizes with HCV NS proteins as a marker of the RC versus structural proteins as markers of virus packaging.

What do the proteins that cause membrane rearrangement have in common?

A literature search of proteins that cause RC-associated membrane rearrangements found that many different NS proteins are involved in membrane rearrangement, leading to the hypothesis that rather than a conserved amino acid sequence being required for membrane association, a conserved protein structure or characteristic is needed. In fact, several positive-strand RNA virus NS proteins contain amphipathic helices that are alpha helical structures in which one side of the helix contains hydrophobic amino acids and the other side of the helix contains hydrophilic amino acids. Amphipathic alpha helices are characteristic components of lipid-associated proteins including hormones and HIV glycoproteins (Segrest et al., 1992). Hepatitis A virus (HAV) (family Picornaviridae) protein 2C, HCV NS4b, and SFV nsp1 all contain

amphipathic helices (Gouttenoire et al., 2009; Kusov et al., 1998; Spuul et al., 2007). In fact, the common characteristic of positive-strand RNA genome virus encoded proteins involved in membrane rearrangements is most likely hydrophobicity. In support of this hypothesis, a comparison of NS4b proteins from the family Flaviviridae found that HCV NS4b is only 23% homologous to other family members at the amino acid sequence level, but all of the NS proteins have four or five transmembrane regions (Welsch et al., 2007). We would like to note that DENV-2 NS3, which Chua et al. (2004) suggested was causing membrane rearrangements that Miller et al. (2007) attributed to NS4a-2K, lacks long stretches of hydrophobic regions like the other NS proteins that have been shown to cause membrane rearrangments (Chua et al., 2004; Miller et al., 2007).

Comparison of the replication complexes of arboviruses

Comparison of membrane rearrangements associated with the replication complexes of arthropod-borne flaviviruses and alphaviruses reveals few structural commonalities other than the size vesicle immediately surrounding the RC. For example, expression of Semliki Forest virus (SFV) nsp1-4 produces the 600-2000 nm cytoplasmic vesicles (CPVs) that are characteristic of alphavirus infections (Kujala et al., 2001). These CPVs contain single membrane enclosed 50 nm spherules along the periphery of the CPV that are the equivalent of the flavivirus RC-containing double membrane vesicles (DMVs) observed with DENV, JEV, and KUNV infected cells (Uchil and Satchidanandam, 2003). In comparison, the DENV RC-containing membranes imaged by Welsch et al. (2009) are located close to the nucleus and very tightly packed with DMVs instead of the RC-associated vesicles arranged along the periphery of a larger

CPV like alphaviruses. Overall, alphavirus and flavivirus RC-associated membranes differ as to size of the packet enclosing the vesicles that contain the RCs, number of membranes surrounding the RC, location within the cell, and how many small vesicles are contained within the outer membranes.

After formation of replication-associated membranes: how do materials flow to and from of the replication complexes?

Several researchers have suggested that RC-associated membranes are completely closed vesicles. Knoops et al. (2008) and Uchil et al. (2003) suggested that SARS coronavirus and DENV RCs are sealed off from the cytoplasm. If this hypothesis is true, how do materials enter and exit the RC-associated membranes? In the case of PV, replication "rosettes" are closed, but the replication complex faces outward, so the replication complex is accessible to the cytoplasm (Bolten et al., 1998). HCV replication-associated membranes have "necks" that are open to the cytoplasm but protect the RC from proteinases and nucleases (Quinkert et al., 2005). SARS coronavirus DMVs appear to be closed and Knoops et al. (2008) offered no suggestions to explain how these might be functional. Welsch et al. (2009) noted that DENV replication-associated vesicles were open or closed depending on the EM preparation method, but concluded that a 10 nm "neck" or pore existed to allow substrates into the replication complex. Uchil et al. (2003) observed closed vesicles and proposed that the JEV genome could exit via a viroporin.

Both alphaviruses and flaviviruses have viroporins, which are small, very hydrophobic viral proteins that can oligomerize to form pores that are involved in the

release of virus particles from cells as well as other functions (Gonzalez, 2003). Many of the +RNA viruses discussed in this chapter have viroporins: PV 2B, SINV 6k, and HCV 7 (Griffin et al., 2003; Lama and Carrasco, 1992; Sanz et al., 2003). More study is needed to determine whether viroporins might play a role in regulating movement of proteins and nucleotides into viral RC-associated membranes.

Re-evaluation of experimental methods

All of the groups used inducible promoters that published detailed methods of how they expressed NS proteins that were suspected to cause virus-associated membrane rearrangements (Egger et al., 2002; Miller et al., 2007; Miller et al., 2006; Westaway et al., 1997a). We speculate that other research groups experienced the same difficulties with constitutive expression that we did.

Umareddy et al. (2007) presented very convincing evidence that in a natural DENV infection, DENV promotes transcription of the eukaryotic initiation factor 2 alpha (eIF-2α) effector protein of the UPR by an unknown mechanism. This up-regulation of eIF-2α prevents the accumulation of the prM, E and NS1 proteins in the ER from triggering the UPR. Perhaps our attempts to express the experimental NS4 constructs outside of a natural virus infection induced ER stress without the up-regulation eIF-2α to counterbalance the ER stress and triggered the UPR. If the UPR is unsuccessful in relieving ER stress, apoptotic cell death is triggered (Paschen, 2003). If expression of DENV NS4 upregulates the UPR outside of a natural infection, this could lead to apoptosis, which could thus explain our observation of almost no viable cells after we transfected mosquito cells with NS4 plasmids and selected with hygromycin. Recently

published guides to the production of recombinant proteins in mammalian cells consider the ER folding limitations and UPR to be major rate limiting factors in protein production (Khan and Schroder, 2008).

Intriguingly, two groups of researchers expressed viral proteins from alphavirus replicons and then evaluated membrane rearrangement via EM. Roosendahl et al. (2006) expressed Kunjin virus NS4a-2k and NS4b from a SFV replicon and observed the membrane rearrangements known as convoluted membranes and paracrystalline arrays. Pedersen et al. (1999) also used an alphavirus expression vector to express equine arteritis virus (EAV) (family Arterivivirdae) nsp1-4 and observed membrane rearrangements. Instead of being concerned that alphavirus induced protein expression would confound the membrane rearrangements caused by the viral proteins, Roosendahl et al. (2006) thoroughly characterized the alphavirus membrane rearrangements without expression of other viral proteins, then examined intracellular membranes again when other viral proteins were expressed.

We initially decided that expression of viral proteins from an alphavirus expression vector was less useful for our experimental purposes than creating protein expressing cell lines like Miller et al. (2006, 2007) because of the confounding membrane rearrangements caused by the alphavirus vector. Unfortunately, we were unable to express DENV NS4 proteins outside of an alphavirus system. So, we reconsidered use of alphavirus expression and used the SINV replicon system to determine whether it was possible to express DENV proteins outside of a natural DENV infection in mosquito cell culture. As discussed earlier, we were unable to express NS4a-2K from the SINV replicon system and we were unable to track V5-tagged NS4a-2k localization in C6/36

cells via IFA. In the end, we decided against examining the possible DENV NS4a-2K induced membrane rearrangement in C6/36 cells after expression from a SINV replicon via EM because we were hesitant to undertake an EM imaging experiment without some preliminary indication of membrane or organelle changes via IFA, and IFA and immunoblot detection of V5-tagged NS4a-2k was unsuccessful.

Future research

As mentioned previously, Cherry et al. (2006) carried out a genome-wide RNAi screen of *Drosophila* host factors that are required for replication of Drosophila C virus (family Dicistroviridae), and they found that COPI coatamer and fatty acid biosynthesis were required for viral replication. These requirements are consistent with the biochemical data from other +RNA virus RC compartments studied such as PV, which is known to interact with COPII coatamer proteins for virus replication, and SINV, which requires lipids for replication (Belov and Ehrenfeld, 2007; Ng et al., 2008). Further evaluation of such mosquito host factors for DENV replication by Sessions et al. (2009) found two UPR proteins were crucial for DENV replication in mosquitoes. In the future, thorough biochemical evaluation of mosquito host factors suggested by genome screens like those by Cherry et al. (2006) and Sessions et al. (2009) may lead to new models of the RC compartment and how NS proteins interact with host proteins.

Overall, the experiments described in this chapter did little to increase our understanding of the role of NS proteins in membrane rearrangement in mosquito cells. In the next chapter, we evaluated whether similar patterns of dsRNA localization,

detection of viral RNAs from gradient fractions of disrupted cells, and EM visualization of vesicles described in Chapter 2 could be repeated in mosquito tissues.

Chapter 4

Evaluation of dengue virus replication-associated membranes in *Aedes aegypti* mosquito midgut cells

Introduction

Although membrane rearrangement associated with flavivirus replication has long been observed, there are few studies that have looked at this membrane rearrangement in the context of the mosquito host. Arboviruses vary in their ability to induce membrane rearrangements in mosquitoes. Researchers studying encephalitic arboviruses such as western equine encephalitis (family Togaviridae) observed severe cytopathology in mosquito midguts (Weaver et al., 1992; Weaver et al., 1988). St. Louis encephalitis virus (family Flaviviridae) caused proliferation of ER in intact cells in the midgut of infected mosquitoes via electron microscopy (EM) (Whitfield et al., 1973). A recent ultrastructural study of West Nile virus (family Flaviviridae) in *Culex pipiens quinquefasciatus* mosquito tissues observed ER membrane proliferation and vesicles similar to those seen in mammalian cells infected with flaviviruses (Girard et al., 2005; Uchil and Satchidanandam, 2003).

The hypothesis examined in this chapter is that vesicles like those isolated from DENV-infected mosquito cell culture can also be isolated from midguts of *Aedes aegypti* mosquitoes infected with DENV. Experiments in this chapter also tested the hypothesis that differences in flavivirus replication and alphavirus replication, as represented by localization of dsRNA that were not apparent in mosquito cell culture, will be observed in mosquito tissues.

In Chapter 2, perinuclear localization of dsRNA was described in mosquito cell culture. Cellular fractionation of detergent-treated cultured mosquito cells revealed DENV RNA in two regions of the gradient, and transmission electron microscopic (TEM) examination of the more buoyant upper fractions of sucrose gradients revealed

50-75 nm membrane structures likely to have originated from the ER. To determine whether these observations were unique to DENV replication in cell culture or relevant to the mosquito, *Ae. aegypti* mosquito midguts were dissected and stained with fluorescent antibodies for dsRNA localization. DsRNA was also examined in the context of DENV envelope and capsid proteins via immunofluorescent microscopy. Temporal and spatial localization patterns of DENV dsRNA and antigens were compared to SINV localization patterns via fluorescent and confocal microscopy. Cellular fractionation experiments and TEM experiments performed on samples from mosquito cell culture in Chapter 2 were repeated on mosquito midgut samples.

In Chapter 2, immunofluorescent microscopic localization of dsRNA was unsuccessful in evaluating replication differences between DENV and SINV. After examining these data, we speculated that differences in replication between DENV and SINV represented by dsRNA staining might be more readily apparent in mosquito tissues. In fact, immunofluorescent microscopic analysis of viral antigen in whole mosquitoes has been used to confirm differences in dissemination between strains of yellow fever virus (McElroy et al., 2008).

The experiments discussed in this chapter were designed to establish a link between DENV replication and proliferation of ER membranes in the mosquito midgut. The data presented here established a link between DENV replication and production of double-membrane vesicles in mosquito tissues, confirmed a vesicle size range including the 50-75 nm diameter range observed in vesicles from mosquito cell culture, verified probable ER origin of the vesicles, and showed ER proliferation in DENV-infected mosquito midguts. Comparison of dsRNA temporal localization between a flavivirus and

two strains of an alphavirus in mosquito midguts revealed temporal differences in replication that were not obvious in mosquito cell culture. The results presented here have implications for the development of an RNAi-based DENV-resistant transgenic mosquito.

Materials & Methods

Cell culture lines

C6/36 (*Aedes albopictus*) cells were obtained from the American Type Culture Collection (ATCC; Manassas, VA). C6/36 cells were grown in Leibowitz 15 (L-15) medium supplemented with 10% heat-inactivated fetal bovine serum (FBS), 100 U/mL penicillin, 100 µg/mL streptomycin, and 0.2 mM L-glutamine at 28°C (growth medium).

Mosquito rearing

Rexville D strain (*Aedes aegypti*) mosquitoes, originally from Puerto Rico, were reared at 28˚C and 80% humidity, with a photoperiod of 12 hr light and 12 hr darkness by the AIDL CORE support program in the insectary of the Virology suite of BRB. Mosquitoes were maintained prior to bloodfeed on sugar cubes and water *ad libitum*.

Viruses

All virus stocks were obtained from the AIDL CORE support system. All titrations were performed via the AIDL CORE support system using the protocol described in Chapter 5 except that plaques were counted instead of picked at the end.

DENV-2 For preparation of virus for artificial bloodmeals, 2 mL DENV-2 strain Jamaica 1409 (Genbank #M20558) were inoculated onto subconfluent C6/36 cells in a 75 cm^2 flask at a multiplicity of infection (MOI) of 0.01 and rocked at room temperature for 1 hr before adding 10 mL of medium. Infected C6/36 cells were maintained in L-15 medium supplemented with 2% FBS, 100 U/mL penicillin, 100 µg/mL streptomycin, 1x

MEM non-essential amino acids, and 0.2 mM L-glutamine at 28°C (maintenance medium) for a total of 14 days with a medium change at 7 dpi. At the end of the 14 day incubation, virus was harvested by using a cell scraper to detach cells, and infected cells suspended in medium were used as the virus component of bloodmeals. The average bloodmeal titer used in these experiments was 1 x 10^7 pfu/mL.

SINV Strains MRE16 (Klimstra et al., 1998; McKnight et al., 1996) and TR339 (Klimstra et al., 1998; McKnight et al., 1996) were grown as follows. For preparation of virus stocks used for artificial bloodmeals, 2 mL virus was inoculated onto C6/36 cells in 75 cm^2 tissue culture flasks at an MOI of 0.01 and rocked at room temperature for 1 hour before adding 10 mL of medium. Infected C6/36 cells were maintained in L-15 maintenance medium for a total of 4 days. Cells were detached from tissue culture flask using a cell scraper, then infected cells suspended in medium were divided into 0.5 mL aliquots and stored at -80°C.

Aliquots of SINV stocks were thawed and used for artificial bloodmeals as described next. The titer of the SINV (MRE16) stock used in the experiments described in this chapter was 7.43 log pfu/mL and the titer of the SINV (TR339) stock was 7.3 log pfu/mL.

Artificial bloodfeed

DENV DENV-2 (JAM1409) was cultured for bloodmeals as described above. Infectious bloodmeals consisted of equal volumes of freshly harvested virus and defibrinated sheep blood (Colorado Serum Company: Boulder, CO) supplemented with a final concentration of 1 mM adenosine triphosphate to stimulate feeding. Control bloodmeals consisted of

the same mixture except mock infected cells and their medium were used. Bloodmeals were provided in water-jacketed feeders with sausage casing membranes warmed by a waterbath set at 37°C and mosquitoes were allowed to feed for no more than 1 hr. At the end of the hour, mosquitoes were briefly cold-anesthetized and sorted. Engorged mosquitoes were maintained on sucrose and water at normal rearing conditions. Every 24 hr post bloodmeal for 14 days, 40 mosquitoes from the infected group and 10 mosquitoes from the mock-infected group were randomly selected, dissected, and prepared for IFA or cellular fractionation.

SINV SINV strains MRE16 and TR339 were cultured for bloodmeals as described above. Bloodmeals were prepared as for DENV except frozen stock virus was used in place of freshly cultured virus. Sorting and maintenance of mosquitoes was as described for DENV bloodmeals. Every 24 hr post bloodmeal for 5 days, 60 mosquitoes from the SINV-infected group and 10 mosquitoes from the mock-infected group were randomly selected, dissected, and prepared for IFA.

Cellular fractionation

Sucrose gradient solutions Sucrose solutions and TNMg buffer were made as described in Chapter 2.

Isolation of vesicles Viral replication-associated vesicles were isolated based on the technique used by Uchil and Satchidanadam with mammalian cells (2003). *Ae. aegypti* (RexD) mosquitoes were fed DENV-containing artificial bloodmeals as described above. An IFA using mAb 3H5-1 was used to verify successful DENV-infection prior to vesicle isolation. At 7, 10, or 14 days post bloodmeal (d pbm) midguts were dissected from 400

infected mosquitoes and placed immediately into TNMg buffer on ice. Midguts were gently harvested by centrifugation (2500 rpm, 5 min) after dissection. Then as described in Chapter 2 for C6/36 cells, the pellet was resuspended and incubated in 1% Triton X100 (TX100) on ice for 1 hr to disrupt cellular plasma membranes, then the heavy membrane fraction, the equivalent of the S16 used by Uchil and Satchidanadan, was sedimented at 16,000 x g for 15 min (2003). Sucrose gradient was prepared using the resuspended S16 pellet and fraction collection was as described in Chapter 2.

Washing fractions Sucrose removal and sample concentration was as described in Chapter 2.

Characterizing RNA in gradient fractions

RNA extraction All solutions were obtained from Amresco (ISC Bioexpress: Kaysville, UT) except the RNase-free PBS, which was obtained from Ambion (Ambion: Austin, TX) as a 25x solution and diluted in nuclease-free water.

Washed fractions obtained from midgut cellular fractionation gradients were analyzed for presence of DENV-2 viral RNA. After concentration by centrifugation, fractions were resuspended in 0.5 mL RNase-free PBS and extracted once using saturated 5:1 phenol-chloroform, and once with 24:1 chloroform-isoamyl alcohol followed by a precipitation in one-tenth volume of 5M ammonium acetate and 2 volumes 100% ethanol. RNA pellets were washed once in 70% ethanol, air dried, and then resuspended in 20 μL nuclease free water.

Strand-specific RT-PCR Viral RNA was detected via strand-specific RT-PCR (ssRT-PCR) using a method developed by Peyrefitte et al. (2003) to minimize false priming

results (Figure 4.1) (Peyrefitte et al., 2003). RNA samples were treated with Turbo DNase (Ambion: Austin, TX) for 30 min as instructed in the kit to remove DNA then stopped using the provided EDTA-containing buffer. RNA was purified by one round of phenol-chloroform extraction followed by an isopropanol precipitation at -20°C for 15 min. RNA was collected by centrifugation for 15 min at 14,000 rpm at 4°C, supernatant was removed, RNA was resuspended in nuclease free water, then used as a template for RT. RNA was transcribed to cDNA via RT using the tagF for anti-genome sense strand and R for genome sense strand (Table 4.1). The RT was carried out using the Invitrogen Superscript III Reverse Transcriptase (Invitrogen: Carlsbad, CA). The conditions were 50°C for 30 min, followed by 70°C for 15 min. The cDNA was purified using a PCR Purification kit (Qiagen: Valencia, CA) to remove RT primers. The cDNA was PCR amplified using the primer pairs tag and R (anti-genome sense), F and R (genome sense). The PCR mixture was as follows: 1.5 mM Mg sulfate, 0.8 mM dNTPs, 1x final concentration of PCR buffer, 2 µL of the cDNA from the RT reaction, 0.2 µM forward primer, 0.2 µM reverse primer, 1 U Platinum Taq, nuclease-free water (Invitrogen: Carlsbad, CA) to 25 µL. PCR parameters were 94°C 2 min, 30 cycles 94°C 30 sec, 60°C 30 sec, 72°C 1 min, followed by a final incubation of 68°C 10 min. Expected product size of 100 bp was verified via agarose gel electrophoresis.

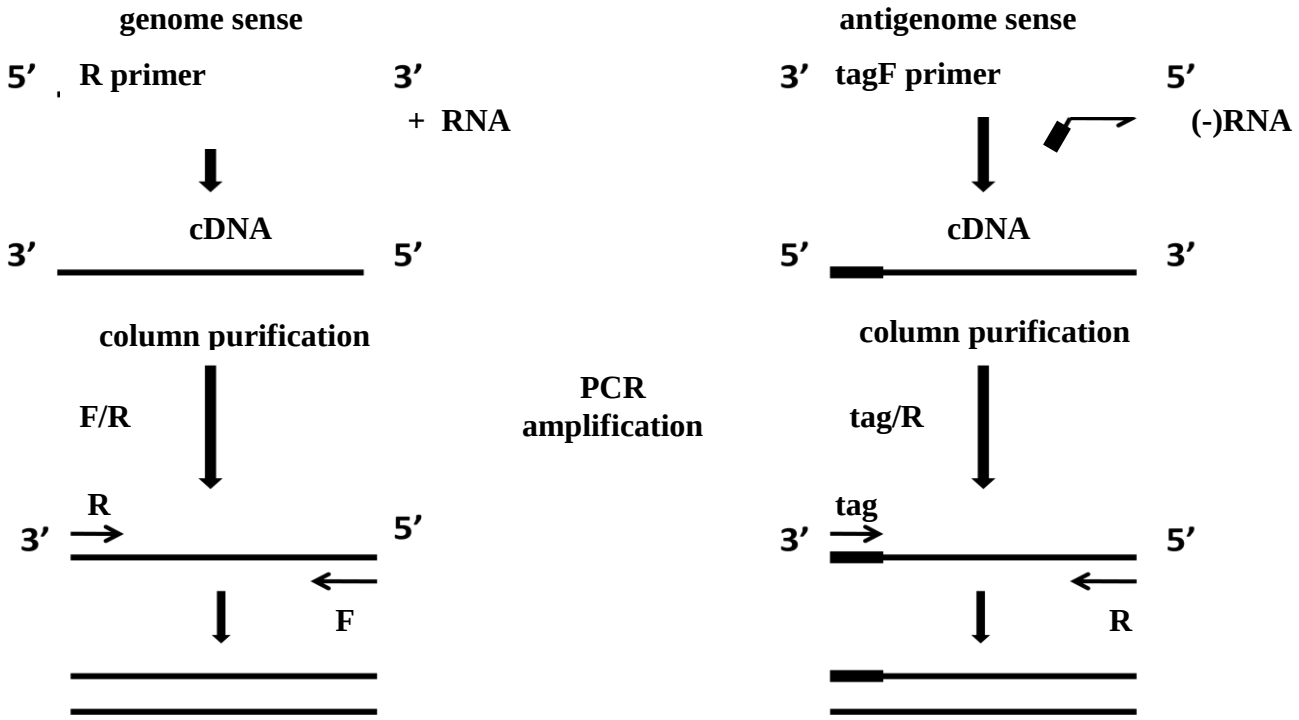

Figure 4.1 Strand-specific RT-PCR (ssRT-PCR) method The ssRT-PCR method designed by Peyrefitte et al. (2003) was used to distinguish between genome sense and anti-genome sense DENV RNA from midguts of mosquitoes infected with DENV. The presence of anti-genome sense RNA was assumed to be indicative of DENV replication. The ssRT-PCR to detect genome sense strand method consists of an initial RT amplification with a reverse (R) primer followed by column purification to remove residual primers and the final PCR step used a forward and reverse primer. The ssRT-PCR to detect anti-genome sense method consists of initial RT amplification with a tagged forward (tagF) primer followed by column purification and finally PCR. The PCR step used a primer specific to the added tag sequence and reverse primer to detect anti genome sense strand. The tagged RT primer and column purification steps increase the specificity of detection of anti-genome sense RNA by reducing false priming.

Table 4.1 Strand-specific RT-PCR primers Primers used for detection of genome sense or anti-genome sense DENV RNA from fractions of cellular fractionation gradient fractions of mosquito midgut tissue, using primers designed by Peyrefitte et al. (2003).

Primer	Purpose	Genomic location	Sequence
KP 99 (tag)	PCR of - strand	none	CGGTCATGGTGGCGAATAA
KP100 (tagF)	RT of - strand	tag, 10565-10541	CGGTCATGGTGGCGAATAAAAGGACTAGAGGTTAGAGGAGACCC
KP101 (F)	PCR of + strand	10565-10541	AAGGACTAGAGGTTAGAGGAGACCC
KP102 (R)	RT of + strand and PCR of +/- strand	10648-10628	CGTTCTGTGCCTGGAATGATG

Verifying strand specific RT-PCR product Gel electrophoresis of RT-PCR products yielded unexpected bands sized 200 bp and 400 bp in addition to 100 bp expected product with the genome sense primers, so products from strand-specific RT-PCR were excised from the agarose gel and extracted using a Gel Extraction kit (Qiagen: Valencia, CA). DNA concentration was determined via absorbance at 260 nm and products sequenced in both forward and reverse directions by the Proteomics and Metabolomics Facility at Colorado State University using an ABI 3130 Genetic Analyzer. We were unable to consistently obtain well separated 400 bp products from genome sense RT-PCR from the anti-genome ssRT-PCR, so these products were not sequenced. Product identity for the 200 bp and 400 bp products from genome sense RT-PCR was verified using the National Center for Biotechnology Information (NCBI) basic local alignment search tool (BLAST).

After examining the BLAST results from the 200 bp and 400 bp PCR product sequences, we decided to check the specificity of the primers via BLAST with automatic adjustment for short input sequence. We also repeated the BLAST search for 400 bp product sequenced with the F primer adjusted for short input sequence. Briefly, the short input sequence adjustments suggested by NCBI were word size 7, expect value 1000, blastn, and removal of the low complexity filter. Next we repeated the 400 bp product sequenced with the F primer BLAST query with the adjustment for short sequence and limited the query to the *Ae. aegypti* genome as this would be the other RNA template present during RT. Since the BLAST of genome sense ssRT-PCR 400 bp PCR product with the F primer with short adjustment and limited to *Ae. aegypti* yielded a few short matches, we reconsidered what primer mismatch would have to occur to give false

primed 400 bp product. Reasoning that to produce a false PCR product, the primer would have to first anneal in the RT, we repeated our query against the *Ae. aegypti* genome using the appropriate RT primer, the R primer, using a BLAST query adjusted for short sequences. The reported primer matches were limited to sequences ≥15 bp since the 200 bp band reported by Peyrefite et al. resulted from a 15 bp upstream primer match, so we knew that 15bp matches were capable of producing unexpected ssRT-PCR products.

Optimization of antibodies

All antibodies used for single and double-staining experiments were optimized on cell culture samples prior to usage in midgut experiments as described in Chapter 2. Occasionally, additional optimization using midguts was required because optimal antibody dilutions or incubation conditions were not identical between cultured cell samples and midgut tissues.

Antibodies for single-label immunofluorescence assays

J2 antibody for detection of dsRNA was obtained from Scions (Scions/English and Scientific Consulting: Hungary http://www.engscicons.de). J2 antibody is a mouse monoclonal antibody (IgG2a) that is highly specific for dsRNA. Research to characterize the antibody showed that dsRNA of length ≥40 bp is recognized in a non-sequence specific manner (Schonborn et al., 1991).

Biotinylated sheep anti-mouse IgG used as secondary antibody and Strepavidin-fluorescein used to detect biotinylated IgG were obtained from Pierce (Pierce/Thermo Fisher Rockford, IL).

Immunofluorescent assay (IFA) for dsRNA

Lyophilized preparations of J2 antibody were reconstituted in 0.5 mL sterile distilled water as recommended by manufacturer, then divided into 10 µL aliquots and frozen at -20˚C for long term storage.

Fixation timepoints were designated as every 24 hours post infection, for as long as needed for the experimental design. Dissected mosquito midguts were immersed in 4% electron microscopy grade paraformadehyde (Electron Microscopy Sciences: Hatfield, PA) diluted in RNase free PBS (Ambion: Austin, TX). Samples were stored at 4°C for 24 hr then centrifuged at 2,500 rpm for 1 min and transferred to microcentrifuge tubes containing RNase-free PBS and stored at 4°C until all timepoints were completed.

Experimental IFAs consisted of incubation with 1:1000 J2 mAb (2 hr) followed by 1:400 biotinylated sheep anti-mouse IgG (1 hr) then strepavidin-fluorescein (1 hr) at 28˚C with gentle rocking (Weber et al. 2007). All antibodies were diluted in PBS with 0.2% bovine serum albumin (BSA) (Sigma: St. Louis, MO) and 0.5% Triton X-100 (TX100) (Sigma: St. Louis, MO). Each incubation was followed by three washes in PBS with 0.01% Tween20 (PBST) (Sigma: St. Louis, MO). All incubations and washes were performed in PCR purification columns with filters removed (Qiagen: Valencia, CA). Midguts were mounted on glass slides using 24 x 60 mm no. 11/2 coverslips (VWR.:

Arlington Heights, IL) using Vectashield with DAPI nuclear stain (Vector Laboratories Inc.: Burlingame, CA) and observed with a Leica DM4500B fluorescent microscope.

Biotinylation of J2 antibody

IFAs for colocalization of dsRNA and DENV envelope and capsid antigens used biotinylated monoclonal antibody J2 prepared with the ProtON Biotin Labeling Kit (Vector Laboratories Inc, Burlingame, CA), which creates a stable linkage between biotin and the antibody. Antibody labeling was carried out as described in Chapter 2.

IFA for localization of dsRNA and DENV proteins

Primary Antibodies

J2 For all assays, biotinylated monoclonal antibody J2 was prepared as described above, then reacted with Streptavidin Alexa Fluor 546 conjugate as described below.

3H5-. Mouse ascites fluid containing monoclonal antibody 3H5-1 to DENV envelope protein was prepared by and obtained from Dr. Irma Sanchez-Vargas (AIDL, Colorado State University).

1A2A-1 Monoclonal antibody specific for DENV capsid protein was obtained from Dr. John Roehrig of CDC DVBID (Fort Collins, CO).

30.11a Mouse ascites fluid containing monoclonal antibody to 30.11a SINV envelope protein was prepared by and obtained from Dr. Irma Sanchez-Vargas (AIDL, Colorado State University).

Secondary antibodies and labels

Streptavidin Alexa Fluor 546 conjugate reacts with biotin to form a stable bond (Invitrogen: Molecular Probes, Eugene, OR). Streptavidin Alexa Fluor 546 conjugate was divided into 50 µL aliquots and stored at -20˚C protected from light.

FITC antimouse IgG antibody was used as the secondary antibody for viral antigen-specific monoclonal antibodies (3H5-1, 30.11a, 1A2A-1) and protein disulfide isomerase PDI antibodies. The FITC antimouse antibody used is a goat polyclonal antibody to mouse IgG heavy and light chain (Abcam: Cambridge, MA).

Localization of DENV envelope antigen and dsRNA

Samples were prepared as described for dsRNA IFAs using *Aedes aegypti* RexD midguts from mosquitoes fed infectious bloodmeals containing DENV-2 (JAM1409) at 1-14 dpi. To ensure that bloodmeals contained infectious virus, a sample of the bloodmeal was titrated by the AIDL CORE support system using the protocol described in Chapter 5 except plaques were counted instead of picked at the end. Experimental IFAs consisted of incubation of infected midguts with 1:400 mAb 3H5-1 (2 hr) followed by 1:400 FITC sheep anti-mouse IgG (1hr) then 1:250 biotin-conjugated mAb J2 (2hr) followed by 1:250 streptavidin Alexa Fluor 546 conjugate (1 hr). All incubations were at 28˚C with rocking. Control IFAs were with monoclonal antibody J2 or 3H5-1 alone and the first two incubations were with PBS with 0.5% TX100 and 0.2% BSA. All antibodies were diluted in PBS with 0.2% BSA (Sigma) and 0.5% TX100 (Sigma); the Strepavidin Alexa Fluor 546 conjugated was diluted in PBS alone. After incubation, samples were washed three times in PBST and distilled water wash after the final incubation. Midguts were mounted on glass slides using 24 x 60 mm no. 11/2 coverslips in Vectashield with

DAPI (Vector Laboratories Inc.: Burlingame, CA) and observed with a Leica DM4500B fluorescent microscope to verify labeling. Relative localization of dsRNA and envelope protein staining was analyzed using confocal microscopy as described below.

Localization of DENV capsid antigen and dsRNA

Samples were prepared as described above for dsRNA. Experimental IFAs consisted of incubations with 1:100 monoclonal antibody 1A2A at 4˚C overnight followed by 1:100 FITC-conjugated sheep anti-mouse IgG (1 hr) then 1:250 monoclonal antibody J2 (2 hr) followed by 1:250 streptavidin Alexa Fluor 546 conjugate (1 hr). All incubations except the initial incubation were at 28˚C with rocking. All washes between and after incubations, mounting, control IFAs, and microscopy were as described above.

Localization of SINV envelope and dsRNA. Mosquitoes were infected as described with SINV-containing artificial bloodmeals. Samples were prepared as described for DENV midgut IFAs, and midguts from RexD mosquitoes fed MRE16, TR339, or mock-infectious bloodmeals were dissected at 1-5 dpi. Experimental IFAs consisted of incubations with 1:150 monoclonal antibody 30.11a (2 hr) followed by 1:100 dilution FITC sheep anti-mouse IgG (1 hr), then 1:250 monoclonal antibody J2 (2 hr) followed by 1:250 Streptavidin Alexa Fluor 546 conjugate (1 hr) with all incubations at 28˚C with rocking. All washes, mounting, control IFAs, and microscopy as described above.

Confocal Microscopy

As in Chapter 2, all three-dimensional imaging and analysis were carried out using the Zeiss Laser Scanning Axiovert Confocal Microscope in the Infectious Diseases

Annex (IDA) on the Foothills campus (Colorado State University). The LSM510 Meta software was used for all imaging.

Confocal settings Confocal settings were optimized for each set of samples as described in Chapter 2. Also, as in Chapter 2, differential interference contrast (DIC) images were only included in results if they added information about the structure of the midgut tissues.

Three-Dimensional Localization Three-dimensional localization of dsRNA within mosquito midguts was as described in Chapter 2. Orthogonal views for analysis were reconstructed from optical Z sections used for three dimensional localization using the LSM510 Meta software orthogonal option.

Electron Microscopy

All electron microscopic imaging was carried out with the assistance of Dr. Suzanne Royer, operating the JEOL 2000 Transmission Electron Microscope in the Anatomy and Zoology building (Colorado State University). All grid preparation was carried out by myself, and embedding after the initial fixation steps was carried out by Dr. Royer.

Sample preparation RexD mosquitoes were fed DENV-2 containing artificial bloodmeals as described above. For vesicle isolation, midguts were dissected from mosquitoes at 7 dpi. Negative controls were prepared from mock infected mosquitoes.

Samples were divided for cell fractionation on sucrose density gradients or microscopy as follows. Fifty midguts were harvested by gently pelleting at 1,500 rpm, 1 min at 4°C. Supernatant was removed and midguts were resuspended in ice-cold PBS

and pelleted at 14,000 rpm, 5 min. Fixative consisting of 62 mM paraformaldehyde with 1 mM glutaraldehyde was added dropwise down the side of the microcentrifuge tube, and samples were allowed to incubate for 10 min at room temperature (RT). Pellet was loosened from the bottom of the tube with a sterile pipette tip and allowed to incubate in fixative for an additional 20 min at RT before transferring to 4°C for storage until embedded and sectioned.

Pre-fixed samples were post-fixed, embedded, and sectioned by Dr. Royer as described in Chapter 2.

Sample preparation: isolated vesicles Vesicle-containing samples were prepared as described previously in the cellular fractionation protocol and mounted on EM grids as described below.

Grid preparation Samples were concentrated as described for cellular fractionation in 0.2 mL TNMg buffer. Samples were stored on ice for transport to the EM center for preparation. Samples were prepared and stained as described in Chapter 2. Samples were immediately examined for imaging after grids were dry.

Characterization of isolated vesicles: detergent sensitivity To determine the detergent sensitivity of vesicles, samples were prepared by the cellular fractionation protocol, except samples were incubated in 1.5% sodium deoxycholate (DOC) on ice instead of TX100 prior to the S16 centrifugation as described in Chapter 2. Grids were prepared as described in Chapter 2. TX100-treated samples from fractions likely to contain vesicles were compared with DOC-treated equivalent fractions.

Imaging Samples were examined by Dr. Royer and myself on the TEM described above. All vesicle images were taken at a magnification of 100,000x, 100 kV. Vesicles were

imaged as described in Chapter 2. Embedded control midgut samples were examined and imaged at a magnification of 30,000, 100 kV for gross morphology changes.

Results

Characterization of sucrose gradient fractions: analysis of viral RNA via strand-specific RT-PCR

DsRNA replicative intermediates consisting of annealed genome sense and anti-genome sense strands of RNA are produced during DENV replication, so if DENV replication occurs within membrane bound compartments, these isolated compartments should contain both genome sense and anti-genome RNAs. To determine whether the viral RNA in the top, more bouyant fractions of cellular fractionation gradients consists of both genome sense and anti-genome sense RNA, a strand-specific RT-PCR method was used.

Anti-genome sense DENV RNA could be amplified from only fractions 1 and 2 of the sucrose gradients used to fractionate mosquito midgut cells at 7 d pbm (Figure 4.2A top row) and from fractions 1-3 in cellular fractionation gradients at 10 and 14 d pbm (Figure 4.2B & C top row). No anti-genome sense strand DENV RNA was amplified from fractions 3-10 of the sucrose gradients used to fractionate mosquito midgut cells at 7 d pbm (Figure 4.2A top row) nor from fractions 4-10 in cellular fractionation gradients at 10 and 14 d pbm. Genome sense ssRT-PCR resulted in observation of genome sense RNA in fractions corresponding with anti-genome sense RNA amplification and in fractions 8-10 at all three timepoints (Figure 4.2A-C bottom row). The strand-specific RT-PCR procedure yielded triplet product bands from cellular fractionation samples (Figure 4.2). Peyrefitte et al. (2003) observed both 100 bp and 200 bp bands after RT-PCR of DENV RNA using the same primers. In addition to the

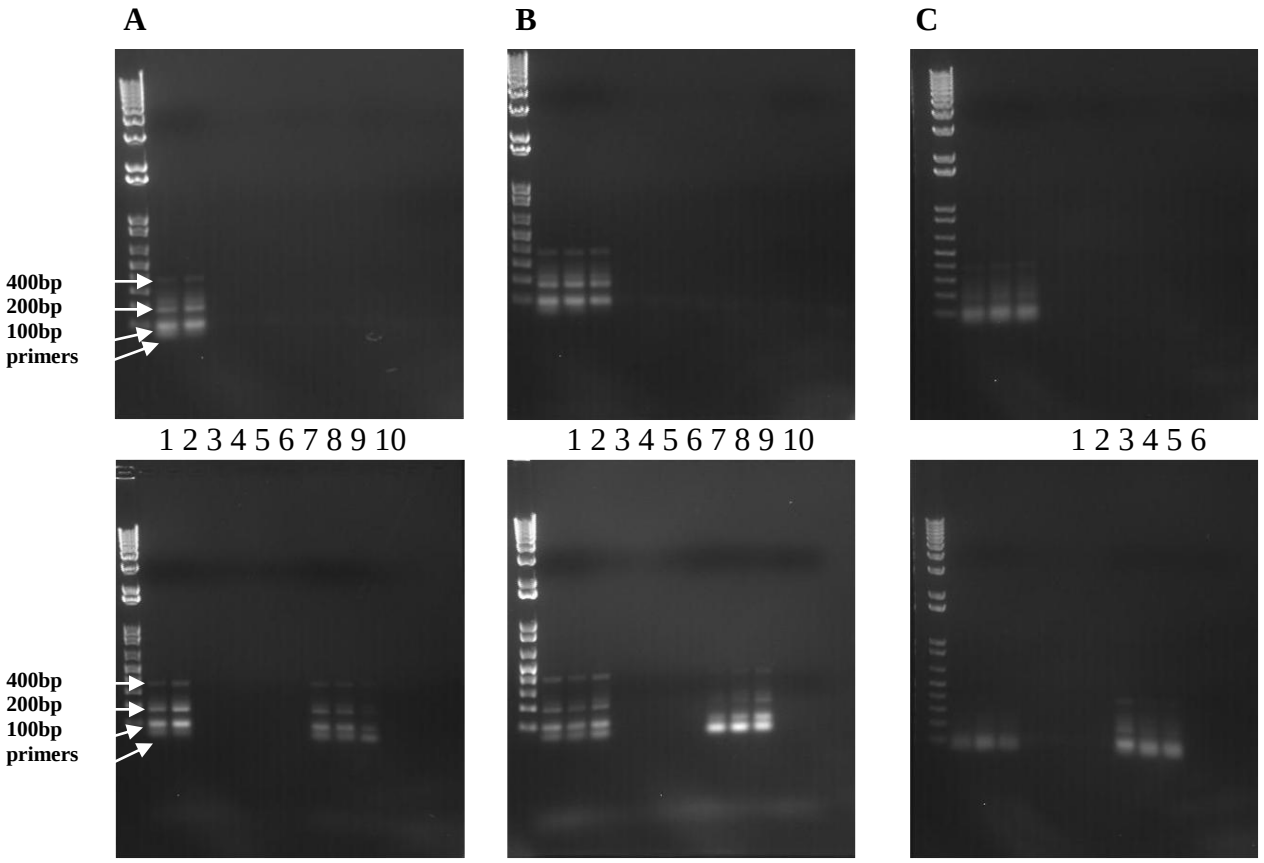

Figure 4.2 Agarose gel electrophoresis of strand-specific RT-PCR products from sucrose gradient fractions of Aedes aegypti mosquito midguts post DENV (JAM1409) containing bloodmeal **A** 7 dpi **B** 10 dpi **C** 14 dpi, top panels contain fractions amplified using primers specific to anti-genome sense DENV RNA and the bottom panels contain samples amplified with primers specific to genome-sense DENV RNA. Each gel shows DNA size markers, fractions 1-10 (top to bottom of sucrose gradient) left to right.

200 bp product we observed a faint band at 400 bp with the genome sense primers and sometimes an indistinct smear with the anti-genome sense primers. To determine whether each of these bands represented specific detection of DENV RNA, the 200 bp and 400 bp product bands were extracted and sequenced by the university sequencing facility using primers F and R. We were unable to sequence the indistinct product amplified with the anti-genome sense primers. Using BLAST alignment, we found that the approximately 200 bp product amplified with F and R primers was DENV-specific and matched the DENV genome from 10603 bp to 10513 bp (Table 4.2a). The 400 bp product amplified with the R primer from the genome sense RT-PCR, resulted in a sequence less than 400 bp in length that was specific to the DENV genome from 10647 bp to 10493 bp. The 400 bp product amplified with the F primer from the genome sense RT-PCR was not found to match the DENV genome. Surprised that the 400 bp sequence did not match the DENV genome, we double-checked all four primers for matches to the DENV genome. Analysis of the BLAST results of the F primer showed a match beginning at 10548 bp and 10493 bp of the DENV genome. BLAST of R showed the intended match at approximately beginning at 10650 bp to the DENV genome and short matches, from 3504 to 3493 and from 3493 to 9301 to 3494 , unlikely to prime synthesis of the 400 bp product. We found short matches between the tag primer and the DENV genome, and matches for either tag or F matches but not both contiguously for the tagF primer which is composed of linked tag and F sequences (Table 4.2b).

Table 4.2a DENV RNA sequence matches for 200 bp and 400 bp unexpected products from strand-specific RT-PCR of sucrose gradient fractions of *Aedes aegypti* mosquito midguts post DENV (JAM1409) containing bloodmeal

PCR product (primer used for sequencing)	GenBank Match JAM1409 (acc. # M20558)	Matching Bases (match ratio)	Notes
200 bp (F)	10603-10645 plus	78/78	confirms Peyrefitte et al.'s observation that the unexpected 200 bp band is strand specific
200 bp (R)	10646-10513 minus	151/154	confirms Peyrefitte et al.'s observation that the unexpected 200 bp band is strand specific
400 bp (F)	no significant similarity		attempted to sequence 3 times, poor quality sequence, sequencing facility noted 2 possible templates once
400 bp (R)	10647-10493	152/154	also aligns with 200bp (R) sequence

Acc# = GenBank accession number. Matching base numbers are the subject nucleotide numbers not the query nucleotide numbers.

Table 4.2 b DENV RNA sequence matches for primers used for strand-specific RT-PCR from sucrose gradient fractions of *Aedes aegypti* mosquito midguts post DENV (JAM1409) containing bloodmeal

Primer	GenBank Match JAM1409 (acc. # M20558)	Matching Bases (match ratio)	Notes
KP99 / tag	3652-3658 plus	7/7	Peyrefitte et al. (2003) states that there was no homology to DENV RNA by BLAST, our results are consistent
KP100 / tagF	10578-10602 plus	25/25	designed to match here
	10493-10515 plus	22/23	mismatch for F region
	7411-7403 minus	9/9	short mismatch
KP101 / F	10548-10602 plus	25/25	designed to match here
	10493-10515 plus	22/23	mismatch for F region
KP102 / R	10685-10665 minus	21/21	designed to match here

Matching base numbers are the subject nucleotide numbers not the query nucleotide numbers. In notes, match indicates homology as intended by primer design and mismatch indicates that match was not intended by primer design.

Table 4.2 b continued DENV RNA sequence matches for primers used for strand-specific RT-PCR from sucrose gradient fractions of *Aedes aegypti* mosquito midguts post DENV (JAM1409) containing bloodmeal

Location of primer mismatches which produce 200 bp and 400 bp products

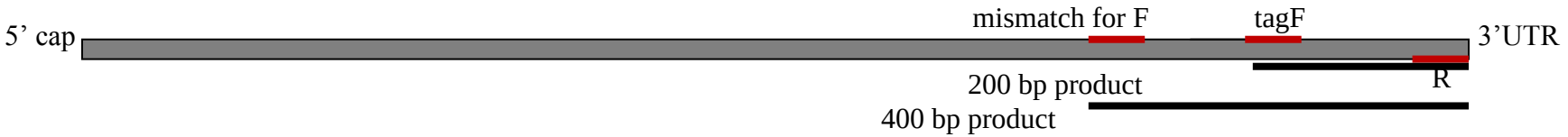

Since the 400 bp product amplified with the F primer yielded only very short sequence matches to the DENV genome via BLAST analysis, and the sequencing facility noted the possible presence of two templates, we hypothesized that the F primer matched unintentionally to another location within the DENV genome besides the 200 bp product yielding mismatch. An adjustment of the BLAST parameters for short query sequences resulted in approximately 50 bp discontinuous matches within the 3' UTR of the DENV genome (Table 4.2c). To identify the possible second template suggested by the sequencing facility, we repeated the BLAST query with limitation to the *Ae. aegypti* genome, based on the hypothesis that mRNA from *Ae. aegypti* would also be present in our samples and observed only short, approximately 22 bp, matches between the 400 bp sequence amplified with the F primer and the *Ae. aegypti* genome (Table 4.2d). We reasoned that a primer mismatch with *Ae. aegypti* mRNA to produce a 400 bp product would have to initially occur during the RT, so we performed a BLAST query with the R primer with automatic adjustments for short sequences and limited the search to the *Ae. aegypti* genome (Table 4.2e). This BLAST search resulted in many short matches to *Ae. aegypti* genome; the reported results were limited to sequences ≥15 bp based on the observation that the 200 bp band found by Peyrefitte et al. (2003) resulted from a 15 bp primer match upstream of the intended site so the ssRT-PCR conditions could result in a product from a 15 bp primer match. This data filter yielded a list of *Ae. aegypti* enzyme mRNAs including acetyl-CoA oxidase, glycogen synthetase, and methylenetetrahydrofolate dehydrogenase.

Table 4.2c DENV RNA Sequence matches for 400bp, F-primed unexpected product bands from of strand-specific RT-PCR products from sucrose gradient fractions of Aedes aegypti mosquito midguts post DENV (JAM1409) containing bloodmeal
BLAST alignment was adjusted for short sequences.

Product (primer)	GenBank Match JAM1409 (acc # M20558)	Matching Bases	Notes
400 bp (F)	10662-10685	22/24	all matches in 3'UTR

Matching base numbers are the subject nucleotide numbers not the query nucleotide numbers.

Table 4.2d *Aedes aegypti* genome sequence matches for 400bp, F-primed unexpected bands of strand-specific RT-PCR products from sucrose gradient fractions of *Aedes aegypti* mosquito midguts post DENV (JAM1409) containing bloodmeal
BLAST alignment was adjusted for short sequences and limited to *Aedes aegypti*.

Product (primer)	GenBank Match	Matching Bases (match ratio)
400 bp (F)	*Aedes aegypti* hypothetical protein partial mRNA (XM_001659297.1 and XM_001648663.1)	554-575 (22/24)

Matching base numbers are the subject nucleotide numbers not the query nucleotide numbers.

Table 4.2e *Aedes aegypti* genome sequence matches for R primer for strand-specific RT-PCR of sucrose gradient fractions of *Aedes aegypti* mosquito midguts post DENV (JAM1409) containing bloodmeal BLAST alignment was adjusted for short sequences and limited to *Aedes aegypti* genome. Only matches ≥15 bp are listed based on the observation that Peyrefitte et al. (2003) noted that their spurious 200 bp band was the result of a 15 bp upstream primer match.

Primer	GenBank Match	Matching Bases (match ratio)	Notes
R	*Aedes aegypti* hypothetical protein partial mRNA (XM_001662311.1)	74-55 (18/20)	
	Aedes aegypti acyl-CoA oxidase partial mRNA (XM_001653267.1)	2258-2275 (16/18)	enzyme involved in fatty acid metabolism
	Aedes aegypti Gustatory receptor28b partial mRNA (XM_001658686.1)	1095-1080 (15/16)	G protein coupled receptor family member
	Aedes aegypti glycogen synthetase partial mRNA (XM_001648654.1)	2282-2267 (15/16)	enzyme that converts glycose to glycogen
	Aedes aegypti aldehyde oxidase partial mRNA (XM_001662355.1)	78-96 (17/19)	enzyme that uses aldehyde to make carboxylic acids
	Aedes aegypti aldehyde oxidase partial mRNA (XM_001654463.1)	141-159 (17/19)	enzyme that uses aldehyde to make carboxylic acids
	Aedes aegypti hypothetical protein partial mRNA (XM_001649518.1)	1723-1707 (15/17)	
	methylenetetrahydrofolate dehydrogenase [*Aedes aegypti*] (XM_001662311.1)	394-409 (15/16)	oxidoreductase family member

Matching base numbers are the subject nucleotide numbers not the query nucleotide numbers.

Localization of dsRNA in midguts of DENV-infected mosquitoes

To determine the pattern of dsRNA in mosquito midgut tissue, we dissected midguts from RexD mosquitoes fed a DENV bloodmeal 7 d pbm, stained for dsRNA, and examined via fluorescent microscopy. DsRNA IFA showed a pattern similar to the infected foci observed in mosquito midguts stained for DENV envelope protein antigen. Staining for dsRNA in midguts of mosquitoes that had been fed a non-infectious bloodmeal showed no immunofluorescence (Figure 4.3). As for midguts stained for DENV envelope protein using 3H5-1, dsRNA foci size observed varied between individual midguts in location, number, and size. Staining for dsRNA with mAb J2 in DENV-infected midguts was less intense than for DENV envelope protein with 3H5-1 but more intense than SINV E1 protein staining with mAb 30.11a in SINV-infected midguts (Figures 4.9 & 4.10).

Localization of dsRNA and DENV E protein in infected mosquitoes

To evaluate whether dsRNA and DENV envelope protein antigen temporally and spatially co-localize in the mosquito midgut, midguts were dissected from *Ae. aegypti* mosquitoes fed infectious or non-infectious bloodmeals at 1-14 d pbm, stained for dsRNA and DENV envelope protein, and examined via fluorescent microscopy. Images from 4-11 dpi that best illustrated changes in DENV envelope and dsRNA staining are shown in Figure 4.4.

There was no staining for DENV envelope protein or dsRNA in mock-infected midguts at any timepoint, indicating that all staining was DENV-specific (Figure 4.4).

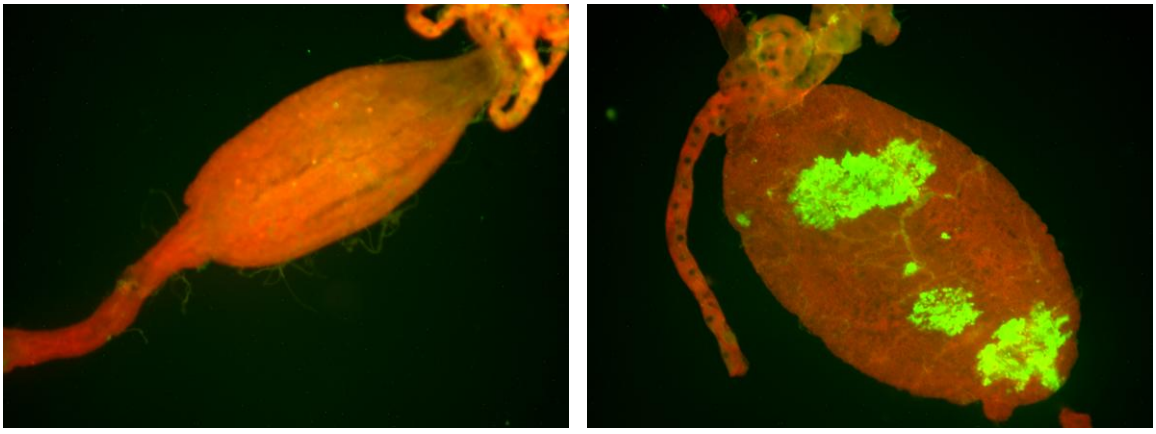

A **B**

Figure 4.3 DsRNA IFA of Aedes aegypti (RexD) mosquitoes at 7 days pbm containing DENV (JAM1409) Midguts from **A** mosquito fed non-infectious bloodmeal and **B** mosquito fed infectious bloodmeal were stained with dsRNA antibody J2 (green) and counterstained with Evans blue (red) (10x, fluorescent). pbm = post bloodmeal

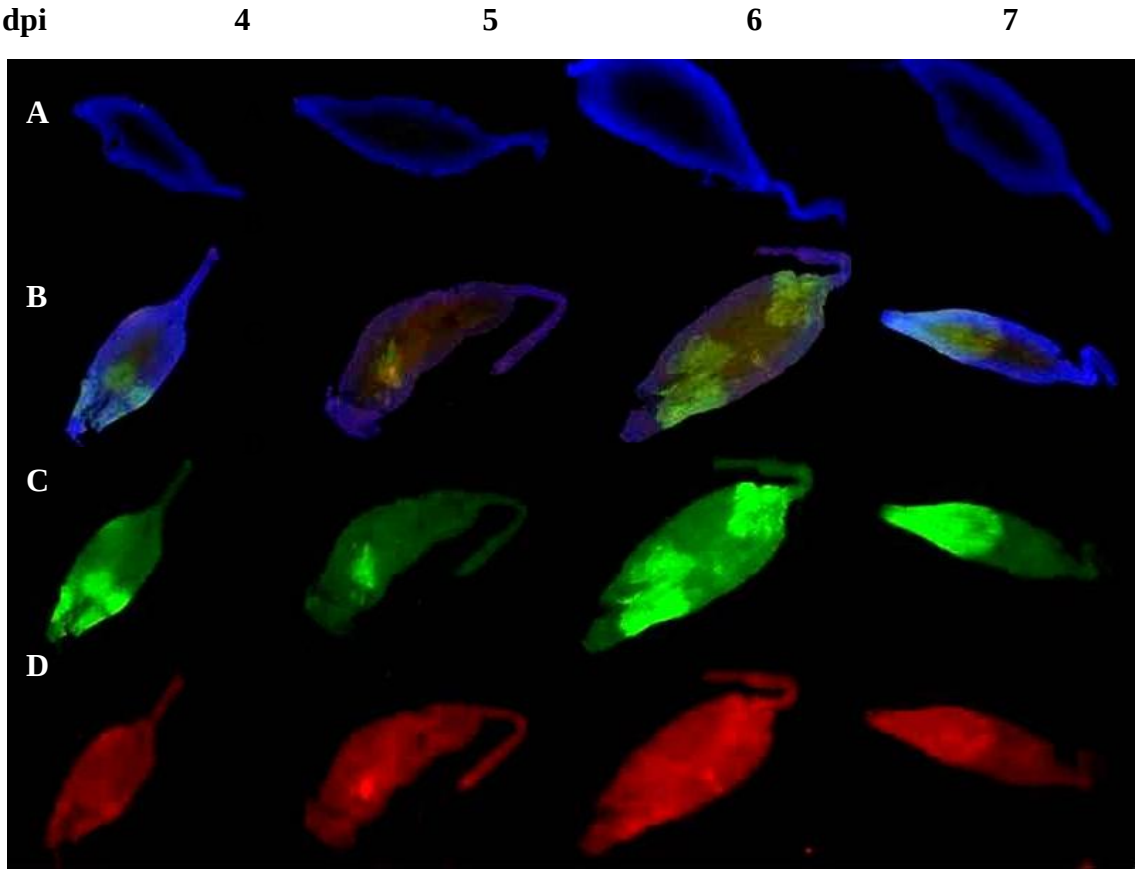

Figure 4.4a Localization of dsRNA and DENV E protein in mosquito midguts (*Aedes aegypti*) 4-7 days pbm Midguts of **A.** mock infected and **B-D** infected mosquitoes were stained for **C** DENV envelope protein (green), **D** dsRNA (red), and **B** C and D merged, **A** and **B** were also stained for nuclei (DAPI) (blue) (10x, fluorescent microscope). DsRNA and DENV envelope protein are visible and approximately co-localized at 4-7days pbm. pbm = post bloodmeal.

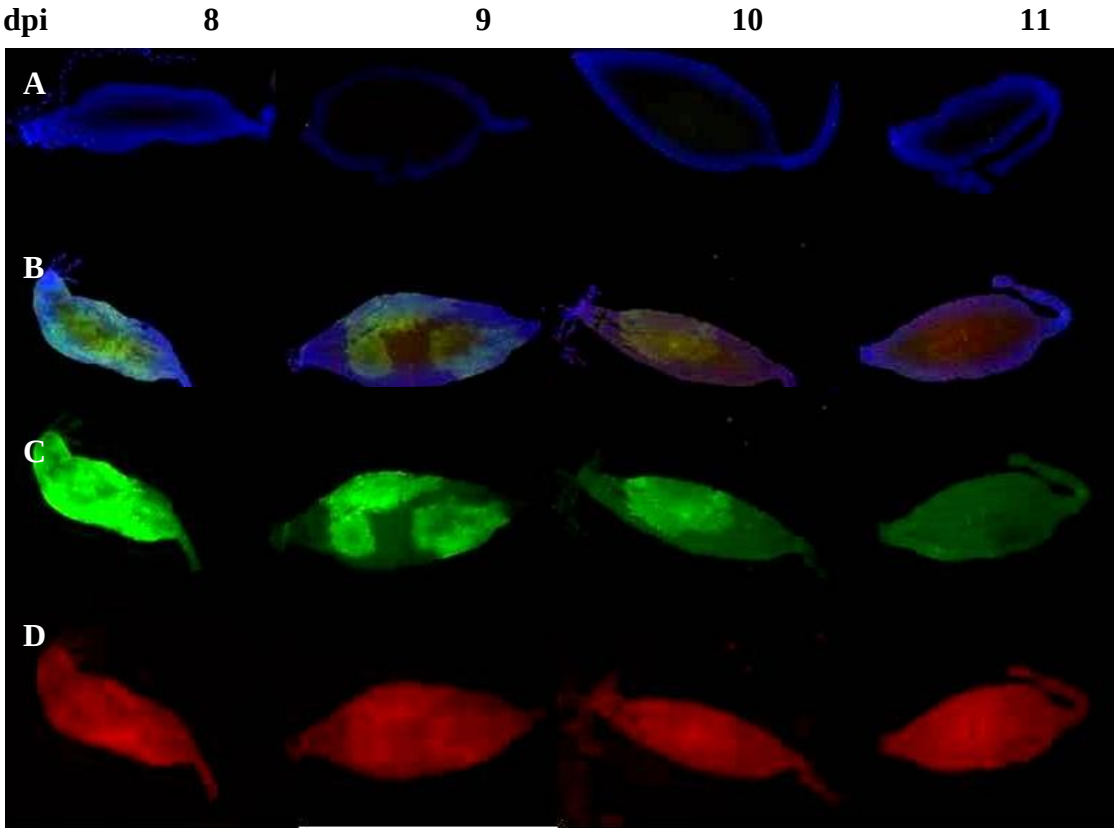

Figure 4.4b Localization of dsRNA and DENV E protein in mosquito midguts (*Aedes aegypti*) 8-11 days pbm Midguts of **A** mock infected and **B-D** infected mosquitoes were stained for **C** DENV envelope protein (green), **D** dsRNA (red), and **B** C, and D merged, **A** and **B** were also stained for nuclei (DAPI) (blue) (10x, fluorescent microscope). DsRNA and DENV envelope protein co-localize 8-11 dpi and intensity of both increases from until 10dpi then begins to wane. pbm = post bloodmeal.

From 1 to 3 days pbm, there was no staining for dsRNA or DENV envelope protein in midguts of mosquitoes fed an infectious bloodmeal. From 4 to 10 days pbm there was an increase in staining for both dsRNA and DENV envelope protein in DENV-infected midguts, followed by a decline in intensity of staining beginning at 11 days pbm and continuing through the end of the timecourse at 14 days pbm. The number of foci and total area of each focus in DENV-infected midguts increased from 4 to 10 days pbm and declined from 10 to 14 days pbm, indicating that there is a tight correlation between production of structural proteins as represented by staining for envelope protein and dsRNA during DENV replication in the mosquito midgut. Antibodies for dsRNA and DENV envelope protein stained similar areas at all timepoints, which is consistent with observations of dsRNA and DENV envelope staining in mosquito cells in Chapter 2. As in Chapter 2, we were unable to see any localization differences between dsRNA and DENV envelope protein via fluorescent microscopy.

Confocal microscopy was used to more closely examine the localization of dsRNA and envelope protein in the midgut of a DENV-infected mosquito. Two regions of a focus of infection in a midgut at 10 d pbm were imaged. The center of the focus was assumed to contain the cells that were first infected by DENV and the edge of the focus was assumed to contain the cells most recently infected by DENV based on observations by Salazar et al. (2006) that DENV moves laterally from the initially infected cells. Figure 4.5 A-E shows the center of the focus of infection and Figure 4.5 F-J shows the edge of the same focus. The DENV envelope antigen staining for entire focus at 10 day pbm resembled a doughnut-like structure with a decrease in intensity of envelope antigen staining in the middle of the focus compared to the outer edge.

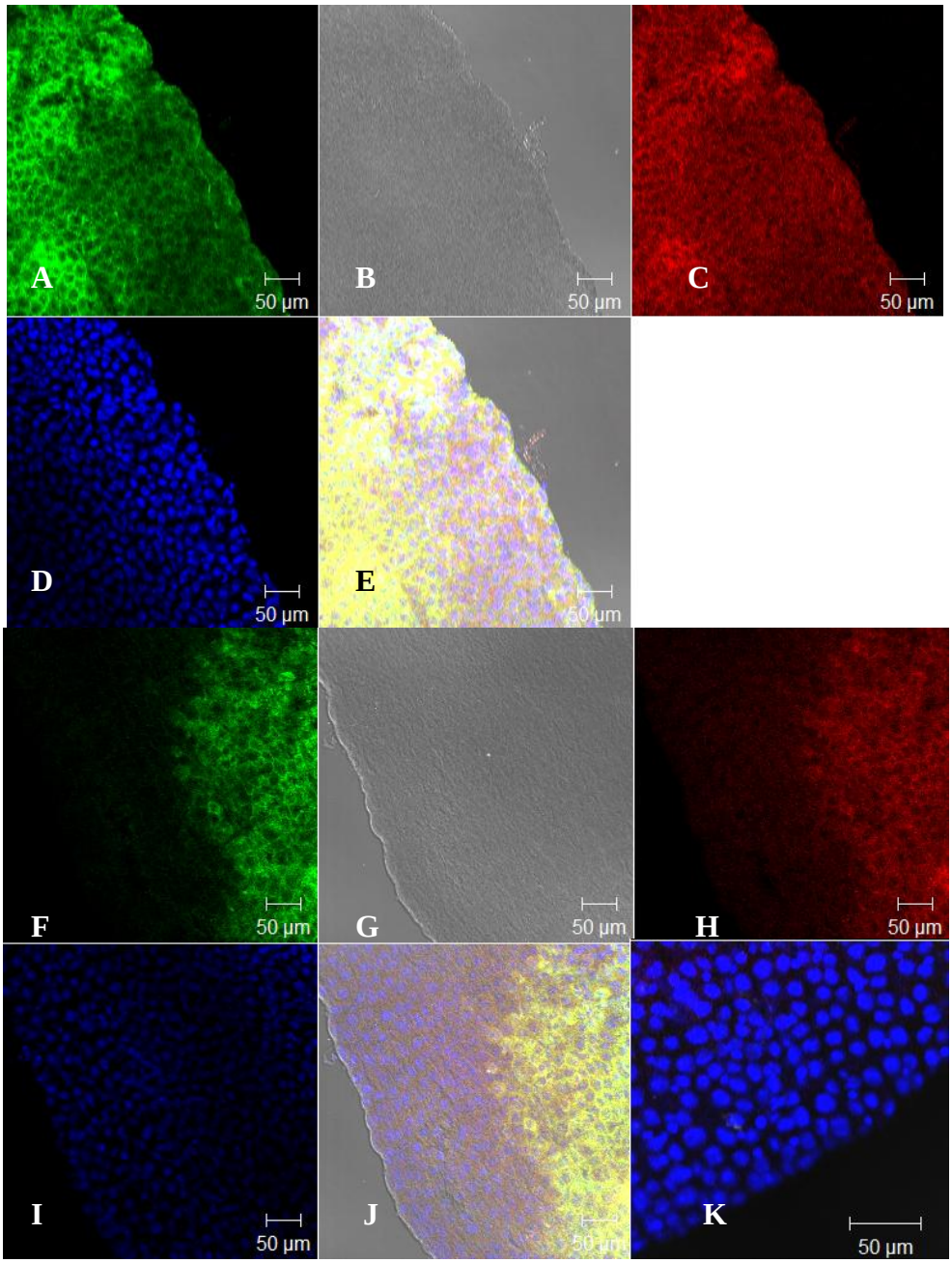

Figure 4.5 Localization of dsRNA and DENV E antigen in 2 regions of a focus of infection in mosquito midgut (Aedes aegypti) at 10 days pbm Midguts were stained for **A & F** DENV envelope protein (green), **B & G** DIC (gray), **C & H** dsRNA (red), **D & I** nuclei, DAPI (blue), and **E & J** A, B, C, and D and F, G, H, and I merged. In merged images, co-localization of dsRNA and E protein appears yellow. Note Image K is also merged but because the midgut was mock-infected, there is no observable staining for DENV envelope protein (green) or dsRNA (red). Images A-E are at the center of the focus of infection; images F-J are on the expanding edge of the focus and represent the most recent DENV infection. Image K (40x confocal) is the uninfected control for the DENV infected midgut shown in A-I (20x confocal). pbm = post bloodmeal

Unfortunately, an entire focus was not imaged. This observation of a decline in viral antigen at 10 dpi is consistent with the observations of Salazar et al. (2007), who also noted a decline in viral antigen staining in mosquito midguts from *Ae. aegypti* colonized from Chetumal, Mexico, at 10 d pbm. Perhaps this decline in viral antigen represents maturation and release of virus into the hemocoel. Again, no temporal or spatial differences were observed between DENV envelope protein and dsRNA localization. This observation is consistent with our observations of DENV envelope protein and dsRNA in mosquito cell cultures in Chapter 2 as well as the observation by Welsch et al. (2009) who noted of tightly associated DENV envelope protein and dsRNA synthesis within mammalian cells.

Localization of dsRNA and DENV capsid antigen in midguts of infected mosquitoes

To determine the temporal expression patterns of dsRNA and DENV capsid protein in mosquito midgut tissue, midguts were dissected from RexD mosquitoes 8-14 days post infectious bloodmeal, stained for dsRNA and DENV capsid, and examined via fluorescent microscopy. We selected the range 8-14 d pbm based on testing to optimize capsid staining in mosquito midguts, which found less variation than in the size of the region stained for DENV capsid antigen at 1-7 d pbm. Observations of capsid staining from 1-7 d pbm were very similar to envelope protein staining in the mosquito midgut, so to broaden our understanding of viral structural protein synthesis relative to dsRNA synthesis in mosquito midguts, we focused our study of capsid antigen staining on timepoints 8-14 d pbm. The size of the area stained for capsid antigen and intensity of staining appeared to peak at 8 d pbm and then wane in both area and intensity by 14 days

(Figure 4.6). The merged image B at day 10 days pbm shows the most representative image of decreased area and intensity of capsid antigen staining. Staining for capsid protein appeared to be slightly more intense on the edges of the stained regions, perhaps because these regions would be the most recently infected and had yet to package and release virus into the hemocoel thus depleting the capsid protein present to form mature DENV virions. This hypothesis is investigated in more detail via confocal microscopy (Figure 4.7).

To more closely examine whether dsRNA and DENV capsid protein co-localize in the midgut of DENV-infected mosquitoes, mosquito midguts stained for both dsRNA and capsid were examined via confocal microscopy. Observations of a focus of DENV infection showed complete co-localization of dsRNA and DENV capsid protein at 20x magnification (Figure 4.7A-E). There was a decrease in intensity of antigen staining in the middle of the focus of infection, which was assumed to be the result of release of mature virions into the hemocoel depleting the capsid protein being produced by the midgut cells. Imaging the same focus at higher magnification, 40x, in an attempt to further investigate the decrease in intensity of staining caused the tissue to tear in the middle of the focus (Figure 4.7F-I). In two-dimensional microscopy, investigation of the torn focus of DENV infection provided no additional insight as to the cause of the decrease in intensity of staining. In midguts of mosquitoes fed mock-infectious bloodmeals, there was slight background fluorescence but no staining for either DENV capsid or dsRNA (Figure 4.7J). A trachea is detectable as a dark area with irregularly shaped edges in the middle of the negative midgut tissue, focusing through the tissue revealed taenidia, confirming the identity of the dark area as a trachea (data not shown).

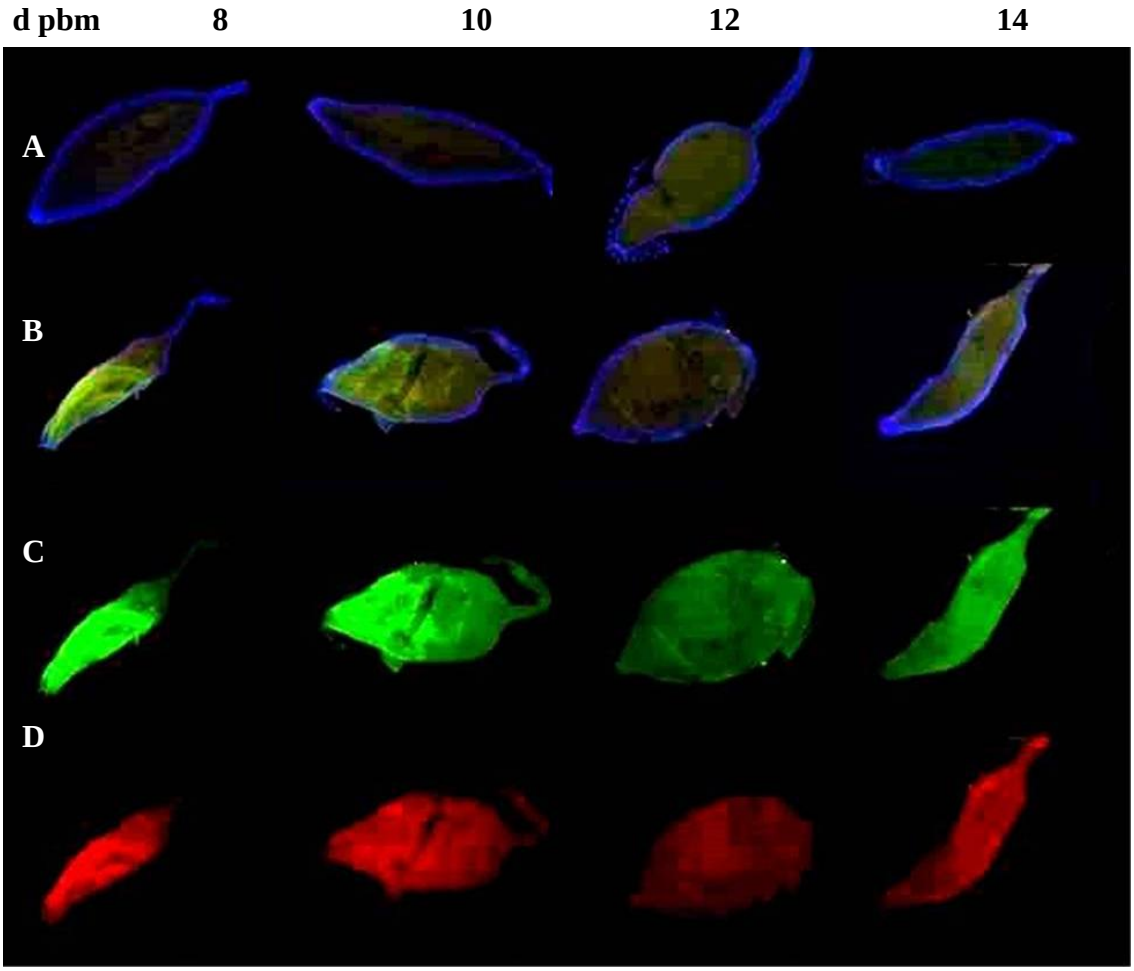

Figure 4.6 Co-localization of dsRNA and DENV capsid protein via IFA in Aedes aegypti (RexD) mosquito midguts at 8-14 days pbm Midguts of **A** mock infected and **B-D** infected mosquitoes were stained for **C** DENV capsid protein (green), **D** dsRNA (red), and **B** C and D merged **A** and **B** were also stained for nuclei (DAPI) (blue) (10x, fluorescent microscope). Staining for capsid protein appears to be slightly more intense on the edges of stained regions. pbm = post bloodmeal.

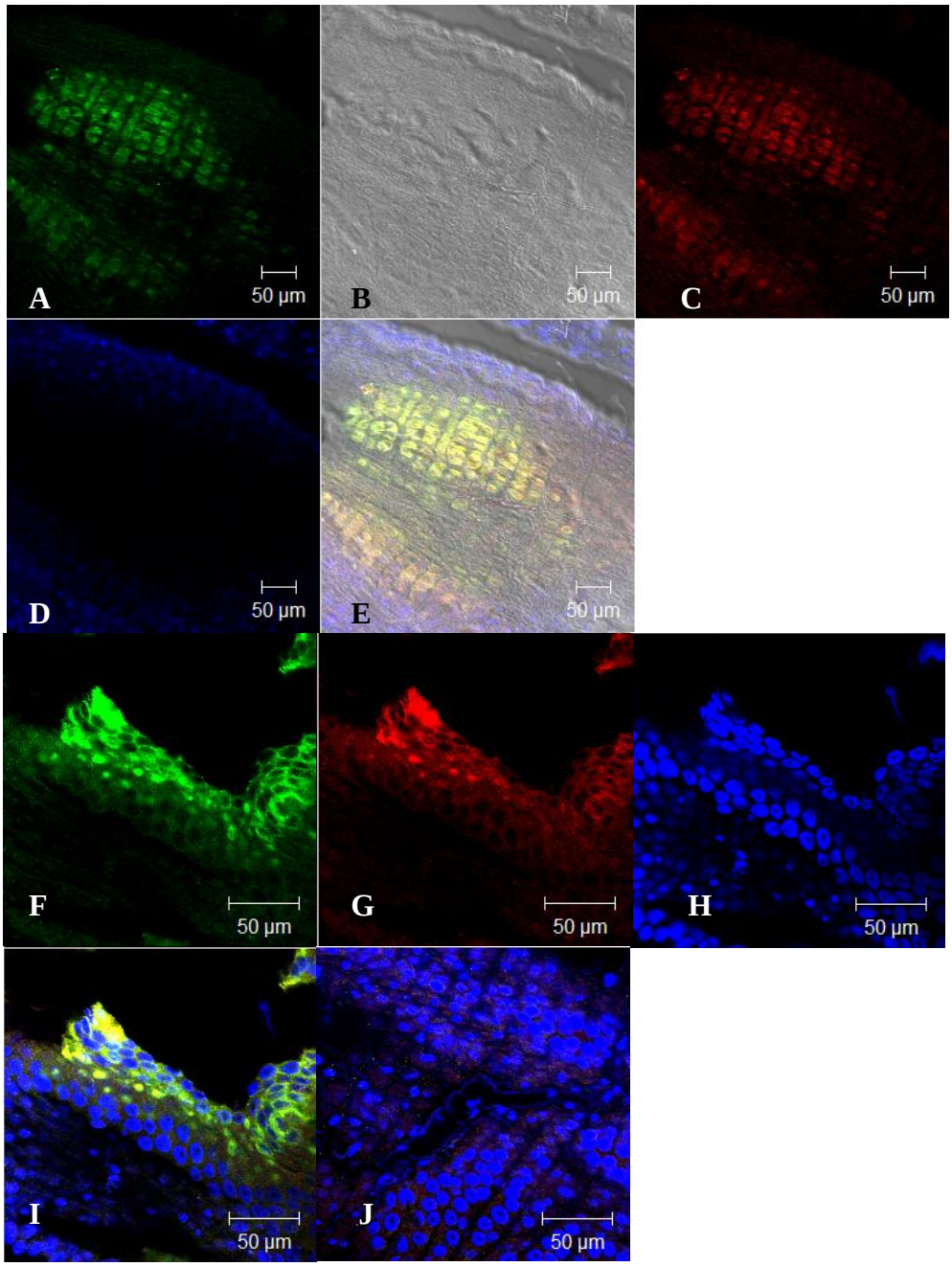

Figure 4.7 Localization of DENV capsid antigen and dsRNA in a viral infected focus at 10 days pbm Infected and mock-infected midguts were stained for **A & F**, DENV capsid protein (green), **B** DIC (gray), **C & G** dsRNA (red), **D & H** nuclei, DAPI (blue), and **E & I** A, B, C, and D and F, G, and H merged. Image J is from a mock-infected midgut and is also merged but because the midgut was un-infected, there is no observable staining for DENV capsid protein (green) or dsRNA (red) (40x, oil confocal). Images A-E are from the intact focus (20x, confocal), images F-I are from the same focus as the tissue began to tear (40x, oil confocal). Images A-E show a focus of infection in the midgut and images F-I show a close-up of the center of the focus. pbm = post bloodmeal

Overall, the temporal and spatial staining for capsid and dsRNA in the midguts of mosquitoes fed infectious bloodmeals (Figure 4.6) was similar to that observed when midguts were stained for DENV envelope protein and dsRNA (Figure 4.5).

Further analysis of the torn midgut tissue, imaged in Figure 4.7 via an optical series focusing through the tissue via confocal microscopy (Figure 4.8), showed a gradual change in staining intensity of DENV capsid protein and dsRNA. A computer-generated orthogonal view allowed us to visualize the Z positioning of each image within the three-dimensional structure of the midgut as indicated by the blue line (top and right panels, Figure 4.8A). Figure 4.8A is a lumen-side view of the focus from Figure 4.7 that shows minimal capsid staining on the lumen-side of the midgut. Examination of the side view of the midgut tissue shows a distinct bias in DENV capsid antigen staining for the hemocoel side of the midgut compared to the lumen side. Figure 4.8B shows a midline view of the same DENV-infected midgut tissue, between the lumen and hemocoel sides. Figure 4.8C is a hemocoel-side view of the focus, which shows more intense capsid antigen staining and a lattice-like structure. Capsid staining is mainly associated with epithelial cells on the hemocoel side of the midgut, suggesting at this 10 day pbm timepoint DENV is being released into the hemocoel coinciding with the timing of what was previously described by Salazar et al. (2007) as a decrease in DENV antigen observed in the midgut. Based on several descriptions of the midgut-associated musculature, which runs both circularly and longitudinally in what Bowers et al. (2003) describe as a "grate work-like banding pattern" around the midgut, it appears that capsid antigen is associated with epithelial cells between the midgut-associated musculature (Bowers et al., 1995; Bowers et al., 2003; Myles et al., 2004). An enlargement of Image

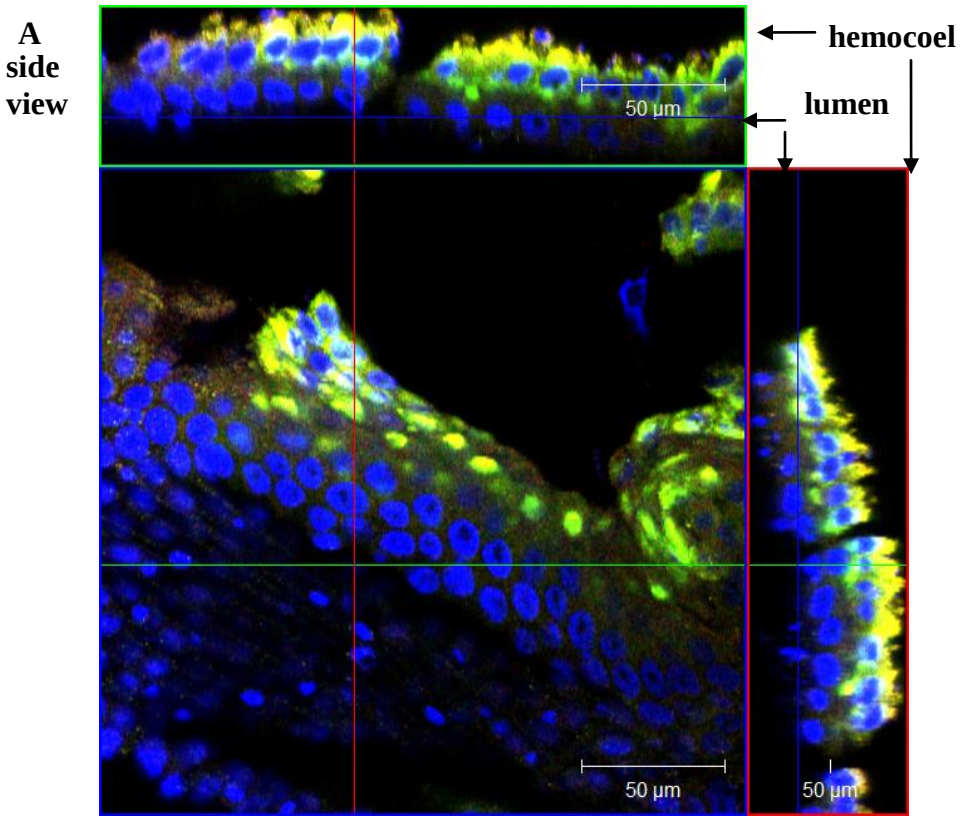

Figure 4.8a Localization of DENV capsid antigen and dsRNA in sections through a focus of DENV infection in a mosquito midgut (Aedes aegypti) at 10 days pbm (orthogonal view) Infected midguts were stained for DENV capsid protein (green), dsRNA (red), and nuclei, DAPI (blue) and these images are shown merged here. This is the same focus of infection that was imaged in **Figure 4.7**. Blue lines indicate the Z-axis location of the tissue section and sections are shown moving from the hemocoel- side of the midgut to the lumen side of the midgut. Image **A** hemocoel-side of midgut tissue, Image **B** midline of midgut tissue, Image **C** lumen-side of midgut tissue. White box in image **C** indicates area that is enlarged and shown in **Figure 4.8b** (40x, oil confocal). pbm = post bloodmeal

B

side view

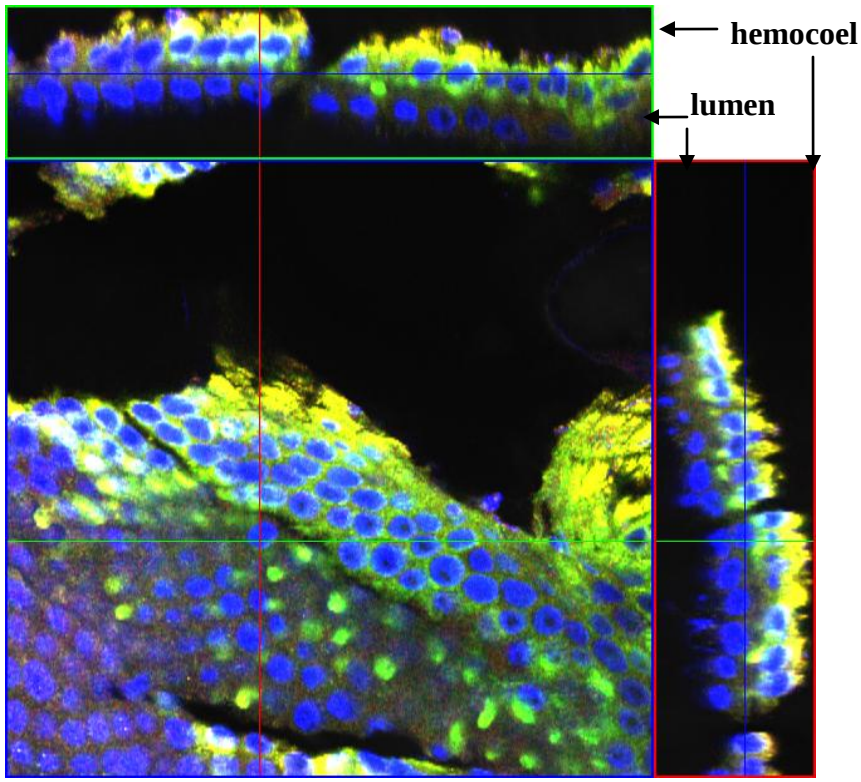

top view midline of midgut tissue side view

C

side view

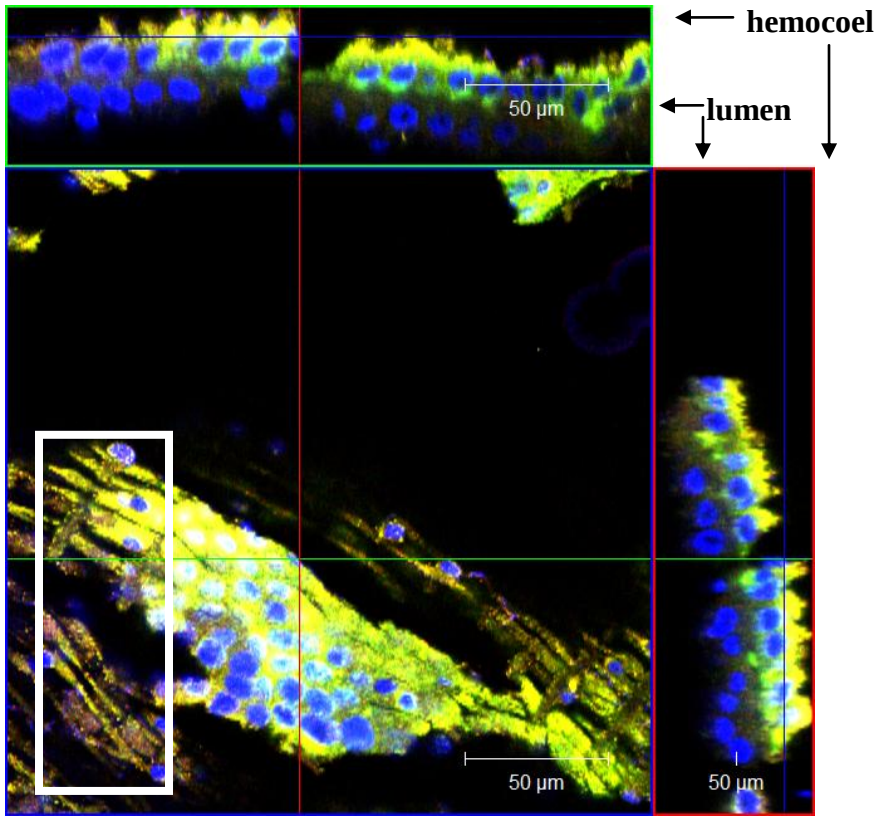

top view lumen-side of midgut tissue side view

D

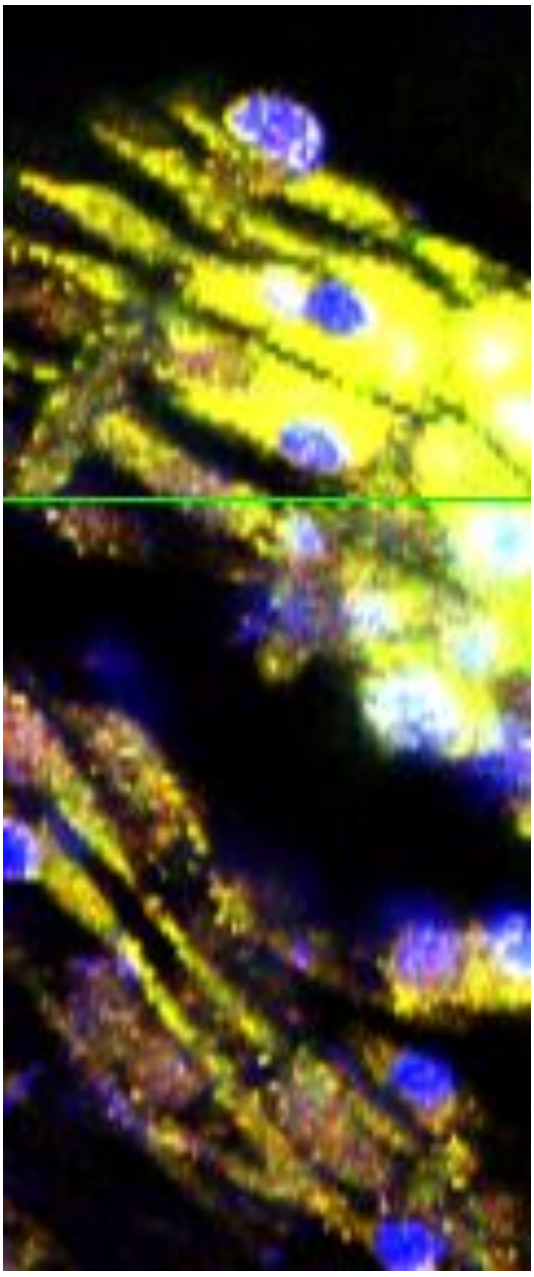

Figure 4.8b Enlargement of DENV capsid antigen and dsRNA staining in lumen-side section of a focus of DENV infection in a mosquito midgut (*Aedes aegypti*) at 10 days pbm Image **D** is an enlargement of the lumen side image shown in **Figure 4.8a, Image C** The checkerboard pattern resembles the pattern made by the the midgut associated musculature which runs longitudinally and transversely around the midgut. The DENV capsid antigen appears to be primarily localized in the epithelial cells between the midgut associated musculature which appears as dark bands at this time post bloodmeal (enlargement of 40x, oil confocal). pbm = post bloodmeal

E

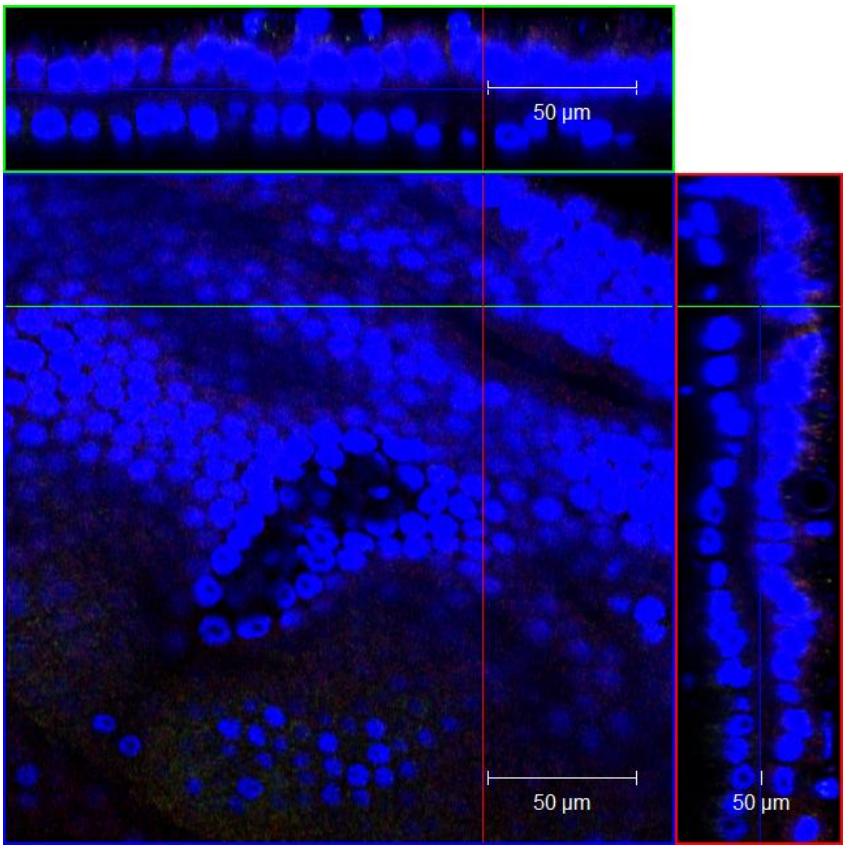

Figure 4.8c Lack of staining of DENV capsid antigen and dsRNA in a section of a mosquito midgut (Aedes aegypti) at 10 days post non-infectious bloodmeal (orthogonal view) Mock-infected midguts were stained for DENV capsid protein (green), dsRNA (red), and nuclei, DAPI (blue) and these images are shown merged here. Note because the midgut was non-infected, there is no observable staining for DENV capsid protein (green) or dsRNA (red). Image **E** midline of midgut tissue. This midgut was the control for the midgut imaged in **Figures 4.8a** and **4.8b** (40x, oil confocal).

C shows capsid antigen between the lattice-like pattern characteristic of the midgut associated musculature (Figure 4.8, Image D). This observation supports observations by Salazar-Sanchez (2006), who stated that DENV-2 antigen was never observed in association with the midgut associated musculature (Salazar-Sanchez, 2006). Mock-infected midguts showed no staining of capsid or dsRNA indicating that all capsid and dsRNA staining was specific to DENV-infection (Figure 4.8c).

Localization of dsRNA and SINV envelope 1 protein in infected mosquito midguts

Spatial and temporal localization of dsRNA relative to SINV E1 envelope protein was examined by feeding *Aedes aegypti* (RexD) mosquitoes infectious bloodmeals containing SINV MRE16 or SINV TR339, dissecting midguts at 1-5 d pbm, and examining them via fluorescent microscopy. In the midguts of the mosquitoes fed the MRE16 strain there was no staining at 1 d pbm, small foci of stained cells at 2-3 days, larger foci at day 4, and by 5 days the intensity of E1 antigen staining in foci had begun to decline (Figure 4.9). In the midguts of the mosquitoes fed the TR339 strain of SINV, there was no staining a 1-3 d pbm, small foci of stained cells at 4 days, and no staining at 5 days (Figure 4.10). Our data are consistent with Myles et al. (2004) who observed that MRE16 and TR339 have similar growth curves in mosquito cell culture, but TR339 titers are much lower than MRE16 titers mosquitoes. The decline in intensity of staining for E1 antigen at 5 d pbm in both the MRE16 and TR339 infected midguts may coincide with release of mature virions into the hemocoel as hypothesized for DENV-infected mosquitoes. No staining for dsRNA or E1 envelope protein was observed in un-infected midguts at any time point, indicating that staining for dsRNA and E1 envelope protein were specific to SINV-infected midguts.

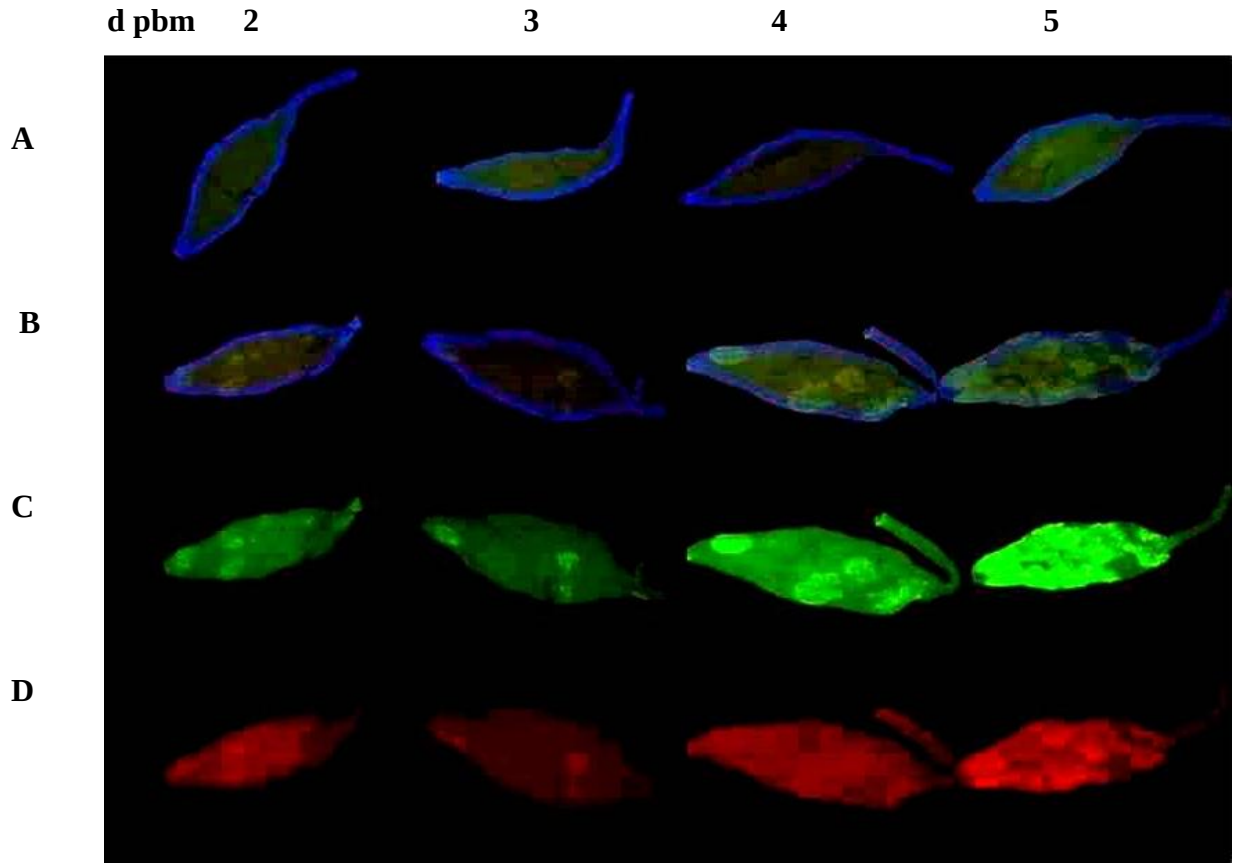

Figure 4.9 Localization of dsRNA and SINV envelope protein in mosquito midguts (Aedes aegypti) at 2-5 days pbm **A** mock infected and **B-D** SINV (MRE16) infected midguts were stained for **C.** SINV E1 envelope protein (green), **D** dsRNA (red) and **B** C and D E merged, **A** and **B** also stained for nuclei, DAPI (blue), (5x, fluorescent microscope). DsRNA and SINV protein co-localize and area stained of both increases from 2-5 days pbm. d pbm = days post bloodmeal

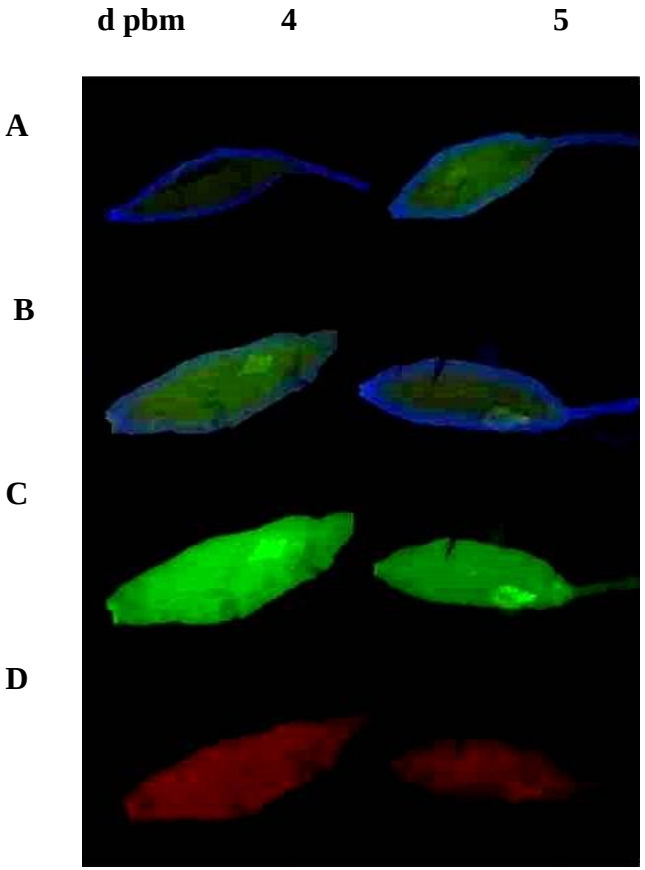

Figure 4.10 Localization of dsRNA and SINV envelope protein in mosquito midguts (Aedes aegypti) at 4 and 5 days pbm A mock infected and **B** SINV virus (TR339) infected midguts were stained for **C** SINV virus E1 envelope protein (green), **D** dsRNA (red) and **B** C and D merged, **A** and **B** were also stained for nuclei, DAPI (blue) (5x, fluorescent microscope). DsRNA and SINV viral protein co-localize and presence of both decreases from 4-5 days pbm. d pbm = days post bloodmeal.

There were more foci observed in MRE16-infected mosquito midguts than in TR339-infected midguts. The staining intensity for E1 envelope protein was greater in MRE-16 infected midguts than in TR339 midguts. Also the proportion of total midguts that had infected foci was greater from the MRE16 midguts than the TR339 midguts. These observations of fewer and less intensely stained foci in TR339-infected midguts compared to MRE16-infected midguts is consistent with observations by Myles et al. (2004), who made similar comparisons of number of infected foci via IFA between the two SINV strains.

To determine where dsRNA and SINV envelope proteins localized in mosquito midguts, the midguts above were further examined via confocal microscopy. There was complete colocalization of dsRNA and SINV E1 envelope protein in midguts of mosquitoes fed SINV strains MRE16 or TR339 and again, the foci from TR339-infected mosquitoes were less intensely stained than the foci observed in MRE16-infected midguts (Figure 4.11 A-E and F-H). As seen previously, midguts of mosquitoes fed non-infectious bloodmeals and stained for dsRNA and SINV E1 envelope protein showed only background levels of staining (Figure 4.11I). As noted for Figure 4.10, there is a qualitative difference in E1 protein staining between MRE16-infected and TR339-infected midguts. TR339-infected midguts stain less intensely for E1 protein antigen. Overall the intensity of dsRNA staining relative to background dsRNA staining in SINV-infected midguts was less than for DENV-infected.

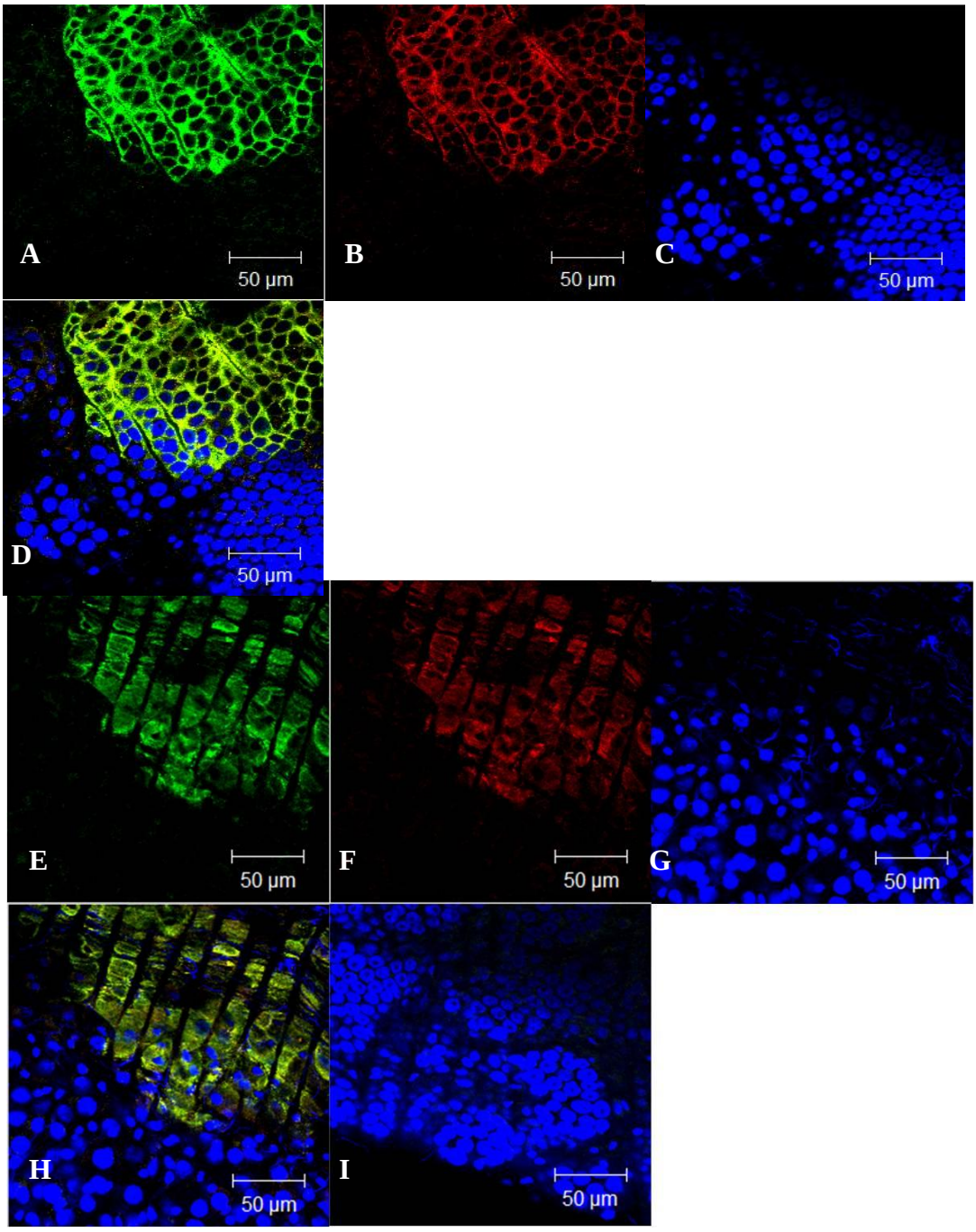

Figure 4.11 Localization of dsRNA and SINV envelope protein in infected cell foci in mosquito midguts (Ae. aegypti) at 4 days pbm Midguts infected with MRE16 **A-D** or TR339 **E-H** or mock-infected **I** stained for **A** & **E** SINV E1 envelope protein (green), **B** & **F**, dsRNA (red), **D** & **G**, nuclei, DAPI (blue), and **D** & **H**, A, B, and C & E, F, and G merged. Note Image I is also merged but because the midgut was mock-infected, there is no observable staining for SINV E1 protein (green) or dsRNA (red) DsRNA and SINV protein co-localize and the patterns of intensity of staining correlate between envelope protein and dsRNA (40x oil, confocal). pbm = post bloodmeal

Transmission electron microscopy

To determine whether detergent-resistant vesicles like those observed in Chapter 2 could be isolated from DENV-infected mosquito midguts, mosquitoes were fed DENV-containing bloodmeals or mock-infected and both groups of midguts were dissected at 7 d pbm, treated with Triton-X100, then fractionated on a sucrose gradient. Fractions from the top of the sucrose gradient were collected, concentrated, and examined via transmission electron microscopy (TEM). Examination of DENV-infected midgut fractions revealed an oval-shaped vesicle with an average diameter of 100 nm and images were taken focusing through vesicle, confirming that the structure was spherical (Figure 4.12). These observations of approximately 100 nm sized vesicles that are specific to DENV-infected materials are consistent with previous work in which detergent-resistant vesicles were isolated from flavivirus-infected mammalian cells and the isolation of infection-induced vesicles from mosquito cell cultures in Chapter 2 (Uchil et al., 2003).

To determine the subcellular origin of the vesicles isolated from infected mosquito midgut tissues, midguts from mosquitoes that had been fed infectious or mock-infectious bloodmeals were dissected and treated with TX100 or DOC. TEM imaging of these materials showed vesicles in TX100-treated DENV-infected midguts but no vesicles in TX100-treated mock-infected midguts, DOC-treated DENV-infected nor DOC-treated mock-infected midguts. These results were consistent with our observations from Chapter 2 and those of Uchil et al. (2003) that DENV RC-associated vesicles were TX100-resistant but DOC-sensitive, which led them to conclude that vesicles associated with flavivirus replication originated from the ER (Figure 4.13).

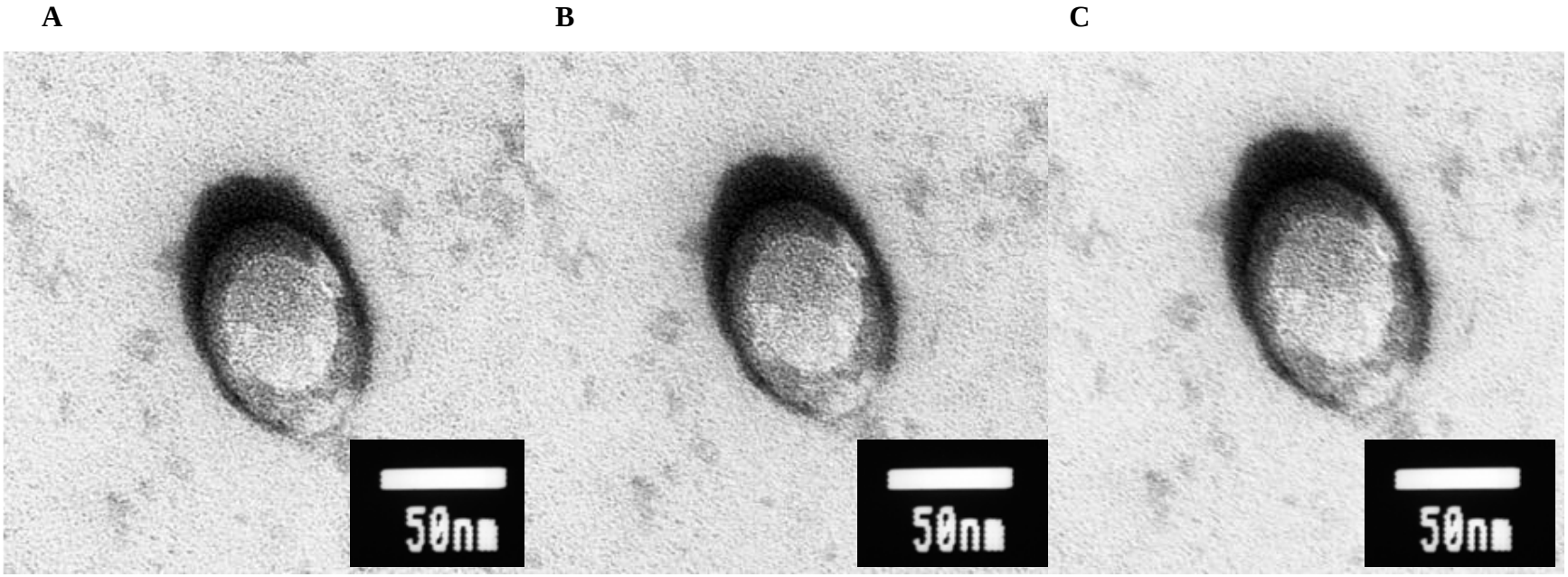

Figure 4.12 Transmission electron micrograph through-focal series of Triton-X100 resistant vesicle isolated from DENV-infected Aedes aegypti mosquito midguts A vesicle from fraction 2 of cell fractionation gradient of TX100-treated mosquito midguts showed the characteristic spherical structure of DENV-associated replication vesicles. All images have the same size bar. (100,000x, 100kV, TEM).

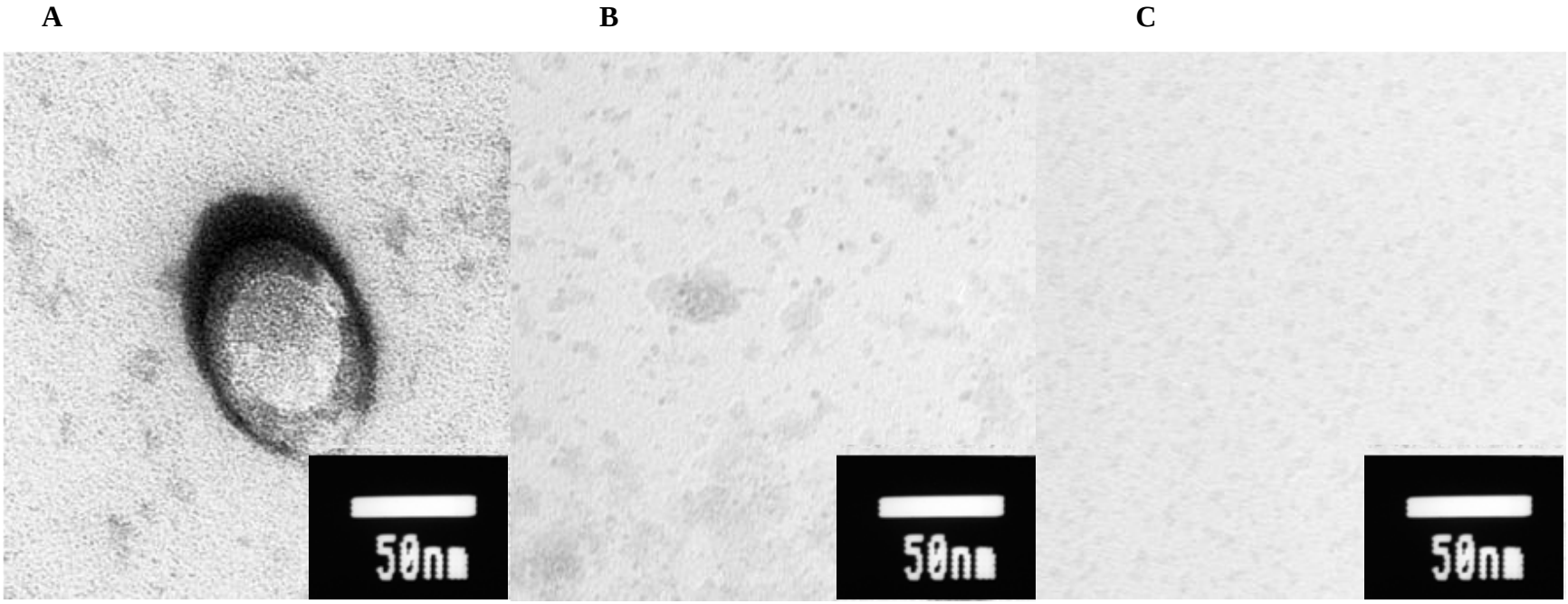

Figure 4.13 Transmission electron micrographs of effects of detergent-treatment of vesicles isolated from DENV (JAM1409) infected Aedes aegypti mosquito midguts at 7 days pbm **A** vesicle from Triton-X100-treated infected mosquito midguts, **B** no vesicles from equivalent gradient fractions of Triton-X100 treated mock infected mosquito midguts, **C** no vesicles from equivalent gradient fractions of sodium deoxycholate treated infected mosquito midguts (100,000x, 100kV, TEM). Resistance to TX100 treatment and lysis caused by DOC treatment suggested an ER origin for vesicles. pbm = post bloodmeal

TEM examination of sucrose gradient fractions from TX100-treated mosquito midguts from showed a variety of sizes of vesicles. The extremes of the vesicle size range were 120 nm (Figure 4.14A) to 50 nm (Figure 4.14 B). Vesicles were only observed in fractions 2 and 3, near the top of the gradient, and not in fractions 1 or 4-10. There was less variation in vesicle sizes from mosquito cell culture described in Chapter 2, 50-75 nm, than in vesicle sizes originating from mosquito midguts. However, the overall 50-120 nm size range encompasses the 50-75 nm range observed by Uchil et al. (2003) using the same methods we used to isolate vesicles. Our TEM vesicle measurements are also consistent with the 87.5 nm average diameter of vesicles from the EM tomography study by Welsch et al. (2009). A wider range of vesicles sizes was observed in TEM images of cellular fractions of mosquito midgut tissues.

To determine where DENV replication-associated vesicles occurred in midgut cells and to confirm that vesicles existed in the original DENV-infected tissues and weren't an artifact of isolation, embedded and sectioned mosquito midguts were examined via TEM. No vesicles were observed from control samples containing mock-infected mosquito midguts, confirming that there were no vesicles in the original mock-infected material.

Unexpectedly, no vesicles were observed in DENV-infected midguts either. However, comparison of images showed differences in the average area covered by ER membranes between infected and mock-infected midguts. Representative sections showed an average of 70% of the imaged area covered by maze-like ER membranes in the DENV- infected mosquito midguts compared to 20% of the area covered by ER

A **B**

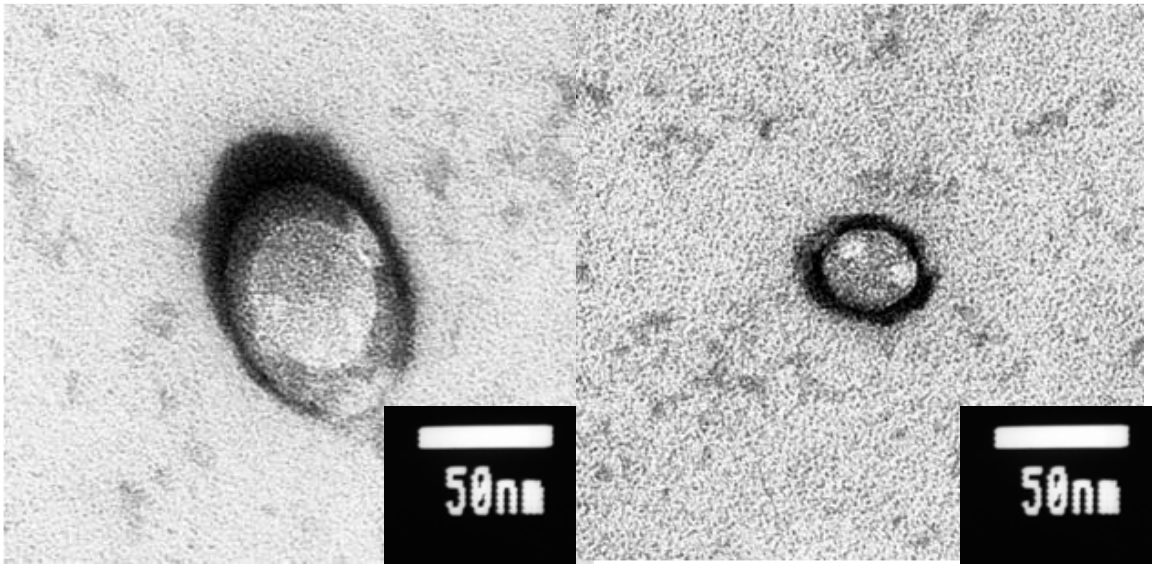

Figure 4.14 Transmission electron micrographs: Size range of vesicles isolated from DENV (JAM1409) infected Aedes aegypti mosquito midguts at 7 days pbm Vesicles isolated from Triton-X100 treated DENV- infected mosquito midguts fractions that are approximately **A** 120nm diameter and **B** 50 nm diameter (100,000x, 100kV, TEM). **pbm** = post bloodmeal

membranes in the mock-infected mosquito midguts (Figure 4.15). This difference in quantity of ER was consistent in all sections observed via TEM from 100 DENV-infected mosquito midguts. These observations are consistent with the observation of Girard et al. (2005) of WNV-infection-induced ER proliferation and the immunofluorescent and immunoEM imaging by Welsch et al. (2009) of ER associated with DENV RC membranes in mammalian cells.

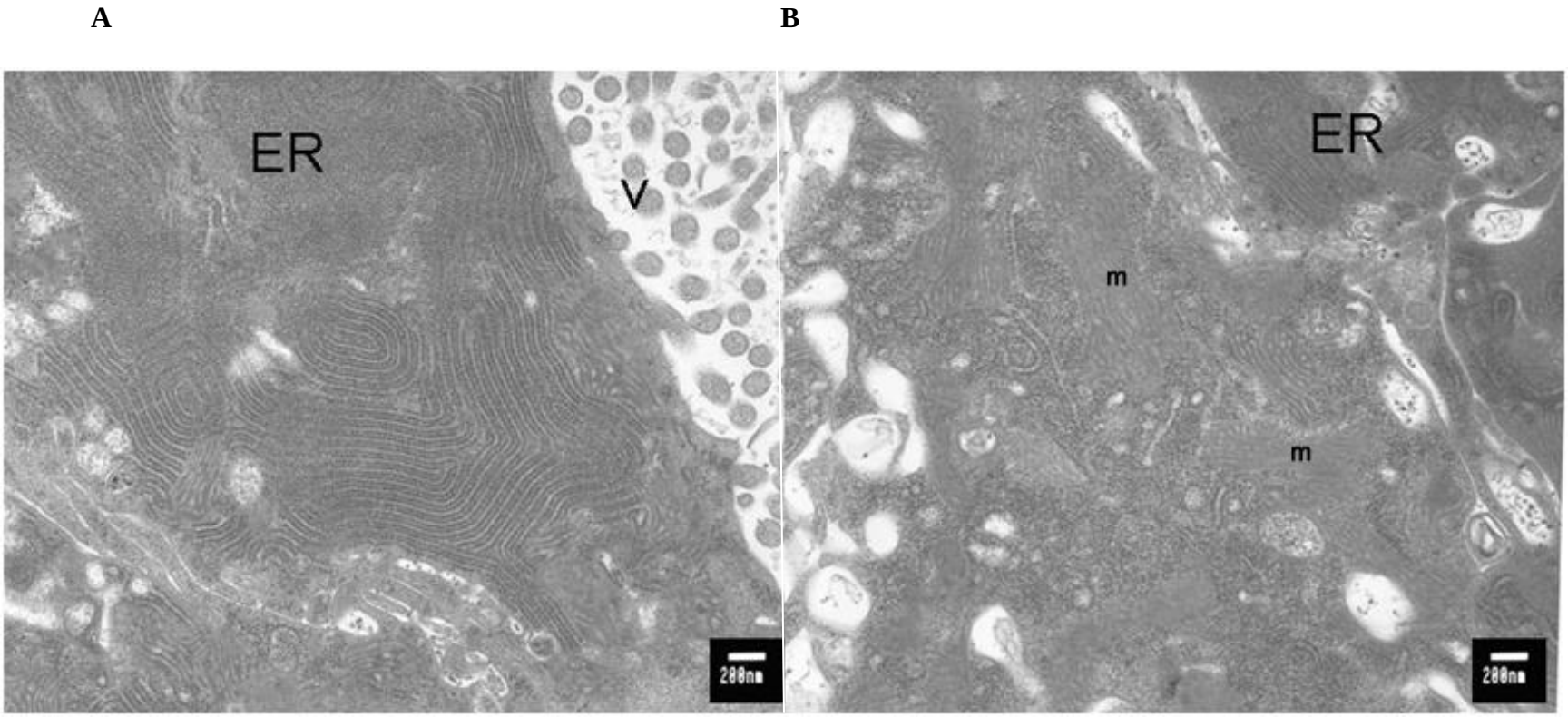

Figure 4.15 Transmission electron micrographs of sections of DENV (JAM1409) infected and mock-infected Aedes aegypti mosquito midguts at 7 days pbm **A** section from infected mosquito midgut, **B** section from mock-infected mosquito midguts, (30,000x, 100kV, TEM). Note larger area of sectioned material covered by contiguous ER membranes in midguts of mosquitoes fed infectious bloomeals compared to mosquitoes fed non-infectious bloodmeals. This observation suggests proliferation of ER membranes. (v = microvilli, m = mitrochondria, ER = endoplasmic reticulum, pbm = post bloodmeal)

Discussion

Characterization of sucrose gradient fractions: analysis of viral RNA via strand specific RT-PCR

We used ssRT-PCR to examine DENV-specific RNA from sucrose gradient fractions of detergent-treated mosquito midguts and amplified genome sense DENV RNA from both buoyant top and dense bottom fractions of the gradients (Figure 4.2, bottom panels). We detected anti-genome sense DENV RNA only in the bouyant top fractions of the sucrose gradients (Figure 4.2, top panels). This pattern of DENV-specific RNA detection in both buoyant top fractions and dense lower fractions is consistent with the RT-PCR results from detergent-treated infected mosquito cell culture fractionation (Chapter 2). The similar localization patterns of DENV RNA between midgut and mosquito cells argues that data from cultured mosquito cells is relevant to the whole mosquito, making the cellular fractionation method useful for the study of DENV RCs because of the timeframe for mosquito cell culture-based experiments is one week versus four weeks for mosquito midgut-based experiments. The use of the ssRT-PCR technique on mosquito midgut samples provided the additional information not available from the RT used in Chapter 2, that DENV-specific RNA in the top fractions was both genome and anti-genome sense. This was a novel use of the method of Peyrefitte et al. (2003) method to evaluate membrane-associated DENV RCs. Overall, the ssRT-PCR data support the hypothesis proposed in Chapter 2 that buoyant fractions contain membrane associated RCs, which contain both genome sense and anti-genome sense DENV RNA and lower, more dense fractions likely contain virions.

The strand-specific RT-PCR method devised by Peyrefitte et al (2003) and used to characterize DENV specific RNAs from mosquito midgut fractions yielded inconsistent results, the yield of the 100 bp product ranged from almost undetectable to clearly observable via agarose gel electrophoresis. The method involved many purification steps, each of which reduced product yield and increased the likelihood of cross-contamination between samples. An interesting follow-up experiment would have been to determine whether these DENV RCs were still active, but this would have required a method of labeling viral RNA and our attempts to directly label DENV RNA for the cellular fractionation experiments in Chapter 2 were unsuccessful.

In trying to optimize the ssRT-PCR assay for detection of anti-genome and genome strand DENV RNA, we found that adjustments in salt and PCR cycle temperature and time parameters that detected anti-genome sense increased the non-specific products from the genome sense RNA. Unfortunately, in using ssRT-PR, we and other researchers have found no data in the literature on the tradeoffs of sensitivity and specificity of this ssRT-PCR technique using tagged primers for detection of arboviruses (Plaskon et al., 2009). Plaskon et al. (2009) used a version of the method of Peyrefitte et al. (2003) for quantitative ssRT-PCR and found that they could minimally detect between 80 and 800 copies of anti-genome RNA from Onyong-nyong virus (ONNV) (family Togaviridae) infected cells. Other researchers have argued that ssRT-PCR methods are still a non-specific method of detection of anti-genome sense RNA because of a snap-back phenomenon in which RNA templates form a transient fold onto themselves, creating an RT primer (Tuiskunen et al., 2009). Tuiskunen et al. (2009) argued that the tagged primer method doesn't overcome this problem and discussed the loss of template

material with the method of Peyrefitte et al. (2003), then offered alternative methods of strand-specific RNA detection which have not been experimentally tested. The critique by Tuiskunen et al. (2009) of Peyrefitte et al. (2003) and other ssRT-PCR techniques was published after these experiments were completed, so we did not have the opportunity to try alternative methods. We agree that ssRT-PCR methods for arbovirus RNA detection need to be improved, but our experimental optimization yielded no evidence for an improved method other than use of different RT and PCR cycling parameters for genome sense versus anti-genome sense detection.

BLAST analysis of unexpected products from strand-specific RT-PCR

BLAST analysis of the 200 bp sized product band ssRT-PCR to detect genome sense RNA of TX100-treated DENV-infected mosquito midguts found that the 200 bp product was completely specific to the DENV genome while the 400 bp product yielded matches to both the DENV genome and mRNAs coding for *Ae. aegypti* enzymes (Table 4.2). This unexpected 400 bp product from ssRT-PCR indicates specificity problems with the ssRT-PCR parameters used for detection of genome sense DENV RNA.

Comparison of methods used to study of DENV RNA replication

A variety of methods, including gradients and chemical inhibitors of protein and RNA synthesis, have been used to study DENV replication in cell culture. An early study of DENV replication in mammalian cells used a cesium chloride gradient to concentrate virus and found RNA that was associated with plaque forming ability in the lower fractions of the gradient (Stevens and Schlesinger, 1965). These data from Stevens and Schlesinger (1965) are consistent with the hypothesis that we proposed in Chapter 2,

that DENV virions were the source the of viral specific RNA in lower fractions of our gradients as well as the ssRT-PCR data that showed only genome sense RNA in the lower fractions.

We found two polarities of DENV-specific RNA in our bouyant sucrose gradients using samples derived from mosquito midguts. Researchers using radiolabeled DENV RNA in mammalian cells typically found 2 sizes of RNA associated with DENV-replication and occasionally a third in gradient fractions: 20S, 26S, and 45S (Stollar et al., 1967). They hypothesized that the 20S RNA was the replicative form of DENV RNA because they only found it early in infection; 26S was an unknown rare form; the 45S RNA was infective. Intriguingly, they found that the 20S RNA descended lower in the sucrose gradient when treated with dimethyl sulfoxide (DMSO), which dissolves polar and non polar compounds. We speculate that the 20S RNA that Stollar et al. (1967) found lower within the sucrose gradient after DMSO-treatment was the membrane-associated RNA that we have been working to characterize. Another study of radiolabeled DENV RNA in mammalian cells found RNA localized to the rough endoplasmic reticulum (rER), which is consistent with our hypothesis for the origin of our bouyant vesicles and our TX100-resistance data (Stohlman et al., 1975). Boulton and Westaway (1976) also gradient fractionated radiolabeled KUNV RNA in mammalian cells, then examined each fraction via EM to discover that KUNV RNA localized with both rough and smooth ER membranes that floated high in the gradient. While the association of RNA with rough and smooth membranes suggests that KUNV RNA may be associated with smooth ER or Golgi membranes as well as rER membranes, it is useful to note that even using a different sucrose gradient method, rER membranes are

buoyant, which is consistent with our observations (Boulton and Westaway, 1976). Uchil et al. (2003) radiolabeled flaviviral RNA in mammalian cells and found the replicative form (RF) or dsRNA of DENV, JEV, and WNV localized to fractions containing buoyant, TX100-resistant membranes in a sucrose gradient. Using quantitative real-time RT-PCR, genome sense and antigenome sense DENV RNA has been detected in *Ae. aegypti* midguts, consistent with our ssRT-PCR detection of both polarities of vRNA at 7, 10, and 14 d pbm (Richardson et al., 2006).

Localization of dsRNA in midguts of DENV-infected mosquitoes via immuno-fluorescent assay

The staining pattern for dsRNA in midguts of RexD mosquitoes 7 days after being fed a bloodmeal containing DENV resembled the staining pattern for DENV-infected foci stained for viral envelope antigen. The similarities between the dsRNA staining pattern and the envelope protein staining pattern we observed in mosquito midguts was intriguing (Figure 4.3). This novel use of mAb J2 to detect dsRNA in mosquito midguts led to the double-staining experiments to determine whether there was complete co-localization between dsRNA and envelope protein staining in the DENV-infected midguts.

Staining mosquito midguts for dsRNA and DENV envelope protein detected no dsRNA or envelope protein antigen 1-3 days pbm, increased staining at 4-10 days pbm, and a decline in staining from 11 to 14 days pbm. This observation of increased antigen staining for DENV envelope protein in mosquito midguts from 4 to 10 days pbm followed by a decline from 11 to 14 days pbm is consistent with the observations of

DENV envelope antigen staining differences between DENV-infected and mock-infected mosquito cells in Chapter 2. Complete co-localization of staining between dsRNA and DENV envelope protein is consistent with the observation by Welsch et al. (2009) that DENV dsRNA replicates in close proximity to virus assembly. The fluorescent microscopy used for these observations lacks the resolution to distinguish between the replication and assembly locations. Confocal microscopic examination of staining for both DENV envelope protein and dsRNA showed that antigen was fading in the center of focus of infection in a mosquito midgut at 10 d pbm (Figure 4.5). Complete co-localization and similar intensities of staining between DENV envelope protein and dsRNA suggested that dsRNA staining is an accurate marker of active DENV replication in mosquito midguts.

It has been shown that virus-specific small RNAs are produced in flavivirus-infected mosquitoes (Sanchez-Vargas et al., 2004); however, because the J2 antibody to dsRNA only detects dsRNA longer than 41 bp in length, we were unable to observe the small RNA markers of the RNAi response via IFA (Brackney et al., 2009; Sanchez-Vargas et al., 2004; Schonborn et al., 1991). Perhaps an EM in situ hybridization (ISH) method, like that of Grief et al. (1997), if it could be adapted to detect small RNAs, would allow us to compare to viral dsRNA as stained by the J2 antibody. A next step would be to compare the viral dsRNA stained with the J2 antibody to ISH-labeled small RNAs between DENV susceptible versus non-susceptible strains of mosquitoes to determine whether the midgut escape barrier (MEB), in which DENV replication is limited to the mdigut and does not disseminate, described by Bennett et al. (2005) could have an RNAi basis. The Carb77 mosquito strain, an RNAi-based DENV-resistant

transgenic mosquito, will be discussed in Chapter 5 as an example of how such DENV resistance in a mosquito might function.

Since there are no other reports of using dsRNA IFA in mosquitoes to compare our data with, we reviewed the immune EM and in situ hybridization studies. EM in situ hybridization using dioxigenin-labeled anti-genome sense DNA probe to genome sense RNA in DENV-infected *Ae. albopictus* cells found RNA in association with the rER and SMS (Grief et al., 1997). Additionally, Grief et al. (1997) observed paracrystalline arrays of virions near SMS in agreement with the model of Welsch et al. (2009) of virus assembly near RNA replication sites. ImmunoEM studies of DENV envelope protein in mosquito and mammalian cell cultures have found envelope protein associated with vacuoles, vesicles, in the rER and around SMS with no spatial differences in localization between cell lines (Barth, 1999; Rahman et al., 1998). Salazar et al. (2006) observed DENV envelope antigen via IFA in mosquito midguts at 3 days post infection, peaking 7-10 days pbm, beginning to fade by 14 days pbm, with some antigen still present as long as 21 dpi in the Chetumal strain of *Ae. aegypti*. The data of Salazar et al. (2006) are very similar to our observations, and they also used the 3H5-1 antibody to DENV envelope as well as a polyclonal human anti-DENV antibody. Franz et al. (2006) observed approximately half of the mosquito midgut was stained for envelope antigen using the 3H5-1 antibody in DENV-infected Higgs' white eye (HWE) strain of *Ae. aegypti* at 7 days pbm. Our data on dsRNA and envelope antigen temporal and spatial localization in DENV-infected *Ae. aegypti* midguts is consistent with published observations in spite of some differences in mosquito strains studied.

Localization of dsRNA and capsid protein in midguts of infected mosquitoes

Staining mosquito midguts for dsRNA and DENV capsid protein showed the same pattern of antigen localization and a decrease in staining from 8 to 14 d pbm which is consistent with the observations of Salazar-Sanchez et al. (2007). Stohlman et al. (1975) also observed a decline in capsid antigen, from 24 hr to 72 hr, isolated from ER-proteins isolated from DENV-infected mammalian cells by gradient fractionation, which they attributed to depletion of capsid protein due to viral maturation. Also the edges of the capsid foci were more intensely stained than the interior of the foci (Figure 4.6). The most recently infected cells would be localized around the edge of foci. These cells in the early stages of DENV infection would have recently begun translation of capsid protein but may have not yet begun packaging and release of mature virus. Viral packaging and release would lead to a reduction of DENV capsid protein available for staining via IFA which could explain why the interior/longer infected cells at the center of foci have less capsid staining.

Confocal microscopic examination of mosquito midguts fed an infectious bloodmeal and stained for DENV capsid and dsRNA showed complete co-localization of the two antigens. The DENV infection appeared to be primarily localized on the hemocoel side of the midgut. Since the midgut sample was at 10 d pbm, this is an older focus of infection, and this localization pattern was consistent with DENV infection beginning on the luminal side of the midgut, then budding through the basal lamina to the hemocoel-side where mature virus would be released into the hemocoel (Figure 4.8 9F to 1A). Other researchers, studying DENV capsid localization via IFA in mammalian cells

noted that capsid localized to the ER and also observed a decline in capsid antigen, which they suggested was depleted by viral maturation (Stohlman et al., 1975).

In agreement with Salazar (2006) we observed DENV capsid antigen localized to the midgut epithelial cells but not associated with midgut-associated musculature (Figure 4.8). Salazar et al. (2007) reported that DENV antigen never associated with midgut-associated musculature in a study of DENV tropisms in *Ae. aegypti* midguts. A review of arbovirus antigens that have been found in association with the mosquito midgut found reports of both flavivirus and alphavirus antigens localized to midgut-associated musculature. A confocal microscopy study by Girard et al. (2004) of WNV in *Culex quinquesfasciatus* found WNV antigen localized to the circular and longitudinal muscles associated with the midgut, using mouse hyperimmune ascites fluid (MHIAF) to WNV by 6 and 8 dpi. An EM study of WNV in *Cx. quinquesfasciatus* noted the membrane proliferation in midgut-associated musculature, which was interpreted as evidence of WNV-replication in these muscles (Girard et al., 2005). Alphavirus researchers have observed SINV antigen in a "grate work-like banding pattern" in intrathoracically inoculated SINV-infected *Ae. albopictus* (Bowers et al., 2003). Myles et al. (2004) observed TR339-infected circular and longitudinal muscles of the posterior midgut of *Ae. aegypti*. Additionally, green fluorescent protein-expressing Venezuelan equine encephalitis virus (VEE) (family Togaviridae) replicons localized to muscle fibers in intrathoracically inoculated *Ochleratatus taeniorhynchus* (Romoser et al., 2004). However, DENV antigens and dsRNA do not associate with the midgut-associated musculature in DENV-infected mosquito midguts.

Localization of dsRNA and SINV envelope protein in infected mosquito midguts

SINV-infected mosquito midguts were stained for dsRNA and SINV envelope protein and examined via fluorescent microscopy. Complete temporal co-localization of dsRNA and SINV envelope protein antigens was observed within samples. However, there were differences in staining between the two strains of SINV, MRE16 and TR339. The larger number of foci in MRE16 infected mosquito midguts compared to the few small, faint foci observed in TR339 infections, is not a novel observation. The localization patterns observed in this experiment were consistent with previous observations of replication differences between the MRE16 and TR339 strains of SINV (Myles et al., 2004).

Comparison of midguts of mosquitoes fed SINV strains MRE16 and TR339 and examined via confocal microscopy showed complete co-localization of dsRNA and envelope protein 1. The differences in staining for SINV E1 antigen between the TR339 and MRE16 stains has been well characterized. In spite of qualitative differences in foci between TR339 and MRE16 in the midgut, Myles et al. (2004) observed no significant difference in titers between the two viruses grown in both mosquito and mammalian cell cultures but did observe significant differences in dissemination between the viruses in mosquitoes.

There was no apparent difference in staining patterns for dsRNA and viral envelope proteins between DENV and SINV at the cellular level in our experiments. Although there were differences in timing and intensity of staining, the known cellular localization differences between flaviviruses and alphaviruses could not be readily evalulated via dsRNA IFA even with the increased resolution of confocal microscopy

(Figures 4.7 & 4.11). The phenomenon of viral antigen localized to the midgut associated musculature seems to be widespread in SINV-infected mosquitoes as Bowers et al. (2004) and Myles et al. (2004) found viral antigen throughout the midgut-associated musculature. It is unclear why this localization difference of SINV antigen with midgut associated musculature and DENV not associated with musculature would occur.

Transmission electron microscopy: through-focal series, detergent resistance, size, localization, and ER proliferation

TEM examination of subcellular fractions from detergent treated mosquito midguts showed non-ionic detergent-resistant spherical structures (Figure 4.12). Comparison of infected and mock infected mosquito midguts treated with TX100 or DOC found vesicles only in infected materials that had been treated with TX100 (Figure 4.13). The lysis of vesicles when treated with DOC is consistent with the biochemical evidence presented by Uchil et al. (2003) and the EM tomography by Welsch et al. (2009) that vesicles in DENV-infected cells originated from the ER. Vesicles were only observed in buoyant fractions near the top of the gradient, and range of vesicle size observed was 50 nm to 120 nm. The gradient position of vesicles coincided with detection of both anti-genome sense and genome sense viral RNA ssRT-PCR results (Figure 4.2). The vesicle size range was similar to observations made from DENV-induced vesicles in mammalian cells and tissues infected with other flaviviruses (Girard et al., 2005; Uchil and Satchidanandam, 2003; Welsch et al., 2009; Westaway et al., 1997b).

As discussed earlier, Uchil and Satchidanadam (2003) found that radiolabeled replicative forms of WNV, DENV, and JEV in mammalian cells correlated with fractions containing vesicles. Also an older study of radiolabeled DENV RNA found replicative forms of viral RNA that were DMSO-sensitive (Stollar et al., 1967). Our data are consistent with published data and expand the observations to mosquito midguts, indicating that DENV replication-associated membranes are relevant to any control measures targeting DENV RNA in mosquito midguts such as the Carb77 transgenic mosquito strain with an enhanced RNAi-response to DENV.

Transmission electron microscopy: ER proliferation

TEM images of embedded and sectioned DENV-infected mosquito midguts showed approximately a 50% increase in area covered by ER membranes compared to mock-infected midguts (Figure 4.15). This observation is consistent with the increase in intensity of PDI-staining observed in infected cells in Chapter 2, which also suggested that DENV replication was associated with proliferation of intracellular membranes in mosquito cells (Figure 2.15). We did not observe evidence of DENV virions in the ER.

Many EM observations of ER involvement in flavivirus replication have been made from cell cultures over the years and fewer observations have been made from mosquito tissues. Ng et al. (1987) observed what they described as ER lengthening during EM imaging of *Ae. albopictus* cell cultures infected with KUNV. Hase et al. (1987) observed virions in the rER of mosquito cells and mammalian cell cultures infected with JEV. Barth et al. (1999) observed SMS in the rER of DENV-infected mammalian and mosquito cell cultures.

Based on the many published records of ER proliferation and virions localized in the ER in flavivirus infected cell cultures, we expected to observe ER proliferation and virions in the ER in DENV-infected mosquitoes. Instead, we observed ER proliferation and no virions in the ER of the midguts of DENV-infected *Ae. aegypti*. Consistent with our EM observations, Whitfield et al. (1973) observed ER proliferation at 6 d pbm in SLE-infected *Cx. quinquefasciatus* and no virions in the ER.

Girard et al. (2005) observed SMS in the rER of midgut cells of *Cx. quinquefasciatus* infected with WNV. We were unable to observe virus or SMS in the midguts of *Ae. aegypti* infected with DENV, but we did see SMS in the ER of infected cultured mosquito cells (Chapter 2), as Barth (1999) observed. In an effort to determine why Girard et al. (2005) observed SMS in the rER and we did not, we compared our sample preparation methods to Girard's methods. Girard et al. (2005) fixed midguts separately and immediately post dissection while our midguts were held on ice and processed as a group of 50, since this was our standard procedure for preparation of cellular fractionation samples, and our goal was to see if vesicles were present in the materials at the beginning of cellular fractionation and not a processing artifact. Another explanation for the differences between our observations and Girard et al. (2005) is that we used DENV-infected mosquito materials and Girard et al. (2005) used WNV-infected materials.

Comparison of electron microscopy observations in arbovirus-infected mosquitoes

Other researchers studying DENV replication in mosquitoes via EM intrathoracically injected *Ae. albopictus* with DENV and followed the morphological

changes over 14 days in negatively stained thin sections and found DENV virions and vesicles in the rER in the midgut, salivary glands, and fat body (Sriurairatna and Bhamarapravati, 1977). Sriurairatna and Bhamarapravati (1977) observed most DENV replication in the SG and less DENV replication in the midgut and fatbody. Perhaps we would have observed more vesicles in our mosquitoes had we examined the salivary glands as Sriurairatna and Bhamarapravati (1977) did. Alternately, the intrathoraric injection technique used may have biased their observations, leading to more evidence of replication, virions and vesicles, in the salivary glands than in the midgut because DENV was not following the natural route of infection and the dose of virus received by the salivary glands was artificially high compared to the natural route of infection.

Comparing the data on DENV to other flaviviruses, researchers studying yellow fever virus (YF) (family Flaviviridae) in intrathoracically injected *Ae. aegypti* mosquitoes found rearrangement of the ER membranes and virions in the salivary glands at 20 days pbm (Bergold and Weibel, 1962). Japanese encephalitis researchers found virus and vesicles localized perinuclearly in the salivary gland cells of intrathoracically injected *Culex pipiens* and *Culex tritaneoniorhychus* (Takahashi and Suzuki, 1979). Whitfield et al. (1973) studied Saint Louis encephalitis virus (SLE) in *Cx. quinquefasciatus* fed on viremic mice and observed ER proliferation, virions in the Golgi body, and more virions in the salivary glands than the midgut late in infection with formation of large paracrystalline arrays observed in the salivary glands after 25 days pbm. The EM study of Girard et al. (2005) of WNV in *Cx. quinquefasciatus* showed membrane proliferation in midgut cells, including a distended ER and virions in the rER. Our observations of ER proliferation are consistent with the SLE and YF studies. We did not see virions in the

ER, Golgi body, or perinuclearly as in the YF, JEV, SLE, or WNV studies but this could be due to timing, dose, route of infection, or tissue differences. The observations of Takahashi and Suzuki (1979) of perinuclear JEV are intriguing because this is consistent with our observations of DENV in mosquito cell culture at early timepoints, but we did not observe this perinuclear localization of DENV antigen in mosquito midguts and had initially attributed it to differences between cell culture and whole tissues. The perinuclear localization of DENV dsRNA was observed in mosquito cell cultures at early timepoints, and our samples were taken from midguts at 7 days pbm.

EM studies of some arboviruses in mosquitoes have observed much more pathology than we did in DENV-infected mosquitoes. A TEM study of WNV in the midguts of a *Cx. pipiens* strain that was found to be resistant to infection with WNV, found apoptotic cells in the midgut. After confirming the hypothesis of apoptosis by acridine orange staining, they suggested that apoptosis may help limit WNV infection of midgut cells. Our midgut cells did not show the level of damage seen in these apoptotic cells.

Weaver et al. (1988) provided *Culesita melanura* a bloodmeal from eastern equine encephalitis virus (EEEV) (family Togaviridae) infected birds and found a great deal of cytopathology in the mosquito midgut. Proliferation of the rER, intracellular virus, and sloughing of the midgut brush border was observed in EEEV-infected *Cs. melanura*, which they argued might modulate EEEV infection (Weaver et al., 1988). A later study of *Cx. tarsalis* allowed to feed on WEEV infected chicks also found midgut lesions and sloughing of the midgut brush border only with higher titer bloodmeals (Weaver et al., 1992). Based on WNV, WEEV, and EEEV observations, DENV

infection is much less pathogenic to midguts than other alphaviruses and flaviviruses. We have proposed the idea that there is a fine balance between DENV replication and the mosquito RNAi defense. As discussed in Chapter 2, Umareddy et al. (2007) proposed that DENV modulates the UPR, so it appears that DENV has co-evolved to a fine balance with the *Ae. aegypti* vector in several different pathways.

Conclusions

The data presented in this chapter suggest that DENV replication occurs in association with vesicles in mosquito midguts. These vesicles are 50-120 nm in diameter, of ER origin, and specific to midgut tissues, which show ER proliferation from DENV- infection. This is the first isolation and characterization of DENV replication-associated membranes from mosquito midguts. These vesicles have similarities to the vesicles observed in Chapter 2 and isolated from DENV-infected mammalian cells. As discussed in Chapter 2, replication of DENV within vesicles may exclude access of Dicer-2 to the dsRNA replicative intermediates. The next chapter will discuss whether genomic mutations allow DENV to thwart an RNAi-based DENV-resistant transgenic mosquito.

Chapter 5

Evasion of RNA interference mediated resistance in transgenic mosquitoes: evaluation of virus escape mutants via sequencing and transgenic mosquito challenge

Introduction

Carb77 is a line of genetically modified *Aedes aegypti* mosquitoes that have reduced vector competence for DENV-2. The Carb77 strain of mosquitoes expresses an inverted repeat sequence from the premembrane (prM) gene of DENV-2. The inverted repeat is expressed under the control of a carboxypeptidase promoter and the transcript forms virus-specific dsRNA at the time DENV acquired in a bloodmeal is initiating replication and therefore most vulnerable (Franz et al., 2006). Carb77 mosquitoes were challenged to test resistance to DENV-2 infection by comparing the DENV-2 titers between Carb77 and the parental white eye strain of *Ae. aegypti* Puerto Rico Rexville D at 7, 10, and 14 days post infection. The results from the challenge experiments showed a small number of Carb77 mosquitoes became infected with DENV (Figure 5.1). The viruses that infected and replicated in the Carb77 mosquitoes were termed "escape variants" in Franz et al. (2006). In this chapter, the "escape variants" will be called "virus escape mutants" because we hypothesized that the escape variants were due to mutations in the DENV genome.

It is unclear why DENV-2 replicated in some individual Carb77 mosquitoes to a significantly higher titer than in other individuals. Reasons for the discrepancy in titers between individual mosquitoes may include variation in virus genome sequence, physiological variation between individual mosquitoes, or physiological damage caused by artificial bloodmeals. Regarding variation in virus genome sequence, viruses exist as quasispecies or a group of genomic sequences which are under constant selection, so the DENV-2 used to challenge the Carb77 mosquitoes exists as a population of varying

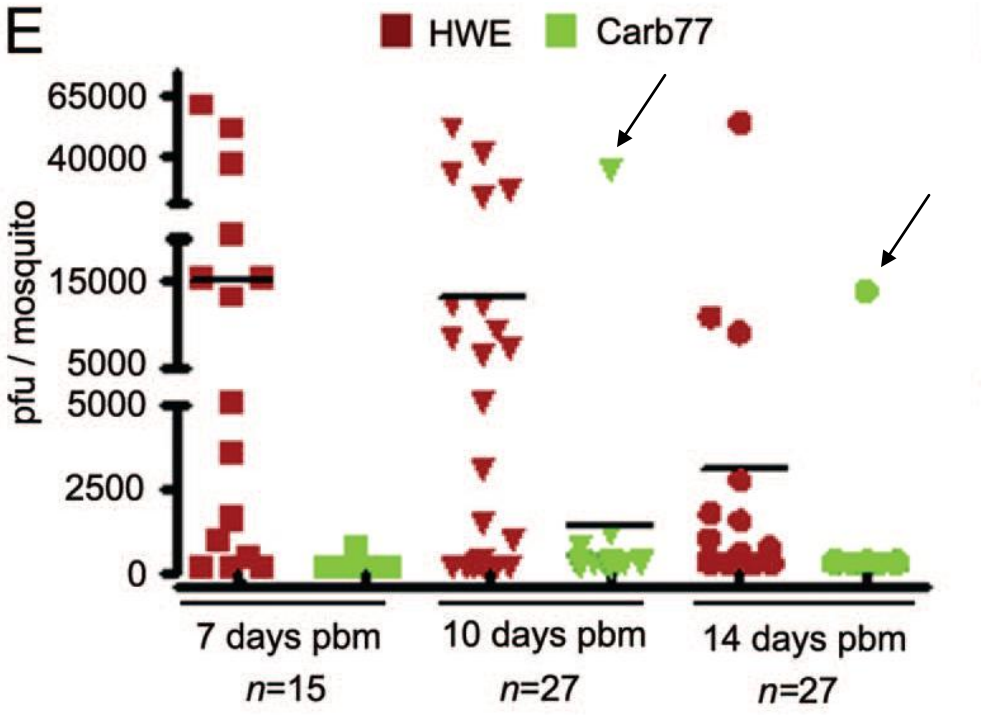

Fig 5.1 Virus escape mutants Whole body plaque titration of DENV-2 in Carb77 and Higgs white eye (HWE) mosquitoes at 7, 10, and 14 days post infection, modified from figure 3 of Franz et al. (2006). Arrows indicate examples of virus escape mutants.

genomic sequences (Domingo et al., 1985; Holland et al., 1982). The prM-primed RNAi response in Carb77 mosquitoes could be exerting a greater than normal selection pressure on DENV-2, leading to the selection of genomes with prM mutations. As for the possibility of variation in physiological state between individual Carb77 mosquitoes, variation in body size, due to larval rearing, has been correlated both positively and negatively with susceptibility to infection with arboviruses in different sudies (Grimstad et al., 1980; Paulson and Hawley, 1991; Schneider et al., 2007; Sumanochitrapon et al., 1998), so variation in body size of individual Carb77 mosquitoes could affect virus titer. Since the Carb77 strain was based on the Higgs white eye (HWE) strain of Rexville D *Ae. aegypti*, which has been reared in the laboratory for many years, it is likely that any genetic variance in body size of the Carb77 family is already constrained. Another possibility as to why some DENV-2 replicates to higher titers in some mosquitoes is physiological damage caused by excessively large bloodmeals taken during artificial bloodfeeding. This leaky midgut theory is used to explain the presence of virus in the hemocoel immediately after a bloodmeal, much faster than the virus could escape from the midgut via replication (Woodring et al., 1996). In fact, EM studies of *Culex taeniopus* have shown that uptake of unusually large bloodmeal volumes allows VEEV to reach the fat body within 1 hr post bloodmeal (pbm) (Weaver, 1986). In the case of the Carb77 mosquitoes, a leaky or bypassed midgut would allow the virus to completely avoid the enhanced RNAi response in the midgut.

We chose to test the hypothesis that variation in virus genome sequence was responsible for the high titer DENV-infections observed in some Carb77 mosquitoes. RNA viruses exist as a quasispecies, so the original DENV-2 containing bloodmeal fed to

the Carb77 mosquitoes would have contained DENV genomes with nucleotide sequence variations differing from the consensus sequence. The DENV genomes with the most nucleotide mutations in the prM region would be less affected by the Carb77 mosquitoes' enhanced RNAi-response directed to the prM region, which could give these viral genomes a fitness advantage. DENV genomes with such a fitness advantage might be observed to replicate to a higher titer in Carb77 mosquitoes as observed in Franz et al. (2006), infect a higher proportion of mosquitoes, and maintain mutations within the prM region of the genome.

Other RNA viruses including poliovirus (PV) (family Picornaviridae), Hepatitis C virus (HCV) (family Flaviviridae), and human immunodeficiency virus-1 (HIV-1) (family Retroviridae) have "escaped" or acquired the ability to replicate in the presence of RNAi-based siRNA or dsRNA therapies (Gitlin et al., 2005; Konishi et al., 2006; Pusch et al., 2003; ter Brake et al., 2008; Westerhout et al., 2005). Gitlin et al. (2005) observed point mutations in the siRNA targeted region of poliovirus, which led to resistance to siRNA treatment in cell culture. Konishi et al. (2006) studied how rapidly HCV mutants would arise in siRNA treated cell culture and found partial resistance to siRNA treatment arose within four weeks. HIV-1 researchers found that point mutations reduced the efficiency of siRNA silencing, mutations that affected the secondary RNA structure of the viral genome affected HIV-1 susceptibility to RNAi, and genome regions that are targeted by siRNAs have an increased frequency of mutation (ter Brake et al., 2008; Westerhout et al., 2005). A recent report by Brackney et al. (2009) used massively parallel sequencing to demonstrate that regions of the WNV genome that are more highly

targeted by RNAi in mosquitoes, as indicated by a greater number of siRNA sequences, are more likely to have imperfect matches between siRNAs and the WNV genome.

The hypothesis tested in this chapter is that mutations in the DENV prM gene allowed the virus escape mutants to replicate to a higher titer in the RNAi-based DENV-resistant transgenic Carb77 mosquitoes. This hypothesis will be referred to as the "escape mutant hypothesis" for ease of discussion. To determine whether the escape mutants evaded RNAi-mediated resistance due to mutations in the targeted prM region of DENV RNA, we analyzed the prM gene sequence of the escape mutant viruses' genomes. Results from this analysis led to further investigation of mutants via full-length genome sequencing and artificial bloodmeals to re-challenge Carb77 mosquitoes with the isolated mutant viruses.

Materials and Methods

Cell culture lines

C6/36 (*Aedes albopictus*) cells were grown in Leibowitz's L-15 medium supplemented with 10% fetal bovine serum (FBS), 100 U/mL penicillin, 100 µg/mL streptomycin, 0.2 mM L-glutamine (growth medium).

LLC-MK2 (rhesus monkey kidney cells, *Macaca mulatta*) cells were grown in MEM supplemented with 8% FBS, 0.2 mM L-glutamine, 1x MEM non-essential amino acids, 100 U/mL penicillin, 100 µg/mL streptomycin, and 1.25 mM Amphotericin B.

Mosquito rearing

All mosquitoes, *Aedes aegypti,* were reared at 28˚C and 80% humidity, with a photoperiod of 12h light and 12h darkness by the AIDL CORE Support program in the insectary of the Virology suite of BRB. Mosquitoes were maintained prior to bloodfeed on sugar cubes and water *ad libitum*. All transgenic mosquito strains were sorted under fluorescent microscope for enhanced green fluorescent protein (egfp) eye marker expression to verify transgenic status prior to use in experiments.

Higgs white eye (HWE) The HWE mosquitoes are a white eye variant derived from the Rexville D strain, originally from Puerto Rico. The basis of the white eye phenotype of the HWE mosquitoes is a mutation in the kynurinine hydroxylase gene that affects eye pigment (Cornel et al., 1997). Lack of eye pigment allows for the visible expression of fluorescent markers in HWE mosquitoes making this mosquito strain uniquely useful for easily screened transgenic mosquitoes.

Carboxypeptidase 77 (Carb77) The Carb77 mosquitoes are the genetic family derived from the original transgenic female mosquito designated number 77. These transgenic mosquitoes were genetically engineered from the HWE strain with a transgene as described previously (Franz et al., 2006). The Carb77 mosquitoes used in this chapter were from generations (G) 9-11, and the mosquitoes used in the challenge experiment reported in this chapter were G_{11}. Note that Carb77 loss of resistance to DENV-2 over G_{14}-$G_{17,}$ as reported by Franz et al. (2009), was not suspected at the time these experiments were designed.

Vitellogenin 40 (Vg40) The Vg40 mosquitoes are another line of transgenic mosquitoes with the same transgene described previously for Carb77 but now under the control of the vitellogenin 1 (Vg1) promoter so that the transgene is expressed in the fatbody (Franz et al., 2009).

Viruses

All virus seed stocks were initially prepared from laboratory stocks maintained by the AIDL CORE support system. All stock titrations were performed by the AIDL CORE support system using the protocol described below.

DENV-2 For preparation of virus for artificial bloodmeals, 2 mL DENV-2 strain Jamaica 1409 (Genbank #M20558) was inoculated onto subconfluent C6/36 cells in a 75 cm^2 tissue culture flask at a multiplicity of infection of 0.01 and rocked at room temperature for 1 hr before adding 10 mL of medium. Infected C6/36 cells were maintained in L-15 medium supplemented with 2% FBS, 100 U/mL penicillin, 100 µg/ mL streptomycin, 1x MEM non-essential amino acids, and 0.2 mM L-glutamine at 28°C for a total of 14 days

with a medium change at 7 dpi. At the end of the 14 day incubation, virus was harvested using a cell scraper to detach cells, and cells plus medium were used as the virus component of bloodmeals.

Plaque purification of virus escape mutants

Twenty DENV samples termed "virus escape mutants" were obtained from Dr. Irma Sanchez-Vargas (AIDL) (Table 5.1). Dr. Sanchez-Vargas originally obtained viruses from bodies of transgenic Carb77 mosquitoes challenged with artificial bloodmeals containing DENV-2 (JAM1409) that were ground and filtered. Mosquitoes were ground in 0.5 mL MEM using disposable pestles, filter sterilized using 0.2 µm Acrodisc syringe filters (VWR) and mixed with 0.5 mL MEM. The samples we received prior to plaque isolation were the filtered mosquito homogenates used for determining titers of individual mosquitoes in Franz et al. (2006). Prior to sequence analysis, virus escape mutants were cloned using three rounds of plaque isolation in mammalian cells followed by amplification in mosquito cell cultures. Three plaques were picked for each virus at each round, to ensure that isolates were not lost during the process.

Initial plaque isolations consisted of titration of viruses from DENV-challenged Carb77 mosquitoes by infection of barely confluent LLC-MK2 cell monolayers in 12-well cell culture plates with serial 10-fold dilutions of mosquito homogenates. Virus dilutions were incubated on LLC-MK2 plates for 1 hr then overlaid with equal parts agar mixture and 2x medium. Agar mixture consisted of sterilized 2% low melting temperature agar in distilled water. Medium consisted of 2x medium 199, 20% FBS,

Table 5.1 Key to origination information for virus escape mutant viruses

Working name of mutant	Virus escape mutant source (Mosquito, days post infection, dates: month day year, mosquito #)		
A	Carb77	7dpi	101305 #12
B	Carb77	7dpi	101305 #22
F	Carb77	13dpi	0626-0628-071106 #3
G	Carb77	13dpi	0626-0628-071106 #5
H	Carb77	7dpi	101305 #17
I	Carb77	7 dpi	0626-0628-07506 #1
J	Carb77	7 dpi	0626-0628-07506 #8
K	Carb77	7dpi	100906-101106-101806 #3
L	Carb77	7dpi	100906-101106-101806 #15
M	Carb77	7dpi	100906-101106-101806 #18
N	Carb77	14dpi	0824-090706 #8
O	Carb77	14dpi	0824-090706 #9
P	Carb77	14dpi	100906-101106-102306 #4
R	Carb77	14dpi	100906-101106-102306 #8
S	Carb77	14dpi	100906-101106-102306 #16
T	Carb77	14dpi	100906-101106-102306 #18
U	Carb77	14dpi	101305 #8
V	Carb77	14dpi	101305 #23
W	Carb77	14dpi	101305 #19
X	Carb77	14dpi	0824-090706 #10

Note: Several HWE control isolates were originally selected for plaque isolation and sequence analysis, but there was a miscommunication regarding labeling of virus stocks, and Carb77 isolates were inadvertently used in place of the HWE isolates. The switch was not discovered until after completion of the experiment.

71 mM sodium bicarbonate, 2% DEAE-Dextran/Hanks balanced salt solution (BSS) mixture made by dissolving 2 g of DEAE-Dextran in 100 mL of 1x Hanks BSS sterilized by filtration, 1x MEM vitamins, 1x MEM amino acids, and 1.25 mM Amphotericin B. All agar and medium components were obtained from Sigma except sodium bicarbonate, MEM vitamins and MEM amino acids, which were obtained from Cellgro, and FBS, which were obtained from Atlas Biologicals, Fort Collins, CO. Once agar solidified, plates were inverted and incubated at 37˚ C for 12 days. Plaques were visualized by staining with 12 mM thiazolyl blue tetrazolium bromide in phosphate buffered saline (PBS) for 4 hr at 37˚C, followed by no more than 4 hr at 4˚C to minimize effect of stain chemicals on virus viability. After plaques were visible, three well-isolated plaques were selected and removed in a plug of agar over the plaque with a sterile Pasteur pipette. Plugs were incubated in 1 mL of L-15 medium supplemented with 10% fetal bovine serum, penicillin, streptomycin, and L-glutamine on ice for 1 hr. Then medium was transferred to one well in a 12-well cell culture plate containing C6/36 cells at approximately 80% confluency. Virus was amplified by growth in C6/36 cells for a period of 7 days (Eckels et al., 1976). At the end of 7 days, medium was collected from C6/36 cells and frozen at 80˚C for use in the next round of plaque purification. One plaque per virus was used for the next round of isolation. Plaque titration and C6/36 cell amplification were repeated twice more.

To confirm that each plaque contained infectious virus, remaining C6/36 cells were stained for DENV E protein. C6/36 cells were scraped off the 12-well culture plates using a sterile pipette tip and placed dropwise onto glass slides. Scraped cellular material was allowed to dry in a cell culture hood for approximately 1 hr then fixed in cold

acetone and air dried. Immunofluorescent assays (IFA) consisted of incubation with 1:400 anti-DENV E protein monoclonal antibody 3H5-21 (2 hr) followed by biotinylated sheep anti-mouse IgG (1hr), and finally with 1:400 streptavidin-fluorescein (1 hr). Each incubation was followed by three washes in PBS. Cells were scored as positive or negative by observation with a Leica DM4500B fluorescent microscope.

Sequencing of prM gene RNA

The prM gene of 3x plaque purified DENV RNA was amplified via high-fidelity RT-PCR using Invitrogen's SuperScript III One-Step RT-PCR System with Platinum Taq High Fidelity kit (Carlsbad, CA) and the following primers (designed by Dr. Alexander Franz): Mnp-antisense-FWD GCAGGCGTGATTATTA and Mnp-antisense-REV AGTCTCTATTTGATATT. Expected amplification product size of 1000 bp was verified via gel electrophoresis and RT-PCR products were purified to remove template RNA using Qiagen's QIAquick PCR Kit (Valencia, CA). The resulting cDNA was TOPO cloned using the Invitrogen TOPO TA cloning kit. TOPO clone transformed colonies were selected with 50 µg/mL ampicillin, PCR was used to determine colonies with prM inserts, and three to four colonies per virus were cultured overnight. Plasmids were purified using Qiagen's QIAprep Spin Miniprep kit and sequenced by the Proteomics and Metabolomics Facility.

Full-length genome sequencing

RNA from virus escape mutants was obtained by extracting total RNA from infected C6/36 cells in 12-well cell culture plates after the third round of purification

according to the manufacturer's instructions using the RNeasy mini kits (Qiagen). To obtain DNA for sequencing, cDNA was transcribed and amplified via high fidelity RT-PCR using Invitrogen's SuperScript III One-Step RT-PCR System with Platinum Taq High Fidelity kit. The DENV-2 (JAM1409) genome was divided into 12 segments consisting of approximately 1000 bp each with 100 bp overlap at the 3' end of each segment for optimal sequencing (Table 5.2). Amplification product sizes were verified to be approximately 1000 bp via gel electrophoresis and RT-PCR products were purified for sequencing using Qiagen's QIAquick PCR Kit (Qiagen). Viral cDNA was sequenced in both forward and reverse directions by the Proteomics and Metabolomics Facility.

Sequence Analysis

Sequences obtained from the prM genes of the virus escape mutants were analyzed using the CLUSTALW – Multiple Sequence Alignment feature from Biology Workbench (San Diego Supercomputer Center, http://workbench.sdsc.edu/). Overlapping sequences from full-length virus escape mutant genomes were analyzed using Contig Express from Invitrogen's VectorNTI Advance 10.

Challenge assay

To determine variation in mosquito disseminated infection between parental DENV-2 (JAM1409) and putative virus escape mutants, *Ae. aegypti* mosquitoes, Carb77 and HWE strains, were provided artificial bloodmeals containing JAM1409 or the virus escape mutant of interest. After three rounds of plaque isolation and amplification in C6/36 cells, escape mutants were sequenced. DENV-2 for infectious bloodmeals was

Table 5.2 Primers for full-length sequencing of virus escape mutants

Primer	Sequence	Genome location (nt)
KP26	AGTTGTTAGTCTACGTGGACCG	1- 22
KP27	CAACCAGCTTCCTCCTGAAACC	1000-978
KP28	TTCATCTTACTGACAGCTGTCG	900-922
KP29	TAACTATTGTTCCATGTTGTG	1900-1879
KP30	ATGGACAAACTACAGCTCAAAG	1800-1822
KP31	CTGTGGAGAGCATTTTCGCC	2800-2780
KP32	AAAGGAATCATGCAGGCAGG	2700-2720
KP33	TTCCCAGGTCTCTAAAGGACATG	3700-3677
KP34	ACATTGATTACTGGGAACATG	3600-3621
KP35	GCTTGATTCTATAGGCTCCATC	4600-4578
KP36	TGGGAAGTGAAGAAACAACGG	4500-4522
KP37	GAGGAAATGGGTCTCTACTTCC	5500-5478
KP38	ATAGCAGCTAGAGGATACATTTC	5400-5423
KP39	GTGCCAGTGGGTCAGAATAG	6400-6380
KP40	AGATGGTTGGATGCTAGGATC	6300-6321
KP41	CTGCTGCTCTTTTCTGAGCTTC	7300-7278
KP42	CAAGCAAAAGCAACCAGAGAAG	7200-7222
KP43	TGACTGAGGGCATATATGGGTTG	8200-8178
KP44	TTTTGCATAAAGGTTCTCAACC	8100-8122
KP45	CTTCTCCTTCCACTCCACTCAGG	9100-9077
KP46	TGGCTTGGAGCACGCTTCTTTAG	9000-9022
KP47	TTGTTGGAACCCAATGTGAC	10000-9980
KP48	GCTATTTGCTCGGCAGTCCC	9900-9920
KP49	AGAACCTGTTGATTCAACAGC	10723-10703

prepared by growth in C6/36 cells as described above. Bloodmeals consisted of equal parts virus-containing cell-medium suspensions and defibrinated sheep blood supplemented with 1 mM adenosine triphosphate to stimulate feeding. Bloodmeals were provided in sausage casing membranes on water-jacketed feeders at 37˚C and mosquitoes were allowed to feed for no more than one hour. At the end of the hour, mosquitoes were cold-anesthetized and sorted. Fully engorged mosquitoes were maintained on sucrose and water at normal rearing conditions. Mosquitoes were collected at 7, and 14 days pbm and stored at -80˚C until individual analysis by plaque assay for infectious virus.

Plaque assay Mosquitoes from the challenge assay were prepared for plaque titration by grinding in 0.5 mL MEM supplemented with 8% FBS, L-glutamine, MEM non-essential amino acids, penicillin, and streptomycin. After grinding, 0.5 mL of medium was added and the suspension was filtered using 0.2 μm Acrodisc syringe filters (VWR). Plaque assay consisted of titration of ten-fold serial dilutions on LLC-MK2 cells in 24-well cell culture plates. Infected LLC-MK2 plates were incubated for 1 hr then overlaid with agar as described above. Plates were inverted and incubated at 37˚C for 12 days. Plaques were visualized as described above and counted.

Statistical analysis To determine whether there were any statistically significant differences in proportion of infected mosquitoes or mean titers between mosquito and virus strain combinations, proportions of infected mosquitoes and mean titers were calculated using Microsoft Excel for all mosquito strain and DENV-2 virus strain combinations at 7 and 14 days pbm. Data was further analyzed using Statistical Analysis Software (SAS) (SAS Institute Inc. Cary, NC). Proportions of infected mosquitoes were analyzed by Fisher's exact test ($\alpha = 0.05$). Proportions of infected mosquitoes were

compared between multiple groups after logit transform and Tukey's error adjustment. Mean virus titers of infected mosquitoes were log-transformed and analyzed by one-way ANOVA ($\alpha = 0.05$) with the Tukey-Kramer error adjustment for unequal sample size. Statistician Dr. James Zumbrunnen (CSU) was consulted regarding appropriate statistical analysis for unequal sample size.

.

Characterization of a large plaque phenotype virus via RT-PCR, sequencing, and midgut IFA

To determine the characteristics of the large plaque-producing escape mutant virus, midguts were dissected from mosquitoes that had been re-challenged with virus escape mutant "P" (VEM P) and fixed with 4% paraformaldehyde in phosphate buffered saline for 24 hr. IFAs were carried out with 1:150 SINV-specific monoclonal antibody 30.11a (2 hr) followed by 1:400 biotinylated sheep anti-mouse IgG (1 hr) then 1:400 strepavidin-fluorescein (1 hr). Midguts were washed three times in PBS after fixation and following each incubation. Midguts were mounted on slides in Vectashield with DAPI (Vector Laboratories: Burlingame, CA) and scored as positive or negative by observation with a Leica DM4500B fluorescent microscope. IFA with DENV monoclonal antibody 3H5-1 as described in Chapter 2 was performed on a subset of midguts from mosquitoes which had been fed infectious bloodmeals containing the large plaque mutant virus.

The RNA of the large plaque phenotype virus escape mutant was characterized via RT-PCR using the SuperScript III One Tube RT-PCR kit (Invitrogen) with SINV specific primer pairs: TE3 E1 FWD 5'CGCAGGCCGCATGAGGATTT3', TE E1 REV

5’GGCTTGAAATTCTTGGTCAT3’, MRE16 E1 FWD 5’CTCAAGCTGCATCTGGG TT3’, MRE16 E1 REV 5’TGCCTGGAACTCCTGGTGGT3’. Expected product size using these primers was 500 bp. Amplification products were separated via gel electrophoresis and extracted using the QIAquick gel extraction kit following the manufacturer’s instructions (Qiagen). Products were sequenced in both forward and reverse directions by the Proteomics and Metabolomics Facility. Sequences were analyzed using the CLUSTALW – Multiple Sequence Alignment feature from Biology Workbench (San Diego Supercomputer Center, http://workbench.sdsc.edu/).

Midgut IFA for dsRNA

To determine whether dsRNA originating from a transgene could be observed in mosquito midguts as it was in FB9.1 cell culture in Chapter 2, midguts were dissected from Carb77 (G_9 - G_{10}) and HWE mosquitoes. Transgenic mosquitoes with RNAi-based DENV-2 resistance phenotype provided a unique opportunity to examine potential interactions between transgene expressed dsRNA and membrane associated RNA as examined in mosquitoes in Chapter 4. Mosquitoes were provided bloodmeals containing DENV JAM1409 or without virus and at 24, 48, and 72 hr pbm, fixed in 4% paraformaldehyde in PBS at 4˚C for 24 hr. IFAs consisted of incubations with 1:1000 dsRNA specific antibody J2 (2 hr) followed by 1:400 biotinylated sheep anti-mouse IgG (1 hr) then 1:400 streptavidin-fluorescein (1 hr). Midguts were washed three times in phosphate buffered saline with 0.2% bovine serum albium (BSA) (Sigma) and 0.5% Triton X-100 (TX100) (Sigma) after fixation and following each incubation. Midguts were mounted on slides in Vectashield with DAPI (Vector Laboratories) and scored as

positive or negative by observation with a Leica DM4500B fluorescent microscope. Note that at this time, the double-staining techniques used to visualize dsRNA and virus antigen in Chapter 4 had not yet been optimized.

The dsRNA IFA experiment was repeated with the Vg40 mosquitoes at 10, 24, and 48 hr pbm. Timepoints were selected based on what is known of the expression of the transgene in the fatbody (Franz et al., 2009). The Vg1 promoter initiates expression of the transgene by 10 hr, peaks at 24 hr, and expression halts by 48 hr (Franz et al., 2009). Fatbody tissue was dissected and fixed by soaking in approximately 100 µL drop of 4% paraformaldehyde in PBS, allowed to dry almost completely in a chemical hood, then slides were stored in PBS at 4˚C. IFAs were as described for midguts.

Results

Sequencing of prM gene RNA

To test the escape mutant hypothesis, a total of 20 virus escape mutants were isolated and the targeted prM genes were sequenced after the final round of three rounds of plaque isolation. Of these virus genomes, two contained the same single, synonymous point mutation (T540C) (Figure 5.2). One of these mutations appeared to be associated with a large plaque phenotype.

Full-length genome sequencing

To determine whether mutations outside the prM region could be responsible for the enhanced replication of the escape mutant viruses in Carb77 mosquitoes, we sequenced the entire genome of virus escape mutant I (VEM I) after the final round of three rounds of plaque isolation. The VEM I genome which contained the T540C mutation in the prM gene. The genome sequences revealed several additional synonymous mutations and several non-synonymous mutations (Table 5.3). A literature search found none of the non-synonymous mutations in the VEM I genome have been correlated with enhanced DENV replication.

The genome of virus escape mutant P was not successfully sequenced and will be discussed in more detail in the discussion of characterization of the large plaque phenotype virus, VEM P. How plaque isolation methods may have biased sequencing results for VEM I will be discussed in detail.

```
cloneIreverse     ATGTTGATTCCAACAGCGATGGCGTTCCATTTAACCACACGTAATGGAGAACCACACATG
clonePreverse     ATGTTGATTCCAACAGCGATGGCGTTCCATTTAACCACACGTAATGGAGAACCACACATG
cloneIforward     ATGTTGATTCCAACAGCGATGGCGTTCCATTTAACCACACGTAATGGAGAACCACACATG
clonePforward     ATGTTGATTCCAACAGCGATGGCGTTCCATTTAACCACACGTAATGGAGAACCACACATG
JAM1409*          ATGTTGATTCCAACAGCGATGGCGTTCCATTTAACCACACGTAATGGAGAACCACACATG

cloneIreverse     ATCGTTGGTAGGCAAGAGAAAGGGAAAAGTCTTCTGTTCAAAACAGAGGATGGTGTTAAC
clonePreverse     ATCGTTGGTAGGCAAGAGAAAGGGAAAAGTCTTCTGTTCAAAACAGAGGATGGTGTTAAC
cloneIforward     ATCGTTGGTAGGCAAGAGAAAGGGAAAAGTCTTCTGTTCAAAACAGAGGATGGTGTTAAC
clonePforward     ATCGTTGGTAGGCAAGAGAAAGGGAAAGTCTTCTGTTCAAAACAGAGGATGGTGTTAAC
JAM1409           ATCGTTGGTAGGCAAGAGAAAGGGAAAAGTCTTCTGTTCAAAACAGAGGATGGTGTTAAC

cloneIreverse     ATGTGCACCCTCATGGCCATAGATCTTGGTGAATTGTGTGAAGATACAATCACGTACAAG
clonePreverse     ATGTGCACCCTCATGGCCATAGATCTTGGTGAATTGTGTGAAGATACAATCACGTACAAG
cloneIforward     ATGTGCACCCTCATGGCCATAGATCTTGGTGAATTGTGTGAAGATACAATCACGTACAAG
clonePforward     ATGTGCACCCTCATGGCCATAGATCTTGGTGAATTGTGTGAAGATACAATCACGTACAAG
JAM1409           ATGTGTACCCTCATGGCCATAGATCTTGGTGAATTGTGTGAAGATACAATCACGTACAAG

cloneIreverse     TGTCCCCTCCTCAGGCAAAATGAACCAGAAGACATAGATTGTTGGTGCAACTCTACGTCC
clonePreverse     TGTCCCCTCCTCAGGCAAAATGAACCAGAAGACATAGATTGTTGGTGCAACTCTACGTCC
cloneIforward     TGTCCCCTCCTCAGGCAAAATGAACCAGAAGACATAGATTGTTGGTGCAACTCTACGTCC
clonePforward     TGTCCCCTCCTCAGGCAAAATGAACCAGAAGACATAGATTGTTGGTGCAACTCTACGTCC
JAM1409           TGTCCCCTCCTCAGGCAAAATGAACCAGAAGACATAGATTGTTGGTGCAACTCTACGTCC
```

Figure 5.2 Alignment of prM gene sequences of virus escape mutants I and P Sequences were aligned with DENV-2 JAM1409 accession #M20558 (415-654nt). Arrow indicates T540C point mutation.

Table 5.3 Non-synonymous mutations in DENV escape mutant I mutations are compared to parental DENV JAM1409 strain

Genome nt position	viral gene	nucleotide published virus		amino acid substitution number within genome
935	E	A	G	L311 M
3915	NS2a	C	T	L 1305 S
3916	NS2a	T	C	L 1305 S
4540	NS3	T	C	V 1513 A
7067	NS3	C	G	I 2355 M
7068	NS3	C	G	H 2356 D
8223	NS5	T	A	S 2741 T

Challenge assay

To evaluate whether VEM I had a replication advantage in mosquitoes relative to JAM1409 as predicted by our escape mutant hypothesis, we challenged Carb77 (G_{11}) and HWE mosquitoes with artificial bloodmeals containing DENV JAM1409 or VEM I. Bloodmeal titers were less than 10-fold different at 5.14 logs pfu/mL and 5.40 logs pfu/mL respectively. We collected mosquitoes at 7 and 14 d pbm and compared the proportion infected mosquitoes and mean titer between JAM1409 and VEM I (Figures 5.3 and 5.4). Proportions of infected mosquitoes were compared between multiple groups after logit transform and Tukey's error adjustment. Mean virus titers of infected mosquitoes were log-transformed and analyzed by one-way ANOVA ($\alpha = 0.05$) with the Tukey-Kramer error adjustment for unequal sample size.

Proportion of mosquitoes infected

At 7 d pbm the proportion of mosquitoes infected for all mosquito strain and DENV-2 strain combinations was 100%, except for Carb77 mosquitoes fed JAM1409 in which 93.3% of the mosquitoes were infected (Table 5.4A). At 14 d pbm 100% of all mosquito strain and DENV-2 strain combinations were infected except 75% HWE mosquitoes fed strain JAM1409 were infected (Table 5.5A). There were no statistically significant differences in the proportions of infected mosquitoes for any of the individual or pairwise comparisons (Tables 5.4 and 5.5). The values for proportion infected comparisons were different for our challenge of Carb77 (G_{11}) and HWE from the

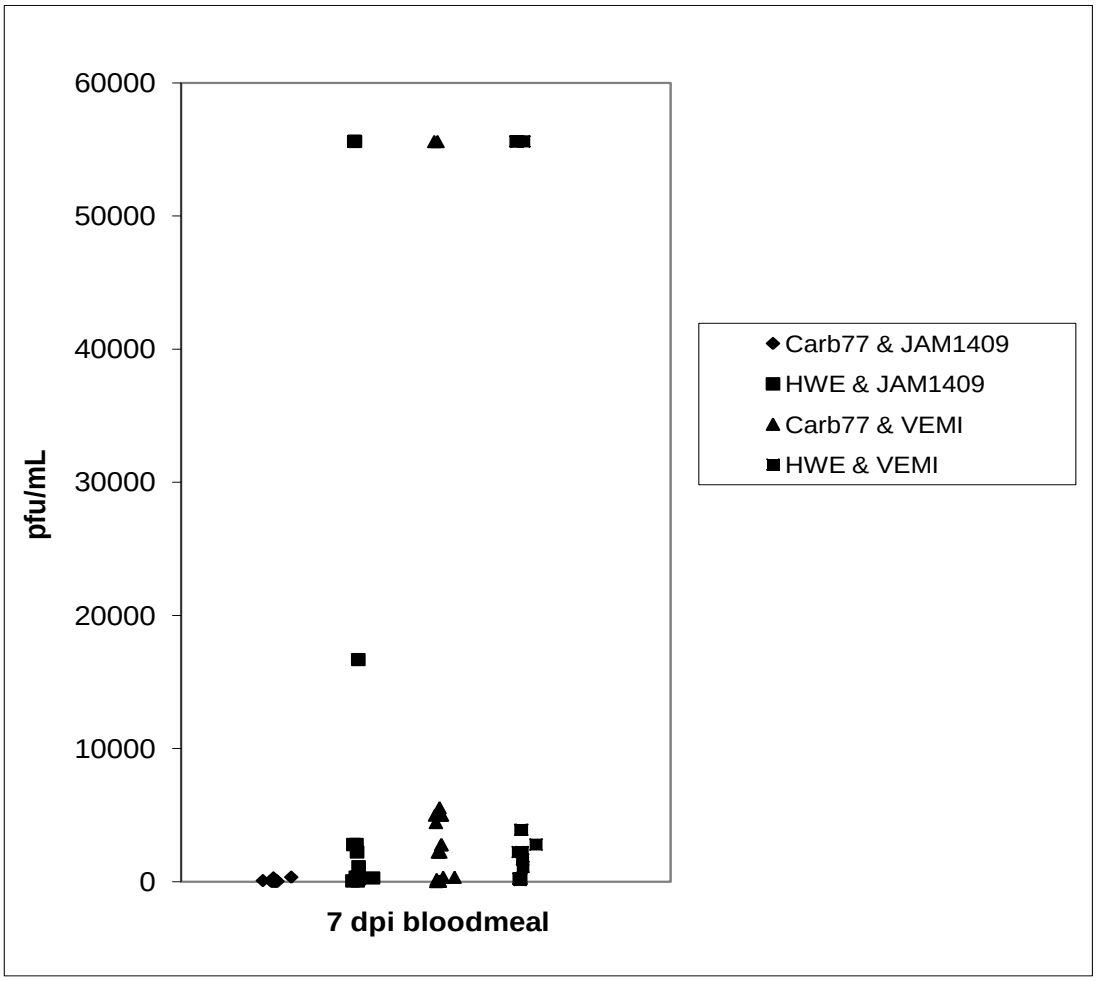

Figure 5.3 Comparison of titers of DENV-2 JAM1409 and virus escape mutant I in Carb77 (G11) and Higgs white eye mosquitoes at 7 days post bloodmeal

Table 5.4A Raw data and analysis for comparison of titers of DENV-2 JAM1409 and virus escape mutant I in Carb77 (G11) and Higgs white eye mosquitoes at 7 days post bloodmeal Fisher exact test ($\alpha = 0.05$) analysis reported for the proportion of infected vs. non-infected females and ANOVA ($\alpha = 0.05$) value reported for the mean virus titers of infected females. Data in table corresponds with titration data above; Carb77 & JAM1409 corresponds with n = 15, 93.3% infected, mean titer 78 pfu/mL and P-value p** 0.9834 and P-value t = 0.0002 compare the proportions infected and mean titers between Carb77 and HWE fed JAM1409.

n	15	15	19	19
% infected	93.3	100	100	100
mean titer*	78	12917	7788	17730

P-value p**	0.9834	1.0000
P-value t***	0.0002	0.2803

* = infected mosquitoes only, ** = proportions of infected vs. non-infected mosquitoes, *** = titers of infected mosquitoes

Table 5.4B ANOVA (α = 0.05) table for mean titers of infected females in Carb77 (G_{11}) and Higgs white eye mosquitoes at 7 days post bloodmeal DENV-2 JAM1409 and virus escape mutant I.

	Carb77 JAM1409	Carb77 VEM I	HWE JAM1409	HWE VEM I
Carb77 JAM1409		0.0003	0.0002	<0.0001
Carb77 VEM I	0.0003		0.9764	0.2803
HWE JAM1409	0.0002	0.9764		0.5757
HWE VEM I	<0.0001	0.2803	0.5757	

Pairwise comparison of mean titers of infected females HWE and Carb77 (G_{11}) across virus strains <0.0001 and pairwise comparison of mean titers of JAM1409 and VEM I across mosquito strains 0.0002.

Table 5.4C Fisher's exact test (α = 0.05) was used to make individual and pairwise comparisons for proportion of infected females in Carb77 (G_{11}) and Higgs white eye mosquitoes at 7 days post bloodmeal with DENV-2 JAM1409 and virus escape mutant I. The comparisons presented in the table are those most relevant for VEM I escape mutant hypothesis.

Sample 1	Sample 2	P-value t
Carb77 fed JAM1409	Carb77 fed VEM I	0.9813
HWE fed JAM1049	HWE fed VEM I	1.000
VEM I (both mosquitoes)	JAM1409 (both mosquitoes)	0.9897

Table 5.4D Fisher's exact test (α = 0.05) was used to make individual and pairwise comparisons for proportion of infected females in Carb77 (G_{11}) and Higgs white eye mosquitoes at 7 days post bloodmeal with DENV-2 JAM1409 and virus escape mutant I. The comparisons presented in the table are those most relevant for determining resistance of Carb77 (G_{11}) mosquitoes.

Sample 1	Sample 2	P-value t
Carb77 fed JAM1409	HWE fed JAM1049	0.9834
Carb77 fed VEM I	HWE fed VEM I	1.0000
Carb77 (both virus strains)	HWE (both virus strains)	0.9897

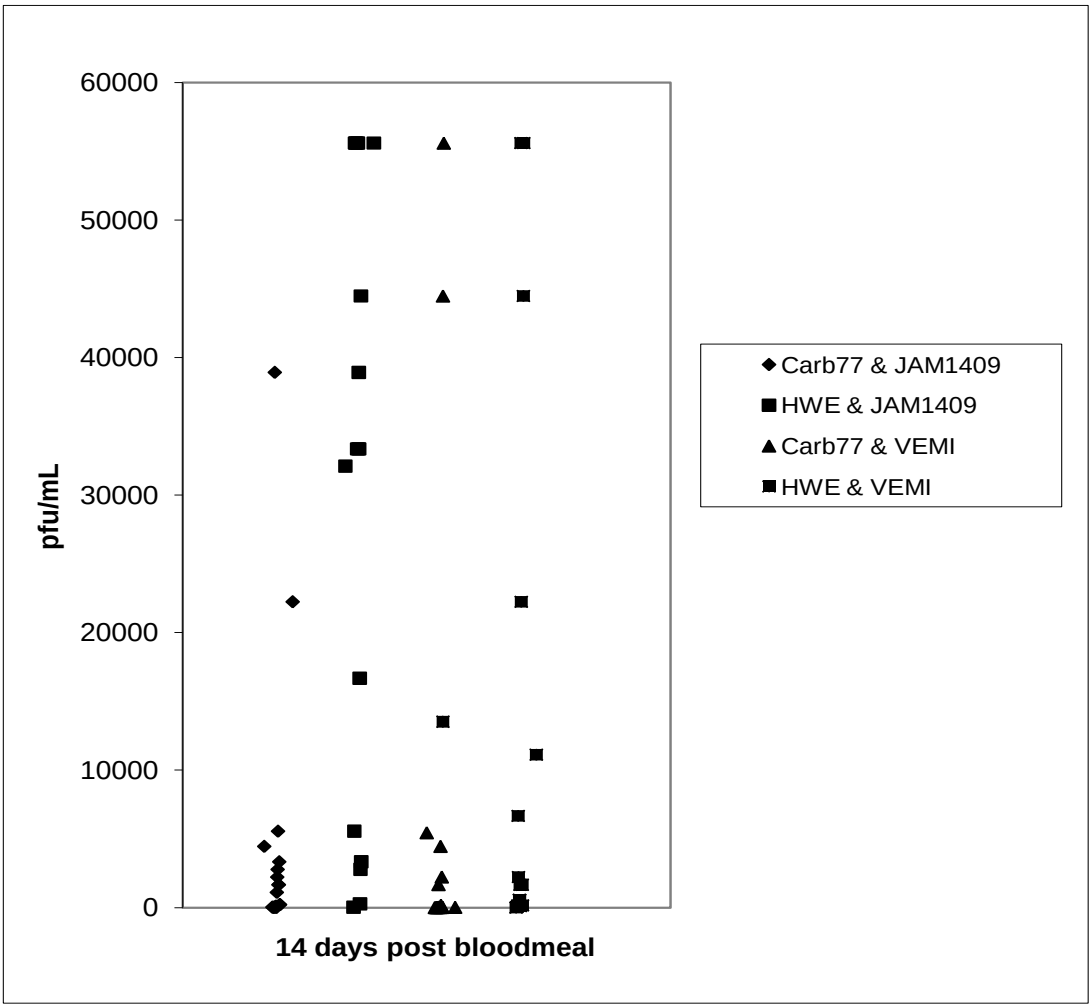

Figure 5.4 Comparison of titers of DENV-2 JAM1409 and virus escape mutant I in Carb77 (G11) and Higgs white eye mosquitoes at 14 days post bloodmeal

Table 5.5A Raw data and analysis for comparison of titers of DENV-2 JAM1409 and virus escape mutant I in Carb77 (G_{11}) and Higgs white eye mosquitoes at 14 days post bloodmeal. Fisher exact test ($\alpha = 0.05$) analysis reported for the proportion of infected vs. non-infected females and ANOVA ($\alpha = 0.05$) value reported for the mean virus titers of infected females. Data in table corresponds with titration data above; Carb77 & JAM1409 corresponds with n = 18, 100% infected, mean titer 4456 pfu/mL and P-value p** 1.0000 and P-value t = 0.0041 compare the proportions infected and mean titers between Carb77 fed JAM1409 and HWE fed JAM1409.

n	18	17	20	15
% infected	100	100	75.0	100
mean titer*	4456	32102	7253	13525

P-value p**	1.0000	0.9814
P-value t***	0.0041	0.0053

* = infected mosquitoes only, ** = proportions of infected vs. non-infected mosquitoes
*** = titers of infected mosquitoes

Table 5.5B ANOVA ($\alpha = 0.05$) table for mean titers of infected females in Carb77 (G_{11}) and Higgs white eye mosquitoes at 14 days post bloodmeal with DENV-2 JAM1409 and virus escape mutant I.

	Carb77 JAM1409	Carb77 VEM I	HWE JAM1409	HWE VEM I
Carb77 JAM1409		0.0943	0.0041	0.6712
Carb77 VEM I	0.0943		<0.0001	0.0053
HWE JAM1409	0.0041	<0.0001		0.1060
HWE VEM I	0.6712	0.0053	0.1060	

Pairwise comparison of mean titers of infected females HWE and Carb77 (G_{11}) across virus strains <0.0001 and pairwise comparison of mean titers of JAM1409 and VEM I across mosquito strains 0.0015.

Table 5.5C Fisher's exact test ($\alpha = 0.05$) was used to make individual and pairwise comparisons for proportion of infected females in Carb77 (G_{11}) and Higgs white eye mosquitoes at 14 days post bloodmeal with DENV-2 JAM1409 and virus escape mutant I. The comparisons presented in the table are those most relevant for VEM I escape mutant hypothesis.

Sample 1	Sample 2	P-value t
Carb77 fed JAM1409	Carb77 fed VEM I	0.9797
HWE fed JAM1049	HWE fed VEM I	1.0000
VEM I (both mosquitoes)	JAM1409 (both mosquitoes)	0.9887

Table 5.5D Fisher's exact test ($\alpha = 0.05$) was used to make individual and pairwise comparisons for proportion of infected females in Carb77 (G_{11}) and Higgs white eye mosquitoes at 14 days post bloodmeal with DENV-2 JAM1409 and virus escape mutant I. The comparisons presented in the table are those most relevant for determining resistance of Carb77 (G_{11}) mosquitoes.

Sample 1	Sample 2	P-value t
Carb77 fed JAM1409	HWE fed JAM1049	1.0000
Carb77 fed VEM I	HWE fed VEM I	0.9814
Carb77 (both virus strains)	HWE (both virus strains)	0.9887

proportion of mosquitoes infected reported by Franz et al. (2009). These data will be discussed for relevance to our hypothesis of an RNAi escape mutant virus and to the Carb77 loss of resistance that was recently reported by Franz et al. (2009).

Mean titer of infected mosquitoes

We did not find significant differences in the proportions of mosquitoes infected when fed JAM1409 versus VEM I as discussed above. We have arranged our results to present the mean titer comparisons of interest for the Carb77 resistance phenotype first. To determine whether the Carb77 (G_{11}) mosquitoes were resistant to challenge with DENV-2, we have presented comparisons of Carb77 and HWE mosquitoes fed the same virus strain. For the escape mutant hypothesis, we have presented comparisons of Carb77 fed JAM1409 versus VEM I as well as HWE fed JAM1409 versus VEM I.

Resistance phenotype

Mean titers for all mosquito and virus combinations at 7 and 14 d pbm are reported in Tables 5.4 and 5.5. For the loss of resistance of Carb77 (G_{11}), the mean titer comparisons of interest at 7 day pbm, are the individual comparisons between HWE fed JAM1409 versus Carb77 fed JAM1409 ($p = 0.0002$), individual comparisons between HWE fed VEM I versus Carb77 fed VEM I ($p = 0.2803$), and the pairwise comparison of mean titer of HWE versus Carb77 across virus strains ($p < 0.0001$). The mean titer comparison between HWE and Carb77 mosquitoes fed JAM1409 and the pairwise comparison of mean titer of HWE versus Carb77 across virus strains were statistically significant at 7 d pbm with lower DENV titers in Carb77 mosquitoes than HWE mosquitoes. The mean titer comparison of HWE and Carb77 mosquitoes fed VEM I at

7 d pbm was not statistically significant, however the titer of VEM I was still lower in Carb77 mosquitoes (Table 5.4A & B).

For the loss of resistance of Carb77 (G_{11}) the mean titer comparisons of interest at 14 d pbm are the individual comparisons between HWE fed JAM1409 versus Carb77 fed JAM1409 ($p = 0.0041$), individual comparisons between HWE fed VEM I versus Carb77 fed VEM I ($p = 0.0053$), and the pairwise comparison of mean titer of HWE versus Carb77 across virus strains ($p < 0.0001$). All comparisons of mean titer of HWE versus Carb77 across virus strains were statistically significant at 14 d pbm with lower titers of both DENV strains in Carb77 than HWE (Table 5.5A & B).

At 7 d pbm, mean titer difference between between HWE versus Carb77 fed VEM I was not statistically significant, but the titer of VEM I in Carb77 is lower than the titer of VEM I in HWE, so titer comparisons were consistent with intact resistance of Carb77 mosquitoes to VEM I. At 14 d pbm, mean titer differences between Carb77 and HWE with all viruses were statistically significant with lower titer DENV in Carb777 than HWE, consistent with intact resistance of Carb77 mosquitoes. Overall, the mean titer of both JAM1409 and Carb77 was lower in Carb77 mosquitoes than in HWE mosquitoes, consistent with Carb77 resistance to DENV-2. Our proportion infected data and mean titer data were not consistent with the data from Franz et al. (2009), which noted that the basis of Carb77 (G_9-G_{13}) resistance was a lower proportion of mosquitoes infected, not a lower mean titer. This discrepancy will be discussed in more detail later in the chapter.

Escape mutant hypothesis

At 7 day pbm the individual comparisons between Carb77 fed JAM1409 versus Carb77 fed VEM I ($p = 0.0003$) and the pairwise comparison of mean titer of VEM I versus JAM1409 across mosquito strains ($p = 0.0002$) were significantly different with higher mean titers of VEM I than JAM1409 in Carb77 and higher mean titers of VEMI than JAM1409 across mosquito strains (Table 5.4B).

The comparisons of interest for the escape mutant hypothesis at 14 d pbm, are the individual comparisons between Carb77 fed JAM1409 versus Carb77 fed VEM I ($p = 0.0943$), and the pairwise comparison of mean titer of VEM I versus JAM1409 across mosquito strains ($p = 0.0015$). The pairwise comparison of mean titer of VEM I versus JAM1409 across mosquito strains was statistically significant at 14 d pbm with higher titer in VEM I than JAM1409. The comparison between Carb77 fed JAM1409 versus Carb77 fed VEM I was not statistically significant at 14 days pbm but VEM I titer was higher than JAM1409 titer in Carb77 mosquitoes.

Overall, the 7 d pbm and 14 d pbm mean titer comparison between Carb77 fed JAM1409 and VEM I were consistent with the hypothesis that DENV-2 strain VEM I may be evading the enhanced RNAi response of the Carb77 mosquito strain. The implications of these comparisons will be discussed in detail later in the chapter.

Characterization of a large plaque phenotype virus via RT-PCR, genome sequencing, and IFA

A ground mosquito filtrate from Carb77 mosquitoes infected with DENV described as exhibiting a "large plaque phenotype" was included in the initial samples provided by Dr. Sanchez-Vargas. This virus became known as virus escape mutant "P" (VEM P) and was difficult to isolate, as the virus several times produced no plaques upon passage in LLC-MK2 cells and required a return to the initial isolate to recommence the plaque purification procedure. Attempts to obtain a full-length genome sequence of this virus escape mutant using DENV RNA specific primers were unsuccessful. Titers were at least one log higher than the DENV-2 (JAM1409) grown under the same conditions (Table 5.6).

RT-PCR on RNA from VEM P with primers specific for SINV strains TE3'2J and MRE16 yielded an amplification product with TE3'2J primers (Figure 5.5). The amplification product shown in Figure 5.5 was sequenced and alignment of that product with SINV TE3'2J genome is shown in Figure 5.6. There were minimal mismatches between the VEM P amplification product and SINV TE3'2J RNA. Midgut IFAs with 30.11a monoclonal antibody showed low levels of infection and a single faint IFA focus was observed on one midgut out of twenty stained (not shown).

Midgut IFA for dsRNA

To determine whether we could detect the dsRNA transcribed from the transgene, IFAs comparing staining of dsRNA in midguts of Carb77 (G_{10}) and HWE mosquitoes after both DENV-2 (JAM1409) infectious and non-infectious bloodmeals were examined

Table 5.6 Titers of DENV-2 JAM1409 and virus escape mutant P, grown under the same conditions

Date grown	**DENV JAM1409 titer**	**virus escape mutant P titer**
Stock 6/17/07	4.67 log pfu/mL	8.03 log pfu/mL
Stock 10/4/2007	3.43 log pfu/mL	4.43 log pfu/mL
Bloodmeal 2/22/08	4.67 log pfu/mL	6 log pfu/mL
Bloodmeal 3/25/08	6.27 log pfu/mL	inconclusive
Bloodmeal 4/2/08	4.82 log pfu/mL	6 log pfu/mL

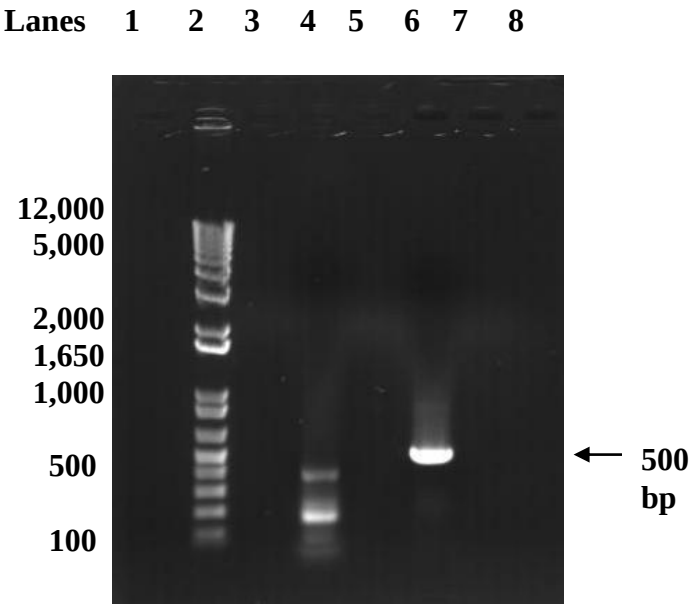

Figure 5.5 RT-PCR of VEM P RNA with primers specific for SINV strains MRE16 and TE3'3J (Lanes 1, 3, 5, 7, and 8 were empty) Lane 2 contained an Invitrogen size marker ladder, lane 4 contained virus escape mutant P amplified with MRE16 specific primers, and lane 6 contained virus escape mutant P amplified with TE3'2J specific primers (3175 – 3674 nt).

```
TE 3' 2J        TACACGCAGG CCGCATCAGG ATTTGAGATG TGGAAAAACA ACTCAGGCCG
VEMP rev        ---TCGCAGG CCGCATCAGG ATTTGAGATG TGGAAAAACA ACTCAGGCCG
VEMP fwd        ---------- ---------- ---------- ---------A AAGTCGGCCG

TE 3' 2J        CCCATTGCAG GAAACCGCAC CTTTCGGGTG TAAGATTGCA GTAAATCCGC
VEMP rev        CCCACTGCAG GAAACCGCAC CTTTCGGGTG TAAGATTGCA GTAAATCCGC
VEMP fwd        CCCACTGCAG GAA-CCGCAC CTTTCGGGTG TAAGATTGCA GTAAATCCGC

TE 3' 2J        TCCGAGCGGT GGACTGTTCA TACGGGAACA TTCCCATTTC TATTGACATC
VEMP rev        TCCGAGCGGT GGACTGTTCA TACGGGAACA TTCCTATTTC TATTGACATC
VEMP fwd        TCCGAGCGGT GGACTGTTCA TACGGGAACA TTCCTATTTC TATTGACATC

TE 3' 2J        CCGAACGCTG CCTTTATCAG GACATCAGAT GCACCACTGG TCTCAACAGT
VEMP rev        CCGAACGCTG CCTTTATCAG GACATCAGAT GCACCACTGG TCTCAACAGT
VEMP fwd        CCGAACGCTG CCTTTATCAG GACATCAGAT GCACCACTGG TCTCAACAGT

TE 3' 2J        CAAATGTGAA GTCAGTGAGT GCACTTATTC AGCAGACTTC GACGGGATGG
VEMP rev        CAAATGTGAA GTCAGTGAGT GCACTTATTC AGCAGACTTC GGCGGGATGG
VEMP fwd        CAAATGTGAA GTCAGTGAGT GCACTTATTC AGCAGACTTC GGCGGGATGG

TE 3' 2J        CCACCCTGCA GTATGTATCC GACCGCGAAG GTCAATGCCC CGTACATTCG
VEMP rev        CCACCCTGCA GTATGTATCC GACCGCGAAG GTCAATGCCC CGTACATTCG
VEMP fwd        CCACCCTGCA GTATGTATCC GACCGCGAAG GTCAATGCCC CGTACATTCG

TE 3' 2J        CATTCGAGCA CAGCAACTCT CCAAGAGTCG ACAGTACATG TCCTGGAGAA
VEMP rev        CATTCGAGCA CAGCAACTCT CCAAGAGTCG ACAGTACATG TCCTGGAGAA
VEMP fwd        CATTCGAGCA CAGCAACTCT CCAAGAGTCG ACAGTACATG TCCTGGAGAA

TE 3' 2J        AGGAGCGGTG ACAGTACACT TTAGCACCGC GAGTCCACAG GCGAACTTTA
VEMP rev        AGGAGCGGTG ACAGTACACT TTAGCACCGC GAGTCCACAG GCGAACTTTA
VEMP fwd        AGGAGCGGTG ACAGTACACT TTAGCACCGC GAGTCCACAG GCGAACTTTA

TE 3' 2J        TCGTATCGCT GTGTGGGAAG AAGACAACAT GCAATGCAGA ATGTAAACCA
VEMP rev        TCGTATCGCT GTGTGGGAAG AAGACAACAT GCAATGCAGA ATGTAAACCA
VEMP fwd        TCGTATCGCT GTGTGGGAAG AAGACAACAT GCAATGCAGA ATGTAAACCA

TE 3' 2J        CCAGCTGACC ATATCGTGAG CACCCCGCAC AAAAATGACC AAGAATTTCA
VEMP rev        CCAGCTGACC CAAT------ ---------- ---------- ----------
VEMP fwd        CCAGCTGACC ATATCGTGAG CACCCCGCAC AAAAATGACC AAGATTTCAA
```

Figure 5.6 Alignment of virus escape mutant P RNA Virus escape mutant P RNA was amplified with TE3'2J specific primers aligned with SINV TE3' 2J genomic RNA (3175-3674 nt). Sequence in yellow differs from the TE3' 2J genomic sequence.

(Figure 5.7). There was higher fluorescence in midguts of Carb77 mosquitoes fed a DENV-infectious bloodmeal compared to either Carb77 fed a non-infectious bloodmeal or HWE fed infectious or non-infectious bloodmeal. The significance of these observations will be discussed later.

Based on results from the Carb77 mosquito IFAs, we wanted to determine whether difficulties with dsRNA IFAs were due to difficulties dissecting midguts soon after bloodmeal or some complication of detecting transgene RNA in whole mosquitoes. We repeated our IFA for dsRNA on the fatbodies of Vg40 mosquitoes. We found more obvious differences in dsRNA fluorescence levels between HWE and the Vg40 mosquitoes than comparison of dsRNA in the midguts of Carb77 and HWE mosquitoes. Also there was variation in dsRNA detection between timepoints in Vg40, with little to no dsRNA detection at 10 hr, detection at 24 hr, and no detection at 48 hr (Figure 5.8). However, it is still unclear where dsRNA from the transgene is localized at the cellular level within the fatbody (Figure 5.9). We observed that fatbody tissues were more difficult to image via fluorescent microscopy than other mosquito tissues such as midguts due to unusually high background fluorescence. We hypothesize that this high background fluorescence may be due to the greater fat content and readily observed lipid droplets.

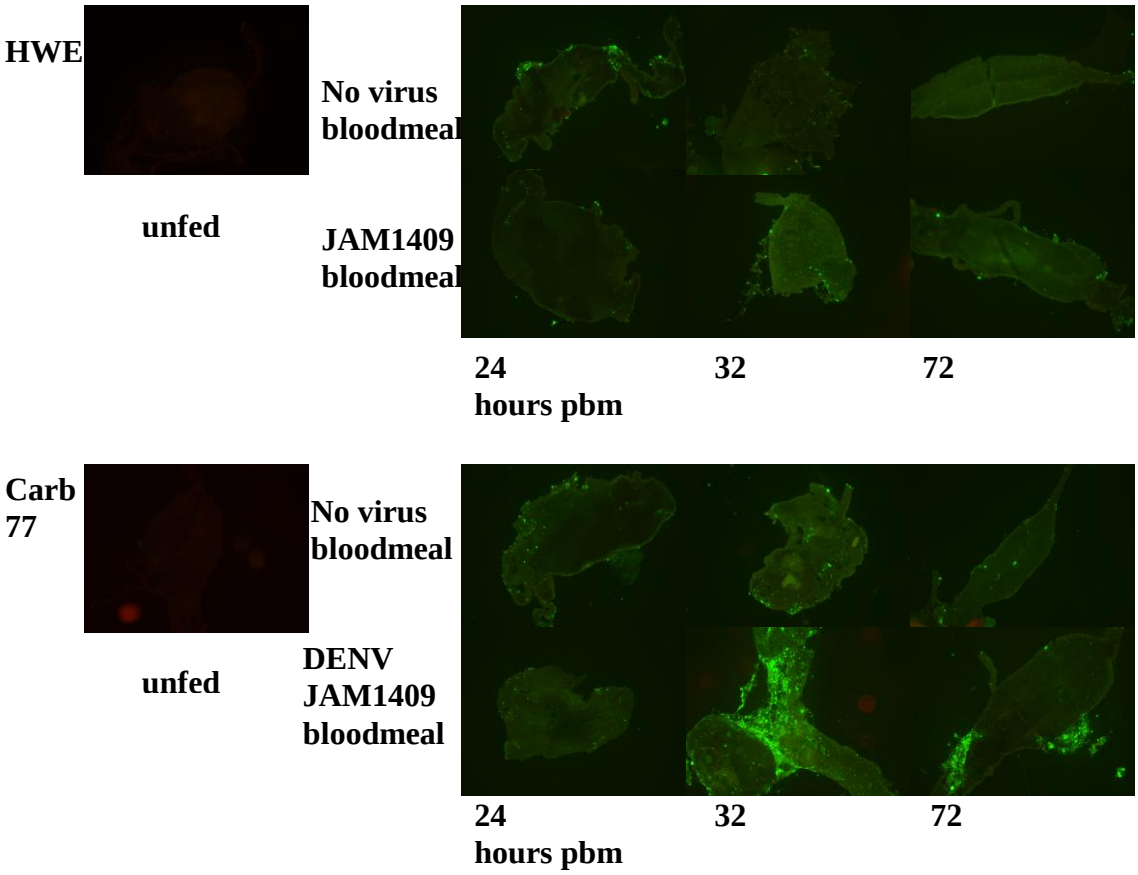

Figure 5.7 DsRNA detection by IFA in midguts in transgenic mosquitoes Carb77 mosquitoes compared to Higgs white eye mosquitoes after DENV-containing or non-infectious bloodmeals. pbm = post bloodmeal

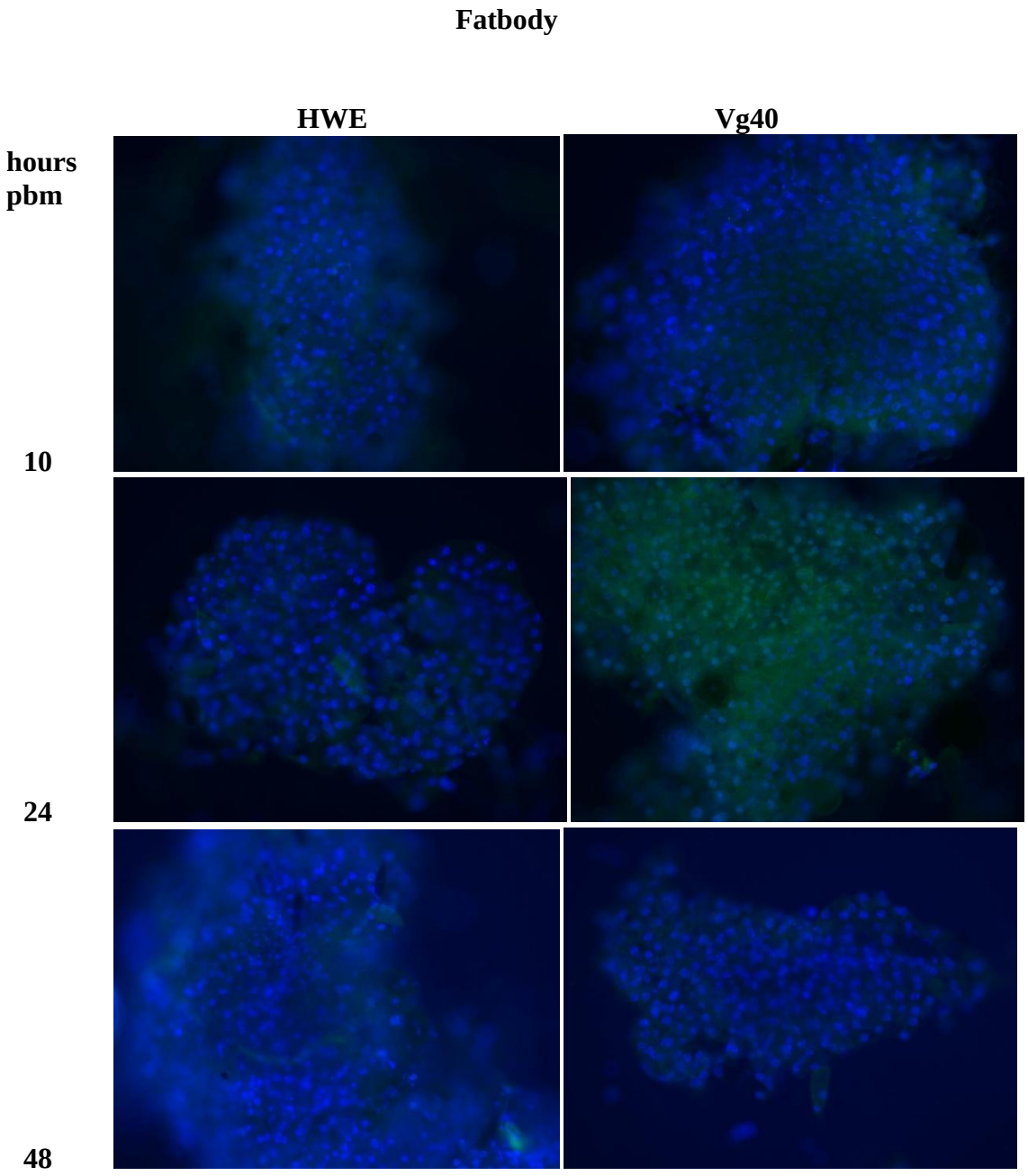

Figure 5.8 DsRNA detection by IFA in fatbodies of transgenic mosquitoes Carb77 mosquitoes compared to Higgs white eye mosquitoes after non-infectious bloodmeals (fluorescent microscope, 20x). hours pbm = hours post bloodmeal

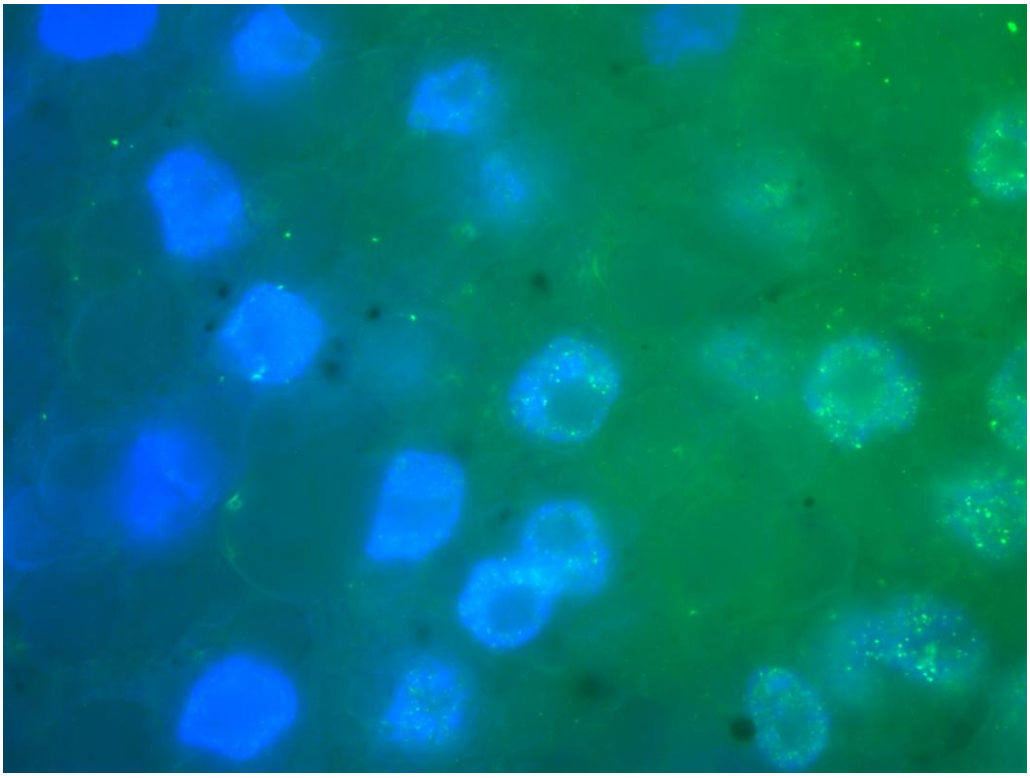

Figure 5.9 DsRNA detection by IFA in fatbody Vg40 mosquitoes 24 hr after non-infectious bloodmeal; higher magnification of 24 hr Vg40 panel in Figure 5.8. (fluorescent microscope, 100x)

Discussion

Sequencing of prM gene RNA

Analysis of the prM gene RNA sequences from virus escape mutants detected non-synonymous mutations in the RNA of only 2 viruses out of 20 tested. Unfortunately, the plaque isolation and amplification of viruses in mosquito cells to increase titers prior to TOPO cloning methodology, modeled on previously published techniques (Chao et al., 2005; Eckels et al., 1976), may not have been the best method to detect mutations in the virus escape mutants. Other researchers have noted that cell culture or animal passage of arboviruses to increase titers to levels useful for further study can lead to changes in virus virulence (Taylor and Marshall, 1975a; Taylor and Marshall, 1975b). Serial passage of DENV in mammalian cell lines or mosquitoes has been shown to cause genotypic changes associated with increased virulence that were attributed to enhanced replication (Cologna et al., 2005; Erb, 2010). Studies have shown that mutations in serially passaged DENV occur rapidly, with most of the mutations occurring within the first five passages, so the three rounds of plaque isolation may have resulted in loss of any original mutations (Lee et al., 1997). Other researchers suggested that arboviruses undergo cell type specific adaptations in mammalian versus mosquito cell cultures, so plaque isolation in LLC-MK2 cells may have resulted in loss of original mutations acquired in mosquitoes (Hanley et al., 2003). The most accurate picture of the mutations in the DENV escape mutants probably would have been obtained by directly sequencing the genomes of viruses isolated from the DENV-challenged Carb77 mosquitoes.

If we could repeat the experiments to analyze possible sequence changes in the virus escape mutant isolates and their potential to escape the Carb77 enhanced RNAi response in nature, we would design an experiment similar to Steve Erb's serial passage experiments of DENV-2 strain 16681 in mosquitoes. We would initially feed Carb77 mosquitoes bloodmeals containing VEM from initial plaque assays in mammalian cells, then grind infected Carb77 mosquitoes and grow the virus in mammalian cells. Carb77 mosquitoes would be provided bloodmeals containing DENV-2 grown in mammalian cells to mimic the alternation of hosts which would occur if Carb77 were to released into the wild thus allowing us to better mimic selection pressure on DENV-2 and better predict genomic mutations. During the experiment we would sequence the VEM after every mosquito passage and evaluate the proportion of mosquitoes infected and mean titers to monitor for increased VEM replication in mosquitoes. Since we cannot re-design the experiment, it would still be informative to sequence the VEM I viruses after each plaque isolation to determine if the isolate mutated during the plaque purification procedure.

Although our methodology might have altered the mutations present in our VEM I sequence, based on our data it does appear that the so-named "virus escape mutants" may have been DENV-2 mutants selected for ability to evade the Carb77 mosquitoes' enhanced RNAi system. VEM I titers in Carb77 mosquitoes were higher than the parental JAM1409 strain, indicating an "escape" of the enhanced RNAi response. Intriguingly, VEM I also replicated to higher titers than JAM1409 in HWE mosquitoes. So, perhaps VEM I is a DENV mutant with increased replication. Of the non-synonymous mutations found in full-length genome sequencing of virus escape

mutant I, a search of current literature found none of these mutations to be associated with previously indentified enhanced replication phenotypes (Table 5.3). However, based on Holmes' study of nonsynonymous mutations in DENV genomes, the level of nonsynonymous mutations within the VEM I genome sequence is typical in quasispecies and the majority of the mutations would be expected to be removed by purifying selection (Holmes, 2003).

Another explanation for unusually high titer of virus in individual Carb77 mosquitoes could be that the artificial bloodmeals result in uptake of an abnormally large bloodmeal or virus dose (Woodring et al., 1996). An abnormally large bloodmeal could create micro-tears in midgut or "leaky midgut," which could result in artificially high titers in individual mosquitoes or "escape viruses." A larger bloodmeal could result in tears in the midgut, allowing DENV-2 to bypass the midgut similar to EM observations of VEE reaching fatbody 1 hr pbm after particularly large bloodmeals (Weaver, 1986). Bloodmeals containing larger doses of virus have been shown to result in greater dissemination rates in mosquitoes than lower volume bloodmeals (Watts et al., 1987). The genomic mutations seen in viruses associated with abnormally high titers are likely related to natural variation in virus sequence due to error-prone replication rather than the result of selection pressure by the Carb77 RNAi response.

Challenge assay

We will first discuss the resistance of the Carb77 (G_{11}) mosquitoes before considering the escape mutant data. Regarding the Carb77 loss of resistance, Franz et al. (2009) noted that Carb77 (G_{12}-G_{15}) resistance was due to lower infection rates, not lower

titers. Our data for Carb77 (G_{11}) showed no statistically significant differences in the proportion of mosquitoes infected, and observable but not always statistically significant differences in mean DENV-2 titers between Carb77 and HWE mosquitoes with lower DENV titers for JAM1409 and VEM I in Carb77 than HWE. We consistently observed a high mosquito infection rate with all mosquito and virus strain combinations. Adelman et al. (2002) found low level infection in DENV-2 resistant transgenic mosquito cell lines in which at least 1% of the cells in every transgenic cell line created were DENV-2 antigen positive via IFA. No DENV-2 resistant transgenic mosquito cell lines were completely resistant to DENV-2 infection. We found that many of the Carb77 (G_{11}) mosquitoes we tested had low titer DENV-2 infections, suggesting that like Dr. Adelman's DENV-2 resistant transgenic mosquito cell lines our Carb77 (G_{11}) mosquitoes were not completely resistant to DENV-2. At 7 d pbm, the mean titer comparison between HWE and Carb77 fed VEM I was not statistically significantly different; however, VEM I titers were lower in Carb77 than HWE. At 14 d pbm mean titer comparisons between HWE and Carb77 fed VEM I were statistically significantly different with lower titers in Carb77 than HWE. The mean titers of HWE and Carb77 mosquitoes fed JAM1409 at 7 and 14 d pbm were statistically significantly different with lower JAM1409 titers in Carb77 than HWE.

Overall, there were observable, if not always statistically significant, differences in mean viral titers between Carb77 and HWE, indicating that, as determined by Franz et al. (2009), Carb77 (G_{11}) mosquitoes were still resistant to infection with DENV-2. In contrast to Franz et al. (2009), we found that the Carb77 (G_{11}) resistance was due to differences in mean titer, not infection rate. Our data more closely resemble those of

Franz et al. (2009) from challenging Carb77 mosquitoes with heterologous strains of DENV-2. Possible reasons for the discrepancy between our data and Franz et al. (2009) include differences in mosquito rearing conditions and different mosquito sorting methods post bloodmeal. To support the hypothesis that differences in mosquito rearing conditions may have affected the proportion of Carb77 mosquitoes infected with DENV-2, few Carb77 (G_{11}) mosquitoes were available at the time of re-challenge assay, and BRB CORE support staff observed that the egg hatch rate was poor due to age of eggs. Regarding sorting mosquitoes after the challenge bloodmeal, if we used only fully or over engorged mosquitoes while Franz et al. (2009) used partially engorged mosquitoes, we would have a higher infection rate than Franz et al. (2009).

Since we concluded that the Carb77 (G_{11}) mosquitoes were resistant at the time of challenge, we will proceed to discuss the implications of the virus escape mutant results. We found lower mean titers of VEM I and JAM1409 in Carb77 mosquitoes than HWE mosquitoes but no significant differences in proportions of Carb77 mosquitoes infected compared to HWE mosquitoes. We observed a few high titer individual mosquitoes in the Carb77 fed both JAM1409 and VEM I at 7 and 14 d pbm, similar to the high titer mosquitoes observed by Franz et al. (2006).

We also noticed an unusual pattern to the mean titers. In the Carb77 mosquitoes fed JAM1409, the mean titers were as follows: 78 pfu/mL (7 d pbm), 4456 pfu/mL (14 d pbm). In the HWE mosquitoes fed JAM1409, the mean titers were as follows: 12917 pfu/mL (7 d pbm), 32102 pfu/mL (14 d pbm) In the Carb77 mosquitoes fed VEM I, the mean titers were as follows: 7788 pfu/mL (7 d pbm), 7253 pfu/mL (14 d pbm). In the HWE mosquitoes fed VEM I, the mean titers were as follows: 17730 pfu/mL (7d pbm),

13525 (14d pbm). In retrospect, it would have been informative to compare the growth curves of JAM1409 and VEM I in both HWE and VEM I mosquitoes, because it appears that mean VEM I titers (7d pbm) peaked earlier than JAM1409 titers (14d pbm). This pattern of differences in mean titers may indicate a difference in growth kinetics between the virus strains within Carb77 (G_{11}) mosquitoes. Since Hanley et al. (2008) observed DENV mutations that were associated with enhanced replication in mosquitoes that were not readily apparent in cell culture, a growth curve comparison of VEM I and Jam1409 in HWE and Carb77 mosquitoes would be more helpful than a growth curve in cell culture to verify this observation.

Ideally, this challenge experiment should be repeated; however, during the timeframe of these experiments the resistance phenotype of the Carb77 family was lost. Recent work by Franz et al. (2009) demonstrated a loss of DENV-2 resistance in Carb77 mosquitoes (G_{14}-G_{17}), and the loss of the resistance phenotype could be due to loss of expression of the transgene. Franz et al. (2009) found no mutations in the transgene; instead expression of the transgene was lost due to some unknown mechanism.

Based on the RNAi escape hypothesis, we would predict one or more mutations in the prM encoding region of the DENV-2 genome and this mutation or mutations would disrupt the complementary base pairing between the inverted repeat transcript and the DENV-2 genome, resulting in corresponding high titer phenotypes. Although we did observe a mutation in the prM sequence, it was only at one nucleotide of the prM gene in two VEM isolates, VEM I and VEM P. The prM region used in construction of the Carb77 mosquito strain is 578 nt long and the total mutation rate for DENV-2 RNA is 0.62×10^{-3} (95% confidence interval 0.49-0.74) substitutions/site/year (Jenkins et al.,

2002). For the prM region, 0.35 nt in the 578 nt sequence would occur based on this natural mutation rate. We observed 2 DENV-2 virus escape mutants with mutations in the prM out of 20 possible virus escape mutants when we would predict 7 virus escape mutants could have mutations based on the mutation rate determined by Jenkins et al. (2002). Our observations are well within the predicted number of mutations for natural mutation rate in DENV RNA, not indicative of the increased rate of mutation that would be predicted for flavivirus RNA under selection by RNAi (Brackney et al., 2009; Holmes, 2003). However, we did observe what appeared to be an increased replication phenotype as represented by a large plaque phenotype virus, VEM P. This observation led us to hypothesize that a DENV-2 isolate might have a high titer phenotype in individual Carb77 mosquitoes due to a mutation outside the prM region. So we attempted to sequence the entire genome of VEM I and VEM P and discovered that VEM P was not DENV-2 but perhaps a DENV and SINV mixture (Table 5.6, Figure 5.5 & 5.6). None of the mutations observed in sequencing of full-length VEM I has been associated with enhanced DENV replication in mosquitoes (Table 5.3). Other arbovirus researchers have observed mutations in viral genomes associated with enhanced replication and transmission in mosquitoes. Chikungunya (CHIK) (family Togaviridae) envelope protein I mutation (E1-A226V), which was associated with the 2005-2006 Reunion Island outbreak, allowed adaptation of CHIKV to *Aedes albopictus* (Tsetsarkin et al., 2007). West Nile virus sequences from the first 5 years post introduction to New York revealed mutations leading to a reduction of extrinsic incubation period (EIP) or time from mosquito infection to transmission (Ebel et al., 2004). Increased DENV replication in mosquitoes has been shown to play a role in DENV-3 strain replacement in Sri Lanka, as

a less virulent strain of DENV-3 was replaced with a more virulent strain (Hanley et al., 2008).

As for the increased infection rate prediction of the RNAi escape hypothesis, the mean infection rate for our Carb77 (G_{11}) challenge experiment was higher than the infection rate shown by Franz et al. (2009) for Carb77 (G_{12}). At 7 day pbm Franz et al. (2009) reported 56.3% HWE and 7.2% Carb77 infection rates, whereas we reported 100% and 93.3% infection rates respectively. At 14 day pbm, infection rates were 100% for all mosquito and virus strain combinations except Carb77 fed VEM I, which was 75% compared to infection rates of 46.7% HWE mosquitoes and 20% Carb77 (G_{12}) mosquitoes at 14 d pbm observed by Franz et al. (2009). The mean titers were consistently different, if not statistically significantly different, between VEM I and JAM1409 in individual comparisons. However, the pairwise differences in mean titers across mosquito strains were statistically significant, which shows overall that VEM I replicated to higher titers than JAM1409 in both mosquito strains at all timepoints.

Overall comparison of DENV viral titers in Carb77 (G_{11}) mosquitoes to HWE mosquitoes, we determine that Carb77 (G_{11}) mosquitoes were still resistant to DENV-2 based on lower mean DENV titers. After determining that Carb77 (G_{11}) mosquitoes were resistant to DENV-2, we evaluated whether VEM I escaped the enhanced RNAi-response of Carb77 mosquitoes. Since VEM I titers are higher than JAM1409 in Carb77, it appears that VEM I may have escaped the enhanced RNAi response of Carb77. Additionally, all comparisons of VEM I titers were higher than JAM1409 titers, except HWE fed VEM I at 14 d pbm compared to HWE fed JAM1409. So, an alternative explanation to the escape mutant hypothesis is that VEM I simply replicates to higher

titer than JAM1409 and a growth curve comparison in mosquitoes is need to verify this observations.

Identification of a large plaque phenotype virus via RT-PCR, sequencing, and midgut IFA

The large plaque phenotype observed in association with virus escape mutant P was attributable to contamination with a SINV, TE3'2J. This contaminant explains the observation of the large plaque phenotype relative to DENV isolates. Since VEM P was initially described as a large plaque phenotype prior to plaque isolation in this study, it is possible that the initial DENV-2 (JAM1409) stock may have been contaminated. The ability to amplify and sequence the DENV prM gene from this escape mutant suggests that the initial VEM P isolate may have been a mixture of DENV and SINV (Figure 5.2). Experiments to identify the large-plaque variant were undertaken because the virus not only made abnormally large plaques but also routinely replicated to a higher titer than DENV in cell culture. However, VEM P was not the DENV with enhanced replication phenotype due to mutations outside the prM region that we had hypothesized.

Brackney et al. (2009) reported an increase in mutation frequency in regions of the WNV genome sequence that were highly targeted by the mosquito RNAi response. So, it is still plausible that DENV RNAi escape mutants could arise from selection pressure of the Carb77 prM-targeting RNAi system. Researchers studying poliovirus offered a solution to RNAi escape viruses, recommending either an increase in the number of siRNAs or use of a dsRNA greater than 1 Kb in length (Gitlin et al., 2005). In the Carb77 mosquito, the prM inverted repeat sequence is 578 nt. While a longer effector

sequence may be practical for a DENV-2 resistant mosquito like Carb77, a chimeric inverted repeat targeting all four DENV serotypes may not be practical for production of transgenic mosquitoes.

Midgut IFA for dsRNA

Presumably the inverted repeat RNA was still being expressed in the Carb77 mosquitoes examined in Figure 5.8; however, Franz et al. (2009) found that Carb77 (G_{17}) was not expressing the inverted repeat RNA as detected by northern blot hybridization. To determine whether detection of dsRNA expression from a transgene was possible in Carb77 mosquito midguts post-bloodmeal, we used J2 monoclonal antibody IFA to dsRNA. Attempts to stain for dsRNA in infected and uninfected Carb77 and HWE midguts shortly after a bloodmeal were less successful than hoped. The J2 dsRNA antibody has previously been used to show dsRNA in foldback RNA-expressing cells (Figure 2.6). Theoretically, the prM foldback expressed by induction of the carboxypeptidase promoter immediately after a bloodmeal should have been detectable in Carb77 mosquitoes with the J2 antibody at 24, 48, and 72 hr pbm. Removal of the bloodmeal from midguts dissected so soon after feeding was difficult and more frequently resulted in midgut fragments rather than intact midguts, making localization of dsRNA to a specific region of the midgut difficult to discern. Additionally, in the case of midguts in which the bloodmeal was not completely removed the residual blood appeared to interfere with fluorescent signal. In the case of the Carb77 mosquitoes, in which dsRNA production is under the control of a bloodmeal induced promoter and is expressed in the midgut, the information gained on location of transgene expression from dsRNA

staining with the J2 antibody is minimal due to the difficulty of removing the bloodmeal without destroying the midgut. Difficulty detecting transgene expression in the mosquito midgut via IFA at early timepoints pbm seems to be a common problem. Researchers studying *Plasmodium*-resistant transgenic mosquitoes expressing salivary gland and midgut peptide (SM1) also had high background fluorescence and torn midgut in IFA images (Ito et al., 2002).

Since we have shown in Chapters 2 and 4 that monoclonal antibody J2 detects dsRNA from inverted repeat-RNA expressing transgenes as well as from DENV replication in mosquito midguts, we might question whether the source of this dsRNA was DENV or transgene transcript. However, based on Chapter 4 timecourse of dsRNA staining in mosquitoes, the source of the fluorescence in the Carb77 samples 32 hrs post bloodmeal should be dsRNA expressing transgene. In retrospect, to confirm that the dsRNA in the Carb77 samples 32 hrs post bloodmeal were expressed from the transgene, we should have used a midgut sample in which we consistently observed dsRNA staining, as a positive control. A 7 day pbm HWE midgut infected with DENV-2 would have been a better positive control for dsRNA staining.

We had planned to develop double-staining for dsRNA or to show early expression of dsRNA (IR) and later no expression viral antigen in bloodfed Carb77 compared to HWE. If we had been able to compare staining for dsRNA and DENV-2 antigen in Carb77 transgenic mosquito midguts, versus HWE midguts then we would have had an interesting model system for evaluating the timing of RNAi and detection of secondary structure of the DENV genome and replicative intermediates as well as exclusion of Dicer from membrane bound replication compartments in whole

mosquitoes. Brackney et al. (2009) and Scott (2009) studying WNV in mosquito midguts and DENV-2 in mosquito cells, observed no bias in which sense, genome or anti-genome, of WNV RNA siRNAs were derived from massively parallel sequencing, indicating that both the viral replicative intermediates and secondary structure are being targeted by RNAi.

Localization of dsRNA in Vg40 transgenic mosquitoes was more successful, confirming the expected temporal and spatial patterns of transgene expression by showing an increase in dsRNA staining in the fatbody at 24 hrs pbm. Imaging tissue with high background fluorescence, such as mosquito fatbody would benefit from careful controls that allow narrowing of the emission window used in confocal microscopy to subtract background. However, the need to use confocal microscopy to image dsRNA in fatbody, may diminish the utility of dsRNA IFA for rapid screening of transgenic mosquitoes.

Overall, dsRNA IFA techniques are potentially a useful addition to the tools used to evaluate expression of transgenes. IFA provides spatial and temporal information about transgene expression. Other research groups who have developed transgenic mosquitoes resistant to malaria via protein effectors such as SM1 and bee venom, have used immunoblot and IFA to provide temporal and spatial data on transgene expression (Ghosh et al., 2001; Ito et al., 2002). Until we began using the J2 dsRNA antibody, we relied mainly on temporal data on effector expressionn based on Northern blot data. Use of the J2 dsRNA antibody helps evaluation of spatial expression of transgenes.

Conclusions

Overall, the results from these experiments suggest that viruses with mutations in RNA are not selected due to pressure from the enhanced RNAi system of the Carb77 family of mosquitoes. Instead, we propose that VEM I is a virus with a increased replication phenotype in both Carb77 and HWE mosquitoes. Repetition of the challenge experiment and sequencing mutant viruses at every isolation step or preferably sequencing immediately after initial isolation would allow us to draw stronger conclusions as to whether the selection of hyper-replicating DENV-2 should be a concern for release of transgenic mosquitoes that are resistant to DENV.

Although these experiments showed no hyper replicating viruses that could be definitively stated to escape the Carb77 enhanced RNAi response, the methods used were not optimal. The deep sequencing study of West Nile virus associated small RNA by Brackney et al. (2009), which provided evidence that RNAi targets viral hotspots leading to increased virus mutation rates, is a cause for concern in design of a RNAi-based DENV virus-resistant transgenic mosquito. The loss of resistance in the Carb77 mosquitoes by an unknown mechanism as discussed by Franz et al. (2009) is also worrisome. While RNAi based resistance in transgenic mosquitoes is promising based on DENV resistance in G_8 through G_{13} of Carb77, these transgenic mosquito systems still require optimization.

Chapter 6

Summary

Although arbovirus replication in the mosquito host has been studied for many years, we still have many unanswered questions. Previous research in our laboratory has shown that arbovirus replication in mosquitoes triggers an RNA interference (RNAi) response, and when RNAi is suppressed, an increase in arbovirus replication is observed (Keene et al., 2004; Sanchez-Vargas et al., 2004). Since there are no approved vaccines or antiviral drugs for the treatment of dengue infections, our laboratories have developed molecular control strategies. Study of dengue virus (DENV) replication in mosquito cell culture and *Aedes aegypti* suggests that there is a fine balance between DENV replication and the antiviral RNAi response (Sanchez-Vargas et al., 2009). A greater understanding of the interaction between DENV and RNAi, enables us to improve molecular control strategies for DENV.

The research described in the previous chapters was based on the hypothesis that DENV replicative RNA may be protected from the RNAi response in the mosquito. Rearrangement and proliferation of intracellular membranes has long been observed in association with flavivirus replication, and replicative forms of viral RNA have been isolated from these membranes in mammalian cell culture (Mackenzie et al., 1999; Uchil and Satchidanandam, 2003). We evaluated the association between viral dsRNA and membranes in mosquito cell culture. DsRNA was observed throughout the cytoplasm in DENV-infected mosquito cell culture. DENV dsRNA co-localized completely with DENV envelope (E) protein via confocal microscopy while DENV capsid (C) protein and dsRNA did not completely co-localize. These observations suggest that dsRNA and E protein are produced in close proximity with mosquito cells while C protein localizes to sites of viral packaging. Our observations are consistent with EM tomography models of

DENV RNA replication in close proximity of viral protein production (Welsch et al., 2009). Additionally, DENV-specific dsRNA was isolated from buoyant fractionations of mosquito cell culture which contained double-membrane vesicles (DMVs) of 50-75 nm when examined by electron microscopy (EM). Observations of increased intensity of ER staining via immunofluorescent microscopy in DENV-infected mosquito cell culture and that DMVs were resistance to treatment with cold non-ionic detergent indicated that DMVs isolated from buoyant fractions probably originated from the endoplasmic reticulum (ER). These observations were consistent with descriptions of ER origin and the morphology of DMVs observed in flavivirus infected mammalian cells (Uchil et al., 2006). Exclusion of DENV-specific dsRNA from the mosquito RNAi response was not clearly established, but we can speculate based on similarities in DENV-induced DMV morphology and size in mammalian and mosquito cell culture that DMV pore size might be sufficient to exclude Dicer from accessing the DENV dsRNA replicative intermediates. DMVs observed in mosquito cell culture are likely to protect dsRNA replicative intermediates from RNAi.

DsRNA localization in mosquito cells was compared between DENV-infections and infection with other arboviruses. DENV dsRNA staining localized throughout the cytoplasm in cell culture and co-localized with ER staining, confirming previous reports of DENV dsRNA replication in the ER. Previous research has shown than SINV replicates within cytoplasmic vacuoles (CPVs) (Gliedman et al., 1975). Like DENV, staining for SINV dsRNA was consistent with published observations of of SINV replication and SINV dsRNA staining localized to large clusters in the cytoplasm.

Expression of DENV NS4a-2K in mammalian cell culture has been shown to cause membrane rearrangements that resemble DENV infection (Miller et al., 2007). To further characterize the DMVs isolated from mosquito cell lines, we attempted to express DENV NS4a and NS4b proteins in mosquito cell culture to determine if they induced DMVs like those observed in DENV-infected mosquito cells. We did not establish whether expression of DENV NS4 causes membrane rearrangement in mosquito cells. We hypothesize that expression of NS4 constructs under a constitutive promoter was overwhelming or toxic to mosquito cells. Future expression studies of DENV NS4a and NS4b in mosquito cells should use inducible expression methods to avoid problems with toxicity. Further studies such as RNAi-based genome screens for host factors involved in virus replication and yeast two hybrid screening are needed to fully understand how DENV NS proteins and host proteins interact to form DMVs.

We isolated DMVs from midguts of DENV-infected *Aedes aegypti* mosquitoes similar to the DMVs that we isolated from DENV- infected mosquito cell culture. We observed a greater variation in the diameter of the DENV associated vesicles isolated from midguts, 50-120 nm in midguts versus 50-75 nm in cell culture. Similar to the DMVs isolated from cell culture, these DMVs were associated with ER proliferation and were resistant to cold non-ionic detergent, suggesting that the membranes originated from the ER. The DENV envelope and SINV envelope 1 proteins both co-localized temporally and spatially with dsRNA in *Ae. aegypti* midguts but SINV viral antigen and dsRNA were observed earlier than DENV. Differences in temporal and spatial localization between flavivirus and alphavirus RCs, as represented by localization of dsRNA and viral antigen, that were not apparent in mosquito cell culture were observed

in mosquito tissues. This discrepancy between observations in mosquito cell culture and mosquitoes may be because C6/36 cells were selected to be extremely permissible to arbovirus replication, whereas arboviruses may encounter midgut escape barriers in mosquitoes (Igarashi, 1978; Myles et al., 2004).

The presence of DENV dsRNA within DMVs has implications for the development of an RNAi-based DENV-resistant transgenic mosquito. To effectively target DENV dsRNA, antiviral responses must either be timed to act on the secondary structure of freshly uncoated viral RNA or as viral RNA moves between DMVs and sites of mature virus packaging. To completely inhibit DENV replication using RNAi, future studies will need to determine the timeframe in which vRNA moves between DMVs to packaging locations or find a method of accessing dsRNA within DMVs.

We isolated viruses that replicated to high titer in the DENV-resistant Carb77 mosquitoes, and determined that the virus escape mutant I (VEM I) replicated to a higher titer than the parental strain. We hypothesized that DENV-2 replicated to a significantly in some individual Carb77 mosquitoes than other individuals due to variation in the prM region targeted by the Carb77 enhanced RNAi response. Since RNA viruses exist as a quasispecies, the original DENV-2 (JAM1409) bloodmeal received by the Carb77 mosquitoes would have contained DENV genomes with nucleotide sequence variations differing from the consensus sequence. The DENV genomes with the most variation, as represented by the nucleotide mutations, in the prM region of their genome would be less affected by the Carb77 mosquitoes' enhanced RNAi-response directed to the prM region, which could give these viral genomes a fitness advantage. A increased fitness phenotype virus might replicate to higher titer in Carb77 mosquitoes, infect a higher proportion of

mosquitoes, and have mutations within the prM region of the genome. However, we found only two VEMs out of twenty viruses sequenced that had mutations in the prM region compared to JAM1409. We sequenced VEM I which did not infect a higher proportion of mosquitoes, replicated to higher titers in Carb77 mosquitoes, and had a single mutation in the prM region. Since the prM region expressed by the Carb77 mosquitoes is 578 nt in length and many siRNAs should be produced from this region minimizing the impact of a single mutation, we hypothesized that a 1 nt mutation could not be responsible for this increase in titer. We sequenced the entire VEM I genome and found no mutations known to be associated with increased replication.

RNA viruses including poliovirus, Hepatitis C virus, and HIV-1 have "escaped" or acquired the ability to replicate in the presence of RNAi-based siRNA or dsRNA therapies (Gitlin et al., 2005; Konishi et al., 2006; Pusch et al., 2003; ter Brake et al., 2008; Westerhout et al., 2005). However there is minimal data available on flavivirus mutations and evasion of RNAi. Brackney et al. (2009) used massively parallel sequencing to demonstrate that regions of the WNV genome that are more highly targeted by RNAi in mosquitoes, as indicated by a greater variation in siRNA sequences, are more likely to have imperfect matches between siRNAs and the WNV genome. Overall, our evaluation of DENV virus escape mutants is inconclusive because the plaque isolation method used could have introduced more mutations than were in the original viruses. Future research should sequence directly from the original isolate.

DsRNA IFA was used to evaluate spatial localization of transgene hairpin RNA with mixed results. DsRNA staining in transgenic mosquitoes with dsRNA expressed in the midgut expression was minimally informative while dsRNA staining for transgenes

expressed in the fatbody were consistent with northern blot data of transgene expression. Prior to use of the J2 dsRNA antibody, we relied mainly on Northern blot data to verify temporal transgene expression. Now the J2 dsRNA antibody can be used to evaluate spatial and temporal information about transgene expression simultaneously.

The research described in this dissertation increased our knowledge of DENV membrane-associated replication complexes and the role they play in the balance between DENV replication and RNAi. In Chapter 2, we studied DENV dsRNA in mosquito cell culture and found dsRNA was be briefly localized perinuclearly then spread throughout the cytoplasm and observed 50-75 nm diameter DMVs of ER origin similar to those isolated from mammalian cells. Comparison of dsRNA localization alphaviruses and flaviviruses in mosquito cell culture found few temporal and spatial differences in dsRNA staining. In Chapter 3, our attempt to induce membrane rearrangement via expression of dengue NS4 and NS4b proteins was largely unsuccessful, but we learned that overexpression of NS4a and NS4b appears to be detrimental to mosquito cells. Future studies of NS4a and NS4b in mosquito cell culture should use inducible expression methods. In Chapter 4, we observed that DENV dsRNA temporally and spatially co-localized with E protein and C protein, and does not localize to midgut associated muscles. Additionally, we observed ER proliferation and isolation of DMVs similar to those isolated from mosquito cell culture. Comparison of dsRNA between SINV and DENV found temporal and spatial expression of dsRNA is closely tied to production of viral antigen. In Chapter 5, methodologically flawed characterization of viruses that escaped the enhanced RNAi response of transgenic mosquitoes revealed no mutations within the targeted viral sequence that could account

for RNAi escape. We also found no mutations in other regions of the genome that could explain the enhanced replication phenotype of VEM I. The increased titer of VEM I relative to the parental JAM1409 stain requires further characterization. Overall, this work suggests that there may be a point in the dengue viral life cycle where the replication complex of viral RNA is protected from the mosquito RNAi response. Since no bias in strand polarity has been observed in flavivirus siRNAs, Dicer must be accessing the DMV-protected anti-genome sense RNA at some point during DENV replication. Future studies of DENV membrane-associated RC will need to characterize movement in and out of RC-associated membranes and whether this can be exploited to find another DENV dsRNA vulnerability for development of transgenic mosquitoes.

References

Adelman, Z. (2000) RNA-mediated resistance to dengue virues 1-4. PhD dissertation., dissertation, Colorado State University, Fort Collins, CO.

Adelman, Z. N., Anderson, M. A., Morazzani, E. M., and Myles, K. M. (2008). A transgenic sensor strain for monitoring the RNAi pathway in the yellow fever mosquito, Aedes aegypti. Insect Biochem Mol Biol *38*, 705-713.

Adelman, Z. N., Sanchez-Vargas, I., Travanty, E. A., Carlson, J. O., Beaty, B. J., Blair, C. D., and Olson, K. E. (2002). RNA silencing of dengue virus type 2 replication in transformed C6/36 mosquito cells transcribing an inverted-repeat RNA derived from the virus genome. J Virol *76*, 12925-12933.

Albertini, A. A., Wernimont, A. K., Muziol, T., Ravelli, R. B., Clapier, C. R., Schoehn, G., Weissenhorn, W., and Ruigrok, R. W. (2006). Crystal structure of the rabies virus nucleoprotein-RNA complex. Science *313*, 360-363.

Amberg, S. M., Nestorowicz, A., McCourt, D. W., and Rice, C. M. (1994). NS2B-3 proteinase-mediated processing in the yellow fever virus structural region: in vitro and in vivo studies. J Virol *68*, 3794-3802.

Anderson, J. R., and Rico-Hesse, R. (2006). Aedes aegypti vectorial capacity is determined by the infecting genotype of dengue virus. Am J Trop Med Hyg *75*, 886-892.

Anderson, R. G., and Jacobson, K. (2002). A role for lipid shells in targeting proteins to caveolae, rafts, and other lipid domains. Science *296*, 1821-1825.

Armstrong, P. M., and Rico-Hesse, R. (2001). Differential susceptibility of Aedes aegypti to infection by the American and Southeast Asian genotypes of dengue type 2 virus. Vector Borne Zoonotic Dis *1*, 159-168.

Armstrong, P. M., and Rico-Hesse, R. (2003). Efficiency of dengue serotype 2 virus strains to infect and disseminate in Aedes aegypti. Am J Trop Med Hyg *68*, 539-544.

Attarzadeh-Yazdi, G., Fragkoudis, R., Chi, Y., Siu, R. W., Ulper, L., Barry, G., Rodriguez-Andres, J., Nash, A. A., Bouloy, M., Merits, A., *et al.* (2009). Cell-to-cell spread of the RNA interference response suppresses Semliki Forest virus (SFV) infection of mosquito cell cultures and cannot be antagonized by SFV. J Virol *83*, 5735-5748.

Barillas-Mury, C., Wizel, B., and Han, Y. S. (2000). Mosquito immune responses and malaria transmission: lessons from insect model systems and implications for vertebrate innate immunity and vaccine development. Insect Biochem Mol Biol *30*, 429-442.

Bartenschlager, R., and Miller, S. (2008). Molecular aspects of Dengue virus replication. Future Microbiol *3*, 155-165.

Barth, O. M. (1999). Ultrastructural aspects of the dengue virus (flavivirus) particle morphogenesis. J Submicrosc Cytol Pathol *31*, 407-412.

Bayne, E. H., Rakitina, D. V., Morozov, S. Y., and Baulcombe, D. C. (2005). Cell-to-cell movement of potato potexvirus X is dependent on suppression of RNA silencing. Plant J *44*, 471-482.

Bechill, J., Chen, Z., Brewer, J. W., and Baker, S. C. (2008). Coronavirus infection modulates the unfolded protein response and mediates sustained translational repression. J Virol *82*, 4492-4501.

Belov, G. A., and Ehrenfeld, E. (2007). Involvement of cellular membrane traffic proteins in poliovirus replication. Cell Cycle *6*, 36-38.

Belov, G. A., Feng, Q., Nikovics, K., Jackson, C. L., and Ehrenfeld, E. (2008). A critical role of a cellular membrane traffic protein in poliovirus RNA replication. PLoS Pathog *4*, e1000216.
Bennasser, Y., Le, S. Y., Benkirane, M., and Jeang, K. T. (2005). Evidence that HIV-1 encodes an siRNA and a suppressor of RNA silencing. Immunity *22*, 607-619.
Bennett, K. E., Beaty, B. J., and Black, W. C. t. (2005). Selection of D2S3, an Aedes aegypti (Diptera: Culicidae) strain with high oral susceptibility to Dengue 2 virus and D2MEB, a strain with a midgut barrier to Dengue 2 escape. J Med Entomol *42*, 110-119.
Bennett, K. E., Olson, K. E., Munoz Mde, L., Fernandez-Salas, I., Farfan-Ale, J. A., Higgs, S., Black, W. C. t., and Beaty, B. J. (2002). Variation in vector competence for dengue 2 virus among 24 collections of Aedes aegypti from Mexico and the United States. Am J Trop Med Hyg *67*, 85-92.
Bergold, G. H., and Weibel, J. (1962). Demonstration of yellow fever virus with the electron microscope. Virology *17*, 554-562.
Black, W. C. t., Bennett, K. E., Gorrochotegui-Escalante, N., Barillas-Mury, C. V., Fernandez-Salas, I., de Lourdes Munoz, M., Farfan-Ale, J. A., Olson, K. E., and Beaty, B. J. (2002). Flavivirus susceptibility in Aedes aegypti. Arch Med Res *33*, 379-388.
Blakqori, G., Delhaye, S., Habjan, M., Blair, C. D., Sanchez-Vargas, I., Olson, K. E., Attarzadeh-Yazdi, G., Fragkoudis, R., Kohl, A., Kalinke, U., *et al.* (2007). La Crosse bunyavirus nonstructural protein NSs serves to suppress the type I interferon system of mammalian hosts. J Virol *81*, 4991-4999.
Bolten, R., Egger, D., Gosert, R., Schaub, G., Landmann, L., and Bienz, K. (1998). Intracellular localization of poliovirus plus- and minus-strand RNA visualized by strand-specific fluorescent In situ hybridization. J Virol *72*, 8578-8585.
Boulant, S., Targett-Adams, P., and McLauchlan, J. (2007). Disrupting the association of hepatitis C virus core protein with lipid droplets correlates with a loss in production of infectious virus. J Gen Virol *88*, 2204-2213.
Boulton, R. W., and Westaway, E. G. (1976). Replication of the flavivirus Kunjin: proteins, glycoproteins, and maturation associated with cell membranes. Virology *69*, 416-430.
Bowers, D. F., Abell, B. A., and Brown, D. T. (1995). Replication and tissue tropism of the alphavirus Sindbis in the mosquito Aedes albopictus. Virology *212*, 1-12.
Bowers, D. F., Coleman, C. G., and Brown, D. T. (2003). Sindbis virus-associated pathology in Aedes albopictus (Diptera: Culicidae). J Med Entomol *40*, 698-705.
Brackney, D. E., Beane, J. E., and Ebel, G. D. (2009). RNAi targeting of West Nile virus in mosquito midguts promotes virus diversification. PLoS Pathog *5*, e1000502.
Calisher, C. H., Karabatsos, N., Dalrymple, J. M., Shope, R. E., Porterfield, J. S., Westaway, E. G., and Brandt, W. E. (1989). Antigenic relationships between flaviviruses as determined by cross-neutralization tests with polyclonal antisera. J Gen Virol *70 (Pt 1)*, 37-43.
Campbell, C. L., Keene, K. M., Brackney, D. E., Olson, K. E., Blair, C. D., Wilusz, J., and Foy, B. D. (2008). Aedes aegypti uses RNA interference in defense against Sindbis virus infection. BMC Microbiol *8*, 47.
Cardosa, J., Ooi, M. H., Tio, P. H., Perera, D., Holmes, E. C., Bibi, K., and Abdul Manap, Z. (2009). Dengue virus serotype 2 from a sylvatic lineage isolated from a patient with dengue hemorrhagic Fever. PLoS Negl Trop Dis *3*, e423.

Catteruccia, F., Godfray, H. C., and Crisanti, A. (2003). Impact of genetic manipulation on the fitness of Anopheles stephensi mosquitoes. Science *299*, 1225-1227.
CDC (2003). Fact Sheet: Dengue and Dengue Hemorrhagic Fever. http://www.cdc.gov/ncidod/dvbid/dengue/facts.htm.
CDC (2008). Dengue: Clinical and Public Health Aspects. http://www.cdc.gov/ncidod/dvbid/dengue/slideset/set1/ii/slide02.htm .
Chan, S. W., and Egan, P. A. (2009). Effects of hepatitis C virus envelope glycoprotein unfolded protein response activation on translation and transcription. Arch Virol.
Chao, D. Y., King, C. C., Wang, W. K., Chen, W. J., Wu, H. L., and Chang, G. J. (2005). Strategically examining the full-genome of dengue virus type 3 in clinical isolates reveals its mutation spectra. Virol J *2*, 72.
Chen, C. H., Huang, H., Ward, C. M., Su, J. T., Schaeffer, L. V., Guo, M., and Hay, B. A. (2007). A synthetic maternal-effect selfish genetic element drives population replacement in Drosophila. Science *316*, 597-600.
Chen, M. C., Lin, C. F., Lei, H. Y., Lin, S. C., Liu, H. S., Yeh, T. M., Anderson, R., and Lin, Y. S. (2009). Deletion of the C-terminal region of dengue virus nonstructural protein 1 (NS1) abolishes anti-NS1-mediated platelet dysfunction and bleeding tendency. J Immunol *183*, 1797-1803.
Cherry, S., and Silverman, N. (2006). Host-pathogen interactions in drosophila: new tricks from an old friend. Nat Immunol *7*, 911-917.
Cho, M. W., Teterina, N., Egger, D., Bienz, K., and Ehrenfeld, E. (1994). Membrane rearrangement and vesicle induction by recombinant poliovirus 2C and 2BC in human cells. Virology *202*, 129-145.
Chu, P. W., and Westaway, E. G. (1992). Molecular and ultrastructural analysis of heavy membrane fractions associated with the replication of Kunjin virus RNA. Arch Virol *125*, 177-191.
Chua, J. J., Ng, M. M., and Chow, V. T. (2004). The non-structural 3 (NS3) protein of dengue virus type 2 interacts with human nuclear receptor binding protein and is associated with alterations in membrane structure. Virus Res *102*, 151-163.
Cirimotich, C. M., Scott, J. C., Phillips, A. T., Geiss, B. J., and Olson, K. E. (2009). Suppression of RNA interference increases alphavirus replication and virus-associated mortality in Aedes aegypti mosquitoes. BMC Microbiol *9*, 49.
Cologna, R., Armstrong, P. M., and Rico-Hesse, R. (2005). Selection for virulent dengue viruses occurs in humans and mosquitoes. J Virol *79*, 853-859.
Cornel, A. J., Benedict, M. Q., Rafferty, C. S., Howells, A. J., and Collins, F. H. (1997). Transient expression of the Drosophila melanogaster cinnabar gene rescues eye color in the white eye (WE) strain of Aedes aegypti. Insect Biochem Mol Biol *27*, 993-997.
Crochu, S., Cook, S., Attoui, H., Charrel, R. N., De Chesse, R., Belhouchet, M., Lemasson, J. J., de Micco, P., and de Lamballerie, X. (2004). Sequences of flavivirus-related RNA viruses persist in DNA form integrated in the genome of Aedes spp. mosquitoes. J Gen Virol *85*, 1971-1980.
Dailey, M., Marrs, G., Satz, J., and Waite, M. (1999). Concepts in imaging and microscopy. Exploring biological structure and function with confocal microscopy. Biol Bull *197*, 115-122.
De Duve, C., and Wattiaux, R. (1966). Functions of lysosomes. Annu Rev Physiol *28*, 435-492.

de Thoisy, B., Dussart, P., and Kazanji, M. (2004). Wild terrestrial rainforest mammals as potential reservoirs for flaviviruses (yellow fever, dengue 2 and St Louis encephalitis viruses) in French Guiana. Trans R Soc Trop Med Hyg *98*, 409-412.
Deleris, A., Gallego-Bartolome, J., Bao, J., Kasschau, K. D., Carrington, J. C., and Voinnet, O. (2006). Hierarchical action and inhibition of plant Dicer-like proteins in antiviral defense. Science *313*, 68-71.
Deubel, V., and Digoutte, J. P. (1981). Morphogenesis of yellow fever virus in Aedes aegypti cultured cells. I. Isolation of different cellular clones and the study of their susceptibility to infection with the virus. Am J Trop Med Hyg *30*, 1060-1070.
Diallo, M., Ba, Y., Sall, A. A., Diop, O. M., Ndione, J. A., Mondo, M., Girault, L., and Mathiot, C. (2003). Amplification of the sylvatic cycle of dengue virus type 2, Senegal, 1999-2000: entomologic findings and epidemiologic considerations. Emerg Infect Dis *9*, 362-367.
Dimopoulos, G. (2003). Insect immunity and its implication in mosquito-malaria interactions. Cell Microbiol *5*, 3-14.
Ding, S. W., Li, H., Lu, R., Li, F., and Li, W. X. (2004). RNA silencing: a conserved antiviral immunity of plants and animals. Virus Res *102*, 109-115.
Dodd, D. A., Giddings, T. H., Jr., and Kirkegaard, K. (2001). Poliovirus 3A protein limits interleukin-6 (IL-6), IL-8, and beta interferon secretion during viral infection. J Virol *75*, 8158-8165.
Domingo, E. (2002). Quasispecies Theory in Virology. Journal of Virology *76*, 463-465.
Domingo, E., and Holland, J. J. (1997). RNA virus mutations and fitness for survival. Annu Rev Microbiol *51*, 151-178.
Domingo, E., Martinez-Salas, E., Sobrino, F., de la Torre, J. C., Portela, A., Ortin, J., Lopez-Galindez, C., Perez-Brena, P., Villanueva, N., Najera, R., and et al. (1985). The quasispecies (extremely heterogeneous) nature of viral RNA genome populations: biological relevance--a review. Gene *40*, 1-8.
Dong, Y., Aguilar, R., Xi, Z., Warr, E., Mongin, E., and Dimopoulos, G. (2006). Anopheles gambiae immune responses to human and rodent Plasmodium parasite species. PLoS Pathog *2*, e52.
Dunn, W. A., Jr. (1990a). Studies on the mechanisms of autophagy: formation of the autophagic vacuole. J Cell Biol *110*, 1923-1933.
Dunn, W. A., Jr. (1990b). Studies on the mechanisms of autophagy: maturation of the autophagic vacuole. J Cell Biol *110*, 1935-1945.
Dzikowski, R., and Deitsch, K. W. (2009). Genetics of antigenic variation in Plasmodium falciparum. Curr Genet *55*, 103-110.
Ebel, G. D., Carricaburu, J., Young, D., Bernard, K. A., and Kramer, L. D. (2004). Genetic and phenotypic variation of West Nile virus in New York, 2000-2003. Am J Trop Med Hyg *71*, 493-500.
Eckels, K. H., Brandt, W. E., Harrison, V. R., McCown, J. M., and Russell, P. K. (1976). Isolation of a temperature-sensitive dengue-2 virus under conditions suitable for vaccine development. Infect Immun *14*, 1221-1227.
Egger, D., Teterina, N., Ehrenfeld, E., and Bienz, K. (2000). Formation of the poliovirus replication complex requires coupled viral translation, vesicle production, and viral RNA synthesis. J Virol *74*, 6570-6580.

Egger, D., Wolk, B., Gosert, R., Bianchi, L., Blum, H. E., Moradpour, D., and Bienz, K. (2002). Expression of hepatitis C virus proteins induces distinct membrane alterations including a candidate viral replication complex. J Virol *76*, 5974-5984.
Egloff, M. P., Decroly, E., Malet, H., Selisko, B., Benarroch, D., Ferron, F., and Canard, B. (2007). Structural and functional analysis of methylation and 5'-RNA sequence requirements of short capped RNAs by the methyltransferase domain of dengue virus NS5. J Mol Biol *372*, 723-736.
Elbashir, S. M., Lendeckel, W., and Tuschl, T. (2001). RNA interference is mediated by 21- and 22-nucleotide RNAs. Genes Dev *15*, 188-200.
Erb, S. (2010). Serial passage of dengue virus 2 16681 in Aedes aegypti, p. communication, ed.
Falgout, B., Pethel, M., Zhang, Y. M., and Lai, C. J. (1991). Both nonstructural proteins NS2B and NS3 are required for the proteolytic processing of dengue virus nonstructural proteins. J Virol *65*, 2467-2475.
Federovitch, C. M., Ron, D., and Hampton, R. Y. (2005). The dynamic ER: experimental approaches and current questions. Curr Opin Cell Biol *17*, 409-414.
Fire, A., Albertson, D., Harrison, S. W., and Moerman, D. G. (1991). Production of antisense RNA leads to effective and specific inhibition of gene expression in C. elegans muscle. Development *113*, 503-514.
Fire, A., Xu, S., Montgomery, M. K., Kostas, S. A., Driver, S. E., and Mello, C. C. (1998). Potent and specific genetic interference by double-stranded RNA in Caenorhabditis elegans. Nature *391*, 806-811.
Franz, A. (2008). personal communication, B. Poole-Smith, ed.
Franz, A. W., Sanchez-Vargas, I., Adelman, Z. N., Blair, C. D., Beaty, B. J., James, A. A., and Olson, K. E. (2006). Engineering RNA interference-based resistance to dengue virus type 2 in genetically modified Aedes aegypti. Proc Natl Acad Sci U S A *103*, 4198-4203.
Franz, A. W., Sanchez-Vargas, I., Piper, J., Smith, M. R., Khoo, C. C., James, A. A., and Olson, K. E. (2009). Stability and loss of a virus resistance phenotype over time in transgenic mosquitoes harbouring an antiviral effector gene. Insect Mol Biol *18*, 661-672.
Frohlich, V. C. (2008). Phase contrast and Differential interference contrast (DIC) microscopy. Journal of Visual Experiments *6*, 844.
Gaines, P. J., Olson, K. E., Higgs, S., Powers, A. M., Beaty, B. J., and Blair, C. D. (1996). Pathogen-derived resistance to dengue type 2 virus in mosquito cells by expression of the premembrane coding region of the viral genome. J Virol *70*, 2132-2137.
Galiana-Arnoux, D., Dostert, C., Schneemann, A., Hoffmann, J. A., and Imler, J. L. (2006). Essential function in vivo for Dicer-2 in host defense against RNA viruses in drosophila. Nat Immunol *7*, 590-597.
Garcia, S., Billecocq, A., Crance, J. M., Prins, M., Garin, D., and Bouloy, M. (2006). Viral suppressors of RNA interference impair RNA silencing induced by a Semliki Forest virus replicon in tick cells. J Gen Virol *87*, 1985-1989.
Garcia, S. B., A Crance, JM Munderloh, U Garin, D Bouloy, M (2005). Nairovirus RNA sequences expressed by a Semliki Forest virus replicon induce RNA interference in tick cells. Journal of Virology *79*, 8942-8947.
Geiss, B. J., Shimonkevitz, L. H., Sackal, C. I., and Olson, K. E. (2007). Recombination-ready Sindbis replicon expression vectors for transgene expression. Virol J *4*, 112.

Getis, A., Morrison, A. C., Gray, K., and Scott, T. W. (2003). Characteristics of the spatial pattern of the dengue vector, Aedes aegypti, in Iquitos, Peru. Am J Trop Med Hyg *69*, 494-505.
Ghosh, A. K., Ribolla, P. E., and Jacobs-Lorena, M. (2001). Targeting Plasmodium ligands on mosquito salivary glands and midgut with a phage display peptide library. Proc Natl Acad Sci U S A *98*, 13278-13281.
Giepmans, B. N. (2008). Bridging fluorescence microscopy and electron microscopy. Histochem Cell Biol *130*, 211-217.
Girard, Y. A., Klingler, K. A., and Higgs, S. (2004). West Nile virus dissemination and tissue tropisms in orally infected Culex pipiens quinquefasciatus. Vector Borne Zoonotic Dis *4*, 109-122.
Girard, Y. A., Popov, V., Wen, J., Han, V., and Higgs, S. (2005). Ultrastructural study of West Nile virus pathogenesis in Culex pipiens quinquefasciatus (Diptera: Culicidae). J Med Entomol *42*, 429-444.
Girard, Y. A., Schneider, B. S., McGee, C. E., Wen, J., Han, V. C., Popov, V., Mason, P. W., and Higgs, S. (2007). Salivary gland morphology and virus transmission during long-term cytopathologic West Nile virus infection in Culex mosquitoes. Am J Trop Med Hyg *76*, 118-128.
Gitlin, L., Stone, J. K., and Andino, R. (2005). Poliovirus escape from RNA interference: short interfering RNA-target recognition and implications for therapeutic approaches. J Virol *79*, 1027-1035.
Gliedman, J. B., Smith, J. F., and Brown, D. T. (1975). Morphogenesis of Sindbis virus in cultured Aedes albopictus cells. J Virol *16*, 913-926.
Gonzalez, M. C., L (2003). Viroporins. FEBS Letters *552*, 28.
Gosert, R., Egger, D., Lohmann, V., Bartenschlager, R., Blum, H. E., Bienz, K., and Moradpour, D. (2003). Identification of the hepatitis C virus RNA replication complex in Huh-7 cells harboring subgenomic replicons. J Virol *77*, 5487-5492.
Gouttenoire, J., Castet, V., Montserret, R., Arora, N., Raussens, V., Ruysschaert, J. M., Diesis, E., Blum, H. E., Penin, F., and Moradpour, D. (2009). Identification of a novel determinant for membrane association in hepatitis C virus nonstructural protein 4B. J Virol *83*, 6257-6268.
Green, T. J., Zhang, X., Wertz, G. W., and Luo, M. (2006). Structure of the vesicular stomatitis virus nucleoprotein-RNA complex. Science *313*, 357-360.
Grief, C., Galler, R., Cortes, L. M., and Barth, O. M. (1997). Intracellular localisation of dengue-2 RNA in mosquito cell culture using electron microscopic in situ hybridisation. Arch Virol *142*, 2347-2357.
Griffin, S. D., Beales, L. P., Clarke, D. S., Worsfold, O., Evans, S. D., Jaeger, J., Harris, M. P., and Rowlands, D. J. (2003). The p7 protein of hepatitis C virus forms an ion channel that is blocked by the antiviral drug, Amantadine. FEBS Lett *535*, 34-38.
Grimstad, P. R., Ross, Q. E., and Craig, G. B., Jr. (1980). Aedes triseriatus (Diptera: Culicidae) and La Crosse virus. II. Modification of mosquito feeding behavior by virus infection. J Med Entomol *17*, 1-7.
Gubler, D. (1989). *Aedes aegypti* and *Aedes aegypti*-borne Disease Control in the 1990s: Top Down or Bottom Up. American Journal of Tropical Medicine and Hygiene *40*, 571-578.

Gubler, D. (2005). The emergence of epidemic dengue fever and dengue hemorrhagic fever in the Americas: a case of failed public health policy. Pan American Journal of Public Health *17*, 221-224.
Gubler, D. J. (1998). Dengue and dengue hemorrhagic fever. Clin Microbiol Rev *11*, 480-496.
Hahn, C. S., Hahn, Y. S., Braciale, T. J., and Rice, C. M. (1992). Infectious Sindbis virus transient expression vectors for studying antigen processing and presentation. Proc Natl Acad Sci U S A *89*, 2679-2683.
Hall, R. A., Scherret, J. H., and Mackenzie, J. S. (2001). Kunjin virus: an Australian variant of West Nile? Ann N Y Acad Sci *951*, 153-160.
Halstead, S. B. (1979). In vivo enhancement of dengue virus infection in rhesus monkeys by passively transferred antibody. J Infect Dis *140*, 527-533.
Halstead, S. B. (2008). Dengue virus-mosquito interactions. Annu Rev Entomol *53*, 273-291.
Halstead, S. N., S Cohen, SN (1970). Observations Related to Pathogenesis of Dengue Hemorrhagic Fever. IV. Relation of Disease Severity to Antibody Response and Virus Recovered. Yale Journal of Biology and Medicine *42*, 311-328.
Hanley, K. A., Manlucu, L. R., Gilmore, L. E., Blaney, J. E., Jr., Hanson, C. T., Murphy, B. R., and Whitehead, S. S. (2003). A trade-off in replication in mosquito versus mammalian systems conferred by a point mutation in the NS4B protein of dengue virus type 4. Virology *312*, 222-232.
Hanley, K. A., Nelson, J. T., Schirtzinger, E. E., Whitehead, S. S., and Hanson, C. T. (2008). Superior infectivity for mosquito vectors contributes to competitive displacement among strains of dengue virus. BMC Ecol *8*, 1.
Harding, H. P., Zhang, Y., and Ron, D. (1999). Protein translation and folding are coupled by an endoplasmic-reticulum-resident kinase. Nature *397*, 271-274.
Harrington, L. C., Edman, J. D., and Scott, T. W. (2001). Why do female Aedes aegypti (Diptera: Culicidae) feed preferentially and frequently on human blood? J Med Entomol *38*, 411-422.
Harris, R., ed. (1999). Negative Staining of Thinly Spread Biological Particulates (Totowa, NI, Humana Press).
Hase, T., Summers, P. L., Eckels, K. H., and Baze, W. B. (1987). An electron and immunoelectron microscopic study of dengue-2 virus infection of cultured mosquito cells: maturation events. Arch Virol *92*, 273-291.
Ho, B. C., Yap, E. H., and Singh, M. (1982). Melanization and encapsulation in Aedes aegypti and Aedes togoi in response to parasitization by a filarioid nematode (Breinlia booliati). Parasitology *85 (Pt 3)*, 567-575.
Holland, J., Spindler, K., Horodyski, F., Grabau, E., Nichol, S., and VandePol, S. (1982). Rapid evolution of RNA genomes. Science *215*, 1577-1585.
Holmes, E. C. (2003). Patterns of intra- and interhost nonsynonymous variation reveal strong purifying selection in dengue virus. J Virol *77*, 11296-11298.
Houseley, J., and Tollervey, D. (2009). The many pathways of RNA degradation. Cell *136*, 763-776.
Huisman, W., Martina, B. E., Rimmelzwaan, G. F., Gruters, R. A., and Osterhaus, A. D. (2009). Vaccine-induced enhancement of viral infections. Vaccine *27*, 505-512.

Huynh, C. Q., and Zieler, H. (1999). Construction of modular and versatile plasmid vectors for the high-level expression of single or multiple genes in insects and insect cell lines. J Mol Biol *288*, 13-20.
Igarashi, A. (1978). Isolation of a Singh's Aedes albopictus cell clone sensitive to Dengue and Chikungunya viruses. J Gen Virol *40*, 531-544.
Irvin, N., Hoddle, M. S., O'Brochta, D. A., Carey, B., and Atkinson, P. W. (2004). Assessing fitness costs for transgenic Aedes aegypti expressing the GFP marker and transposase genes. Proc Natl Acad Sci U S A *101*, 891-896.
Ito, J., Ghosh, A., Moreira, L. A., Wimmer, E. A., and Jacobs-Lorena, M. (2002). Transgenic anopheline mosquitoes impaired in transmission of a malaria parasite. Nature *417*, 452-455.
Jackson, W. T., Giddings, T. H., Jr., Taylor, M. P., Mulinyawe, S., Rabinovitch, M., Kopito, R. R., and Kirkegaard, K. (2005). Subversion of cellular autophagosomal machinery by RNA viruses. PLoS Biol *3*, e156.
Jacobson, K., and Dietrich, C. (1999). Looking at lipid rafts? Trends Cell Biol *9*, 87-91.
Jasinskiene, N., Coates, C. J., Benedict, M. Q., Cornel, A. J., Rafferty, C. S., James, A. A., and Collins, F. H. (1998). Stable transformation of the yellow fever mosquito, Aedes aegypti, with the Hermes element from the housefly. Proc Natl Acad Sci U S A *95*, 3743-3747.
Jenkins, G. M., Rambaut, A., Pybus, O. G., and Holmes, E. C. (2002). Rates of molecular evolution in RNA viruses: a quantitative phylogenetic analysis. J Mol Evol *54*, 156-165.
Kabeya, Y., Mizushima, N., Ueno, T., Yamamoto, A., Kirisako, T., Noda, T., Kominami, E., Ohsumi, Y., and Yoshimori, T. (2000). LC3, a mammalian homologue of yeast Apg8p, is localized in autophagosome membranes after processing. EMBO J *19*, 5720-5728.
Kapoor, M., Zhang, L., Ramachandra, M., Kusukawa, J., Ebner, K. E., and Padmanabhan, R. (1995). Association between NS3 and NS5 proteins of dengue virus type 2 in the putative RNA replicase is linked to differential phosphorylation of NS5. J Biol Chem *270*, 19100-19106.
Keene, K. M., Foy, B. D., Sanchez-Vargas, I., Beaty, B. J., Blair, C. D., and Olson, K. E. (2004). RNA interference acts as a natural antiviral response to O'nyong-nyong virus (Alphavirus; Togaviridae) infection of Anopheles gambiae. Proc Natl Acad Sci U S A *101*, 17240-17245.
Khakpoor, A., Panyasrivanit, M., Wikan, N., and Smith, D. R. (2009). A role for autophagolysosomes in dengue virus 3 production in HepG2 cells. J Gen Virol *90*, 1093-1103.
Khan, S. U., and Schroder, M. (2008). Engineering of chaperone systems and of the unfolded protein response. Cytotechnology *57*, 207-231.
Khatoon, L., Baliraine, F. N., Bonizzoni, M., Malik, S. A., and Yan, G. (2009). Prevalence of antimalarial drug resistance mutations in Plasmodium vivax and P. falciparum from a malaria-endemic area of Pakistan. Am J Trop Med Hyg *81*, 525-528.
Khromykh, A. A., Varnavski, A. N., Sedlak, P. L., and Westaway, E. G. (2001). Coupling between replication and packaging of flavivirus RNA: evidence derived from the use of DNA-based full-length cDNA clones of Kunjin virus. J Virol *75*, 4633-4640.
Kim, M., Mackenzie, J. M., and Westaway, E. G. (2004). Comparisons of physical separation methods of Kunjin virus-induced membranes. J Virol Methods *120*, 179-187.

Kitchener, S., Leggat, P., Brennan, L., and McCall, B. (2002). Importation of dengue by soldiers returning from East Timor to north Queensland, Australia. Journal of Travel Medicine *9*, 180-183.
Klimstra, W. B., Ryman, K. D., and Johnston, R. E. (1998). Adaptation of Sindbis virus to BHK cells selects for use of heparan sulfate as an attachment receptor. J Virol *72*, 7357-7366.
Klionsky, D. J., and Emr, S. D. (2000). Autophagy as a regulated pathway of cellular degradation. Science *290*, 1717-1721.
Knipe, D. H., P, ed. (2005). Fields Virology, 5th edn (Lippincott Williams & Wilkins).
Knoops, K., Kikkert, M., Worm, S. H., Zevenhoven-Dobbe, J. C., van der Meer, Y., Koster, A. J., Mommaas, A. M., and Snijder, E. J. (2008). SARS-coronavirus replication is supported by a reticulovesicular network of modified endoplasmic reticulum. PLoS Biol *6*, e226.
Kokoza, V., Ahmed, A., Cho, W. L., Jasinskiene, N., James, A. A., and Raikhel, A. (2000). Engineering blood meal-activated systemic immunity in the yellow fever mosquito, Aedes aegypti. Proc Natl Acad Sci U S A *97*, 9144-9149.
Konishi, M., Wu, C. H., Kaito, M., Hayashi, K., Watanabe, S., Adachi, Y., and Wu, G. Y. (2006). siRNA-resistance in treated HCV replicon cells is correlated with the development of specific HCV mutations. J Viral Hepat *13*, 756-761.
Kopek, B. G., Perkins, G., Miller, D. J., Ellisman, M. H., and Ahlquist, P. (2007). Three-dimensional analysis of a viral RNA replication complex reveals a virus-induced mini-organelle. PLoS Biol *5*, e220.
Koukiekolo, R., Sagan, S. M., and Pezacki, J. P. (2007). Effects of pH and salt concentration on the siRNA binding activity of the RNA silencing suppressor protein p19. FEBS Lett *581*, 3051-3056.
Kuhn, R. J., Zhang, W., Rossmann, M. G., Pletnev, S. V., Corver, J., Lenches, E., Jones, C. T., Mukhopadhyay, S., Chipman, P. R., Strauss, E. G., *et al.* (2002). Structure of dengue virus: implications for flavivirus organization, maturation, and fusion. Cell *108*, 717-725.
Kujala, P., Ikaheimonen, A., Ehsani, N., Vihinen, H., Auvinen, P., and Kaariainen, L. (2001). Biogenesis of the Semliki Forest virus RNA replication complex. J Virol *75*, 3873-3884.
Kumar, M., and Carmichael, G. G. (1998). Antisense RNA: function and fate of duplex RNA in cells of higher eukaryotes. Microbiol Mol Biol Rev *62*, 1415-1434.
Kuno, G. (2007). Research on dengue and dengue-like illness in East Asia and the Western Pacific during the First Half of the 20th century. Rev Med Virol *17*, 327-341.
Kuno, G. (2009). Emergence of the severe syndrome and mortality associated with dengue and dengue-like illness: historical records (1890 to 1950) and their compatibility with current hypotheses on the shift of disease manifestation. Clin Microbiol Rev *22*, 186-201, Table of Contents.
Kurtz, J. (2004). Memory in the innate and adaptive immune systems. Microbes Infect *6*, 1410-1417.
Kusov, Y. Y., Probst, C., Jecht, M., Jost, P. D., and Gauss-Muller, V. (1998). Membrane association and RNA binding of recombinant hepatitis A virus protein 2C. Arch Virol *143*, 931-944.

Kyle, J. L., and Harris, E. (2008). Global spread and persistence of dengue. Annu Rev Microbiol *62*, 71-92.
Lama, J., and Carrasco, L. (1992). Expression of poliovirus nonstructural proteins in Escherichia coli cells. Modification of membrane permeability induced by 2B and 3A. J Biol Chem *267*, 15932-15937.
Lambrechts, L., Koella, J. C., and Boete, C. (2008). Can transgenic mosquitoes afford the fitness cost? Trends Parasitol *24*, 4-7.
Lee, C. J., Lin, H. R., Liao, C. L., and Lin, Y. L. (2008a). Cholesterol effectively blocks entry of flavivirus. J Virol *82*, 6470-6480.
Lee, E., Weir, R. C., and Dalgarno, L. (1997). Changes in the dengue virus major envelope protein on passaging and their localization on the three-dimensional structure of the protein. Virology *232*, 281-290.
Lee, H. K., and Iwasaki, A. (2008). Autophagy and antiviral immunity. Curr Opin Immunol *20*, 23-29.
Lee, H. K., Lund, J. M., Ramanathan, B., Mizushima, N., and Iwasaki, A. (2007). Autophagy-dependent viral recognition by plasmacytoid dendritic cells. Science *315*, 1398-1401.
Lee, Y. R., Lei, H. Y., Liu, M. T., Wang, J. R., Chen, S. H., Jiang-Shieh, Y. F., Lin, Y. S., Yeh, T. M., Liu, C. C., and Liu, H. S. (2008b). Autophagic machinery activated by dengue virus enhances virus replication. Virology *374*, 240-248.
Lee, Y. S., Nakahara, K., Pham, J. W., Kim, K., He, Z., Sontheimer, E. J., and Carthew, R. W. (2004). Distinct roles for Drosophila Dicer-1 and Dicer-2 in the siRNA/miRNA silencing pathways. Cell *117*, 69-81.
Leung, J. Y., Pijlman, G. P., Kondratieva, N., Hyde, J., Mackenzie, J. M., and Khromykh, A. A. (2008). Role of nonstructural protein NS2A in flavivirus assembly. J Virol *82*, 4731-4741.
Levashina, E. A. (2004). Immune responses in Anopheles gambiae. Insect Biochem Mol Biol *34*, 673-678.
Levashina, E. A., Moita, L. F., Blandin, S., Vriend, G., Lagueux, M., and Kafatos, F. C. (2001). Conserved role of a complement-like protein in phagocytosis revealed by dsRNA knockout in cultured cells of the mosquito, Anopheles gambiae. Cell *104*, 709-718.
Li, C., Marrelli, M. T., Yan, G., and Jacobs-Lorena, M. (2008a). Fitness of transgenic Anopheles stephensi mosquitoes expressing the SM1 peptide under the control of a vitellogenin promoter. J Hered *99*, 275-282.
Li, F., and Ding, S. W. (2006). Virus counterdefense: diverse strategies for evading the RNA-silencing immunity. Annu Rev Microbiol *60*, 503-531.
Li, L., Lok, S. M., Yu, I. M., Zhang, Y., Kuhn, R. J., Chen, J., and Rossmann, M. G. (2008b). The flavivirus precursor membrane-envelope protein complex: structure and maturation. Science *319*, 1830-1834.
Li, S., Ye, L., Yu, X., Xu, B., Li, K., Zhu, X., Liu, H., Wu, X., and Kong, L. (2009). Hepatitis C virus NS4B induces unfolded protein response and endoplasmic reticulum overload response-dependent NF-kappaB activation. Virology *391*, 257-264.
Li, W. X., Li, H., Lu, R., Li, F., Dus, M., Atkinson, P., Brydon, E. W., Johnson, K. L., Garcia-Sastre, A., Ball, L. A., *et al.* (2004). Interferon antagonist proteins of influenza and vaccinia viruses are suppressors of RNA silencing. Proc Natl Acad Sci U S A *101*, 1350-1355.

Liang, X. H., Kleeman, L. K., Jiang, H. H., Gordon, G., Goldman, J. E., Berry, G., Herman, B., and Levine, B. (1998). Protection against fatal Sindbis virus encephalitis by beclin, a novel Bcl-2-interacting protein. J Virol *72*, 8586-8596.
Lichner, Z., Silhavy, D., and Burgyan, J. (2003). Double-stranded RNA-binding proteins could suppress RNA interference-mediated antiviral defences. J Gen Virol *84*, 975-980.
Lindenbach, B. D., and Rice, C. M. (1999). Genetic interaction of flavivirus nonstructural proteins NS1 and NS4A as a determinant of replicase function. J Virol *73*, 4611-4621.
Lingel, A., Simon, B., Izaurralde, E., and Sattler, M. (2005). The structure of the flock house virus B2 protein, a viral suppressor of RNA interference, shows a novel mode of double-stranded RNA recognition. EMBO Rep *6*, 1149-1155.
Liu, Q., Rand, T. A., Kalidas, S., Du, F., Kim, H. E., Smith, D. P., and Wang, X. (2003). R2D2, a bridge between the initiation and effector steps of the Drosophila RNAi pathway. Science *301*, 1921-1925.
Lowenberger, C. (2001). Innate immune response of Aedes aegypti. Insect Biochem Mol Biol *31*, 219-229.
Lu, Y. E., and Kielian, M. (2000). Semliki forest virus budding: assay, mechanisms, and cholesterol requirement. J Virol *74*, 7708-7719.
Lustig, S., Jackson, A. C., Hahn, C. S., Griffin, D. E., Strauss, E. G., and Strauss, J. H. (1988). Molecular basis of Sindbis virus neurovirulence in mice. J Virol *62*, 2329-2336.
Lyle, J. M., Bullitt, E., Bienz, K., and Kirkegaard, K. (2002). Visualization and functional analysis of RNA-dependent RNA polymerase lattices. Science *296*, 2218-2222.
Ma, L., Jones, C. T., Groesch, T. D., Kuhn, R. J., and Post, C. B. (2004). Solution structure of dengue virus capsid protein reveals another fold. Proc Natl Acad Sci U S A *101*, 3414-3419.
Mackenzie, J. M., Jones, M. K., and Westaway, E. G. (1999). Markers for trans-Golgi membranes and the intermediate compartment localize to induced membranes with distinct replication functions in flavivirus-infected cells. J Virol *73*, 9555-9567.
Mackenzie, J. M., Jones, M. K., and Young, P. R. (1996). Immunolocalization of the dengue virus nonstructural glycoprotein NS1 suggests a role in viral RNA replication. Virology *220*, 232-240.
Mackenzie, J. M., Kenney, M. T., and Westaway, E. G. (2007). West Nile virus strain Kunjin NS5 polymerase is a phosphoprotein localized at the cytoplasmic site of viral RNA synthesis. J Gen Virol *88*, 1163-1168.
Mackenzie, J. M., Khromykh, A. A., Jones, M. K., and Westaway, E. G. (1998). Subcellular localization and some biochemical properties of the flavivirus Kunjin nonstructural proteins NS2A and NS4A. Virology *245*, 203-215.
Mackenzie, J. M., and Westaway, E. G. (2001). Assembly and maturation of the flavivirus Kunjin virus appear to occur in the rough endoplasmic reticulum and along the secretory pathway, respectively. J Virol *75*, 10787-10799.
MacRae, I. J., Zhou, K., Li, F., Repic, A., Brooks, A. N., Cande, W. Z., Adams, P. D., and Doudna, J. A. (2006). Structural basis for double-stranded RNA processing by Dicer. Science *311*, 195-198.
Malhotra, J. D., and Kaufman, R. J. (2007). The endoplasmic reticulum and the unfolded protein response. Semin Cell Dev Biol *18*, 716-731.

Maori, E., Tanne, E., and Sela, I. (2007). Reciprocal sequence exchange between non-retro viruses and hosts leading to the appearance of new host phenotypes. Virology *362*, 342-349.
Marie, M., Dale, H. A., Sannerud, R., and Saraste, J. (2009). The function of the intermediate compartment in pre-Golgi trafficking involves its stable connection with the centrosome. Mol Biol Cell *20*, 4458-4470.
Marrelli, M. T., Li, C., Rasgon, J. L., and Jacobs-Lorena, M. (2007). Transgenic malaria-resistant mosquitoes have a fitness advantage when feeding on Plasmodium-infected blood. Proc Natl Acad Sci U S A *104*, 5580-5583.
Marrelli, M. T., Moreira, C. K., Kelly, D., Alphey, L., and Jacobs-Lorena, M. (2006). Mosquito transgenesis: what is the fitness cost? Trends Parasitol *22*, 197-202.
McBride, W. J., and Bielefeldt-Ohmann, H. (2000). Dengue viral infections; pathogenesis and epidemiology. Microbes Infect *2*, 1041-1050.
McElroy, K. L., Girard, Y. A., McGee, C. E., Tsetsarkin, K. A., Vanlandingham, D. L., and Higgs, S. (2008). Characterization of the antigen distribution and tissue tropisms of three phenotypically distinct yellow fever virus variants in orally infected Aedes aegypti mosquitoes. Vector Borne Zoonotic Dis *8*, 675-687.
McIntosh, R., Nicastro, D., and Mastronarde, D. (2005). New views of cells in 3D: an introduction to electron tomography. Trends Cell Biol *15*, 43-51.
McKnight, K. L., Simpson, D. A., Lin, S. C., Knott, T. A., Polo, J. M., Pence, D. F., Johannsen, D. B., Heidner, H. W., Davis, N. L., and Johnston, R. E. (1996). Deduced consensus sequence of Sindbis virus strain AR339: mutations contained in laboratory strains which affect cell culture and in vivo phenotypes. J Virol *70*, 1981-1989.
Medigeshi, G. R., Lancaster, A. M., Hirsch, A. J., Briese, T., Lipkin, W. I., Defilippis, V., Fruh, K., Mason, P. W., Nikolich-Zugich, J., and Nelson, J. A. (2007). West Nile virus infection activates the unfolded protein response, leading to CHOP induction and apoptosis. J Virol *81*, 10849-10860.
Meister, G., and Tuschl, T. (2004). Mechanisms of gene silencing by double-stranded RNA. Nature *431*, 343-349.
Messer, W. B., Gubler, D. J., Harris, E., Sivananthan, K., and de Silva, A. M. (2003). Emergence and global spread of a dengue serotype 3, subtype III virus. Emerg Infect Dis *9*, 800-809.
Miller, S., Kastner, S., Krijnse-Locker, J., Buhler, S., and Bartenschlager, R. (2007). The non-structural protein 4A of dengue virus is an integral membrane protein inducing membrane alterations in a 2K-regulated manner. J Biol Chem *282*, 8873-8882.
Miller, S., and Krijnse-Locker, J. (2008). Modification of intracellular membrane structures for virus replication. Nat Rev Microbiol *6*, 363-374.
Miller, S., Sparacio, S., and Bartenschlager, R. (2006). Subcellular localization and membrane topology of the Dengue virus type 2 Non-structural protein 4B. J Biol Chem *281*, 8854-8863.
Modis, Y., Ogata, S., Clements, D., and Harrison, S. C. (2004). Structure of the dengue virus envelope protein after membrane fusion. Nature *427*, 313-319.
Molinari, M., Galli, C., Piccaluga, V., Pieren, M., and Paganetti, P. (2002). Sequential assistance of molecular chaperones and transient formation of covalent complexes during protein degradation from the ER. J Cell Biol *158*, 247-257.

Molnar, A., Csorba, T., Lakatos, L., Varallyay, E., Lacomme, C., and Burgyan, J. (2005). Plant virus-derived small interfering RNAs originate predominantly from highly structured single-stranded viral RNAs. J Virol *79*, 7812-7818.
Mongkolsapaya, J., Dejnirattisai, W., Xu, X. N., Vasanawathana, S., Tangthawornchaikul, N., Chairunsri, A., Sawasdivorn, S., Duangchinda, T., Dong, T., Rowland-Jones, S., *et al.* (2003). Original antigenic sin and apoptosis in the pathogenesis of dengue hemorrhagic fever. Nat Med *9*, 921-927.
Moore, C. G., Francy, D. B., Eliason, D. A., and Monath, T. P. (1988). Aedes albopictus in the United States: rapid spread of a potential disease vector. J Am Mosq Control Assoc *4*, 356-361.
Munoz-Jordan, J. L., Sanchez-Burgos, G. G., Laurent-Rolle, M., and Garcia-Sastre, A. (2003). Inhibition of interferon signaling by dengue virus. Proc Natl Acad Sci U S A *100*, 14333-14338.
Myles, K. M., Pierro, D. J., and Olson, K. E. (2004). Comparison of the transmission potential of two genetically distinct Sindbis viruses after oral infection of Aedes aegypti (Diptera: Culicidae). J Med Entomol *41*, 95-106.
Myles, K. M., Wiley, M. R., Morazzani, E. M., and Adelman, Z. N. (2008). Alphavirus-derived small RNAs modulate pathogenesis in disease vector mosquitoes. Proc Natl Acad Sci U S A *105*, 19938-19943.
Napoli, C., Lemieux, C., and Jorgensen, R. (1990). Introduction of a Chimeric Chalcone Synthase Gene into Petunia Results in Reversible Co-Suppression of Homologous Genes in trans. Plant Cell *2*, 279-289.
Nayak, V., Dessau, M., Kucera, K., Anthony, K., Ledizet, M., and Modis, Y. (2009). Crystal structure of dengue virus type 1 envelope protein in the postfusion conformation and its implications for membrane fusion. J Virol *83*, 4338-4344.
Ng, C. G., Coppens, I., Govindarajan, D., Pisciotta, J., Shulaev, V., and Griffin, D. E. (2008). Effect of host cell lipid metabolism on alphavirus replication, virion morphogenesis, and infectivity. Proc Natl Acad Sci U S A *105*, 16326-16331.
Ng, M. L. (1987). Ultrastructural studies of Kunjin virus-infected Aedes albopictus cells. J Gen Virol *68 (Pt 2)*, 577-582.
NIAID (2008). NIAID Experts See Dengue as Potential Threat to U.S. Public Health. In NIH News.
Nimmo, D. D., Alphey, L., Meredith, J. M., and Eggleston, P. (2006). High efficiency site-specific genetic engineering of the mosquito genome. Insect Mol Biol *15*, 129-136.
Niwa, M. (2006). Chaperones. In The unfolded protein response unfolds. http://www.springerlink.com/content/7765081066201361.
Noisakran, S., Dechtawewat, T., Avirutnan, P., Kinoshita, T., Siripanyaphinyo, U., Puttikhunt, C., Kasinrerk, W., Malasit, P., and Sittisombut, N. (2008). Association of dengue virus NS1 protein with lipid rafts. J Gen Virol *89*, 2492-2500.
Nykanen, A., Haley, B., and Zamore, P. D. (2001). ATP requirements and small interfering RNA structure in the RNA interference pathway. Cell *107*, 309-321.
O'Brochta, D. A., Sethuraman, N., Wilson, R., Hice, R. H., Pinkerton, A. C., Levesque, C. S., Bideshi, D. K., Jasinskiene, N., Coates, C. J., James, A. A., *et al.* (2003). Gene vector and transposable element behavior in mosquitoes. J Exp Biol *206*, 3823-3834.

Olson, K. E., Adelman, Z. N., Travanty, E. A., Sanchez-Vargas, I., Beaty, B. J., and Blair, C. D. (2002). Developing arbovirus resistance in mosquitoes. Insect Biochem Mol Biol *32*, 1333-1343.
Orvedahl, A., and Levine, B. (2008). Viral evasion of autophagy. Autophagy *4*, 280-285.
Panyasrivanit, M., Khakpoor, A., Wikan, N., and Smith, D. R. (2009). Co-localization of constituents of the dengue virus translation and replication machinery with amphisomes. J Gen Virol *90*, 448-456.
Paschen, W. (2003). Shutdown of translation: lethal or protective? Unfolded protein response versus apoptosis. J Cereb Blood Flow Metab *23*, 773-779.
Paskewitz, S. M., Brown, M. R., Lea, A. O., and Collins, F. H. (1988). Ultrastructure of the encapsulation of Plasmodium cynomolgi (B strain) on the midgut of a refractory strain of Anopheles gambiae. J Parasitol *74*, 432-439.
Paulson, S. L., and Hawley, W. A. (1991). Effect of body size on the vector competence of field and laboratory populations of Aedes triseriatus for La Crosse virus. J Am Mosq Control Assoc *7*, 170-175.
Pedersen, K. W., van der Meer, Y., Roos, N., and Snijder, E. J. (1999). Open reading frame 1a-encoded subunits of the arterivirus replicase induce endoplasmic reticulum-derived double-membrane vesicles which carry the viral replication complex. J Virol *73*, 2016-2026.
Peyrefitte, C. N., Pastorino, B., Bessaud, M., Tolou, H. J., and Couissinier-Paris, P. (2003). Evidence for in vitro falsely-primed cDNAs that prevent specific detection of virus negative strand RNAs in dengue-infected cells: improvement by tagged RT-PCR. J Virol Methods *113*, 19-28.
Pietiainen, V. M., Marjomaki, V., Heino, J., and Hyypia, T. (2005). Viral entry, lipid rafts and caveosomes. Ann Med *37*, 394-403.
Plaskon, N. E., Adelman, Z. N., and Myles, K. M. (2009). Accurate strand-specific quantification of viral RNA. PLoS One *4*, e7468.
Plongthongkum, N., Kullawong, N., Panyim, S., and Tirasophon, W. (2007). Ire1 regulated XBP1 mRNA splicing is essential for the unfolded protein response (UPR) in Drosophila melanogaster. Biochem Biophys Res Commun *354*, 789-794.
Prentice, E., Jerome, W. G., Yoshimori, T., Mizushima, N., and Denison, M. R. (2004). Coronavirus replication complex formation utilizes components of cellular autophagy. J Biol Chem *279*, 10136-10141.
Puig-Basagoiti, F., Tilgner, M., Bennett, C. J., Zhou, Y., Munoz-Jordan, J. L., Garcia-Sastre, A., Bernard, K. A., and Shi, P. Y. (2007). A mouse cell-adapted NS4B mutation attenuates West Nile virus RNA synthesis. Virology *361*, 229-241.
Pusch, O., Boden, D., Silbermann, R., Lee, F., Tucker, L., and Ramratnam, B. (2003). Nucleotide sequence homology requirements of HIV-1-specific short hairpin RNA. Nucleic Acids Res *31*, 6444-6449.
Qu, F., and Morris, T. J. (2005). Suppressors of RNA silencing encoded by plant viruses and their role in viral infections. FEBS Lett *579*, 5958-5964.
Qu, L., McMullan, L. K., and Rice, C. M. (2001). Isolation and characterization of noncytopathic pestivirus mutants reveals a role for nonstructural protein NS4B in viral cytopathogenicity. J Virol *75*, 10651-10662.
Quinkert, D., Bartenschlager, R., and Lohmann, V. (2005). Quantitative analysis of the hepatitis C virus replication complex. J Virol *79*, 13594-13605.

Rahman, S., Matsumura, T., Masuda, K., Kanemura, K., and Fukunaga, T. (1998). Maturation site of dengue type 2 virus in cultured mosquito C6/36 cells and Vero cells. Kobe J Med Sci *44*, 65-79.
Rasgon, J. L., and Scott, T. W. (2003). Wolbachia and cytoplasmic incompatibility in the California Culex pipiens mosquito species complex: parameter estimates and infection dynamics in natural populations. Genetics *165*, 2029-2038.
Reggiori, F., and Klionsky, D. J. (2002). Autophagy in the eukaryotic cell. Eukaryot Cell *1*, 11-21.
Richardson, J., Molina-Cruz, A., Salazar, M. I., and Black, W. t. (2006). Quantitative analysis of dengue-2 virus RNA during the extrinsic incubation period in individual Aedes aegypti. Am J Trop Med Hyg *74*, 132-141.
Roehrig, J. T., Bolin, R. A., and Kelly, R. G. (1998). Monoclonal antibody mapping of the envelope glycoprotein of the dengue 2 virus, Jamaica. Virology *246*, 317-328.
Romoser, W. S., Wasieloski, L. P., Jr., Pushko, P., Kondig, J. P., Lerdthusnee, K., Neira, M., and Ludwig, G. V. (2004). Evidence for arbovirus dissemination conduits from the mosquito (Diptera: Culicidae) midgut. J Med Entomol *41*, 467-475.
Roosendaal, J., Westaway, E. G., Khromykh, A., and Mackenzie, J. M. (2006). Regulated cleavages at the West Nile virus NS4A-2K-NS4B junctions play a major role in rearranging cytoplasmic membranes and Golgi trafficking of the NS4A protein. J Virol *80*, 4623-4632.
Rosen, L. (1977). The Emperor's New Clothes revisited, or reflections on the pathogenesis of dengue hemorrhagic fever. Am J Trop Med Hyg *26*, 337-343.
Rothman, A. L. (2004). Dengue: defining protective versus pathologic immunity. J Clin Invest *113*, 946-951.
Rothman, A. L., and Ennis, F. A. (1999). Immunopathogenesis of Dengue hemorrhagic fever. Virology *257*, 1-6.
Rudnick, A., and Chan, Y. C. (1965). Dengue Type 2 Virus in Naturally Infected Aedes albopictus Mosquitoes in Singapore. Science *149*, 638-639.
Rust, R. C., Landmann, L., Gosert, R., Tang, B. L., Hong, W., Hauri, H. P., Egger, D., and Bienz, K. (2001). Cellular COPII proteins are involved in production of the vesicles that form the poliovirus replication complex. J Virol *75*, 9808-9818.
Salazar-Sanchez, M. I. (2006) Determinants of dengue type 2 virus infection in the mosquito *Aedes aegypti* PhD dissertation, dissertation, Colorado State Univeristy, Fort Collins, CO.
Salonen, A., Ahola, T., and Kaariainen, L. (2005). Viral RNA replication in association with cellular membranes. Curr Top Microbiol Immunol *285*, 139-173.
Sanchez-Vargas, I., Scott, J. C., Poole-Smith, B. K., Franz, A. W., Barbosa-Solomieu, V., Wilusz, J., Olson, K. E., and Blair, C. D. (2009). Dengue virus type 2 infections of Aedes aegypti are modulated by the mosquito's RNA interference pathway. PLoS Pathog *5*, e1000299.
Sanchez-Vargas, I., Travanty, E. A., Keene, K. M., Franz, A. W., Beaty, B. J., Blair, C. D., and Olson, K. E. (2004). RNA interference, arthropod-borne viruses, and mosquitoes. Virus Res *102*, 65-74.
Sangiambut, S., Keelapang, P., Aaskov, J., Puttikhunt, C., Kasinrerk, W., Malasit, P., and Sittisombut, N. (2008). Multiple regions in dengue virus capsid protein contribute to nuclear localization during virus infection. J Gen Virol *89*, 1254-1264.

Sanz, M. A., Madan, V., Carrasco, L., and Nieva, J. L. (2003). Interfacial domains in Sindbis virus 6K protein. Detection and functional characterization. J Biol Chem *278*, 2051-2057.
Schlegel, A., Giddings, T. H., Jr., Ladinsky, M. S., and Kirkegaard, K. (1996). Cellular origin and ultrastructure of membranes induced during poliovirus infection. J Virol *70*, 6576-6588.
Schneider, J. R., Mori, A., Romero-Severson, J., Chadee, D. D., and Severson, D. W. (2007). Investigations of dengue-2 susceptibility and body size among Aedes aegypti populations. Med Vet Entomol *21*, 370-376.
Schonborn, J., Oberstrass, J., Breyel, E., Tittgen, J., Schumacher, J., and Lukacs, N. (1991). Monoclonal antibodies to double-stranded RNA as probes of RNA structure in crude nucleic acid extracts. Nucleic Acids Res *19*, 2993-3000.
Schutz, S., and Sarnow, P. (2006). Interaction of viruses with the mammalian RNA interference pathway. Virology *344*, 151-157.
Scott, J. (2009). siRNAs in Mosquito cell culture, p. communication, ed.
Segrest, J. P., Jones, M. K., De Loof, H., Brouillette, C. G., Venkatachalapathi, Y. V., and Anantharamaiah, G. M. (1992). The amphipathic helix in the exchangeable apolipoproteins: a review of secondary structure and function. J Lipid Res *33*, 141-166.
Sessions, O. M., Barrows, N. J., Souza-Neto, J. A., Robinson, T. J., Hershey, C. L., Rodgers, M. A., Ramirez, J. L., Dimopoulos, G., Yang, P. L., Pearson, J. L., and Garcia-Blanco, M. A. (2009). Discovery of insect and human dengue virus host factors. Nature *458*, 1047-1050.
Sethuraman, N., Fraser, M. J., Jr., Eggleston, P., and O'Brochta, D. A. (2007). Post-integration stability of piggyBac in Aedes aegypti. Insect Biochem Mol Biol *37*, 941-951.
Shelly, S., Lukinova, N., Bambina, S., Berman, A., and Cherry, S. (2009). Autophagy is an essential component of Drosophila immunity against vesicular stomatitis virus. Immunity *30*, 588-598.
Shepard, D. S., Suaya, J. A., Halstead, S. B., Nathan, M. B., Gubler, D. J., Mahoney, R. T., Wang, D. N., and Meltzer, M. I. (2004). Cost-effectiveness of a pediatric dengue vaccine. Vaccine *22*, 1275-1280.
Shi, S. T., Lee, K. J., Aizaki, H., Hwang, S. B., and Lai, M. M. (2003). Hepatitis C virus RNA replication occurs on a detergent-resistant membrane that cofractionates with caveolin-2. J Virol *77*, 4160-4168.
Shu, P., Chien, L., Chang, S., Su, C., Kuo, Y., Liao, T., Ho, M., Lin, T., and Huang, J. (2005). Fever screening at airports and imported dengue. Emerging Infectious Diseases *11*, 460-462.
Sidjanski, S., Mathews, G. V., and Vanderberg, J. P. (1997). Electrophoretic separation and identification of phenoloxidases in hemolymph and midgut of adult Anopheles stephensi mosquitoes. J Parasitol *83*, 686-691.
Sijen, T., Fleenor, J., Simmer, F., Thijssen, K. L., Parrish, S., Timmons, L., Plasterk, R. H., and Fire, A. (2001). On the role of RNA amplification in dsRNA-triggered gene silencing. Cell *107*, 465-476.
Sijen, T., and Plasterk, R. H. (2003). Transposon silencing in the Caenorhabditis elegans germ line by natural RNAi. Nature *426*, 310-314.
Silva, J. C., and Kidwell, M. G. (2004). Evolution of P elements in natural populations of Drosophila willistoni and D. sturtevanti. Genetics *168*, 1323-1335.

Smit, J. M., Bittman, R., and Wilschut, J. (1999). Low-pH-dependent fusion of Sindbis virus with receptor-free cholesterol- and sphingolipid-containing liposomes. J Virol *73*, 8476-8484.
Snowden, F. M. (2008). Emerging and reemerging diseases: a historical perspective. Immunol Rev *225*, 9-26.
Soldan, S. S., Plassmeyer, M. L., Matukonis, M. K., and Gonzalez-Scarano, F. (2005). La Crosse virus nonstructural protein NSs counteracts the effects of short interfering RNA. J Virol *79*, 234-244.
Southern, J. A., Young, D. F., Heaney, F., Baumgartner, W. K., and Randall, R. E. (1991). Identification of an epitope on the P and V proteins of simian virus 5 that distinguishes between two isolates with different biological characteristics. J Gen Virol *72 (Pt 7)*, 1551-1557.
Spuul, P., Salonen, A., Merits, A., Jokitalo, E., Kaariainen, L., and Ahola, T. (2007). Role of the amphipathic peptide of Semliki forest virus replicase protein nsP1 in membrane association and virus replication. J Virol *81*, 872-883.
Sriburi, R., Jackowski, S., Mori, K., and Brewer, J. W. (2004). XBP1: a link between the unfolded protein response, lipid biosynthesis, and biogenesis of the endoplasmic reticulum. J Cell Biol *167*, 35-41.
Sriurairatna, S., and Bhamarapravati, N. (1977). Replication of dengue-2 virus in Aedes albopictus mosquitoes. An electron microscopic study. Am J Trop Med Hyg *26*, 1199-1205.
Stevens, T. M., and Schlesinger, R. W. (1965). Studies on the nature of dengue viruses. I. Correlation of particle density, infectivity, and RNA content of type 2 virus. Virology *27*, 103-112.
Stohlman, S. A., Wisseman, C. L., Jr., Eylar, O. R., and Silverman, D. J. (1975). Dengue virus-induced modifications of host cell membranes. J Virol *16*, 1017-1026.
Stollar, B. D., Koo, R., and Stollar, V. (1978). Immunofluorescent detection of nuclear double-stranded RNA in situ in Vero and mosquito cells. Science *200*, 1381-1383.
Stollar, V., Schlesinger, R. W., and Stevens, T. M. (1967). Studies on the nature of dengue viruses. III. RNA synthesis in cells infected with type 2 dengue virus. Virology *33*, 650-658.
Suaya, J. A., Shepard, D. S., Siqueira, J. B., Martelli, C. T., Lum, L. C., Tan, L. H., Kongsin, S., Jiamton, S., Garrido, F., Montoya, R., *et al.* (2009). Cost of dengue cases in eight countries in the Americas and Asia: a prospective study. Am J Trop Med Hyg *80*, 846-855.
Suhy, D. A., Giddings, T. H., Jr., and Kirkegaard, K. (2000). Remodeling the endoplasmic reticulum by poliovirus infection and by individual viral proteins: an autophagy-like origin for virus-induced vesicles. J Virol *74*, 8953-8965.
Sumanochitrapon, W., Strickman, D., Sithiprasasna, R., Kittayapong, P., and Innis, B. L. (1998). Effect of size and geographic origin of Aedes aegypti on oral infection with dengue-2 virus. Am J Trop Med Hyg *58*, 283-286.
Szittya, G., Molnar, A., Silhavy, D., Hornyik, C., and Burgyan, J. (2002). Short defective interfering RNAs of tombusviruses are not targeted but trigger post-transcriptional gene silencing against their helper virus. Plant Cell *14*, 359-372.
Takahashi, M., and Suzuki, K. (1979). Japanese encephalitis virus in mosquito salivary glands. Am J Trop Med Hyg *28*, 122-135.

Takeda, A., Sugiyama, K., Nagano, H., Mori, M., Kaido, M., Mise, K., Tsuda, S., and Okuno, T. (2002). Identification of a novel RNA silencing suppressor, NSs protein of Tomato spotted wilt virus. FEBS Lett *532*, 75-79.
Tanaka, Y., Guhde, G., Suter, A., Eskelinen, E. L., Hartmann, D., Lullmann-Rauch, R., Janssen, P. M., Blanz, J., von Figura, K., and Saftig, P. (2000). Accumulation of autophagic vacuoles and cardiomyopathy in LAMP-2-deficient mice. Nature *406*, 902-906.
Taylor, M. P., Burgon, T. B., Kirkegaard, K., and Jackson, W. T. (2009). Role of microtubules in extracellular release of poliovirus. J Virol *83*, 6599-6609.
Taylor, M. P., and Kirkegaard, K. (2007). Modification of cellular autophagy protein LC3 by poliovirus. J Virol *81*, 12543-12553.
Taylor, W. P., and Marshall, I. D. (1975a). Adaptation studies with Ross River virus: laboratory mice and cell cultures. J Gen Virol *28*, 59-72.
Taylor, W. P., and Marshall, I. D. (1975b). Adaptation studies with Ross River virus: retention of field level virulence. J Gen Virol *28*, 73-83.
ter Brake, O., von Eije, K. J., and Berkhout, B. (2008). Probing the sequence space available for HIV-1 evolution. AIDS *22*, 1875-1877.
Thein, S. M., MA Shwe, TN Aye, M Zaw, A Aye, K Aye, KM Aaskov, J (1997). Risk Factors in Dengue Shock Syndrome. American Journal of Tropical Medicine and Hygiene *56*, 566-572.
Travanty, E. (2005) RNA interference and dengue virus replication in insect cells culuture and *Aedes aegypti* mosquitoes. PhD dissertation, Colorado State University, Fort Collins, CO.
Tsetsarkin, K. A., Vanlandingham, D. L., McGee, C. E., and Higgs, S. (2007). A single mutation in chikungunya virus affects vector specificity and epidemic potential. PLoS Pathog *3*, e201.
Tuiskunen, A., Leparc-Goffart, I., Boubis, L., Monteil, V., Klingstrom, J., Tolou, H. J., Lundkvist, A., and Plumet, S. (2009). Self-priming of reverse transcriptase impairs strand specific detection of dengue virus RNA. J Gen Virol.
Uchil, P. D., Kumar, A. V., and Satchidanandam, V. (2006). Nuclear localization of flavivirus RNA synthesis in infected cells. J Virol *80*, 5451-5464.
Uchil, P. D., and Satchidanandam, V. (2003). Architecture of the flaviviral replication complex. Protease, nuclease, and detergents reveal encasement within double-layered membrane compartments. J Biol Chem *278*, 24388-24398.
Umareddy, I., Chao, A., Sampath, A., Gu, F., and Vasudevan, S. G. (2006). Dengue virus NS4B interacts with NS3 and dissociates it from single-stranded RNA. J Gen Virol *87*, 2605-2614.
Umareddy, I., Pluquet, O., Wang, Q. Y., Vasudevan, S. G., Chevet, E., and Gu, F. (2007). Dengue virus serotype infection specifies the activation of the unfolded protein response. Virol J *4*, 91.
van der Goot, F. G., and Harder, T. (2001). Raft membrane domains: from a liquid-ordered membrane phase to a site of pathogen attack. Semin Immunol *13*, 89-97.
Vance, V., and Vaucheret, H. (2001). RNA silencing in plants--defense and counterdefense. Science *292*, 2277-2280.
Vasilakis, N., and Weaver, S. C. (2008). The history and evolution of human dengue emergence. Adv Virus Res *72*, 1-76.

Vezzani, D., and Carbajo, A. E. (2008). Aedes aegypti, Aedes albopictus, and dengue in Argentina: current knowledge and future directions. Mem Inst Oswaldo Cruz *103*, 66-74.
Watts, D. M., Burke, D. S., Harrison, B. A., Whitmire, R. E., and Nisalak, A. (1987). Effect of temperature on the vector efficiency of Aedes aegypti for dengue 2 virus. Am J Trop Med Hyg *36*, 143-152.
Wearing, H. J., and Rohani, P. (2006). Ecological and immunological determinants of dengue epidemics. Proc Natl Acad Sci U S A *103*, 11802-11807.
Weaver, S. C. (1986). Electron microscopic analysis of infection patterns for Venezuelan equine encephalomyelitis virus in the vector mosquito, Culex (Melanoconion) taeniopus. Am J Trop Med Hyg *35*, 624-631.
Weaver, S. C., Lorenz, L. H., and Scott, T. W. (1992). Pathologic changes in the midgut of Culex tarsalis following infection with Western equine encephalomyelitis virus. Am J Trop Med Hyg *47*, 691-701.
Weaver, S. C., Scott, T. W., Lorenz, L. H., Lerdthusnee, K., and Romoser, W. S. (1988). Togavirus-associated pathologic changes in the midgut of a natural mosquito vector. J Virol *62*, 2083-2090.
Weber, F., Wagner, V., Rasmussen, S. B., Hartmann, R., and Paludan, S. R. (2006). Double-stranded RNA is produced by positive-strand RNA viruses and DNA viruses but not in detectable amounts by negative-strand RNA viruses. J Virol *80*, 5059-5064.
Welsch, C., Albrecht, M., Maydt, J., Herrmann, E., Welker, M. W., Sarrazin, C., Scheidig, A., Lengauer, T., and Zeuzem, S. (2007). Structural and functional comparison of the non-structural protein 4B in flaviviridae. J Mol Graph Model *26*, 546-557.
Welsch, S., Miller, S., Romero-Brey, I., Merz, A., Bleck, C. K., Walther, P., Fuller, S. D., Antony, C., Krijnse-Locker, J., and Bartenschlager, R. (2009). Composition and three-dimensional architecture of the dengue virus replication and assembly sites. Cell Host Microbe *5*, 365-375.
Westaway, E. G., Khromykh, A. A., Kenney, M. T., Mackenzie, J. M., and Jones, M. K. (1997a). Proteins C and NS4B of the flavivirus Kunjin translocate independently into the nucleus. Virology *234*, 31-41.
Westaway, E. G., Khromykh, A. A., and Mackenzie, J. M. (1999). Nascent flavivirus RNA colocalized in situ with double-stranded RNA in stable replication complexes. Virology *258*, 108-117.
Westaway, E. G., Mackenzie, J. M., Kenney, M. T., Jones, M. K., and Khromykh, A. A. (1997b). Ultrastructure of Kunjin virus-infected cells: colocalization of NS1 and NS3 with double-stranded RNA, and of NS2B with NS3, in virus-induced membrane structures. J Virol *71*, 6650-6661.
Westerhout, E. M., Ooms, M., Vink, M., Das, A. T., and Berkhout, B. (2005). HIV-1 can escape from RNA interference by evolving an alternative structure in its RNA genome. Nucleic Acids Res *33*, 796-804.
Whitehead, S. S., Blaney, J. E., Durbin, A. P., and Murphy, B. R. (2007). Prospects for a dengue virus vaccine. Nat Rev Microbiol *5*, 518-528.
Whitfield, S. G., Murphy, F. A., and Sudia, W. D. (1973). St. Louis encephalitis virus: an ultrastructural study of infection in a mosquito vector. Virology *56*, 70-87.
WHO (2008). Dengue/DHF Management of Dengue Epidemic (SEA/DEN/1) Annex 8 : Clinical Case Definition for Dengue Haemorrhagic Fever (WHO).

Wilson, R., Orsetti, J., Klocko, A. D., Aluvihare, C., Peckham, E., Atkinson, P. W., Lehane, M. J., and O'Brochta, D. A. (2003). Post-integration behavior of a Mos1 mariner gene vector in Aedes aegypti. Insect Biochem Mol Biol *33*, 853-863.
Woodring, J., Higgs, S., and Beaty, B., eds. (1996). Natural Cycles of Vector-Borne Pathogens (Niwot, CO, University Press of Colorado).
Yap, T. L., Xu, T., Chen, Y. L., Malet, H., Egloff, M. P., Canard, B., Vasudevan, S. G., and Lescar, J. (2007). Crystal structure of the dengue virus RNA-dependent RNA polymerase catalytic domain at 1.85-angstrom resolution. J Virol *81*, 4753-4765.
Yelina, N. E., Savenkov, E. I., Solovyev, A. G., Morozov, S. Y., and Valkonen, J. P. (2002). Long-distance movement, virulence, and RNA silencing suppression controlled by a single protein in hordei- and potyviruses: complementary functions between virus families. J Virol *76*, 12981-12991.
You, S., and Padmanabhan, R. (1999). A novel in vitro replication system for Dengue virus. Initiation of RNA synthesis at the 3'-end of exogenous viral RNA templates requires 5'- and 3'-terminal complementary sequence motifs of the viral RNA. J Biol Chem *274*, 33714-33722.
Yu, C. Y., Hsu, Y. W., Liao, C. L., and Lin, Y. L. (2006). Flavivirus infection activates the XBP1 pathway of the unfolded protein response to cope with endoplasmic reticulum stress. J Virol *80*, 11868-11880.
Zhang, X., Yuan, Y. R., Pei, Y., Lin, S. S., Tuschl, T., Patel, D. J., and Chua, N. H. (2006). Cucumber mosaic virus-encoded 2b suppressor inhibits Arabidopsis Argonaute1 cleavage activity to counter plant defense. Genes Dev *20*, 3255-3268.
Zhao, Z., Thackray, L. B., Miller, B. C., Lynn, T. M., Becker, M. M., Ward, E., Mizushima, N. N., Denison, M. R., and Virgin, H. W. t. (2007). Coronavirus replication does not require the autophagy gene ATG5. Autophagy *3*, 581-585.